HUMAN-YEAST CROSS-SPECIES COMPLEMENTATION OF CHROMOSOME INSTABILITY GENES

by

Akil Hamza

B.Sc., University of Ottawa, 2009

M.Sc., University of Ottawa, 2012

A DISSERTATION SUBMITTED IN PARTIAL FULFILLMENT OF

THE REQUIREMENTS FOR THE DEGREE OF

DOCTOR OF PHILOSOPHY

in

THE FACULTY OF GRADUATE AND POSTDOCTORAL STUDIES

(Biochemistry and Molecular Biology)

THE UNIVERSITY OF BRITISH COLUMBIA

(Vancouver)

October 2019

The following individuals certify that they have read, and recommend to the Faculty of Graduate and Postdoctoral Studies for acceptance, the dissertation entitled:

Human-yeast cross-species complementation of chromosome instability genes

Submitted by Akil Hamza in partial fulfillment of the requirements for

the degree of Doctor of Philosophy

in Biochemistry and Molecular Biology

Examining Committee:

Philip Hieter, Medical Genetics
Supervisor

Corey Nislow, Pharmaceutical Sciences
Supervisory Committee Member

Elizabeth Conibear, Medical Genetics
Supervisory Committee Member

James Kronstad, Microbiology and Immunology
University Examiner

Christopher Loewen, Cell & Developmental Biology
University Examiner

ABSTRACT

Humanized yeast offer a valuable resource with which to model and study human biology. Using cross-species complementation, model organisms like the budding yeast, *Saccharomyces cerevisiae*, can be utilized to measure the impact of tumor-specific mutations and screen for genetic vulnerabilities of genes overexpressed in cancer. To this end, we performed three parallel screens, one-to-one complementation screens for essential and nonessential yeast genes implicated in chromosome instability (CIN) and a pool-to-pool screen that queried all possible essential yeast genes for rescue of lethality by all possible human homologs. Our work identified 65 human cDNAs that can replace the null allele of essential yeast genes, including the nonorthologous pair y*RFT1*/h*SEC61A1*. For the nonessential yeast genes, 20 human-yeast complementation pairs were determined to be replaceable in 44 assays that test rescue of chemical sensitivity and/or CIN defects. For five human-yeast complementation pairs expressing human cDNAs encoding h*LIG1*, h*SSRP1*, h*PPP1CA*, h*PPP1CC* and h*PPP2R1A*, we introduced 45 tumor-specific missense mutations and assayed for growth defects and sensitivity to DNA-damaging agents in yeast. This set of human-yeast gene complementation pairs allows human genetic variants to be readily characterized in yeast, generating a prioritized list of somatic mutations that could contribute to chromosome instability in human tumors. We also selected a human-yeast pair expressing h*FEN1*, which is frequently overexpressed in cancer and is an anti-cancer therapeutic target, to perform synthetic dosage lethal (SDL) screens using ectopic overexpression of wild-type and catalytically inactive h*FEN1* in yeast. The SDL screens identified homologous recombination (HR) repair mutants as synthetic dosage lethal with overexpression of catalytically-inactive hFen1. The SDL interactions were dependent on binding of hFen1 to

DNA suggesting that toxicity was a result of catalytically inactive hFen1 becoming trapped on DNA and resulting in DNA damage. Our study establishes the utility of using cross-species complementation and ectopic overexpression to generate human-yeast genetic interaction networks and to model protein-inhibitor interactions using genetic approaches. Overall, these data establish the utility of this cross-species experimental approach.

LAY SUMMARY

Yeast is a single-celled organism that has played an important role in studying and modelling human biology and disease. Many of the genes that operate in yeast cells have similar roles in human cells. However, compared to human cells, yeast can be easily manipulated at the level of the DNA. As a result, genetic experiments in yeast are quicker, cheaper and can be carried out in high-throughput assays. In this study, we tested the extent to which a human gene can replace the similar yeast gene and operate in a yeast cell. These 'humanized' yeast cells can be used as a tool to study the human gene and its role in diseases such as cancer. Therefore, we used some of these humanized yeast cells as a platform to test mutations found in cancer and model the activity of a cancer specific drug target.

PREFACE

A modified version of chapters 2 and 4 that includes Figures 2.1, 2.2, 2.6, 4.1, 4.2 and Table 2.1 has been published in the journal *Genetics* (Hamza, A., Tammpere, E., Kofoed, M., Keong, C., Chiang, J., Giaever, G., Nislow, C., and Hieter, P. (2015) Complementation of yeast genes with human genes as an experimental platform for functional testing of human genetic variants. *Genetics* 201, 1263-74). I performed all experiments, analyzed and interpreted all data, generated the figures and wrote the paper under the supervision of P. Hieter. E. Tammpere, C. Keong and M. Kofoed helped in the screening of essential yeast genes for Figures 2.1 and 2.2. J. Chiang, G. Giaever, and C. Nislow provided reagents and tools for the screening of essential genes. The reuse and reprint of all published work is with permission from the journal referenced.

A modified version of chapters 2, 3 and 4 that includes Figures 2.3, 3.2, 4.6, 4.7, 4.8, 4.9 and Table 2.2 has been prepared in a manuscript, submitted and is currently under revision (Hamza, A., Driessen, M., Tammpere, E., O'Neil, NJ., and Hieter, P. (2019) Modelling inhibitor-protein interactions using humanized yeast identifies synthetic dosage lethal targets of nuclease defective Fen1. *Manuscript under revision*). I performed all experiments, analyzed and interpreted all data, generated the figures and wrote the paper under the supervision of P. Hieter. M. Driessen constructed strains for Figure 3.2. E. Tammpere helped in the screening of the nonessential yeast genes for Figure 2.3. NJ. O'Neil helped in the design of experiments for Figure 4.6 and edited the paper.

Chapter 3: Work on complementation of the yeast complexes was designed and performed by Akil Hamza and Maureen Driessen. Strain construction was mostly carried out by M. Driessen, while experiments, data analysis and all figures included in this chapter of the dissertation were performed by A. Hamza.

TABLE OF CONTENTS

LIST OF TABLES

LIST OF FIGURES

LIST OF SYMBOLS, ABBREVIATIONS & ACRONYMS

Δ	Deletion, null mutant
5-FOA	5-fluoroorotic acid
aa	Amino acid
ALF	A-like faker
ATP	Adenosine triphosphate
BiM	Bi-mater
CAR	Cohesin-associated region
cDNA	Complementary DNA
CEN	Centromeric or centromere
CIN	Chromosome instability
CPT	Camptothecin
CRISPR	Clustered Regularly Interspaced Short Palindromic Repeats
CTF	Chromosome transmission fidelity
DAmP	Decreased abundance by mRNA perturbation
DNA	Deoxyribonucleic acid
dCIN	Dosage chromosome instability
dNTP	Deoxynucleoside triphosphate
G418	Geneticin
GCR	Gross chromosomal rearrangement
GFP	Green fluorescent protein
GO	Gene ontology
HD	Huntington's disease
HR	Homologous recombination
HU	Hydroxyurea
LiAc	Lithium acetate
LOH	Loss of heterozygosity
MM	Magic media (medium)
MMS	Methyl methanesulfonate
NES	Nuclear export signal
NLS	Nuclear localization signal

OD_{600}	Optical density at 600nm
ORF	Open reading frame
PAM	Protospacer adjacent motif
PARP	Poly ADP-ribose polymerase
PCR	Polymerase chain reaction
PEG	Polyethylene glycol
PNK	Polynucleotide Kinase
RNA	Ribonucleic acid
RPM	Rotations per minute
SC	Synthetic complete (medium)
SDL	Synthetic dosage lethality or synthetic dosage lethal
SDS-PAGE	Sodium dodecyl sulfate polyacrylamide gel electrophoresis
SGA	Synthetic genetic array
sgRNA	Single guide RNA
SL	Synthetic lethality or synthetic lethal
SS-DNA	Single stranded DNA
TS	Temperature-sensitive
WT	Wild-type
YKO	Yeast knockout
YPD	Yeast peptone dextrose (medium)

ACKNOWLEDGEMENTS

I would like to thank my supervisor Dr. Philip Hieter for his guidance, support, and patience during my graduate studies. He has my deepest gratitude.

I also thank my committee members Dr. Corey Nislow and Dr. Elizabeth Conibear for their scientific input and helpful suggestions during my dissertation work.

I thank the Hieter lab members that I have worked with over the years. It was a pleasure and a privilege.

I am especially indebted to Maureen Driessen for her amazing work and help. And to Nigel O'Neil for his support, advice and feedback throughout the years.

I acknowledge scholarship support from the Canadian Institutes of Health Research and the University of British Columbia.

A special thanks to my family for their enduring support.

In particular, I would like to thank my wife, Waged, for her continuous encouragement, love, patience and kind words. Thanks for all the times you came to the lab with me to keep me company. I am grateful that we completed our PhDs together and that was only possible because we had each other.

DEDICATION

To my parents, for all of your love and support.

CHAPTER 1: INTRODUCTION

1.1 Yeast genetics to study chromosome instability

1.1.1 Chromosome instability in cancer

Chromosome instability (CIN) is characterized by an increased rate of chromosome gain, loss, or rearrangement causing aneuploidy, in which cells have abnormal numbers of chromosomes, chromosomal segments, gene amplifications and/or novel gene fusions (Tanaka and Hirota, 2016). Genetic instability on the chromosome-level is detrimental to cellular regulation, growth, and viability, and is an enabling characteristic of cancer development and progression (Hanahan and Weinberg, 2011; Negrini et al., 2010). Cancer is a multigenic disease that arises from the sequential accumulation of genetic alterations in key genes that affect normal cellular proliferation (Loeb, 2011; Stratton et al., 2009). These genetic alterations include mutations such as gain-of-function mutations in oncogenes (whose activation gives the cell a selective growth advantage) and loss-of-function mutations in tumor-suppressor genes (whose inactivation gives the cell a selective growth advantage). Other genetic alterations include gene amplifications of oncogenes and deletions of tumor-suppressor genes that cause dosage imbalance, and chromosomal rearrangements that create oncogenic fusion proteins (Vogelstein et al., 2013). CIN increases the probability for these genetic alterations to occur, and as such, is an important contributing factor to tumorigenesis.

1.1.2 Yeast assays identify chromosome instability genes

The simplicity and genetic tractability of the budding yeast, *Saccharomyces cerevisiae*, makes it a model experimental system to delineate conserved biological pathways and processes such as those involved in CIN (Botstein and Fink, 2011; Measday and Stirling, 2016; Rine, 2014). Yeast-based assays enable measuring CIN using readouts that assay loss

of endogenous genomic loci or marked artificial chromosome fragments. One of the earliest screens utilized random mutagenesis to isolate yeast mutants defective in the maintenance of circular mini-chromosomes (Maine et al., 1984). Another study designed a colony-colour visual assay, termed chromosome transmission fidelity (CTF) assay, and used random mutagenesis to identify mutants that mis-segregate a nonessential artificial chromosome fragment (Spencer et al., 1990). Other yeast-based assays such as the haploid a-like faker (ALF) and diploid bi-mater (BiM) measure loss of the endogenous mating type *MAT* locus (Haber, 1974; Yuen et al., 2007). Similar to the BiM assay, another diploid assay measures loss-of-heterozygosity (LOH) of the *MET15*/*met15*Δ heterozygous diploid (Andersen et al., 2008). This assay is also a colony-colour visual assay that assesses hemi- or homozygosity of the *MET15* locus. In addition, the gross chromosomal rearrangements (GCR) assay measures simultaneous loss of two counter-selectable markers, *CAN1* (Whelan et al., 1979) and *URA3* (Boeke et al., 1987), that are linked in a distal portion of a chromosome arm (Chen and Kolodner, 1999). Overall, the CIN assays measure different possible mechanisms of genetic marker loss. CTF detects whole chromosome loss while the GCR assay measures chromosome rearrangements that are typically terminal deletions. BiM and LOH predominantly detect whole chromosome loss, mitotic recombination, and to a lesser extent chromosome rearrangement and terminal deletions. ALF detects whole chromosome loss, terminal deletions, and to a lesser extent gene conversion events. In aggregate, these assays can be used comprehensively to identify the spectrum of genes important for chromosome maintenance processes.

The development of yeast genomic collections such as the knockout collection for the nonessential genes (Giaever et al., 2002), the temperature-sensitive collection for the

essential genes (Ben-Aroya et al., 2008; Li et al., 2011) and plasmid-based collections for overexpression of all yeast genes (Ho et al., 2009; Hu et al., 2007), has facilitated high-throughput and genome-wide screens to identify genes that function in chromosome stability. Approximately 4700 nonessential yeast genes have been screened as deletion alleles for increased CIN using the CTF, ALF, BiM (Yuen et al., 2007), GCR (Smith et al., 2004) and LOH assays (Andersen et al., 2008). The CTF, ALF and GCR assays were also utilized to screen ~90% of essential yeast genes as temperature-sensitive alleles (at semi-permissive temperatures) or hypomorphic alleles (DAmP collection) (Stirling et al., 2011). Collectively, these studies and others identified 323 essential and 369 nonessential yeast genes that are mutable to a CIN phenotype in at least one of the tested assays (Stirling et al., 2011). Moreover, several large-scale screens identified ~300 yeast genes that cause CIN upon overexpression as measured by CTF (Duffy et al., 2016; Frumkin et al., 2016; Zhu et al., 2015), ALF (Duffy et al., 2016) and LOH assays (Tutaj et al., 2018). A comparison of these dosage CIN (dCIN) genes to the loss-of-function CIN genes revealed only a partial overlap suggesting that genetic alterations causing loss or gain of genes can cause CIN (Duffy et al., 2016).

Analysis of the yeast CIN/dCIN genes list revealed that the major processes required for the maintenance of chromosome stability are those that function in the cell cycle and various DNA transactions including DNA replication/repair, chromosome segregation/cohesion and transcription (Duffy et al., 2016; Measday and Stirling, 2016). An important application of this list is that it serves as a resource to identify candidate human CIN/dCIN genes with potential relevance to cancer. For instance, the majority of colorectal cancers exhibit chromosome instability and a candidate gene sequencing approach of more

than 200 human homologs of yeast CIN genes identified recurrent somatic gene mutations in a panel of colorectal tumor samples (Barber et al., 2008; Wang et al., 2004). Notably, a subset of these tumor-specific variants were found in genes that function in the cohesion pathway, thus highlighting a role for this pathway in cancer biology (Barber et al., 2008; Hill et al., 2016; Losada, 2014; Wang et al., 2004). Another study utilized the yeast dCIN gene list to direct the search for candidate human dCIN genes amplified in tumors. This approach identified human *TDP1* to be elevated in rhabdomyosarcomas and follow-up experiments confirmed that rhabdomyosarcoma cell lines showed increased CIN as a result of higher *TDP1* levels (Duffy et al., 2016). Yeast can also be utilized to identify chemical sensitivities to cytotoxic agents caused by CIN gene mutations that may be exploited to selectively target tumor cells (O'Neil et al., 2017). For instance, genotoxic agents that act by alkylation are common cancer chemotherapy drugs and yeast mutants that are sensitive to these agents identify candidate human genes required for DNA damage response (Svensson et al., 2012).

1.1.3 Yeast genetics to target the cancer genotype

Tumor-specific genetic alterations, such as CIN mutations, represent vulnerabilities that can be leveraged to selectively kill tumor cells relative to normal cells (O'Neil et al., 2017). This can be achieved by disrupting second-site targets in cells based on an established genetic interaction with the tumor-specific alteration. This approach exploits the concept of synthetic lethality (SL), which occurs when the perturbations of two genes individually is viable but combining those perturbations results in lethality. These perturbations can be reduction- or loss-of-function gene mutations, knockout, or knockdown, or through chemical inhibition of the protein itself. Another form of SL, synthetic dosage lethality (SDL), is based on the overexpression of a protein product. SDL occurs when overexpression of a gene

causes lethality in combination with the perturbation of a second-site target (Kroll et al., 1996).

Hartwell and colleagues, in 1997, first suggested that the concept of synthetic lethal genetic interactions in model organisms could be applied (cross-species) to identify potential anti-cancer therapeutic drug targets (Hartwell et al., 1997). Since then, high-throughput methodologies in yeast, such as synthetic genetic array (SGA) technology, have enabled the generation of large-scale genetic interaction networks that include SL (Tong et al., 2001) and SDL (Measday et al., 2005) interactions. SGA can be used to cross a yeast strain bearing a query mutation to arrays composed of mutant strains (ex. nonessential deletion collection). SGA then allows examination of genetic interactions on a genome-wide scale using an automated system to generate double mutants from single mutants and compare their relative fitness (Baryshnikova et al., 2013). Yeast-based SL and SDL screens that queried CIN/dCIN genes have successfully identified conserved genetic interactions in human cancer cells. For instance, a yeast SL interaction between *RAD54* and *RAD27* was reproduced with the human cognate gene pairs, *RAD54B* and *FEN1* (ortholog of y*RAD27*) in a colorectal cancer cell line (McManus et al., 2009). Another study used established yeast SL genetic interactions to generate a conserved human SL genetic network of commonly mutated CIN genes in colorectal cancer. This approach identified the DNA replication enzyme, *FEN1*, as a conserved second-site target and further demonstrated that *FEN1* inhibitors sensitized *MRE11A*-depleted human cell lines (van Pel et al., 2013). Moreover, a genome-wide SDL screen identified the deletion mutant of the histone deacetylase, *RPD3*, as sensitive to overexpression of yeast *TDP1*. The SDL interaction was conserved in a rhabdomyosarcoma

cell line that had elevated levels of human *TDP1* and was sensitive to histone deacetylase inhibitors (Duffy et al., 2016).

Over the past two decades, most genetic interaction screens in yeast have relied on genome-wide deletion or temperature-sensitive mutation collections that result in a loss- or reduction-of-function phenotype. While these approaches are effective in identifying SL genetic interactions that may be relevant to the development of a cancer therapeutic, they may not accurately model a genetic interaction between a tumor mutation and the chemical inhibition of a synthetic lethal partner protein. For instance, synthetic lethal genetic interactions discovered using loss-of-function mutations may show limited efficacy when phenocopied by small molecule inhibitors due to residual enzyme activity. Moreover, lethal interactions that require the formation of a toxic intermediate in the form of a compound-protein or protein-DNA complex would not be discovered by genetic screens using loss-of-function mutations. Two prominent examples of synthetic lethal-based therapeutics whose effectiveness is a result of cytotoxic protein-DNA complexes are PARP and topoisomerase inhibitors. PARP inhibitors that 'trap' PARP on the DNA at sites of DNA damage are more effective at killing BRCA-mutated cancer cells than PARP knockout or knockdown (Murai et al., 2012; Pommier et al., 2016). Topoisomerase inhibitors prevent the resolution of the DNA-topoisomerase intermediate, and although the inhibitors were not developed as synthetic lethal-based therapeutics, their efficacy is due in part to synthetic lethal interactions with tumor-specific mutations affecting DNA replication and repair (Delgado et al., 2018). The trapping of PARP and topoisomerase indicate that synthetic lethal genetic interactions based on a DNA trapping mechanism should be investigated for other DNA-associated cancer targets. This can be accomplished using yeast genetics by introducing catalytically

inactivating mutations that model protein trapping inhibitors as an alternative to gene deletions. In this way, synthetic lethal genetic interactions can be assessed when the target protein is present, retains DNA binding, but is inactivated. For instance, catalytically inactive forms of yeast *RAD27* or the human ortholog, *FEN1*, bind DNA substrates with high affinity (Shen et al., 1996, 1997), while ectopic expression of the yeast or human inactive forms in the presence of wild-type *RAD27* causes genetic instability and DNA damage in a yeast system (Becker et al., 2018; Greene et al., 1999). As such, yeast can be utilized to screen on a large-scale for second-site mutations that cannot tolerate expression of the yeast or human inactive proteins and in turn, generate genetic interaction networks that potentially mimic the activity of chemically inhibited proteins more accurately.

1.2 Humanized yeast to study human biology

Advances in synthetic biology have facilitated the construction of humanized yeast as a tool to study and model conserved biological processes. Yeast can be humanized using two different approaches: heterologous expression in which a human gene is expressed ectopically in yeast or cross-species complementation in which the human gene complements a mutation in the cognate yeast gene.

1.2.1 Heterologous expression of human genes in yeast

Irrespective of orthology, heterologous expression of human genes that induce a phenotypic readout in wild-type yeast cells can be leveraged to elucidate the pathological functions of disease genes (Cooper et al., 2006), identify drug targets (Jo et al., 2017), and screen for chemical inhibitors (Perkins et al., 2001). Two studies systematically overexpressed human cDNAs in wild-type yeast cells to identify human proteins that induce

growth inhibition. One study screened a panel of 38 human cDNAs encoding proteins involved in cell growth and signal transduction resulting in the identification of 12 genes (~30%) that repressed yeast growth upon overexpression (Tugendreich et al., 2001). A more comprehensive screen overexpressed 10,302 human cDNAs (encompassing ~50% of human cDNAs) in yeast and identified 583 human genes (~6%) that caused growth defects (Sekigawa et al., 2010). In cases where expression of a human protein causes growth inhibition, a restoration of growth assay can be used to screen for chemical inhibition of the human protein (Sekigawa et al., 2010). Phenotypic readouts also include yeast-based reporter assays that measure transactivation or enzymatic activity of the human protein. For example, human tumor-suppressor genes *TP53* and *PTEN* have no orthologs in yeast. Nevertheless, heterologous expression in yeast has facilitated the study of 2,314 *TP53* (Kato et al., 2003) and 7,244 *PTEN* (Mighell et al., 2018) single amino-acid variants by means of yeast reporter assays. In addition, yeast can be utilized as an *in vivo* system to explore biological mechanisms of the human protein. For instance, fluorescently-tagged human cohesin genes *STAG1* and *STAG2* were expressed in yeast to study their subcellular localization and determine their nuclear localization (NLS) and export (NES) signals (Tarnowski et al., 2012).

1.2.2 Human-yeast cross-species complementation

Cross-species complementation refers to the ability of a gene (or set of genes) to complement the loss-of-function phenotype of its homolog (or set of homologs) in another species. Homolog is as an umbrella term that encompasses orthologs (genes derived from speciation and that typically perform the same biological function across species) and paralogs (genes related by duplication and that generally perform biologically distinct yet mechanistically related functions) (Koonin, 2005). With approximately 20,000 human and

6,000 yeast protein-coding genes, roughly 60% (3595/6000) of yeast protein-coding genes have identifiable human homologs (corresponding to 6,626 human genes) (Yeastmine Database) (Balakrishnan et al., 2012), while 87% of yeast protein domains are found in a human protein (Peterson et al., 2013). Thus, although humans and yeast diverged approximately one billion years ago (Laurent et al., 2016), there is extensive conservation of protein sequence that in some cases allow human genes to replace yeast genes and function cross-species.

Complementation of yeast mutations by human genes has been utilized to isolate human genes and to elucidate the functional homology between human and yeast proteins. Some of the earliest examples of human-yeast complementation included a study that demonstrated chimeric human-yeast or full length human *RAS* genes could complement yeast *ras*Δ mutants (Kataoka et al., 1985), and a study that used a temperature-sensitive mutant in the *S. pombe CDC2* gene to isolate the human ortholog from a cDNA library (Lee and Nurse, 1987). Since then, hundreds of studies testing individual genes have revealed >200 human-yeast complementation pairs (reviewed in (Dunham and Fowler, 2013; Heinicke et al., 2007; Laurent et al., 2016; Osborn and Miller, 2007)). Several studies systematically tested for human-yeast complementation pairs. One screened for rescue of lethality caused by inducible loss-of-function of 25 essential yeast genes (repressible promoter) following transformation of a human cDNA library (i.e., pool-to-one screens) and identified six essential genes that were rescued by a human ortholog (Zhang et al., 2003). More recently, 176/414 essential yeast genes (as null and/or temperature-sensitive mutants and/or using a repressible promoter) were found to be replaceable by their 1:1 human ortholog (one-to-one screens) (Kachroo et al., 2015). We have also screened 621 essential yeast gene null mutants for

complementation by all potential human homologs in two parallel screens (one-to-one screens for the essential yeast CIN genes and pool-to-pool screens for all possible essential yeast genes) (see Chapter 2 and (Hamza et al., 2015)). Another recent study focused on human disease genes and screened 125 orthologous essential yeast genes (as temperature-sensitive mutants) to determine 25 essential genes that can be rescued by a human ortholog at the nonpermissive temperature (one-to-one screens) (Sun et al., 2016). A follow-up study that also focused on human disease genes tested 1,060 human-yeast paralog pairs and identified 34 complementation pairs whereby the human gene rescues temperature sensitivity of conditional essential yeast mutants (one-to-one screens) (Yang et al., 2017).

Human-yeast complementation has also been attempted at the level of entire yeast complexes and pathways. There are several examples of complementation of two-subunit yeast complexes. Complementation of depleted iron-sulfur (Fe-S) assembly yeast proteins Yae1 or Lto1 required co-expression of human orthologs *YAE1D1* and *ORAOV1* for restoration of growth and Fe-S cluster assembly in yeast (Paul et al., 2015). Similarly, depletion of either member of a yeast glycosyltransferase complex composed of *ALG13* and *ALG14* required co-expression of their human orthologs for restoration of growth (Gao et al., 2005). Other notable examples demonstrating human complementation of double deletion mutants of two-subunit yeast complexes include the DBF4-dependent kinase (DDK) complex composed of human *CDC7*/*DBF4* (Davey et al., 2011), the mRNA export complex composed of human *NXF1*/*NXT1* (Katahira et al., 1999), and the N-terminal acetyltransferase complex composed of human *NAA10*/*NAA15* (Arnesen et al., 2009). For all these cases, complementation was only achieved by co-expression of both human subunits in yeast, suggesting that heterologous combinations of yeast and human subunits were not functional.

Another study found that simultaneous expression of a human mitochondrial translocase complex composed of *TIMM8A* and *TIMM13* rescued the cold-sensitivity phenotype of yeast *tim8*Δ*tim13*Δ mutants and facilitated the import of a human protein (Tim23) into yeast mitochondria, however it is not known if expression of either human protein on its own could complement the corresponding yeast single mutant as this was not tested (Rothbauer et al., 2001). In one case, a subunit of human tRNA m^1A58 methyltransferase complex (*TRM61*) partially rescued growth defects of a conditional mutant of yeast *TRM61*, but the other human subunit (*TRM6*) was unable to complement yeast *TRM6*. However, co-expression of both human subunits fully rescued viability and methyltransferase activity of conditional mutants of yeast *TRM61* and *TRM6* (Ozanick et al., 2005).

In some cases, co-expression of both members of a human complex is not sufficient for complementation as the human proteins may require amino-acid sequence modifications to function in yeast. For instance, the mitochondrial targeting sequences of both human subunits of a mitochondrial metallopeptidase complex (*SPG7*/*AFG3L2*) were replaced by the targeting sequence of yeast *YTA10* to form human-yeast hybrid proteins. Co-expression of both subunits was then required to rescue growth of the single and double deletions of yeast orthologs *YTA10*/*YTA12* on nonfermentable carbon sources (Atorino et al., 2003). This was also the case for another mitochondrial protein, yeast *MIP1*, which encodes mitochondrial DNA (mtDNA) polymerase gamma. While yeast contains only a single catalytic subunit for mtDNA polymerase, human mtDNA polymerase gamma is a complex composed of the orthologous catalytic subunit (*POLG*), and accessory subunit (*POLG2*) which has no homolog in yeast. The accessory interaction domain on *POLG* is also not conserved in yeast *MIP1*. Nevertheless, expression of *POLG* fused to the yeast mitochondrial targeting sequence

partially rescued growth of a *mip1*Δ strain, but a full rescue was observed only when *POLG* was co-expressed with the human accessory subunit *POLG2* (Qian et al., 2014).

Attempts to humanize entire yeast pathways and complexes larger than two subunits are limited. Recently, it was demonstrated that the core yeast nucleosome composed of four histone subunits (H3, H4, H2A, H2B) can be entirely replaced with the human nucleosome in a rare event that required adaptation of yeast cells (Truong and Boeke, 2017). When all four histone subunits were replaced simultaneously, a viable humanized strain was observed only after plating 10^7 yeast cells. After isolating eight colonies with all four human histones being expressed, whole-genome sequencing revealed the humanized strains had higher levels of aneuploidy and contained suppressor mutations in genes functioning in chromosome segregation and cell-cycle progression. The study confirmed that the suppressor mutations enhanced humanization frequency and also showed that substituting five human amino-acid residues (two in H3 and three in H2A) with the corresponding yeast equivalents resulted in a more robust complementation.

Large-scale screens testing complementation of single yeast genes by human genes revealed that complementation patterns of single yeast genes in a pathway were similar, such that if a yeast gene in a pathway was replaceable by a human gene, then other yeast genes in that pathway also tended to be replaceable. For instance, 17 of 19 yeast genes in the sterol biosynthesis pathway can be replaced by the corresponding human ortholog (Kachroo et al., 2015); similarly, human complementation was demonstrated for all eight yeast genes of the heme biosynthesis pathway (Kachroo et al., 2017). While these studies tested single genes, only one study engineered a yeast strain that replaced an entire yeast pathway based on human-yeast complementation. The study demonstrated the 12-step adenine biosynthesis

yeast pathway can be entirely replaced as a full human pathway transplantation (Agmon et al., 2017). The fully engineered strain was utilized to study regulation of human proteins in the pathway and identify suppressor mutations that enhanced growth of the humanized yeast.

1.2.3 Using complementation to assess human genetic variants in yeast

While the pace of discovery of human genetic variants in tumors, patients, and diverse populations has rapidly accelerated, deciphering their functional consequence has become rate-limiting. Model organisms like the budding yeast can be utilized to fill this gap and serve as a platform for testing human genetic variants. There are several approaches for studying human genetic variants in yeast. Based on sequence conservation, human variants can be tested by introducing mutations in conserved sites of the yeast ortholog. However, such sequence-based efforts restrict the number of variants that can be studied, and inferences based on this approach can be misleading as the impact of a nonsynonymous substitution in the context of the yeast protein may not accurately predict the same effect in the context of the human protein (Marini et al., 2010). A more desirable approach is to functionally test variants directly in the context of the human protein sequence by utilizing cross-species complementation to humanize the yeast strain. The main advantages of this approach are that human gene variants can be characterized in their native context while screening rapidly in a model eukaryote.

In comparison to computational predictions, yeast-based complementation assays have been shown to have a higher predictive power on the functional effect of missense mutations. One study utilized complementation of human-yeast ortholog pairs to compare 101 disease and 78 non-disease variants found in 22 human disease genes (Sun et al., 2016). A similar analysis was repeated utilizing complementation of human-yeast paralog pairs to

compare 19 disease and 16 non-disease variants found in seven human disease genes (Yang et al., 2017). In both studies, the human disease genes rescued viability of yeast temperature-sensitive mutants at the restrictive temperature and genetic variants were assessed based on their ability to complement in comparison to the wild-type allele. Based on the assumption that disease variants are deleterious, complementation assays were more likely to identify disease variants as unable to complement yeast mutants compared to the non-disease variants. For instance, complementation using human paralogs identified 15 of 19 disease variants that impact complementation compared to only 4 of 16 non-disease variants (Yang et al., 2017). When compared to computational predictions, both studies revealed that complementation assays better predicted deleterious alleles for the subset of disease variants and non-deleterious alleles for the subset of non-disease variants.

An application of complementation to study human genetic variants from diverse populations was demonstrated in a study of the folate-dependent methylenetetrahydrofolate reductase (*MTHFR*) enzyme. In this study (Marini et al., 2008), the coding regions of the *MTHFR* gene from 564 individuals of diverse ethnicities were sequenced to identify 14 nonsynonymous substitutions. In order to assess the impact of these variants and their responsiveness to folate, a yeast strain was engineered with a deletion of the yeast ortholog (*MET13*) and deletion of *FOL3* to facilitate titration of intracellular folate levels. After confirming that expression of human *MTHFR* rescued growth of *fol3*Δ*met13*Δ in the presence of intracellular folate, the 14 variants were assessed for their ability to complement the same yeast strain when supplemented with varying levels of folate. Complementation assays identified five variants which impacted the ability of human *MTHFR* to complement

the yeast deletion strain and demonstrated that complementation of four of these variants can be restored by elevating intracellular folate levels.

A similar approach was used to study human disease variants found in the cystathionine-b-synthase (*CBS*) gene, which encodes a metabolic enzyme that converts homocysteine to cystathionine. Deficiency in *CBS* causes an accumulation of homocysteine, which leads to the development of homocystinuria and other human diseases. By utilizing complementation of the yeast ortholog (*CYS4*) as a platform to assess disease variants found in homocystinuria patients, 84 *CBS* missense mutations were tested for their ability to complement yeast *cys4*Δ compared to the wild-type *CBS* gene. Yeast growth and enzymatic assays identified 71 variants that displayed phenotypic readouts different than the wild-type *CBS* gene including human disease alleles in which their ability to complement *cys4*Δ was rescued by addition of *CBS* cofactors vitamin B6 or heme (Mayfield et al., 2012).

Another study employed complementation in yeast to assess 12 missense argininosuccinate lyase (*ASL*) mutations found in patients diagnosed with argininosuccinic aciduria (ASAuria). Expression of human *ASL* complemented the growth defect of yeast *arg4*Δ mutants in arginine-deficient media, whereas all 12 mutants resulted in either a loss-of-function or reduction-of-function of the human protein (Trevisson et al., 2009). The study further demonstrated the utility of yeast-based complementation assays to assess clinically-relevant combinations of *ASL* mutations. ASL proteins function as a homotetrameric complex, and in cases of heterozygous mutations, ASL forms a tetrameric complex composed of different subunits derived from different alleles of the gene. Since yeast can exist as haploid or diploid, different heteroallelic combinations of *ASL* mutations were expressed in *arg4*Δ homozygous diploid mutants and compared to the clinical phenotypes of

the patients. For instance, complementation assays of *arg4*Δ haploid mutants revealed that hR182Q and hR297Q are both loss-of-function alleles that cannot rescue viability of the yeast mutant. However, heteroallelic co-expression of hR182Q/hR297Q rescued growth of *arg4*Δ homozygous diploid mutants, indicating a rescue of the enzymatic activity of the ASL tetramer. Conversely, hR113Q and hR236W variants resulted in loss-of-function when expressed either as single or as heteroallelic mutations. These results from yeast-based assays were consistent with the hR182Q/hR297Q patient displaying a 'mild' phenotype, and the hR113Q/hR236W patient displaying a 'severe' phenotype.

Complementation assays have also been used to correlate cancer risk with tumor-specific variants. In an effort to identify inherited mutations in breast cancer patients that are wild-type for *BRCA1/2*, one study sequenced the serine/threonine protein kinase, *CHEK2*, to identify candidate tumor-specific variants in Ashkenazi Jewish families with high incidence of breast cancer (Shaag et al., 2005). Two *CHEK2* variants were identified and tested in yeast-based complementation assays for their ability to rescue viability of *rad53*Δ mutants. Growth assays revealed hS428F as a loss-of-function mutation, and hP85L as a fully functional allele, as measured by complementation of the yeast phenotype. The frequency of these alleles was then assessed in 1848 Ashkenazi Jewish breast cancer patients and 1673 controls to reveal hP85L as a neutral allele, and the hS428F variant as associated with an increased breast cancer risk of about 2-fold. Overall, these studies highlight the utility of yeast-based complementation experiments to differentiate disease-linked from neutral variants.

1.2.4 Generating human-yeast genetic interaction networks

Yeast high-throughput tools facilitate the interrogation of genetic interactions on a genome-wide scale with relative simplicity. The resultant yeast genetic networks are generated in a systematic and unbiased approach and can be used to predict genetic interactions in humans (Lehner, 2007). Alternatively, human genes can be screened in yeast to generate cross-species human-yeast genetic networks. To date, this approach has been used extensively to study neurodegenerative diseases and is primarily based on the heterologous expression of human genes in yeast (reviewed in (Gitler, 2008)). A common manifestation of neurodegenerative diseases is the accumulation of misfolded proteins that aggregate. Expression of these human disease-associated proteins in yeast also leads to the formation of aggregates that are toxic to yeast in a dose-dependent manner (Jo et al., 2017; Tardiff et al., 2014). Genome-wide screens that utilize collections of yeast deletion and overexpression strains can be used to discover yeast genes that suppress or enhance the human gene-induced toxicity. For example, Huntington's disease (HD) is caused by expansions of polyglutamine tracts (<37: normal, >40: pathogenic) in the huntingtin (Htt) protein. Heterologous expression of the Htt protein causes polyglutamine length-dependent aggregation and cytotoxicity in yeast (Gitler, 2008). Genome-wide screens probing the nonessential yeast deletion collection identified loss-of-function mutants that enhanced (Willingham et al., 2003) or suppressed (Giorgini et al., 2005) Htt toxicity. The same study (Willingham et al., 2003) screened a Parkinson’s disease-associated protein, α-synuclein, which also forms aggregates and causes toxicity in yeast in a dose-dependent manner. The results of the two screens yielded a non-overlapping set of yeast mutants that were sensitive to Htt or α-synuclein expression, which suggested that yeast-based screening can unravel

distinct mechanisms and regulation of heterologous human disease proteins. Another study demonstrated the utility of the yeast overexpression library to screen for yeast genes that enhanced or suppressed α-synuclein cytotoxicity (Cooper et al., 2006). Similar genome-wide yeast screens have also identified toxicity modifiers for Alzheimer's-associated (Treusch et al., 2011) and amyotrophic lateral sclerosis (ALS)-associated (Jo et al., 2017) genes. Although the human-yeast genetic networks were based on the expression of non-orthologous human genes in yeast, they were instrumental in deciphering cellular mechanisms of disease genes and identifying potential targets for therapy.

1.3 Research aims

The utility of yeast-based assays to identify conserved human CIN/dCIN genes has been demonstrated. Given that chromosomal instability is prevalent in cancer biology, human CIN/dCIN genes that have tumor-specific mutations or are overexpressed in cancer cells outline a potential link between CIN and tumorigenesis. Yeast as a surrogate system, can be utilized to study these links by cross-species complementation. The central hypothesis of this study is that human complementation of yeast chromosome instability genes facilitates studying CIN processes relevant to cancer in a yeast system. The first aim of this thesis is to identify human candidate CIN genes that complement yeast CIN genes either as single replacements (Chapter 2) or as a complex/pathway transplantation (Chapter 3). The second aim is to demonstrate applications of human-yeast complementation to study cancer relevant processes of human CIN/dCIN genes (Chapter 4). This includes (i) screening tumor-specific variants for functionality and sensitivity to DNA damaging agents and (ii) generating human-yeast genetic interaction networks based on the DNA trapping mechanism for a human gene overexpressed in cancer and which is a target for anti-cancer therapeutic development.

CHAPTER 2: SYSTEMATIC IDENTIFICATION OF HUMAN-YEAST CROSS-SPECIES COMPLEMENTATION PAIRS

2.1 Introduction

Yeast genome-wide screens for CIN genes have resulted in the compilation of ~700 genes required for chromosome stability (Stirling et al., 2011). Human homologs of the yeast CIN genes are candidate human CIN genes whose expression in yeast can be tested for complementation of a loss-of-function phenotype. While cross-species complementation can be scored by any measurable phenotype, the most straight-forward phenotype to assay and quantify is the rescue of growth defects. Complementation of essential yeast genes by candidate human gene homologs can be tested for the ability of a human cDNA to rescue lethality caused by (i) a null allele (deletion in a haploid strain), (ii) a conditional allele under restrictive conditions (e.g., temperature-sensitive strain), or (iii) downregulation by a repressible promoter (e.g., Tet system) (Kachroo et al., 2015). In contrast, nonessential yeast genes, the majority of which cause minimal growth defects when disrupted, can only be screened for complementation in conditional assays that induce measurable growth phenotypes. This can be accomplished by growing the nonessential gene mutants in restrictive media conditions (e.g. alternate sugar sources) (Guimier et al., 2016), adding chemicals to sensitize the yeast strain, or converting the nonessential yeast gene to an essential gene by disrupting a synthetic lethal partner (Greene et al., 1999).

At the onset of this project, the majority of complementation studies were restricted to testing individual human-yeast gene pairs (reviewed in (Dunham and Fowler, 2013)), while only one study systematically assayed for rescue-of-lethality of 25 essential yeast genes using a human cDNA library (Zhang et al., 2003). Since then, several systematic studies for

human-yeast complementation pairs were reported that focused on essential yeast genes (Kachroo et al., 2015; Sun et al., 2016; Yang et al., 2017), including our own work (Hamza et al., 2015). The aim of this project was to systematically screen for human-yeast complementation pairs on a large-scale with a focus on genes functioning in chromosome stability. In this chapter, we report the screening of 621 essential yeast gene null mutants for complementation by all potential human homologs in two parallel screens ("one-to-one" screens for 199 essential CIN genes corresponding to 322 candidate complementation pairs, and a "pool-to-pool" screen for all possible essential yeast genes). To expand the list of complementation pairs beyond those discovered for essential yeast genes, we screened a subset of 112 nonessential yeast CIN genes for rescue of drug sensitivity and/or CIN defects by their human homologs.

2.2 Methods

2.2.1 One-to-one complementation screen of essential yeast CIN genes

Expression vectors: Human cDNAs in Gateway-compatible entry clones were obtained from hORFeome V8.1 (Yang et al., 2011) and shuttled into yeast destination vectors (Alberti et al., 2007) using LR clonase II (Invitrogen) to generate expression clones. The destination vector used was pAG416GPD-ccdB-HA (*URA3*, CEN, constitutive GPD promoter, C-terminal HA tag) with a stop codon contributed by the vector backbone resulting in a 55-amino-acid C-terminal extension. The identity of the human cDNA was confirmed by sequencing the expression vector using a common primer that hybridizes to the vector backbone (CAGGAAACAGCTATGAC).

Complementation assays: Generated expression vectors were transformed into the corresponding haploid-convertible heterozygous diploid knockout yeast strain (Pan et al., 2004) and transformants were selected on SC−Ura media. Transformants were then inoculated in liquid sporulation media (1% w/v potassium acetate, 0.005% w/v zinc acetate, and 0.3mM histidine) (Pan et al., 2007) to a cell density of ∼1–2 OD_{600} at 25°C with shaking for 5 days and sporulation efficiency was assessed using microscopy. Following sporulation, 50µl of cells were resuspended in 1ml water of which 100µl was plated on the haploid selection media MM−Ura (−Leu −His −Arg −Ura + 50µg/ml canavanine + 200µg/ml G418) (Pan et al., 2007) and incubated at 30°C. To confirm that the generated essential yeast haploid knockout is dependent on the expression vector, cells were then replica plated on MM+5-FOA (0.1%) (−Leu −His −Arg + 50µg/ml canavanine + 200µg/ml G418 + 5-FOA) and incubated at 30°C.

2.2.2 Pool-to-pool complementation screen of essential yeast genes

Expression vectors: The same experimental outline was followed as the one-to-one screen with the following modifications and additional steps. Human cDNAs were randomly grouped into 13 pools with each pool comprising up to 96 unique entry clones. Each of the 13 pools of entry clones were shuttled en masse into a yeast destination vector to generate 13 pools of expression vectors (Arnoldo et al., 2014). The destination vector used was pAG416GPD-ccdB (*URA3*, CEN, constitutive GPD promoter) with a stop codon contributed by the vector backbone resulting in a 50-amino-acid C-terminal extension. To ensure sufficient coverage of each expression vector within a pool, the bulk LR reaction was repeated three times to obtain a minimum of 10,000 transformants for 100-fold coverage (∼96 entry clones × 100).

Complementation assays: The same experimental outline was followed as the one-to-one screen except with the following modifications. Heterozygous yeast strains were pinned in a 96-well array format on YPD + G418 (200µg/ml) agar plates and incubated at 30°C. Colonies were then scraped and pooled (by suspension in 1ml YPD) and inoculated in 250ml YPD and allowed to grow for only two generations to prevent competitive outgrowth before proceeding with LiAc/SS-DNA/PEG transformation (see (Pan et al., 2007) for protocol on high-efficiency transformation). The 250ml yeast culture was then divided into 13 equal aliquots into which 13 pools of expression vector DNAs were transformed. Creating pools of transforming DNA and cells to be transformed was done to ensure equal representation of yeast strains across all pools. To ensure sufficient coverage of each yeast strain/vector combination in sufficient numbers, the transformation was repeated a second time for each pool to obtain a minimum of 6 million transformants for 100-fold coverage (621 yeast strains × ~96 expression vectors × 100). Transformed diploid colonies were then scraped, pooled, and inoculated in 13 separate 50ml sporulation cultures as previously described in methods. Sporulated cultures were then pelleted, resuspended in water, and plated on MM−Ura for haploid selection, after which the haploid-converted cells were scraped, pooled, and re-plated again on MM−Ura to obtain single colonies, which were confirmed by replica-plating to MM+5-FOA. For each pool, ~20–50 5-FOA-sensitive colonies were isolated. To determine the identity of the yeast strain, genomic DNA was prepped from phenol/chloroform extractions and the yeast barcode was amplified using the U1/D1 primers to allow sequencing of the UPTAG/DNTAG using the kanB or kanC primers (Giaever et al., 2002). To determine the identity of the rescuing human cDNA, expression vectors were isolated and sequenced using a common primer that hybridizes to the vector backbone

(CAGGAAACAGCTATGAC). Each potential hit (a rescued yeast colony) was reconfirmed by retransformation of the extracted plasmid into the corresponding heterozygous diploid as described for the one-to-one screen. To confirm the nonorthologous hit, both extracted pAG416GPD-h*SEC61A1* and newly generated pAG416GPD-h*SEC61A1*-HA expression vectors along with pAG416GPD-h*RFT1*-HA and GAL-inducible y*SEC61* from the FLEX array (Hu et al., 2007) were separately transformed into the *RFT1*/*rft1*Δ heterozygous diploid yeast strain and the experiment was carried out as described for the one-to-one screen.

2.2.3 Complementation screen of nonessential yeast CIN genes

Expression vectors and yeast strains: Human cDNAs in Gateway-compatible entry clones (Yang et al., 2011) were shuttled into the yeast destination vector pAG416GPD-ccdB+6Stop (*URA3*, CEN, constitutive GPD promoter, 6-amino-acid C-terminal extension) (Alberti et al., 2007; Kachroo et al., 2015) using LR Clonase II (Invitrogen) to generate expression clones. Expression vectors and the vector control pRS416 (*URA3*) (Sikorski and Hieter, 1989) were transformed into the corresponding *MAT*α yeast haploid knockout strain (Giaever et al., 2002) and wild-type strain BY4742 (*MAT*α *his3*Δ*1 leu2*Δ*0 lys2*Δ*0 ura3*Δ*0*) (Brachmann et al., 1998) and transformants were selected on SC−Ura media.

Growth assays to assess rescue of chemical sensitivities: Chemical sensitivity complementation assays for yeast strains with *URA3*-marked vectors were carried out in SC−Ura media (+/- chemical) at 30°C. For spot assays, wild-type and mutant strains from saturated cultures were serially diluted in 10-fold increments and plated onto media with or without chemicals at the following concentrations: 0.01% MMS, 200mM HU, 15µg/ml benomyl, 8% ethanol, 100ng/ml cycloheximide, 5µg/ml CPT, 10µg/ml bleomycin. For growth curve validations, cultures were grown to mid-log phase then diluted to OD_{600}=0.1 in

200µl media +/- chemical at the indicated concentrations. OD_{600} readings were measured every 30 minutes over a period of 24h in a TECAN M200 plate reader and plates were shaken for 10 minutes before each reading. Strains were tested in 3 replicates per plate per condition and area under the curve (AUC) was calculated for each replicate. Strain fitness was defined as the AUC of each yeast strain relative to the AUC of the control strain (BY4742 + pRS416) grown on the same plate in the same media condition.

A-like faker assays (Yuen et al., 2007): On each plate, isolates of wild-type *MAT*α BY4742 and *MAT*α deletion strains containing *URA3*-marked vectors were patched in 1-cm^2 squares on SC−Ura and incubated at 30°C for 2 days. Patches were mated to a *MAT*α *his1* tester lawn by replica plating on YPD followed by incubation at 30°C for 24h. The mated lawn was replica-plated to SC-6 (−Ura −Lys −Ade −His −Trp −Leu) media and incubated for 2 days at 30°C to select for His^+ products. Complementation of the ALF phenotype was assessed by comparing the number of colonies per patch to the wild-type control patch on the same plate.

2.2.4 Generating lists and analysis for the complementation screens

A comprehensive list of essential yeast CIN genes was obtained from (Stirling et al., 2011), while a list of essential yeast genes was obtained from the Yeast Deletion Project (Giaever et al., 2002). A list of human genes was generated from two sources: Yeastmine (Balakrishnan et al., 2012) and Ensembl BioMart (Kinsella et al., 2011) databases. For the nonessential yeast CIN genes (Stirling et al., 2011; Yuen et al., 2007), a list of human homologs was generated from Yeastmine (Balakrishnan et al., 2012). Gene Ontology (GO) processes and other features used to analyze the complementation sets were obtained from Yeastmine and each feature was represented as a proportion of the total number of genes input for each gene set. Significance for each feature was calculated using the hypergeometric distribution and

subjected to the Bonferroni correction to obtain the adjusted P-value (critical value: 0.05). Sequence identity (%) in relation to the yeast gene was determined for all possible human–yeast pairs using the Ensembl BioMart database or NWalign (Y. Zhang, *http://zhanglab.ccmb.med.umich.edu/NW-align*). Significance between the % sequence identity of complementation pairs and % sequence identity of all human–yeast pairs included in this study was calculated using a Mann–Whitney test.

2.3 Results

2.3.1 Systematic identification of human-yeast complementation pairs for the essential yeast genes

A comprehensive list of yeast CIN genes revealed that many essential genes are mutable to a CIN phenotype (323 CIN genes/∼1100 essential genes, or ∼29%) (Stirling et al., 2011). We tested all possible essential yeast CIN gene null mutants for complementation by all potential human homologs in a series of one-to-one screens. While one-to-one screening reduces the number of false negatives that can arise as an artifact of the skewed representation associated with pooled screening, it does not allow identification of unexpected or nonorthologous complementation pairs. Therefore, we set up a pool-to-pool screen to test all possible essential (CIN and non-CIN) yeast genes for complementation by all sequence-related human homologs that are available as full-length cDNA clones.

To set up both screens (Figure 2.1 and Figure 2.2), we used Gateway cloning to enable the systematic shuttling of DNA fragments between cloning vectors (Hartley et al., 2000). Briefly, a human cDNA of interest flanked by recombination sites on an entry clone can be transferred to Gateway-compatible destination vectors in a single-step reaction to

create yeast expression vectors. We used the human ORFeome V8.1, which is a Gateway-compatible clone library of sequence-confirmed human cDNAs (Yang et al., 2011) as the source of human ORFs. We also used the Gateway-compatible library of yeast expression vectors, which offers a selection of promoters (constitutive GPD vs. inducible GAL), plasmid copy number (2µ vs. CEN backbone), N- or C-terminal tags, and auxotrophic markers (Alberti et al., 2007). To express human cDNAs in yeast, we selected a centromere-based backbone and a constitutive promoter to reduce plasmid copy-number variation and minimize potential toxicity that can arise from overexpression of human cDNAs in yeast (Sekigawa et al., 2010; Tugendreich et al., 2001). To test for complementation of essential gene null mutations, we assayed for rescue of lethality of the haploid yeast gene deletion following sporulation of the "haploid-convertible" heterozygous diploids (Pan et al., 2004).

To design and execute the complementation assays, we compiled all sequence homologs of essential yeast genes generated from multiple sources using the Yeastmine database (Balakrishnan et al., 2012), Ensembl BioMart database (Kinsella et al., 2011) and to a lesser extent through manual curation. Each candidate complementation pair (human cDNA and cognate yeast gene mutation) was included in our screens based on the availability and quality control of both the human cDNA in the hORFeome collection and the corresponding yeast strain in the heterozygous collection. In an effort to be as comprehensive as possible, our screens tested all possible complementation pairs even when the least diverged candidate ortholog was not available in the hORFeome collection. For instance, y*CDC42* is a rho-like GTPase required for the establishment of cell polarity (Johnson, 1999). The list of homologs for y*CDC42* included genes such as h*CDC42*, h*RHOJ*, h*RHOV*, h*RHOU*, and other related members of the RHO family of small GTPases. Of these homologs, the least diverged

ortholog, h*CDC42* (80% sequence identity, previously shown to complement the yeast deletion mutant (Kachroo et al., 2015), was not available in the human ORFeome V8.1 collection and therefore not tested in this study. We did test h*RHOJ* (60% sequence identity) and determined that it does not complement the null allele of y*CDC42*. In total, we tested 199 essential CIN deletion mutants for rescue of lethality by 320 human cDNAs one-by-one (322 candidate complementation pairs) (Figure 2.1A and Table A.1) and 621 essential gene deletion mutants for rescue of lethality by 1010 human cDNAs pool-to-pool (1076 candidate complementation pairs) (Figure 2.2A and Table A.2). Our screens identified 65 human cDNAs that complement the null allele of 58 essential yeast genes, including a complementation pair of nonorthologous proteins (yeast Rft1 and human Sec61A1) (Table 2.1). When compared to a curated list of complementation pairs available from the Yeastmine database and other published reports, our work identified 20 novel complementation pairs in which the human cDNA rescues lethality of the yeast null allele (Table A.3).

2.3.2 Systematic identification of human-yeast complementation pairs for the nonessential yeast CIN genes

A comprehensive list of yeast CIN genes revealed that of the ~4700 nonessential yeast genes, 369 are mutable to a CIN phenotype as deletion alleles (Stirling et al., 2011; Yuen et al., 2007). In contrast to essential genes, most haploid deletion strains for nonessential genes display no growth defects when grown under standard laboratory conditions (Giaever et al., 2002). To establish our complementation assays, we tested the ability of human gene expression to rescue the chemical sensitivity and/or CIN defects of the nonessential yeast deletion mutant. The chemicals utilized to induce growth defects included

methyl methane sulfonate (MMS) [alkylating agent] (Beranek, 1990), benomyl [destabilizes microtubules] (Gupta et al., 2004), hydroxyurea (HU) [impedes DNA replication] (Koc et al., 2004), camptothecin (CPT) [topoisomerase inhibitor] (Hsiang et al., 1989), bleomycin [induces DNA strand breaks] (Chen et al., 2008), cycloheximide [protein synthesis inhibitor] (Schneider-Poetsch et al., 2010) and ethanol [impacts many cellular pathways including cell cycle and morphogenesis] (Stanley et al., 2010). To test rescue of CIN defects, we used the a-like faker (ALF) assay, which measures loss of the *MAT*α locus leading to de-differentiation to an a-mating phenotype and subsequent mating to a *MAT*α tester strain (Stirling et al., 2011; Yuen et al., 2007). In this assay, the ability of haploid cells to mate with a tester strain of the same mating type and form diploids reflects loss, deletion or inactivation of the *MAT*α locus.

To set up the complementation assays, we generated a list of human sequence homologs of nonessential yeast CIN genes using the Yeastmine database (Balakrishnan et al., 2012) (Figure 2.3A). Each human open reading frame (ORF) was shuttled via Gateway cloning into a yeast expression vector (single copy centromeric plasmid, constitutive GPD promoter) (Alberti et al., 2007; Kachroo et al., 2015) (Figure 2.3B). For each yeast strain, we queried the Saccharomyces Genome Database (SGD) to determine if the yeast deletion mutant has fitness defects in the presence of at least one of the indicated chemicals. We also searched previously published reports (Stirling et al., 2011; Yuen et al., 2007) to identify mutants that display increased diploid mating products in ALF assays compared to the wild-type strain. Overall, this established assayable phenotypes to test 112 nonessential yeast CIN deletion mutants for complementation by 117 human cDNAs (121 candidate complementation pairs tested across 317 complementation assays) (Figure 2.3C and Table

A.4). Our screens identified 20 human cDNAs that rescue the chemical sensitivity and/or CIN defects of 20 nonessential yeast mutants (Table 2.2 and Figure A.1). Successful complementation pairs were validated by growth curves and encompassed 44 assays that ranged from 1 to 4 assays per pair. For instance, we demonstrate that h*TBCC* expression rescues *cin2*Δ sensitivity to benomyl (Figure 2.3D), while h*FEN1* expression rescues *rad27*Δ sensitivity to MMS, ethanol and cycloheximide, as well as rescuing CIN defects of *rad27*Δ strains in the ALF assay (Figure A.1). Based on a curated list of complementation pairs available from the Yeastmine database, our work identified 13 novel complementation pairs (Table A.3).

2.3.3 Assessing features of yeast genes that predict replaceability

We used Yeastmine to assess GO terms and looked for features that predict replaceability of yeast genes. The yeast complementation set (n=78) is composed predominantly of metabolic genes (Figure 2.4). In general, the complemented yeast genes encode proteins that localize to the cytoplasm rather than the nucleus or other nuclear-associated regions (Figure 2.5A). When grouped by molecular function, the complementation set is more likely to include proteins that display catalytic activity (Figure 2.5B). Even though the complemented yeast genes display no difference in the number of genetic interactions (Figure 2.5C), there is a marked difference in the number of physical interactions in this set: replaceable yeast proteins tend to have fewer physical interactions (Figure 2.5D) and are less likely to be part of macromolecular complexes (Figure 2.5E). However, it was more likely for a yeast gene to be replaceable if other subunits of the same complex were also replaceable. For example, the complementation set included heterodimers (ex. y*RPB4*/y*RPB7* and y*RAD1*/y*RAD10*), subunits of the prefoldin complex (y*GIM4*, y*GIM5*,

y*PAC10*) and proteasome complex (y*RPN5*, y*SEM1*, y*PUP3*, y*RPT6*, y*RPT1*, y*PRE5*). Yeast genes in the same pathway also tended to be similarly replaceable as the complementation set included members of the sterol biosynthesis pathway (y*ERG1*, y*ERG12*, y*ERG26*, y*IDI1*) and heme biosynthesis pathway (y*HEM15*, y*HEM3*). We further show that replaceable yeast genes are more likely to be shorter in length (Figure 2.5F).

Complementation pairs tend to have higher than average sequence identity, but sequence identity alone is a poor predictor of replaceability as evidenced by the observations that high sequence identity does not guarantee replaceability and complementation pairs can have low sequence identity (Figure 2.5G). We assessed whether replaceability by one human homolog predicts the same outcome for additional human homologs. In one case, we found that the glycolytic enzyme y*PGK1* can be replaced by either h*PGK1* (66% sequence identity) or h*PGK2* (63% sequence identity), human proteins that share 87% sequence identity and catalyze the same reaction but are differentially expressed (McCarrey and Thomas, 1987). In another example, the phosphatase y*GLC7* can be replaced by the isozymes h*PPP1CA* (84% sequence identity) and h*PPP1CC* (84% sequence identity), human proteins that are 91% identical and part of the highly conserved PP1 subfamily of protein phosphatases (Ceulemans and Bollen, 2004). In contrast, some yeast genes such as y*DIB1*, y*IDI1*, and y*SMT3* are only replaceable by one of multiple human homologs, whereas others like y*CMD1*, y*MSS4*, and y*CDC28* are replaceable by several (but not all) human homologs. For these cases and the previously mentioned y*CDC42*, we observed that replaceable human proteins share higher sequence identity with the yeast protein than the nonreplaceable ones (Table A.5), suggesting that the least diverged homologs were the most likely to complement. The only contradiction of this observation is h*SEC61A1*, which can replace the nonorthologous y*RFT1* and rescue

lethality of *rft1*Δ (Figure 2.6). Sec61 forms an ER membrane channel and is required for co-translational and post-translational translocation of proteins into the ER (Osborne et al., 2005), while Rft1 also functions at the ER membrane and is implicated in the translocation of lipid-linked oligosaccharides into the ER (Helenius et al., 2002). We further demonstrated that h*RFT1* cannot complement y*RFT1* (also shown by (Kachroo et al., 2015)), and that overexpression of the yeast ortholog of h*SEC61A1*, y*SEC61*, also fails to rescue lethality of *rft1*Δ. The fact that h*SEC61A1* also fails to complement y*SEC61* (Table A.1) highlights the unexpected and complex manner in which the human protein acts to functionally substitute for the nonorthologous yeast protein. Overall, our observations and other complementation studies (Kachroo et al., 2015; Sun et al., 2016; Yang et al., 2017) suggest that human/yeast protein sequence identity is a poor predictor of replaceability.

To assess whether the same features observed for the complementation set (n=78) apply to different subsets, the same analysis was repeated on 4 different groups: essential genes (n=58) (Figure A.2), essential/nonessential CIN genes (n=48), essential CIN genes (n=28), and nonessential CIN genes (n=20) (Figure A.3). The most striking differences were features that separated essential from nonessential genes. Overall, replaceable essential genes were more likely to show cytoplasmic localization, have fewer physical interactions, and were less likely to be part of macromolecular complexes than replaceable nonessential genes. These differences can be attributed to two major reasons: (i) the set of replaceable essential genes had a higher proportion of metabolic enzymes compared to the set of nonessential genes (Figure 2.4), and (ii) the experimental design of the complementation assays since the essential set was screened with yeast expression vectors that add C-terminal tags to the human ORFs (which may impact complementation of subunits of a protein complex),

whereas the nonessential set was screened with a yeast expression vector that only adds 6-amino-acids to the C-terminus. In contrast, the most prominent features common between replaceable essential and nonessential yeast genes are yeast gene size and human/yeast protein sequence identity.

2.4 Discussion

The work presented in this study extends the growing list of human-yeast complementation pairs that will serve as an important resource for model organism and human biology. Many factors impact replaceability of yeast genes by human genes. Different types of yeast strains permit different complementation readouts; therefore, choosing the appropriate yeast strain depends on what is required for downstream applications. We restricted our complementation assays to testing rescue of lethality of the haploid yeast gene knockout because rescue of a yeast conditional allele or downregulated yeast gene can represent partial or indirect complementation. This is evident in the results of (Kachroo et al., 2015), which indicate that <60% (32/56) of the 69 human orthologs identified by rescue of temperature-sensitive alleles are able to rescue the null allele. Similarly, ~60% (24/39) of the 44 human orthologs identified by rescue of downregulated yeast genes are able to rescue the null allele. If the main objective is to use yeast as a platform to characterize the functional consequence of human gene variants, then complementation of the null allele may be more desirable for mainly two reasons. First, expressing human cDNAs in a yeast deletion mutant diminishes the possibility of misleading phenotypic readouts by eliminating unwanted side effects of the residual yeast protein that is present in partial loss-of-function alleles. Second, the use of null alleles distinguishes those human proteins that are truly substituting for the

essential function of the yeast protein from those human proteins that are suppressing a growth phenotype by a secondary mechanism that may or may not relate to the conserved function.

Other factors that impact replaceability include the conditions used to express the human cDNA in yeast to account for dosage, toxicity, or timing of expression. Examples of what can be manipulated include picking a suitable promoter (endogenous yeast promoter vs. constitutive vs. inducible), integration of human cDNA vs. episomal vector-based expression, and inclusion of epitope tags. For instance, one study found that complementation of y*HEM4* by h*UROS* required expression of the human protein using the endogenous yeast promoter of the corresponding ortholog as the use of a constitutive promoter induced toxicity (Kachroo et al., 2017). Our study also used yeast expression vectors that introduce C-terminal extensions, which can interfere with replaceability by some human proteins (Kachroo et al., 2015). In general, there are no sets of conditions that satisfy the replaceability requirements of all candidate complementation pairs, as each human-yeast gene pair is unique. Even when no complementation is observed, partial fusions to create chimeric human-yeast proteins may allow complementation and provide a useful resource for specific applications (Zhou and Reed, 1998).

The experimental design of systematic complementation assays impacts the scope of the results that are obtained. Testing complementation pairs one-by-one reduces the number of false negatives inherent in pooled screening. This was observed in our study: our one-to-one screen identified 34 complementation pairs corresponding to 28 yeast strains, while our pool-to-pool screen identified 12 of these complementation pairs corresponding to 12 yeast strains, resulting in a 35% recovery rate from the pooled screen. This modest recovery rate

may be due to several factors: (i) even with 100-fold coverage, shorter cDNAs are shuttled more efficiently from entry clones to destination vectors in Gateway's LR reaction, resulting in a potentially skewed representation of some expression vectors within a pool; (ii) competitive outgrowth can result in a skewed representation of yeast strains pre- and post-transformation; (iii) even with 100-fold coverage, pool-to-pool transformation reduces the chances of a particular human cDNA complementing the matched yeast strain, especially given the possibility of skewed representation of expression vectors and yeast strains; (iv) toxicity from some human cDNAs can skew representation of yeast strains within a pool; (v) sporulation efficiencies of different yeast strains skew haploid selection; and (vi) sequence coverage of rescued haploids will impact the scope of the results. Nevertheless, the advantage of pooled screening is the potential for identification of nonorthologous complementation pairs, as demonstrated in this study. With the development of better screening methods and updated collections, the potential for discovery of additional nonorthologous complementation pairs will aid in deciphering biological mechanisms that would otherwise be overlooked.

Interestingly, and by an-as-yet-unknown mechanism, y*RFT1* (Requires Fifty-Three) was first isolated as a partial loss-of-function mutation suppressed by expressing human p53 in yeast; however, p53 does not complement *rft1*Δ (Koerte et al., 1995). It was later demonstrated that yRft1 is required for efficient N-linked glycosylation of glycoproteins (Ng et al., 2000), a process that involves assembly of a lipid-linked oligosaccharide at the ER membrane followed by transfer of the oligosaccharide from the lipid anchor to selected asparagine residues of nascent polypeptides in the lumen of the ER. The lipid-linked oligosaccharide is assembled in a multi-step process and is composed of the lipid anchor

dolichol pyrophosphate (Dol-P-P) and the completely assembled 14-residue oligosaccharide $Glc_3Man_9GlcNAc_2$ (reviewed in (Burda and Aebi, 1999)). Briefly, this process involves adding the first seven saccharide moieties to the lipid anchor on the cytoplasmic side of the ER to form the intermediate $Man_5GlcNAc_2$-P-P-Dol. This intermediate is then translocated across the ER membrane to face the lumenal side before addition of the last seven saccharide moieties to form the fully assembled $Glc_3Man_9GlcNAc_2$-P-P-Dol. Translocation of the lipid-linked intermediate is proposed to be facilitated by membrane proteins termed flippases, which have yet to be identified. Initially, yeast genetic experiments determined that yRft1's role in N-linked protein glycosylation is due to a defect in this translocation process and was thus proposed to be the flippase (Helenius et al., 2002). However, biochemical *in vitro* assays utilizing reconstituted proteoliposomal systems (Frank et al., 2008; Sanyal et al., 2008) and sealed microsomal vesicles (Rush et al., 2009) demonstrated that yRft1 was not required for the flipping process. As such, the current model is that yRft1 is not the flippase as indicated by *in vitro* assays, but is required for the translocation process *in vivo*, potentially by acting as a link or chaperone between $Man_5GlcNAc_2$-P-P-Dol and the still elusive flippase.

Human Sec61A1/ySec61 is the largest subunit of the conserved heterotrimeric Sec61 complex which is also composed of hSec61B/ySbh1 and hSec61G/ySss1. This complex spans the ER membrane forming a channel with a hydrophobic interior that allows co-translational and post-translational translocation of proteins into the ER (reviewed in (Osborne et al., 2005)). Although both Sec61 and Rft1 proteins function at the ER membrane and are implicated in a translocation process, albeit of different cargo, they have not been reported to physically or genetically interact. Therefore, the mechanism by which human Sec61 protein replaces the essential yet still unknown function of the yeast Rft1 protein is at

best a speculation without further experimentation. Given that hSec61 complements *rft1*Δ, it is possible that the human protein has compensated for the translocation of the intermediate $Man_5GlcNAc_2$-P-P-Dol into the ER. One scenario is that hSec61 functions as the chaperone between the intermediate and the unknown flippase in the same presumed role as yRft1. However, this raises the question of why hRft1 which shares more homology with its yeast ortholog (26% sequence identity) than hSec61 (18% sequence identity) is not able to carry out that function. Another possibility is that hSec61 is entirely bypassing the flippase and providing an alternative route for the lipid-linked intermediate into the ER lumen. The implication of this hypothesis is that Sec61 as a membrane channel is not specific to nascent polypeptides but can translocate other substrates. However, the fact that y*RFT1* is an essential gene indicates that ySec61 protein cannot compensate for the translocation process and bypass the flippase even when overexpressed. This would suggest that if hSec61 is providing an alternative route, then this function is specific or carried out more efficiently by the human protein. Additional and more direct experiments to answer these questions will yield more insight into the biological mechanism of both proteins.

Systematic human-yeast complementation screens (our study and other recent large-scale screens) have mainly focused on scoring rescue-of-lethality of essential yeast genes (Hamza et al., 2015; Kachroo et al., 2015; Sun et al., 2016; Yang et al., 2017; Zhang et al., 2003). Here, we expanded these screens beyond essentiality and tested a subset of nonessential yeast genes to identify 20 complementation pairs that are replaceable in 44 assays that test rescue of chemical sensitivity and/or CIN defects. For some human-yeast pairs, we demonstrated that the human gene can complement the yeast gene in multiple complementation assays. Although we did not identify any in this study, there are reported

cases of complementation pairs that complement some but not all mutant phenotypes (Davey et al., 2011; Tamburini et al., 2005; Yamagata et al., 1998). For instance, h*WRN* (homolog of y*SGS1*) suppressed the increased rate of illegitimate recombination (CIN assay) of *sgs1*Δ but could not rescue *sgs1*Δ sensitivity to hydroxyurea (Yamagata et al., 1998). Overall, in addition to the 65 complementation assays we identified for the essential yeast genes, our study also defines 44 complementation assays for the nonessential yeast genes. In total, this translates to 109 yeast cell-based platforms to elucidate human protein function, characterize human gene variants and study conserved protein domains based on human-yeast complementation relationships.

Table 2.1. Human genes that complement essential yeast deletion mutants

Yeast Systematic Name	Yeast Standard Name	Human Entrez Gene ID	Human Standard Name	Yeast Gene Brief Description[d]
YBL020W	*RFT1* [a]	29927	*SEC61A1*	Membrane protein required for translocation of Man5GlcNac2-PP-Dol
YBR002C	*RER2*	79947	*DHDDS*	Cis-prenyltransferase involved in dolichol synthesis
YBR029C	*CDS1*	8760	*CDS2*	Phosphatidate cytidylyltransferase (CDP-diglyceride synthetase)
YBR109C	*CMD1* [b]	801; 805; 808	*CALM1; CALM2; CALM3*	Calmodulin
YBR160W	*CDC28* [b]	983; 1017	*CDK1; CDK2*	Cyclin-dependent kinase (CDK) catalytic subunit
YBR252W	*DUT1*	1854	*DUT*	deoxyuridine triphosphate diphosphatase (dUTPase)
YCR012W	*PGK1* [b]	5230; 5232	*PGK1* [c]*; PGK2*	3-phosphoglycerate kinase
YDL045C	*FAD1* [b]	80308	*FLAD1* [c]	Flavin adenine dinucleotide (FAD) synthetase
YDL064W	*UBC9* [b]	7329	*UBE2I*	SUMO-conjugating enzyme involved in the Smt3p conjugation pathway
YDL120W	*YFH1*	2395	*FXN*	Mitochondrial matrix iron chaperone
YDL147W	*RPN5* [b]	5718	*PSMD12* [c]	Subunit of the CSN and 26S proteasome lid complexes
YDL164C	*CDC9* [b]	3978	*LIG1* [c]	DNA ligase found in the nucleus and mitochondria
YDL205C	*HEM3*	3145	*HMBS*	Porphobilinogen deaminase
YDR050C	*TPI1* [b]	7167	*TPI1*	Triose phosphate isomerase, abundant glycolytic enzyme
YDR086C	*SSS1*	23480	*SEC61G*	Subunit of the Sec61p translocation complex (Sec61p-Sss1p-Sbh1p)
YDR208W	*MSS4* [b]	8394; 8395	*PIP5K1A; PIP5K1B* [c]	Phosphatidylinositol-4-phosphate 5-kinase
YDR236C	*FMN1*	55312	*RFK*	Riboflavin kinase, produces riboflavin monophosphate (FMN)
YDR404C	*RPB7* [b]	5436	*POLR2G*	RNA polymerase II subunit B16
YDR454C	*GUK1*	2987	*GUK1*	Guanylate kinase
YDR510W	*SMT3* [b]	7341	*SUMO1* [c]	Ubiquitin-like protein of the SUMO family
YEL026W	*SNU13* [b]	4809	*NHP2L1*	RNA binding protein
YEL058W	*PCM1*	5238	*PGM3*	Essential N-acetylglucosamine-phosphate mutase
YER094C	*PUP3* [b]	5691	*PSMB3*	Beta 3 subunit of the 20S proteasome
YER112W	*LSM4*	25804	*LSM4*	Lsm (Like Sm) protein
YER133W	*GLC7* [b]	5499; 5501	*PPP1CA; PPP1CC*	Type 1 serine/threonine protein phosphatase catalytic subunit
YER136W	*GDI1*	2665	*GDI2*	GDP dissociation inhibitor
YFL017C	*GNA1* [b]	64841	*GNPNAT1* [c]	Glucosamine-6-phosphate acetyltransferase
YGL001C	*ERG26*	50814	*NSDHL*	C-3 sterol dehydrogenase
YGL030W	*RPL30* [b]	6156	*RPL30*	Ribosomal 60S subunit protein L30
YGL048C	*RPT6*	5705	*PSMC5*	ATPase of the 19S regulatory particle of the 26S proteasome
YGR024C	*THG1*	54974	*THG1L*	tRNAHis guanylyltransferase
YGR075C	*PRP38*	55119	*PRPF38B*	Unique component of the U4/U6.U5 tri-snRNP particle

Yeast Systematic Name	Yeast Standard Name	Human Entrez Gene ID	Human Standard Name	Yeast Gene Brief Description[d]
YGR175C	*ERG1*	6713	*SQLE*	Squalene epoxidase
YGR185C	*TYS1*	8565	*YARS*	Cytoplasmic tyrosyl-tRNA synthetase
YGR277C	*CAB4*	80347	*COASY*	Subunit of the CoA-Synthesizing Protein Complex (CoA-SPC)
YGR280C	*PXR1*	54984	*PINX1*	Essential protein involved in rRNA and snoRNA maturation
YIL083C	*CAB2*	79717	*PPCS*	Subunit of the CoA-Synthesizing Protein Complex (CoA-SPC)
YJL097W	*PHS1*	201562	*PTPLB*	Essential 3-hydroxyacyl-CoA dehydratase of the ER membrane
YJR006W	*POL31*[b]	5425	*POLD2*	Subunit of DNA polymerase delta (polymerase III)
YKL013C	*ARC19*[b]	10093	*ARPC4*[c]	Subunit of the ARP2/3 complex
YKL024C	*URA6*[b]	51727	*CMPK1*[c]	Uridylate kinase
YKL033W	*TTI1*[b]	9675	*TTI1*	Subunit of the ASTRA complex, involved in chromatin remodeling
YKL035W	*UGP1*[b]	7360	*UGP2*[c]	UDP-glucose pyrophosphorylase (UGPase)
YKL145W	*RPT1*	5701	*PSMC2*	ATPase of the 19S regulatory particle of the 26S proteasome
YKL189W	*HYM1*	51719; 81617	*CAB39; CAB39L*	Component of the RAM signaling network
YML069W	*POB3*[b]	6749	*SSRP1*	Subunit of the heterodimeric FACT complex (Spt16p-Pob3p)
YML077W	*BET5*[b]	58485	*TRAPPC1*	Core component of transport protein particle (TRAPP) complexes I-III
YMR208W	*ERG12*	4598	*MVK*	Mevalonate kinase
YMR308C	*PSE1*[b]	3843	*IPO5*	Karyopherin/importin that interacts with the nuclear pore complex
YMR314W	*PRE5*[b]	5682	*PSMA1*	Alpha 6 subunit of the 20S proteasome
YOL133W	*HRT1*	9978	*RBX1*	RING-H2 domain core subunit of multiple ubiquitin ligase complexes
YOR143C	*THI80*	27010	*TPK1*	Thiamine pyrophosphokinase
YOR149C	*SMP3*[b]	80235	*PIGZ*	Alpha 1,2-mannosyltransferase
YOR176W	*HEM15*	2235	*FECH*	Ferrochelatase
YOR236W	*DFR1*	1719	*DHFR*	Dihydrofolate reductase involved in tetrahydrofolate biosynthesis
YPL117C	*IDI1*[b]	3422	*IDI1*[c]	Isopentenyl diphosphate:dimethylallyl diphosphate isomerase
YPR082C	*DIB1*[b]	10907	*TXNL4A*[c]	17-kDa component of the U4/U6aU5 tri-snRNP
YPR113W	*PIS1*	10423	*CDIPT*	Phosphatidylinositol synthase

[a] Complementation by non-orthologous gene.

[b] Yeast CIN gene.

[c] Complementation identified by both screens.

[d] Brief description obtained from Yeastmine.

Table 2.2. Human genes that complement nonessential yeast deletion mutants

Yeast systematic name	Yeast standard name	Human Entrez Gene ID	Human standard name	Complementation Assay[a]	Yeast gene brief description[b]
YAL016W	*TPD3*	5518	*PPP2R1A*	MMS, HU, ALF	Regulatory subunit A of the heterotrimeric PP2A complex
YBR026C	*ETR1*	51102	*MECR*	Ethanol, Cycloheximide	2-enoyl thioester reductase
YDR226W	*ADK1*	204	*AK2*	Ethanol	Adenylate kinase, required for purine metabolism
YDR363W-A	*SEM1*	7979	*SHFM1*	HU, Ethanol, ALF	19S proteasome regulatory particle lid subcomplex component
YEL003W	*GIM4*	5202	*PFDN2*	Benomyl, Ethanol	Subunit of the heterohexameric cochaperone prefoldin complex
YEL029C	*BUD16*	8566	*PDXK*	Ethanol	Putative pyridoxal kinase
YGL058W	*RAD6*	7320	*UBE2B*	MMS, HU, Bleomycin, ALF	Ubiquitin-conjugating enzyme (E2)
YGR078C	*PAC10*	7411	*VBP1*	Ethanol, Cycloheximide, ALF	Part of the heteromeric co-chaperone GimC/prefoldin complex
YGR180C	*RNR4*	6241	*RRM2*	MMS, HU, Bleomycin	Ribonucleotide-diphosphate reductase (RNR) small subunit
YIL052C	*RPL34B*	6164	*RPL34*	Ethanol	Ribosomal 60S subunit protein L34B
YJL115W	*ASF1*	55723	*ASF1B*	MMS, CPT, ALF	Nucleosome assembly factor
YJL140W	*RPB4*	5433	*POLR2D*	HU, MMS	RNA polymerase II subunit B32
YKL113C	*RAD27*	2237	*FEN1*	MMS, Ethanol, Cycloheximide, ALF	5' to 3' exonuclease, 5' flap endonuclease
YLR418C	*CDC73*	79577	*CDC73*	HU	Component of the Paf1p complex
YML094W	*GIM5*	5204	*PFDN5*	Ethanol, Cycloheximide	Subunit of the heterohexameric cochaperone prefoldin complex
YML095C	*RAD10*	2067	*ERCC1*	MMS, HU	Single-stranded DNA endonuclease (with Rad1p)
YOL012C	*HTZ1*	3015	*H2AFZ*	MMS, HU, Ethanol	Histone variant H2AZ
YOR002W	*ALG6*	29929	*ALG6*	Ethanol	Alpha 1,3 glucosyltransferase
YPL022W	*RAD1*	2072	*ERCC4*	MMS, HU	Single-stranded DNA endonuclease (with Rad10p)
YPL241C	*CIN2*	6903	*TBCC*	Benomyl	GTPase-activating protein (GAP) for Cin4p

[a] Complementation assays are shown in Figure A.1.

[b] Brief description obtained from Yeastmine.

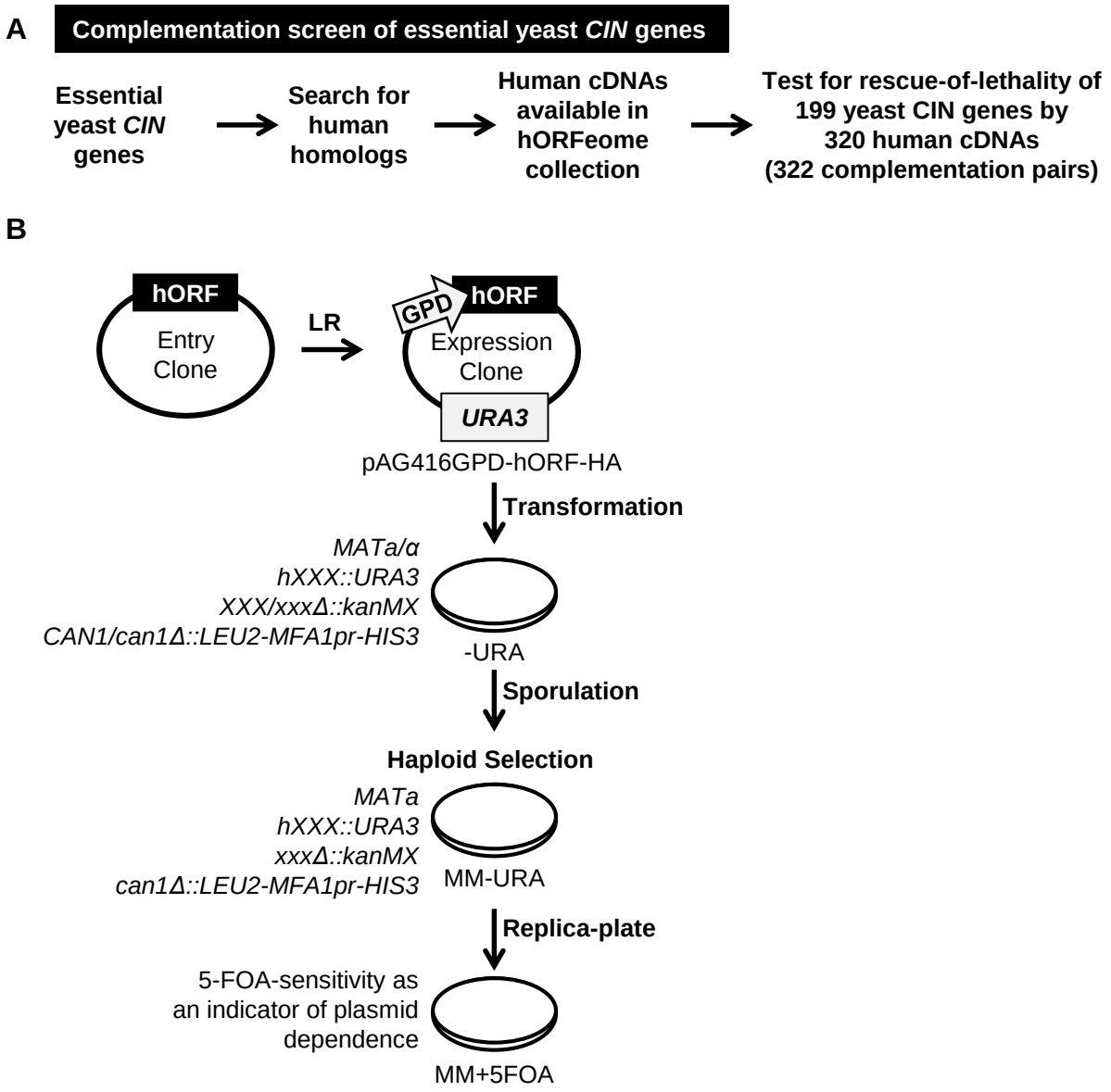

Figure 2.1. Overview of the complementation screen for the essential yeast CIN genes.
(A) Pipeline outlining which human-yeast pairs were included in the complementation screen. **(B)** Flowchart for the complementation screens. Human cDNAs were shuttled from entry clones to indicated yeast destination vector to generate yeast expression vectors. Single expression vectors were then transformed to matched haploid convertible heterozygous diploids and maintained on −Ura media. Following sporulation, heterozygous diploids were plated on haploid selection media (MM−Ura). "Rescued" haploids were tested for plasmid dependency by replica plating on MM+5-FOA.

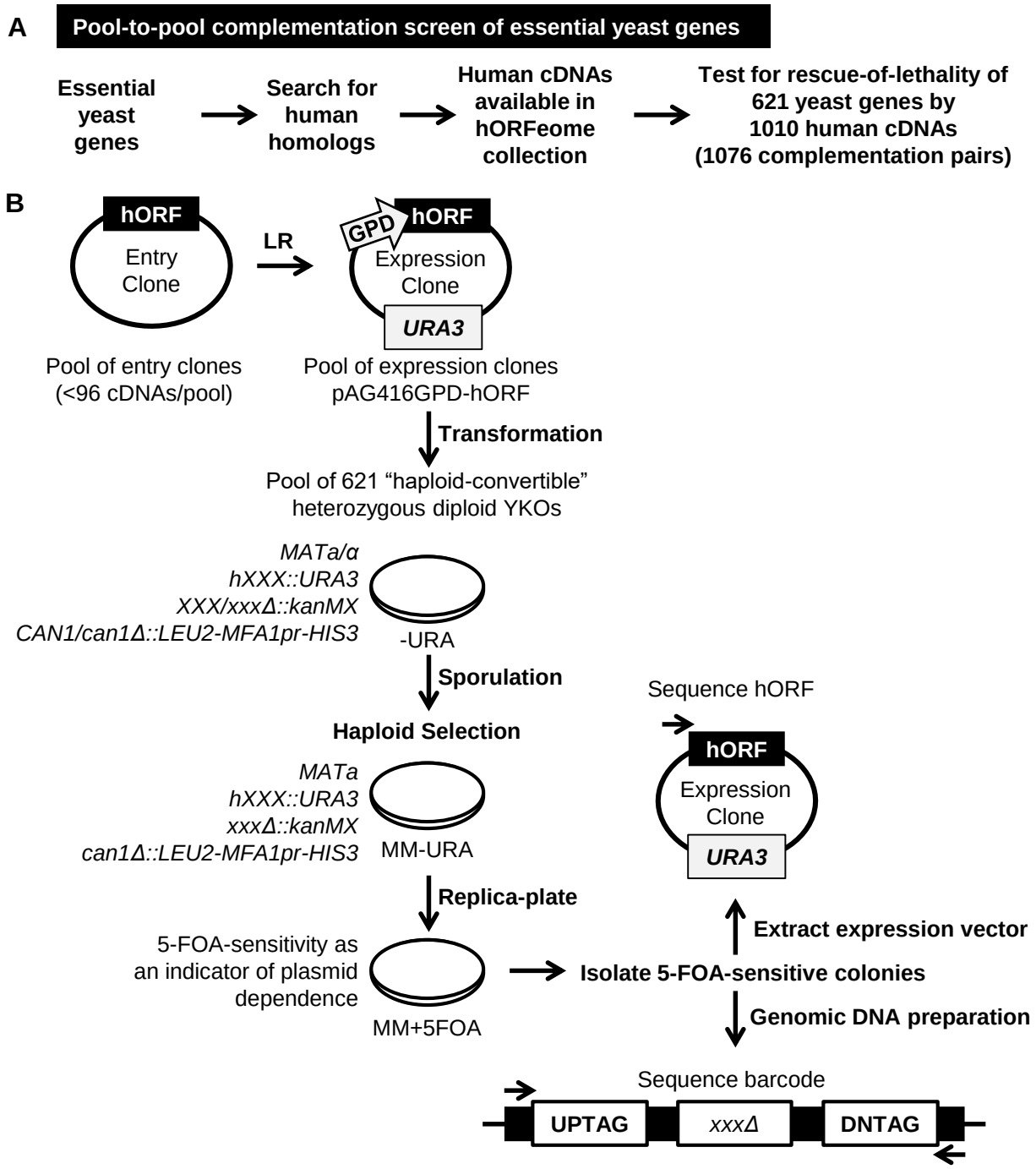

Figure 2.2. Overview of the complementation screen for the essential yeast genes.
(A) Pipeline outlining which human-yeast pairs were included in the complementation screen. **(B)** Flowchart for the complementation screens. Human cDNAs were shuttled from entry clones to indicated yeast destination vector to generate yeast expression vectors. Pooled expression vectors were then transformed to pooled haploid convertible heterozygous diploids and maintained on −Ura media. Following sporulation, heterozygous diploids were plated on haploid selection media (MM−Ura). "Rescued" haploids were tested for plasmid dependency by replica plating on MM+5-FOA. For the pooled screen, 5-FOA-sensitive colonies were isolated for sequencing of yeast barcode and expression vectors.

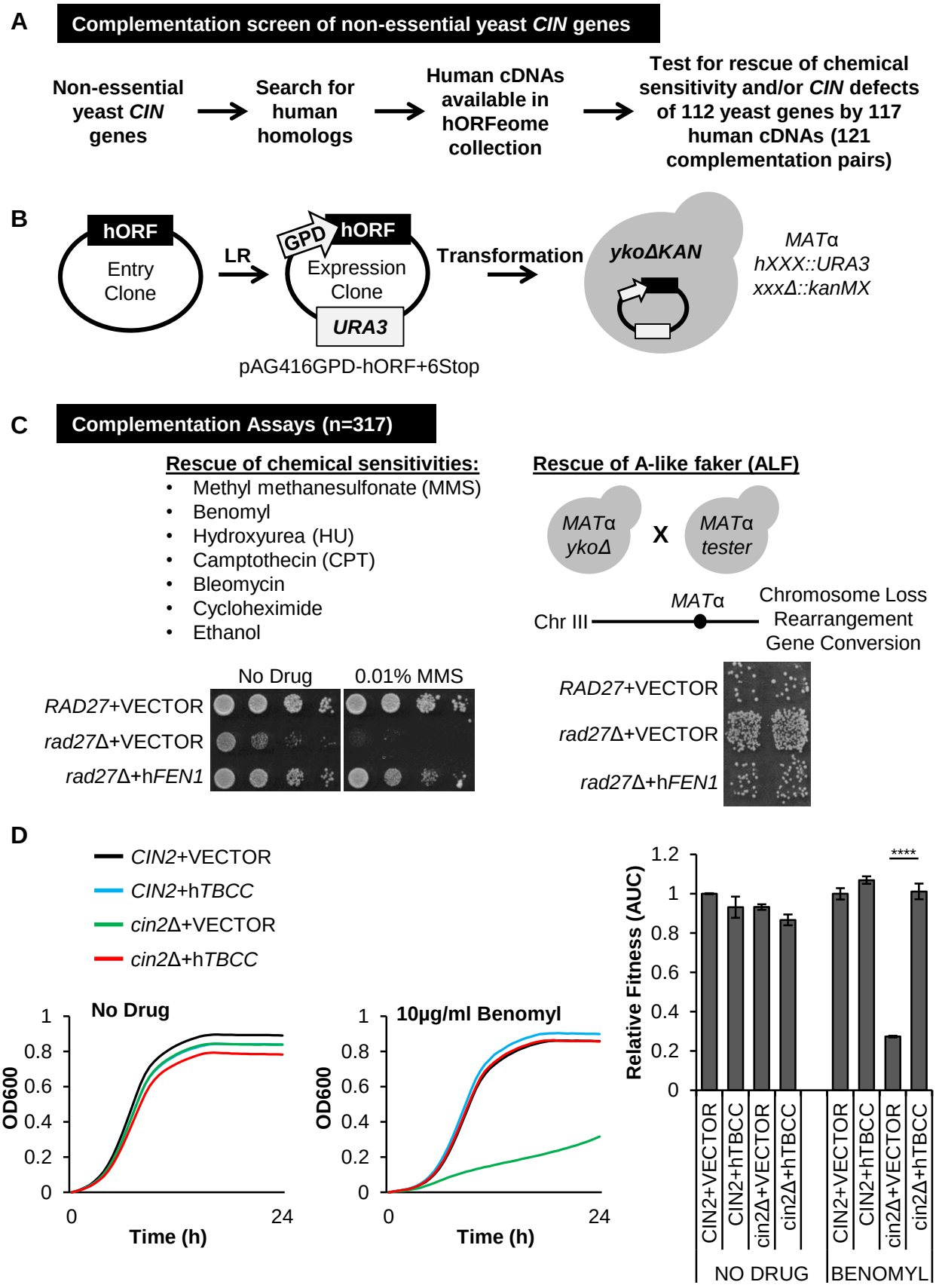
A
Complementation screen of non-essential yeast CIN genes
Non-essential yeast CIN genes
Search for human homologs
Human cDNAs available in hORFeome collection
Test for rescue of chemical sensitivity and/or CIN defects of 112 yeast genes by 117 human cDNAs (121 complementation pairs)
B
hORF
Entry Clone
LR
GPD
hORF
Expression Clone
URA3
pAG416GPD-hORF+6Stop
Transformation
ykoΔKAN
MATα
hXXX::URA3
xxxΔ::kanMX
C
Complementation Assays (n=317)
Rescue of chemical sensitivities:
Methyl methanesulfonate (MMS)
Benomyl
Hydroxyurea (HU)
Camptothecin (CPT)
Bleomycin
Cycloheximide
Ethanol
No Drug
0.01% MMS
RAD27+VECTOR
rad27Δ+VECTOR
rad27Δ+hFEN1
Rescue of A-like faker (ALF)
MATα yokoΔ
X
MATα tester
Chr III
MATα
Chromosome Loss
Rearrangement
Gene Conversion
RAD27+VECTOR
rad27Δ+VECTOR
rad27Δ+hFEN1
D
CIN2+VECTOR
CIN2+hTBCC
cin2Δ+VECTOR
cin2Δ+hTBCC
No Drug
10µg/ml Benomyl
OD600
Time (h)
Relative Fitness (AUC)
****
CIN2+VECTOR
CIN2+hTBCC
cin2Δ+VECTOR
cin2Δ+hTBCC
NO DRUG
BENOMYL

Figure 2.3. Overview of the complementation screen for the nonessential yeast genes.
(A) Pipeline outlining which human-yeast pairs were included in the complementation screen. **(B)** Human cDNAs cloned in the indicated yeast expression vector or a vector control were transformed into the corresponding haploid yeast knockout mutant (*yko*Δ) and maintained on −Ura media. **(C)** Yeast strains were spotted in 10-fold dilution on media +/- chemical based on the reported sensitivity of the yeast mutant to the 7 chemicals. Complementation was scored based on the ability of human cDNA expression to rescue fitness defects of the yeast knockout strain. In the presented example, h*FEN1* expression rescues *rad27*Δ sensitivity to MMS. Growth curve validations for identified hits are shown in Figure A.1. For ALF (a-like fakers), α-type mutant strains containing *URA3*-marked vectors were mated to a *MAT*α tester strain and growth of diploid progeny was assessed on selective media. Loss, deletion or inactivation of the *MAT*α locus allows *MAT*α cells to mate as a-type cells. Complementation was scored based on the ability of human cDNA expression to decrease ALF frequency of the yeast knockout strain. In the presented example (2 independent isolates per strain), h*FEN1* expression decreases the elevated frequency of ALF cells that result from deletion of y*RAD27*. **(D)** Liquid growth curve assays were used to validate complementation observed in spot assays. In the presented example, h*TBCC* expression rescues *cin2*Δ sensitivity to benomyl. Each represented curve is the average of three replicates per media condition. Fitness of each strain was quantified by calculating area under the curve (AUC) of each replicate independently. Strain fitness was defined as the AUC of each yeast strain relative to the AUC of the wild-type strain containing the vector control and grown in the same media condition (mean +/- SD). Student's t-test. ****$p<0.0001$.

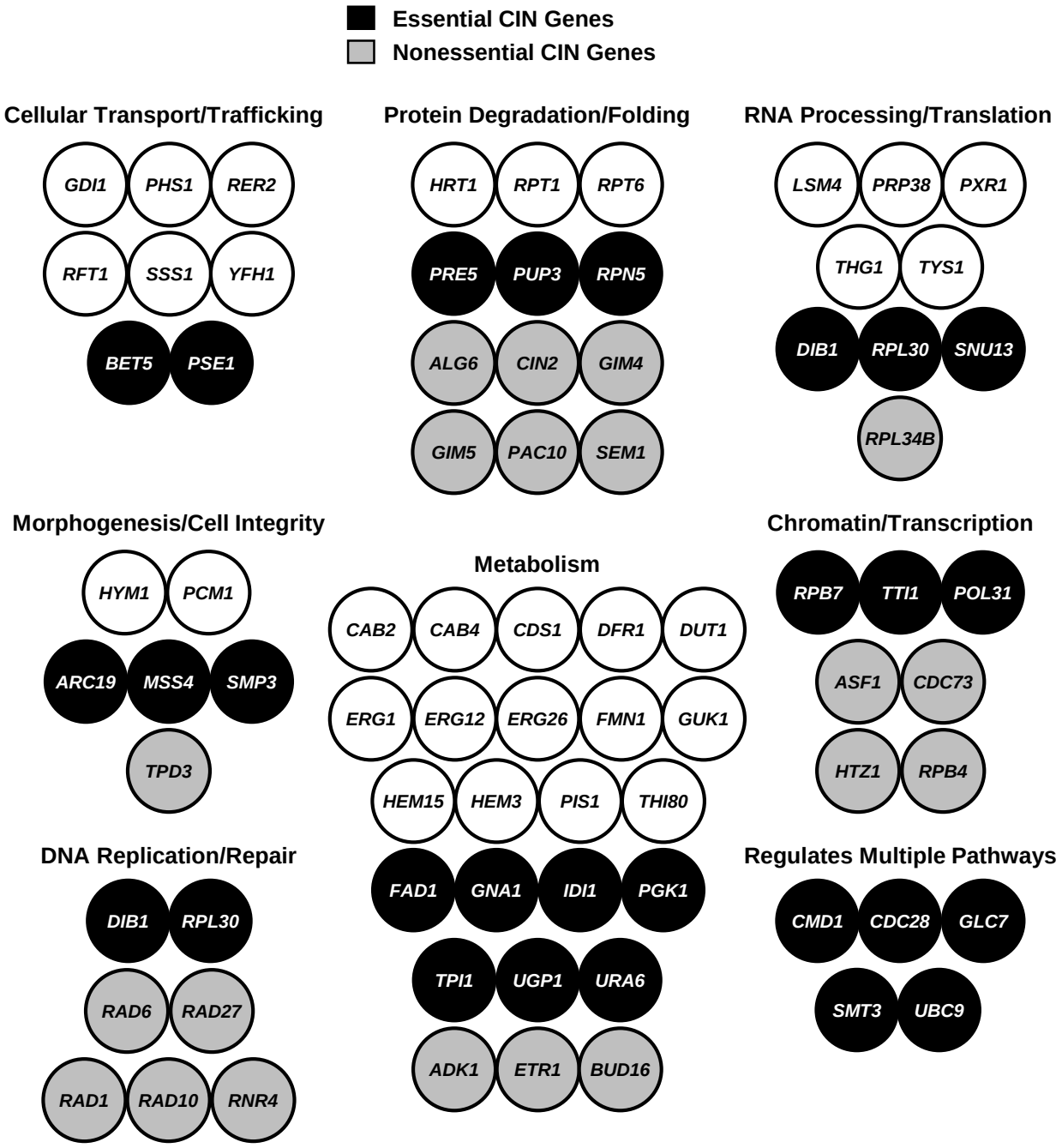

Figure 2.4. Yeast genes that are replaceable by human genes.
A total of 78 yeast genes are represented by nodes and grouped according to cellular processes (Yeastmine). Yeast *CIN* genes are represented by black and grey nodes.

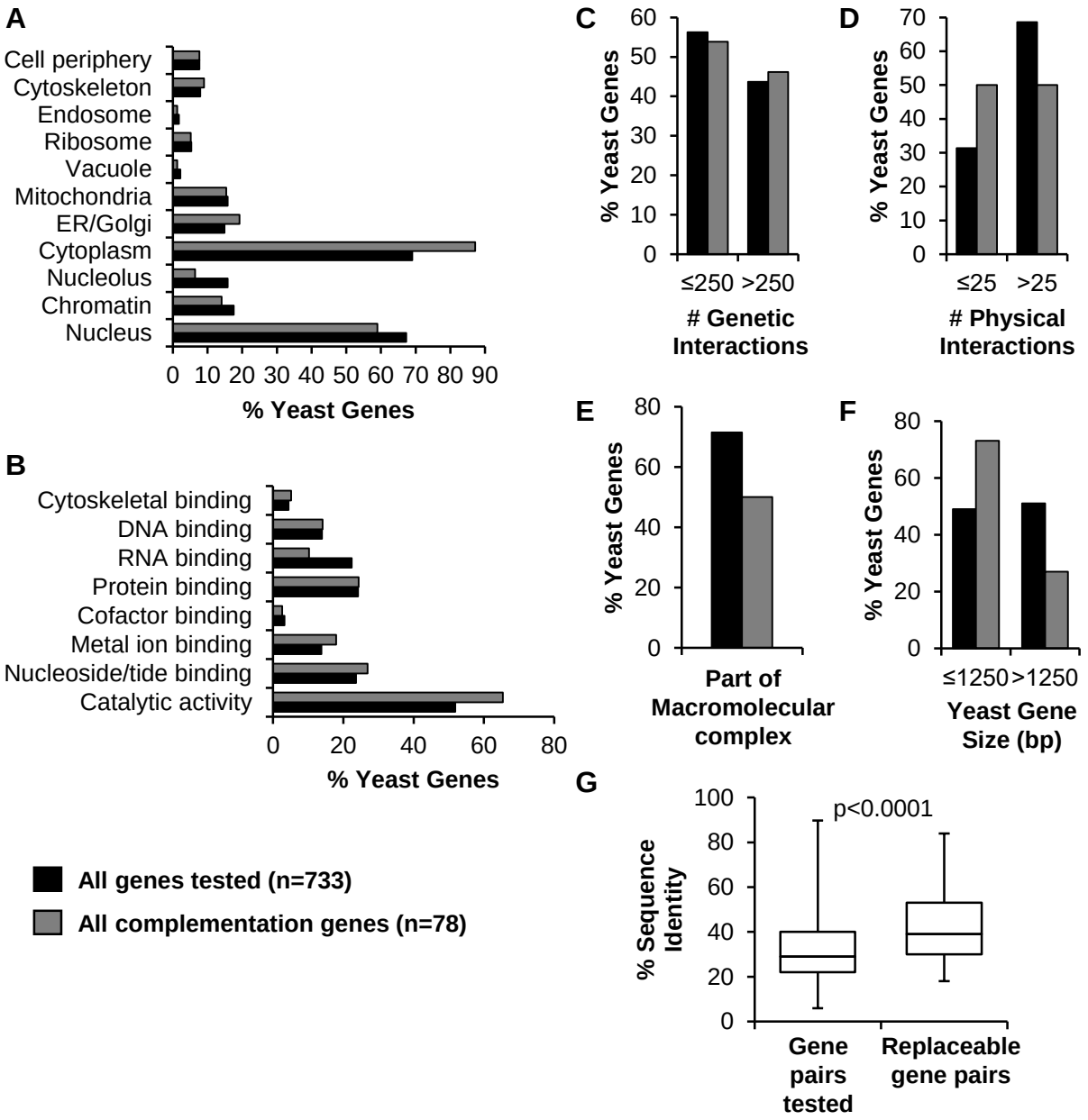

Figure 2.5. Analyzing features of yeast genes that predict replaceability including
(A) localization patterns, **(B)** molecular function, **(C)** no. of genetic interactions, **(D)** no. of physical interactions, **(E)** part of macromolecular complexes, **(F)** yeast gene size, and **(G)** human–yeast sequence identity. Localization data, Gene Ontology (GO) terms, no. of genetic/physical interactions, and gene size for each yeast gene were obtained from Yeastmine and each feature is represented as a proportion of the total number of genes input for each set (n = 733 for all yeast genes included in all screens and n = 78 for the complementation genes). Overall, the complementation set was enriched for yeast proteins that localize to the cytoplasm (P=1.4E-03), have less physical interactions (P=3.1E-03), are less likely to be part of macromolecular complexes (P=2.7E-04), and have smaller gene size (P=7.1E-05). For sequence identity, "Gene pairs tested" refers to the 1197 human–yeast pairs included in this study corresponding to 733 yeast genes and "Replaceable gene pairs" refers to the 85 complementation pairs corresponding to 78 yeast genes. The box plot highlights the median and range of sequence identity for each set of gene pairs.

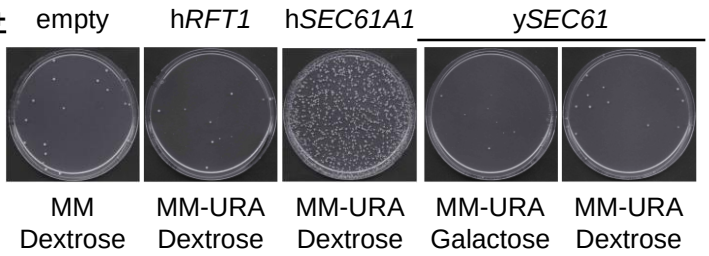

Figure 2.6. h*SEC61A1* complements y*RFT1*.
Expression vectors (h*RFT1* and h*SEC61A1* under the control of the GPD constitutive promoter and y*SEC61* under the control of the GAL-inducible promoter) were transformed into the *RFT1*/*rft1*Δ heterozygous diploid yeast strain and plated on haploid selection media (MM−Ura) following sporulation. Complementation was scored by higher than background growth on MM−Ura as shown and confirmed by testing for plasmid dependency on MM+5-FOA and tetrad dissection.

CHAPTER 3: ASSESSING COMPLEMENTATION OF MULTI-SUBUNIT YEAST COMPLEXES

3.1 Introduction

Our study (Chapter 2) and other large-scale complementation screens determined that a major predictive feature for cross-species complementation is that genes in the same pathway, process or complex tend to be similarly replaceable or non-replaceable (Hamza et al., 2015; Kachroo et al., 2017; Kachroo et al., 2015; Sun et al., 2016). Human genes were more likely to complement if they had a higher proportion of interacting partners that also complemented and vice versa. Alternatively, some human-yeast cognate pairs may require replacing the entire yeast multi-protein complex/pathway for complementation. This has been attempted at the level of two and four-subunit yeast complexes with varying success (reviewed in section 1.2.2). The experiments described in this chapter assess cross-species complementation of yeast multi-protein complexes for which individual subunits are not replaceable on their own. This includes a two-subunit endonuclease complex composed of nonessential yeast genes and the multi-subunit cohesin complex/pathway composed of one nonessential and eight essential yeast genes.

Testing complementation of multi-subunit yeast complexes presents several technical challenges in the experimental design including (i) inactivation of multiple yeast genes in the same strain, (ii) limitations on the number of yeast selection markers for genomic editing and simultaneous expression of multiple human genes in yeast, and (iii) stable and endogenously regulated human gene expression that accounts for stoichiometric balance of complex subunits. Concurrent expression of multiple human genes in yeast can be accomplished with individual vectors for each human gene, a single vector containing all human genes, or

following genomic integration. Tandem expression from a single vector is more preferable than multiple individual vectors given that multiple vectors introduce more variability in expression which can impact complex stoichiometry, while also limiting availability of yeast selection markers (Ryan et al., 2014). In turn, integration of the human ORF in the genome to replace the cognate yeast gene is preferred in comparison to vector-based maintenance as it allows stable gene expression under the endogenous yeast promoter, while also ensuring less heterogeneity within the yeast population without the need for selective growth media. To facilitate iterative genome editing of multiple yeast genes by marker-less deletion or replacement with human genes, the CRISPR/Cas9 system (DiCarlo et al., 2013) can be used for engineering of yeast strains. Here, we demonstrate the utility of the CRISPR/Cas9 system to engineer humanized yeast for complementation assays of yeast multi-protein complexes.

3.2 Methods

3.2.1 CRISPR/Cas9 gene modifications

The CRISPR/Cas9 toolkit and protocols were obtained from the Ellis lab (see *https://benchling.com/pub/ellis-crispr-tools* by William Shaw). The toolkit consists of an sgRNA (single guide RNA) entry vector (pWS082) and yeast expression vectors that facilitate constitutive expression of a yeast optimized Cas9 ORF and the sgRNA. Yeast transformation of a linearized Cas9 expression vector along with a linearized sgRNA fragment with flanking homology will reconstitute a Cas9-sgRNA expression vector based on gap repair of the linearized fragments (Figure 3.1).

sgRNA design and assembly: Guide RNAs consist of a 20-nucleotide sequence preceding the PAM site ‘NGG’. sgRNA sequences were designed using the Benchling wizard ‘Design and

Analyze Guides' and CRISPR sites were selected based on their on-target and off-target scores (higher on-target scores indicate higher expected activity while higher off-target scores indicate less off-target activity). Guides were ordered as complimentary oligos with the following overhangs: 5'-GACTTT$(n)^{20}$-3' and 3'-AA$(n)^{20}$CAAA-5' (Lee et al., 2015). Each oligo was phosphorylated separately by treating with PNK (Polynucleotide Kinase) for 1h at 37°C [1µl oligo (100µM), 1µl 10x T4 DNA ligase buffer, 7µl dH_2O, 1µl PNK] before annealing both oligos [10µl of each phosphorylated oligo, 180µl dH_2O] by slow cooling from 96°C to 23°C (-0.1°C /s) in a thermocycler. Oligos were assembled into the sgRNA entry vector (pWS082) by Golden Gate assembly [4.5µl dH_2O, 2µl annealed oligos, 0.5µl pWS082, 1µl 10x T4 DNA ligase buffer, 1µl BsmBI restriction enzyme, 1µl T4 DNA ligase] in a thermocycler [42°C for 2 minutes, 16°C for 5 minutes, repeat steps 1-2 (10x), 60°C for 10 minutes, 80°C for 10 minutes]. 1µl of the reaction mixture was transformed into competent *E. coli* DH5α cells and non-GFP colonies were selected under blue light, mini-prepped and verified by sequencing using the forward and reverse primers (F: GGGCTGTTAGTTATGCAACG; R: CACTGCCTGGAATGTCCAGC). The sgRNA cassette was linearized with EcoRV [13.2µl dH_2O, 2µl 10x NEB buffer 3.1, 4µl sgRNA plasmid (200ng/µl), 0.8µl EcoRV] by incubating 1h at 37°C then for 20 minutes at 80°C. Digestion was confirmed by agarose gel electrophoresis (undigested: 2.9kb; digested: 1.0kb + 1.9 kb).

Cas9-sgRNA expression vector construction and transformation: Cas9 vectors were linearized using BsmBI for 1h at 55°C [3µl dH_2O, 6µl 10x NEB buffer 3.1, 50µl Cas9 plasmid (100 ng/ul), 1µl BsmBI] and gel purified. CRISPR components were transformed using a high-efficiency LiAc/SS-DNA/PEG transformation protocol (Pan et al., 2007) and

each transformation included 100ng of linearized Cas9-sgRNA vector, 200ng of digested sgRNA vector and ~2µg of PCR amplified donor DNA. For some deletions, donor DNA was constructed by annealing two complimentary oligos composed of flanking homology to the left and right of the deletion site. To confirm CRISPR-mediated insertions or deletions, DNA was isolated from yeast transformants using a rapid DNA isolation method termed GC preparations (Blount et al., 2016). Transformants were screened by PCR using primers that flank the region of homology on the donor DNA and verified by sequencing. To ensure loss of the Cas9-sgRNA vector, transformants were streaked on non-selective media and colonies were confirmed to have lost the plasmid by observing lack-of-growth on selective media.

3.2.2 Utilizing CRISPR/Cas9 to humanize 2-subunit yeast complexes by integration

Yeast strains: To create yeast strains with integrated human cDNAs, donor DNA generated by PCR was co-transformed into wild-type *MAT*α BY4742 (Brachmann et al., 1998) along with linear fragments encoding Cas9 and a sgRNA targeted to the coding region of either y*RAD1*, y*RAD10*, y*MMS4* or y*MUS81* (Table A.6). Donor DNA for h*MUS81* was obtained by PCR using the entry clone from hORFeome V8.1 (Yang et al., 2011) as template and primers were designed to include a stop codon. Donor DNA for h*ERCC4* and h*EME1* was obtained by PCR using clones from the Mammalian Gene Collection (Dharmacon) as template. Donor DNA for h*ERCC1* was generated using pAG416GPD-h*ERCC1*+6Stop as template in the PCR resulting in a PCR product that also contained the *CYC1* terminator. The double deletion strains *mus81Δ mms4Δ* and *rad1Δ rad10Δ* were made by CRISPR-mediated deletion of *MMS4* and *RAD10* in the *mus81Δ::kanMX* and *rad1Δ::kanMX MAT*α deletion strains (Giaever et al., 2002), respectively (Table A.6).

Growth assays to assess rescue of chemical sensitivities: Chemical sensitivity complementation assays for yeast strains with integrated human cDNAs were carried out in SC media (+/- chemical) at 30°C. For liquid growth assays, cultures were grown to mid-log phase then diluted to OD_{600}=0.1 in 200µl media +/- 0.01% MMS or 150mM HU. OD_{600} readings were measured every 30 minutes over a period of 48h in a TECAN M200 plate reader and plates were shaken for 10 minutes before each reading. Strains were tested in 3 replicates per plate per condition and area under the curve (AUC) was calculated for each replicate. Strain fitness was defined as the AUC of each yeast strain relative to the AUC of the control strain (BY4742) grown on the same plate in the same media condition.

3.2.3 Utilizing CRISPR/Cas9 to humanize the multi-subunit cohesin complex/pathway

Expression vectors: The neochromosomes yCL3A, hC, hCL, hCL2A, hCL6A, hL, h2A, hS/S and h3P (see Figure 3.6) were synthesized and constructed by Neochromosome Inc. Human cohesin genes *NIPBL* and *SMC3* cloned in the yeast expression vector pEGH-A (*URA3*, 2µ, inducible GAL promoter, N-terminal GST tag) were derived from the Ultimate ORF collection (Invitrogen). The remaining human cohesin genes were obtained as Gateway-compatible entry clones from the hORFeome V8.1 collection (Yang et al., 2011) and shuttled into yeast destination vectors pAG416GPD-ccdB+6Stop (*URA3*, CEN, constitutive GPD promoter, 6-amino-acid C-terminal extension) or pAG425GAL-hORF+6Stop (*LEU2*, 2µ, inducible GAL promoter, 6-amino-acid C-terminal extension) (Alberti et al., 2007; Kachroo et al., 2015) using LR Clonase II (Invitrogen) to generate expression clones. Neochromosome derivatives of hC with different deletions were constructed by CRISPR-mediated deletions using donor DNA generated from annealed oligos and sgRNAs targeted to the corresponding human ORFs (Table A.7). Neochromosome yCL3A-*smc1*Δ*smc3*Δ was

constructed by CRISPR-mediated deletion of y*SMC1* and y*SMC3* using donor DNA generated from annealed oligos and sgRNAs targeted to linker sequences on the vector (Table A.8). GAL-inducible expression vectors of yeast cohesin genes were obtained from the FLEX collection (Hu et al., 2007).

Yeast strains: Expression vectors containing human or yeast cohesin genes and vector controls pRS415 (*LEU2*), pRS416 (*URA3*) or pRS413 (*HIS3*) (Sikorski and Hieter, 1989) were transformed into indicated yeast strains and maintained on selective media. Yeast strains included wild-type *MAT*α BY4742 (Brachmann et al., 1998), conditional temperature-sensitive mutants of cohesin genes (Li et al., 2011), *rad61*Δ from the *MAT*α yeast haploid knockout collection (Giaever et al., 2002) and yeast cohesin deletion strains (ΔC, ΔCL, ΔCL2A and ΔCL3A) (see Figure 3.12). To create the multi-subunit yeast cohesin deletion strains (4, 6, 8, and 9 gene deletions), donor DNA generated by PCR was co-transformed into a yCL3A-containing BY4742 strain along with linear fragments encoding Cas9 and sgRNAs targeted to the endogenous terminators of the yeast genes (except for y*SCC4*, which targeted the ORF). Gene deletions were completed sequentially starting with the 4 core cohesin genes (ΔC to ΔCL3A) and confirmed by PCR. A range of Cas9-sgRNA expression vectors with differing selection markers were utilized for the iterative gene deletions such that once a transformant was confirmed for a single deletion, a new round of transformation was started without the need to rid the cells of the previous CRISPR/Cas9 machinery (as described in *https://benchling.com/pub/ellis-crispr-tools*). Donor DNA was obtained from PCR using yeast genomic DNA as template and primers were designed such that one primer contained (5’ to 3’) ~60bp homology to the region upstream of the yeast ORF and ~25bp homology to the endogenous terminator of the yeast gene, while the other primer was designed to be

homologous to the endogenous terminator in a region downstream of the corresponding primer pair (Table A.9).

Complementation and growth assays: For spot assays, wild-type and mutant strains were grown to saturation at 25°C then serially diluted in 10-fold increments and plated (5µl each spot) onto selective media at 25°C, 30°C and 37°C. For liquid growth assays, cultures were grown to mid-log phase then diluted to OD_{600}=0.1 in 200µl media +/- 0.0075% MMS. OD_{600} readings were measured every 30 minutes over a period of 24h in a TECAN M200 plate reader and plates were shaken for 10 minutes before each reading. Strains were tested in 3 replicates per plate per condition and area under the curve (AUC) was calculated for each replicate. Strain fitness was defined as the AUC of each yeast strain relative to the AUC of the control strain (BY4742 + vector controls) grown on the same plate in the same media condition. For induction in galactose media, yeast strains were grown to mid-log phase in both dextrose or galactose media before diluting to OD_{600}=0.1 in the same media +/- 0.0075% MMS. All liquid growth assays were done at 30°C. To assess complementation of cohesin deletion mutants, yeast strains were grown to saturation in SC−Leu−His at 30°C to allow loss of *URA3*-marked vectors. Strains were then plated on SC−Leu−His and SC−Leu−His+5-FOA (0.1%) to select for Ura^- segregants via the plasmid shuffle strategy (Boeke et al., 1987) and incubated at 30°C. Plates containing 5-FOA were incubated for a minimum of 10 days and any viable colonies were streaked on new 5-FOA plates before isolation of vector DNA by GC preparations. To confirm presence/absence of *URA3*-marked yCL3A, two sites corresponding to the *URA3* gene and a yeast cohesin gene on the vector were chosen as template for PCR. In all cases tested, 5-FOA resistant colonies were confirmed to contain yCL3A and viability of the cohesin deletion mutants was attributed to

the presence of the yeast cohesin genes on yCL3A. Presumably, the 5-FOA^{R} (Ura^{-}) phenotype was due to mutations in the *URA3* gene present on yCL3A.

3.3 Results

3.3.1 Humanizing two-subunit yeast endonuclease complexes composed of nonessential yeast genes

In chapter 2, the complementation screens showed that either member of the y*RAD1*/y*RAD10* endonuclease complex was replaceable by their respective human orthologs h*ERCC4* or h*ERCC1* individually. Conversely, for another endonuclease complex composed of y*MUS81*/y*MMS4*, neither subunit was replaceable by either h*MUS81* or h*EME1* individually. To examine if both members of the complex were required simultaneously for successful complementation, CRISPR/Cas9-based genomic engineering was used to replace the ORFs of both members of the yeast complex with the corresponding human orthologs. This generated yeast strains in which the human gene ORFs were integrated in the genome and under control of the native yeast gene regulation. Unlike h*ERCC4*/h*ERCC1* which could be successfully replaced as a complex (Figure 3.2A), the combined h*MUS81*/h*EME1* complex failed to complement its yeast heterodimer counterpart (Figure 3.2B).

3.3.2 Humanizing multi-subunit yeast cohesin complexes composed of essential yeast genes

The cohesin multi-protein complex is essential for genome stability and functions in many cellular pathways including sister chromatid cohesion, chromatin structure/organization, DNA repair, and transcriptional regulation. Genes encoding human cohesin subunits are mutated in a range of tumor types and may result in genomic instability,

alterations in chromatin organization and susceptibility to DNA damage (Hill et al., 2016; Losada, 2014). The impact of cohesin mutations on the structure and function of the complex and its contribution to tumorigenesis remains unknown. Accordingly, a cohesin-humanized yeast system can provide an *in vivo* platform to study the impact of these variants in relation to cohesin biology.

The mitotic cohesion pathway includes the DNA-associated multi-subunit cohesin complex composed of four core members (y*SMC1*, y*SMC3*, y*MCD1*, y*IRR1*), a loader two-subunit complex (y*SCC2* and y*SCC4*) and accessory subunits y*PDS5*, y*ECO1*, y*RAD61*, y*ESP1* and y*PDS1* (Figure 3.3A). We directly tested whether some of the yeast cohesion pathway genes could be individually rescued by their corresponding human orthologs, and in all cases, single human/yeast genes replacements failed to rescue viability (Figure 3.3B, Figure 3.4 and Figure 3.5).

The core cohesin subunits form a ring-like complex that embraces sister chromatids and mediates their cohesion from the onset of DNA replication until the onset of anaphase and chromosome segregation (reviewed in (Makrantoni and Marston, 2018; Marston, 2014). Loading of the cohesin complex onto chromosomes is a dynamic turnover process between the loading activity of the yScc2/yScc4 loader complex and the accessory subunits yPds5/yRad61 that promote release of the complex from DNA. This turnover is stabilized by yEco1-mediated acetylation of the core subunit ySmc3 which creates a functional linkage that establishes cohesion between sister chromatids. At the metaphase to anaphase transition, ubiquitin-mediated degradation of securin, yPds1, releases and activates separase, yEsp1, which in turn cleaves the core subunit yMcd1 to allow chromosome separation.

Although the cohesin complex is evolutionarily conserved, there are mechanistic differences between yeast and human cohesion biology (reviewed in (Brooker and Berkowitz, 2014; Nasmyth and Haering, 2009; Peters et al., 2008). For instance, there are two human homologs of yeast cohesin genes y*IRR1*, y*PDS5* and y*ECO1* that seem to have some redundant functions. Further, human sororin (h*CDCA5*), which has no homolog in yeast, functions in counteracting the releasing activity of hWapl (yRad61) by competing for binding to hPds5. Disrupting the interaction between sororin and hPds5 facilitates the hWapl-mediated removal of cohesin from chromosome arms during prophase. Unlike yeast, which requires cleavage of yMcd1 for cohesin removal along the entire chromosome, human cohesin bound to chromosome arms dissociates during prophase in a cleavage-independent process, after which centromeric cohesin is removed in a cleavage-dependent process similar to yeast (Waizenegger et al., 2000). The extent to which these functional differences between yeast and human cohesion biology will impact complementation is unknown.

Given that this complex is composed of multiple subunits and regulated by multiple proteins, we postulated that complementation may require replacing the entire complex with or without the associated regulatory proteins. Since we did not know the minimum subunit requirement for complementation of the yeast cohesin complex, we designed a series of neochromosomes (synthetic chromosomes) each containing an increasing number of human cohesin genes. The human cohesin neochromosomes included hC (4 core subunits), hCL (4 core + 2 loader subunits), hCL2A (4 core + 2 loader + 2 accessory subunits) and hCL6A (4 core + 2 loader + 6 accessory subunits) (Figure 3.6). The difference between hCL2A and hCL6A is the addition of 4 human genes that either have a nonessential yeast ortholog (y*RAD61*; h*WAPL*), a human gene that has no known homolog in yeast (h*CDCA5*), or human

genes that form a separate two-subunit complex composed of separase (y*ESP1*; h*ESPL1*) and its inhibitor securin (y*PDS1*; h*PTTG1*). To allow flexibility in setting up complementation assays with multiple combinations of human genes, we designed additional neochromosomes including hL (2 loader subunits), h2A (2 accessory subunits), hS/S (2 accessory subunits: separase and securin), and h3P (3 human paralogs). Since three human cohesin genes have multiple paralogs, we included the least diverged homologs (h*STAG2*, h*PDS5B*, h*ECO1*) in neochromosomes hC, hCL, hCL2A and hCL6A, but designed the separate h3P to include h*STAG1*, h*PDS5A* and h*ECO2*. For all human cohesin neochromosomes, each human gene was codon optimized and flanked by the endogenous promoter and endogenous terminator of the corresponding yeast ortholog (except for h*CDCA5* which has no known yeast homolog, and so was designed with the yeast promoter of y*RPL13A* and terminator of y*RPL22B*).

In parallel, we also designed a yeast cohesin neochromosome (yCL3A) which contained 9 genes (4 core + 2 loader + 3 accessory subunits) (Figure 3.6). Each yeast gene was flanked by the endogenous yeast promoter and a heterologous terminator to allow CRISPR-mediated targeting of the endogenous chromosomal gene, and to minimize any chance of recombination between the yeast and human cohesin neochromosomes. We confirmed that yCL3A can replace the endogenous yeast cohesin genes by testing rescue of temperature sensitivity of seven yeast cohesin temperature-sensitive strains (Figure 3.7A).

We assessed the impact of human cohesin expression in wild-type yeast. Expression of hC caused fitness defects in yeast and the effect was more pronounced with concurrent expression of the human loaders (hCL) and accessory proteins (hCL2A, hCL6A) (Figure 3.7B). However, expression of the human loaders (hL) and accessory proteins (h2A) alone

did not impact fitness of yeast indicating that expression of the human core genes caused the growth defects.

To examine whether a particular combination of human genes may be required for complementation, we tested the ability of human gene expression to rescue conditional lethality of yeast cohesin temperature-sensitive (TS) strains. When grown at the restrictive temperature, human cohesin gene expression did not rescue lethality of yeast TS strains in multiple tested combinations (Figure 3.8, Figure 3.9 and Figure 3.10). In fact, some yeast TS strains displayed fitness defects as a result of human cohesin expression at the permissive temperatures. This effect was not restricted to conditional mutants of essential yeast genes as hCL6A caused severe fitness defects in a deletion strain of the nonessential y*RAD61* gene (Figure 3.9).

The apparent fitness defects observed in some yeast cohesin single mutants may result from mixed human-yeast subunits which may impact complementation. Therefore, we also tested the ability of human gene expression to rescue lethality of yeast cohesin deletion strains. By utilizing CRISPR/Cas9-based genomic engineering, we constructed a series of strains with multiple genomic deletions of yeast cohesin genes in the presence of yCL3A. Given that yCL3A was designed such that each yeast gene was flanked by a different heterologous terminator, we constructed sgRNAs to target Cas9 to the endogenous terminators of the yeast genes. This facilitated CRISPR-mediated deletion of the genomic copies while sparing yCL3A from any modification. Human cohesin neochromosomes, which were designed to include the endogenous terminators of the corresponding yeast orthologs, were then transformed into the deletion strains. Since yCL3A was marked by *URA3*, we tested complementation by plating on 5-FOA, which selects for cells that have lost

the *URA3*-marked neochromosome. Human cohesin genes failed to complement yeast cohesin gene deletions in multiple tested combinations (Figure 3.11). For instance, hC was tested for the ability to complement a yeast strain (termed ΔC) with deletions of the 4 core cohesin essential genes: *smc1*Δ *smc3*Δ *mcd1*Δ *irr1*Δ. In order to eliminate the possibility that a determent to complementation is the inability of human core genes to disengage from DNA without a species-specific separase, we included hS/S in different combinations with the other human cohesin neochromosomes. When complementation was not observed, we included h3P to address if different paralogs were required. Overall, multiple human-yeast gene replacement experiments did not result in human complementation of yeast cohesin gene deletions (summarized in Figure 3.12).

Although no complementation was observed, an investigation into the cause of yeast growth defects that result from expression of human cohesin genes can expand our understanding of biological properties of human and yeast cohesin proteins. Spot assays demonstrated that expression of human cohesin proteins from the various neochromosomes in wild-type yeast caused fitness defects that varied depending on the particular constellation of proteins being expressed (Figure 3.7B). Furthermore, this toxicity was amplified in some cohesin mutant strain backgrounds (Figure 3.8, Figure 3.9 and Figure 3.10). Since yeast cohesin mutants exhibit cohesion defects, chromosome instability, and DNA damage (Marston, 2014; Stirling et al., 2011), we predicted that ectopic expression of human cohesin genes in yeast may impact these processes and, for example, cause sensitivity to DNA damaging agents. Using liquid growth assays, we determined that expression of human cohesin genes from hC, hCL, hCL2A and hCL6A sensitized wild-type yeast to the alkylating agent, MMS (Figure 3.13 and Figure 3.14). The resultant yeast fitness defects were

suppressed by expression of yeast cohesin genes from yCL3A (i.e. 2 copies of each yeast gene), and the suppression was weaker in strains that lacked the genomic copies of yeast cohesin genes (i.e. 1 copy of each yeast gene).

Unlike hC, hCL, hCL2A and hCL6A, human cohesin neochromosomes that lack human core genes (hL and h2A) had no impact on fitness of wild-type yeast in the presence or absence of MMS (Figure 3.13 and Figure 3.14). To deduce which core gene(s) were the source of toxicity, we overexpressed human core genes separately in wild-type yeast and found that h*SMC1A* and h*SMC3* caused the strongest fitness defects upon overexpression (Figure 3.15A). We used CRISPR/Cas9 to delete human core genes from hC and confirmed that hC-*smc1a*Δ*smc3*Δ (containing only h*RAD21* and h*STAG2*) was the only combination of core gene deletions that suppressed MMS (Figure 3.15B) and cohesin mutant (Figure 3.15C) sensitivity. To pinpoint which yeast genes in yCL3A rescued the fitness defects resulting from expression of h*SMC1A* and h*SMC3*, we transformed GAL-inducible plasmids of each yeast gene in combination with hC and found that overexpression of yeast cohesin genes separately was not sufficient to rescue hC toxicity (Figure 3.16A). Since toxicity was caused by a combination of h*SMC1A* and h*SMC3*, we tested whether the corresponding yeast orthologs (y*SMC1* and y*SMC3*) were both required for rescue of fitness defects. Indeed, we found that unlike yCL3A, the yeast cohesin neochromosome yCL3A-*smc1*Δ*smc3*Δ (containing six other yeast genes) could not rescue fitness defects and MMS sensitivity of yeast containing hC (Figure 3.16B). Taken together, these results suggest that increased levels of ySmc1 and ySmc3 minimize toxicity that occurs when their human counterparts are ectopically expressed in yeast.

3.4 Discussion

In general, a major limitation to cross-species complementation involving multi-protein complexes is the potential for interactions of the human protein subunits with the cognate yeast interaction partners. We presented the example of humanizing two related endonucleases that each form heterodimers and function in similar DNA repair processes with some functional overlap (Dehe and Gaillard, 2017; Kikuchi et al., 2013). In one case, each subunit of the yRad1/yRad10 endonuclease was replaceable indicating that each human ortholog was able to form a heterodimer with the other yeast subunit. In contrast, yMus81/yMms4 was non-replaceable even when combining both human subunits in the yeast strain. While these results are consistent with previous findings that showed genes in the same complex tended to be similarly replaceable or non-replaceable (Hamza et al., 2015; Kachroo et al., 2017; Kachroo et al., 2015; Sun et al., 2016), there are reported cases of two-subunit yeast complexes that are only replaceable when both human protein orthologs are expressed (Arnesen et al., 2009; Davey et al., 2011; Gao et al., 2005; Katahira et al., 1999; Ozanick et al., 2005; Paul et al., 2015). In another study, the four-subunit yeast nucleosome was shown to be replaceable by the human nucleosome only after a rare event that allowed yeast cells to adapt and acquire suppressor mutations (Truong and Boeke, 2017). A more robust complementation was observed after converting five human histone amino-acid residues to the amino-acids found in their yeast counterparts, thus revealing the importance of interactions in the success of a human complementation experiment. Overall, our results suggest that the major limitation to predict the ability of some yeast complexes to be humanized is the lack of information on the minimum complex/pathway members that need to be replaced simultaneously. While replacing one subunit of yRad1/yRad10 was sufficient

for complementation, yMus81/yMms4 may have required replacing additional human proteins to regulate the functions of the endonuclease (Dehe and Gaillard, 2017). Thus, attempts to discover and test the minimum requirements for humanization can provide new avenues to study important properties of human proteins.

We demonstrated a sequential complementation strategy for the yeast cohesion pathway starting from one-to-one complementation assays to expressing up to 15 human genes in a nine-deletion yeast strain background. Although complementation was not detected in multiple growth and viability assays, we determined that expression of the cohesin core proteins hSmc1a and hSmc3 was detrimental to yeast fitness. This toxicity was amplified in several conditions including concurrent expression of the human cohesin loader complex, addition of DNA damaging agents, and in some yeast cohesin mutant genetic backgrounds. The h*SMC1A*/h*SMC3*-induced toxicity occurred despite expressing both human genes using the endogenous promoter and terminator of the corresponding yeast ortholog, thereby ensuring native transcriptional regulation. Based on the data presented in this study, we cannot rule out that the toxicity associated with expression of hSmc1a and hSmc3 may prevent complementation of growth and viability defects of yeast cohesin mutants. There is precedent for this as expression of h*UROS* using a constitutive promoter induced toxicity in yeast which prevented complementation of y*HEM4*, while replaceability was only observed once toxicity was eliminated by expressing h*UROS* using the endogenous yeast promoter of the corresponding ortholog (Kachroo et al., 2017). However, we do note that we did not observe complementation of some cohesin complexes even in the absence of toxicity. For instance, human cohesin loaders (hL) and separase/securin (hS/S) form distinct two-subunit complexes with specialized functions separate from the cohesin core complex, and although

their expression does not result in toxicity in yeast, they cannot complement temperature-sensitive mutants of their corresponding yeast orthologs.

There are several possible mechanisms of h*SMC1A*/h*SMC3*-induced toxicity in yeast. These two proteins contain intramolecular anti-parallel coiled coil domains that fold back on themselves at the hinge region and heterodimerize to form a hinge domain at one end and an ATPase domain at the other. Binding of yMcd1/hRad21 at the ATPase domain interconnects and stabilizes their dimerization and recruits the other cohesin subunits. One possible mechanism for the toxicity associated with expression of h*SMC1A* and h*SMC3* is that their protein products sequester the yeast cohesin subunits away from DNA causing an overall reduction of functional yeast cohesin complexes. Given that DNA repair is compromised when yeast cohesin levels are decreased to 30% of wild-type levels (Heidinger-Pauli et al., 2010a), this mechanism may explain how the human proteins sensitize wild-type yeast to DNA damaging agents and decrease fitness of some yeast CIN mutants. This could also explain how extra copies of the yeast proteins, ySmc1 and ySmc3, rescue the fitness defects. However, these observations also support an alternative mechanism whereby the human cohesin proteins are loaded onto DNA, which in turn contributes to DNA damage and/or mis-regulation of the yeast cohesin function. This is the most likely scenario based on additional observations: (i) the sources of toxicity are the only cohesin proteins that embrace the DNA, and since toxicity is observed upon expression of either h*SMC1A* or h*SMC3*, this may indicate that the DNA-bound core cohesin complex is possibly composed of entirely human subunits or as a mixture of human-yeast subunits, and (ii) the toxicity is amplified upon concurrent expression of the human loader complex suggesting that while the human

core proteins may be loaded by the yeast loader complex, this process might be more efficiently accomplished using the human loader.

If the human cohesin core complex associates with yeast DNA, one potential problem that may impact complementation is that the full-human or mixed human-yeast core complex is mis-localized on the DNA to regions not typically associated with cohesin binding which may affect cohesion, chromatin structure/organization, DNA repair, or transcription. One of the required steps in the loading mechanism is ATP hydrolysis by the Smc1/Smc3 ATPase domains, which enables entrapment and translocation of the core proteins to cohesin-associated regions (CARs) on the DNA (Marston, 2014). Smc1/Smc3 mutant heterodimers deficient in ATP hydrolysis are loaded onto DNA docking sites by the loader complex but fail to translocate to CAR regions (Hu et al., 2011). This results in an unstable association of the core proteins at the docking sites, which in turn prevents loading of wild-type cohesin core complexes. This is supported by results demonstrating that expression of a y*SMC3*-hydrolysis deficient mutant is tolerated in a y*SMC3* wild-type background but not a *smc3-42* mutant strain with reduced ySmc3 activity (Heidinger-Pauli et al., 2010b). Further, overexpression of the y*SMC3*-hydrolysis deficient mutant in a y*SMC3* wild-type background causes lethality, indicating that toxicity occurs when the ratio of the ATPase mutant protein is increased compared to the wild-type protein. These results mirror our observations showing that endogenously-regulated expression of human cohesin proteins from neochromosomes cause toxicity in some yeast cohesin mutants that presumably have reduced cohesin activity, while overexpression of single h*SMC1a* or h*SMC3* causes severe growth defects in a yeast wild-type background. If the human Smc1a/Smc3 subunits are ATPase deficient when expressed in yeast, then a fully-human or mixed human-yeast core complex

will load onto DNA docking sites but then fail to translocate to yeast CAR regions. Given that ATP hydrolysis requires both Smc1 and Smc3 domains (Elbatsh et al., 2016), then extra copies of both yeast proteins may increase the ratio of the wild-type yeast complex in comparison to the supposedly ATPase-deficient human subunits and rescue toxicity.

If human subunits are loaded onto yeast DNA, another potential problem that may impact complementation is the inability of DNA-bound human cohesin containing hRad21 to be cleaved by the human separase. It has been previously reported that human separase cannot cleave yeast Mcd1, and yeast separase cannot cleave human Rad21, although it is unclear whether these results are based on *in vivo* or *in vitro* experiments (Waizenegger et al., 2002). In our assays, we expressed human separase alongside its inhibitor human securin to facilitate cleavage of human Rad21. However, we cannot conclusively conclude that human securin is targeted for degradation by yeast proteins and as such, there is the possibility that human separase remains inactivated. Cohesin cleavage by separase is also enhanced by the yCdc5/hPlk1-mediated phosphorylation of yMcd1/hRad21 separase recognition sites (Alexandru et al., 2001). Although we did not include hPlk1 in our assays, it has been previously reported that h*PLK1* can complement a y*CDC5* loss-of-function mutant (Lee and Erikson, 1997). However, it is still possible that hPlk1 can substitute for yCdc5 and phosphorylate yeast substrates such as yMcd1, but yCdc5 may be unable to phosphorylate the equivalent human substrates, such as hRad21, when they are expressed in yeast. An example of this type of one-directional complementation, albeit in the reverse direction, is the centromeric histone H3-variant, y*CSE4*/h*CENP-A*, where the yeast protein is able to rescue lethality induced by depletion of hCENP-A (Wieland et al., 2004), but the human protein is unable to rescue lethality of conditional or deletion mutants of y*CSE4* (Chapter 2

and (Stoler et al., 1995)). Thus, an investigation into the phosphorylation status of hRad21 and the efficiency of its cleavage in a cohesin-humanized yeast system are important follow-up experiments.

The numerous interaction partners and modes of regulation of the cohesin complex highlight the challenge to pinpoint the minimum requirements for humanization of the yeast cohesion pathway. In addition to loading/unloading of the human subunits and their localization on yeast DNA, additional regulation mechanisms, such as y*ECO1*/h*ESCO*-mediated acetylation of y*SMC3*/h*SMC3*, need to be examined for species specificity and catalytic activity when expressed ectopically in yeast. Failure to acetylate hSmc3 by yEco1 or hEsco1/2 causes an inability to establish cohesion following DNA replication (Zhang et al., 2008). Furthermore, given the multi-functional roles of the cohesion pathway, yeast assays can be utilized to differentiate the ability of the human subunits to complement separate cellular functions of the pathway. In this study, we focused on rescue-of-lethality as an indicator of complementation, however, complementation can also be assessed separately for rescue of cohesion defects, chromatin condensation defects, or DNA repair defects (Heidinger-Pauli et al., 2010a; Marston, 2014). The specialized assays may reveal a subset of functional roles that are rescued by the human subunits, despite failure to rescue viability.

The four-subunit nucleosome complementation study yielded viable humanized colonies after a prolonged period of 20 days that required adaptation of yeast cells and the acquisition of yeast suppressor mutations (Truong and Boeke, 2017). In our study, we did not observe complementation even after a prolonged incubation period on 5-FOA plates. However, unlike the human histones which do not induce toxicity in yeast, we cannot rule out the possibility that h*SMC1A*/h*SMC3*-associated toxicity prohibits the ability of yeast cells

to adapt and incorporate the human cohesin complex. For our complementation assays, we also included human sororin, which has no homolog in yeast, given its interactions and important role in the cohesion pathway in human cells. Such a requirement has been shown before for y*MIP1* complementation, which required co-expression of the ortholog, h*POLG*, with a human accessory subunit that has no homolog in yeast, h*POLG2* (Qian et al., 2014). Although we did not observe rescue of viability by the human cohesin proteins described in this work, yeast can still be utilized as *in vivo* system to study biological properties of human cohesin proteins. For instance, the cohesin core subunits, h*STAG1* and h*STAG2*, were expressed in yeast to study their subcellular localization and determine their nuclear localization (NLS) and export (NES) signals (Tarnowski et al., 2012). Our study outlines a set of tools that include a series of human cohesin neochromosomes designed for expression in yeast, that can be applied to study biological properties of this important pathway.

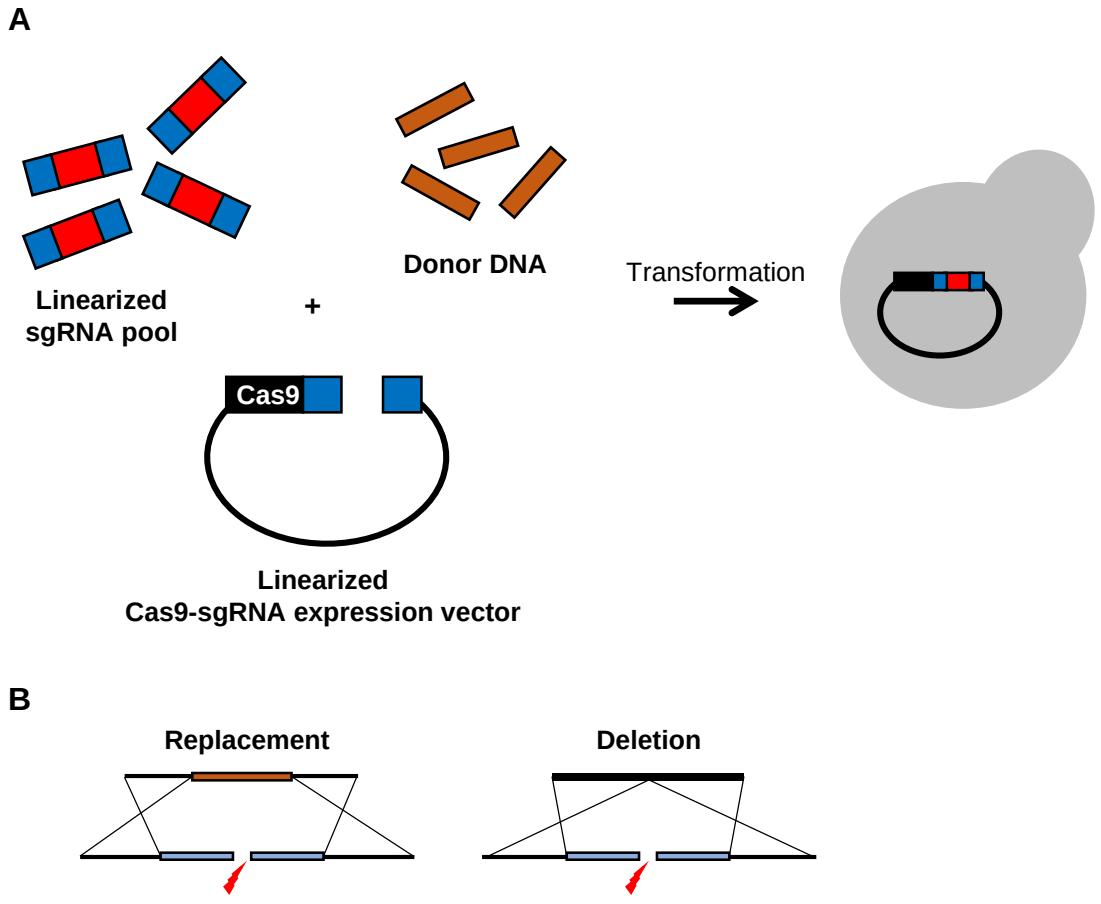

Figure 3.1. CRISPR/Cas9 strategy for gene replacements or deletions.
(A) Figure adapted from (Shaw, W., *https://benchling.com/pub/ellis-crispr-tools*). Yeast transformation of a linearized Cas9 expression vector along with a linearized sgRNA fragment with flanking homology will reconstitute a Cas9-sgRNA expression vector based on gap repair of the linearized fragments. The marker on the Cas9-sgRNA vector is used for selection of yeast transformants. The use of multiple sgRNA cassettes allows for multiplexed Cas9 targeting in a single transformation. **(B)** Co-transformation of donor DNA allows the targeted CRISPR-mediated replacement or deletion of an ORF. In this study, yeast ORFs were deleted or replaced by the cognate human ORFs for complementation assays.

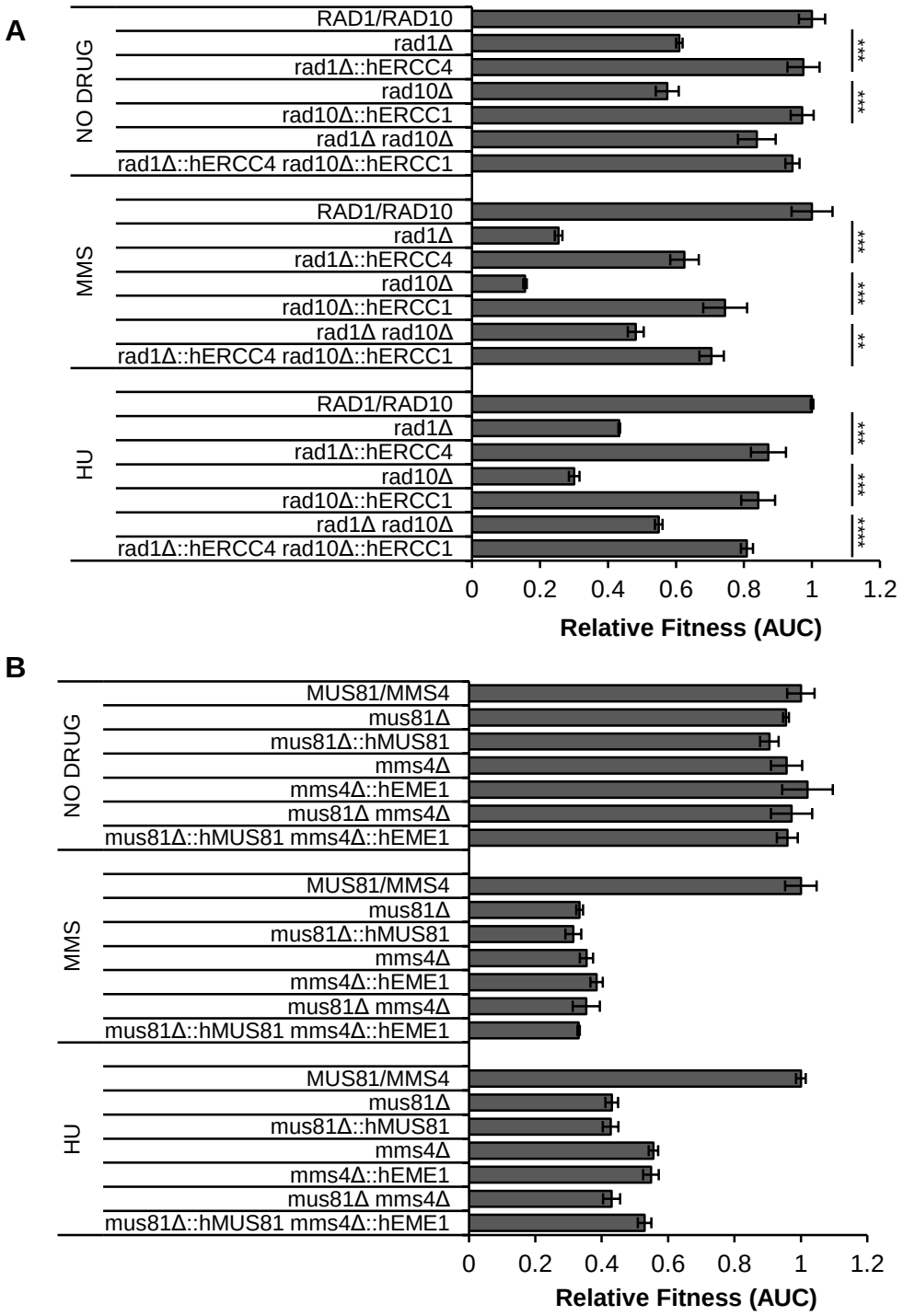

Figure 3.2. Testing complementation of two-subunit yeast complexes.
(A) hErcc4/hErcc1 expression (separately or together) rescues *rad1Δ/rad10Δ* sensitivity to MMS (0.01%) and HU (150mM). Student's t-test. **p<0.01; ***p<0.001; ****p<0.0001. **(B)** hMus81/hEme1 expression (separately or together) does not rescue *mus81Δ/mms4Δ* sensitivity to MMS and HU. Each strain was tested in three replicates per condition and area under the curve (AUC) value was calculated for each replicate independently. Strain fitness was defined as the AUC of each yeast strain relative to the AUC of the wild-type (BY4742) strain grown in the same media condition (mean +/- SD). Corresponding growth curves are shown in Figure A.4.

A

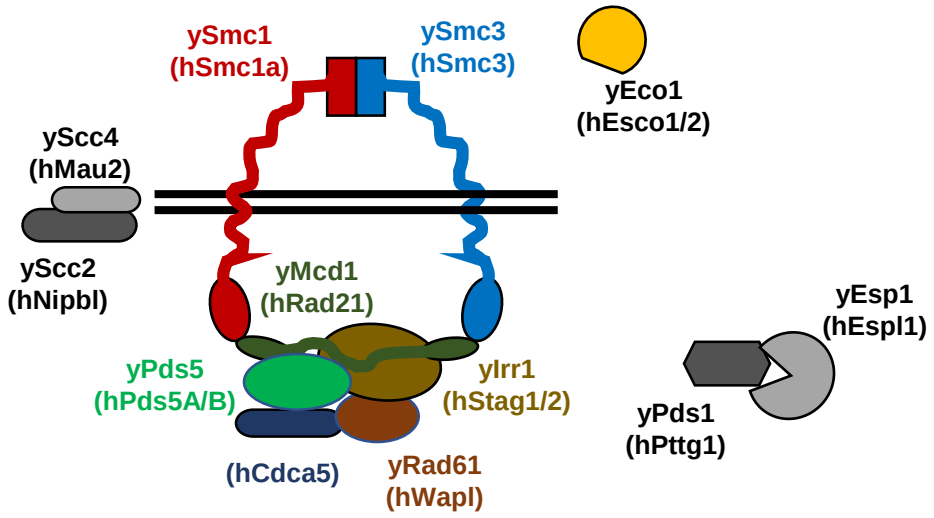

B

	YEAST GENE	YEAST PROTEIN	HUMAN GENE	HUMAN PROTEIN	% IDENTITY	COMPLEMENTATION (This study or PMID)
Core complex	*SMC1*	1225aa	*SMC1A*	1233aa	32	NO (Chap. 3)
	SMC3	1230aa	*SMC3*	1217aa	33	
	MCD1	566aa	*RAD21*	631aa	26	NO (Chap. 2,3)
	IRR1	1150aa	*STAG2*	1268aa	24	NO (Chap. 2,3) (22715410)
			STAG1	1258aa	23	NO (22715410)
Loader complex	*SCC2*	1493aa	*NIPBL*	2804aa	25	NO (Chap. 3)
	SCC4	624aa	*MAU2*	613aa	18	NO (Chap. 2)
Accessory	*PDS5*	1277aa	*PDS5B*	1447aa	23	
			PDS5A	1337aa	21	
	ECO1	281aa	*ESCO1*	840aa	32	NO (Chap. 2,3)
			ESCO2	601aa	30	
	RAD61	647aa	*WAPL*	1190aa	27	NO (Chap. 2)
	--------		*CDCA5*	252aa		
	ESP1	1630aa	*ESPL1*	2120aa	25	
	PDS1	373aa	*PTTG1*	202aa	16	NO (Chap. 3)

Figure 3.3. Complementation of the yeast cohesin complex.
(A) Schematic diagram depicting the cohesin core complex, loader complex, and associated accessory proteins. Human protein names are in parenthesis. **(B)** Comparing yeast and human subunits of the cohesin complex and associated accessory proteins. Individual human cohesin subunits do not complement yeast cohesin genes as seen from data in Chapter 2 and 3 of this study. In Chapter 2, complementation was assessed in deletion mutant backgrounds in the one-to-one screens, while in Chapter 3, complementation was assessed in temperature-sensitive strains (Figures 3.4 and 3.5).

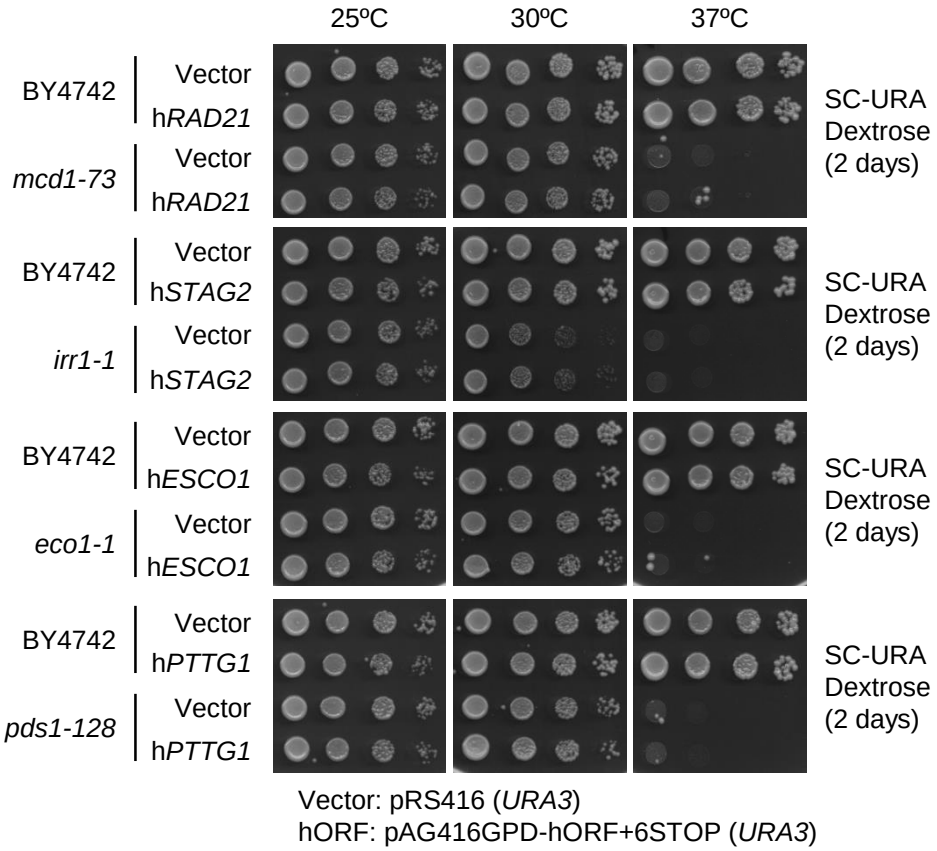

Figure 3.4. Testing complementation of single cohesin mutants by constitutive expression of human cohesin genes.
Wild-type (BY4742) and yeast temperature-sensitive strains transformed with indicated plasmids were spotted in 10-fold serial dilutions to test rescue of temperature sensitivity. Constitutive expression of human orthologs does not rescue temperature sensitivity of yeast strains.

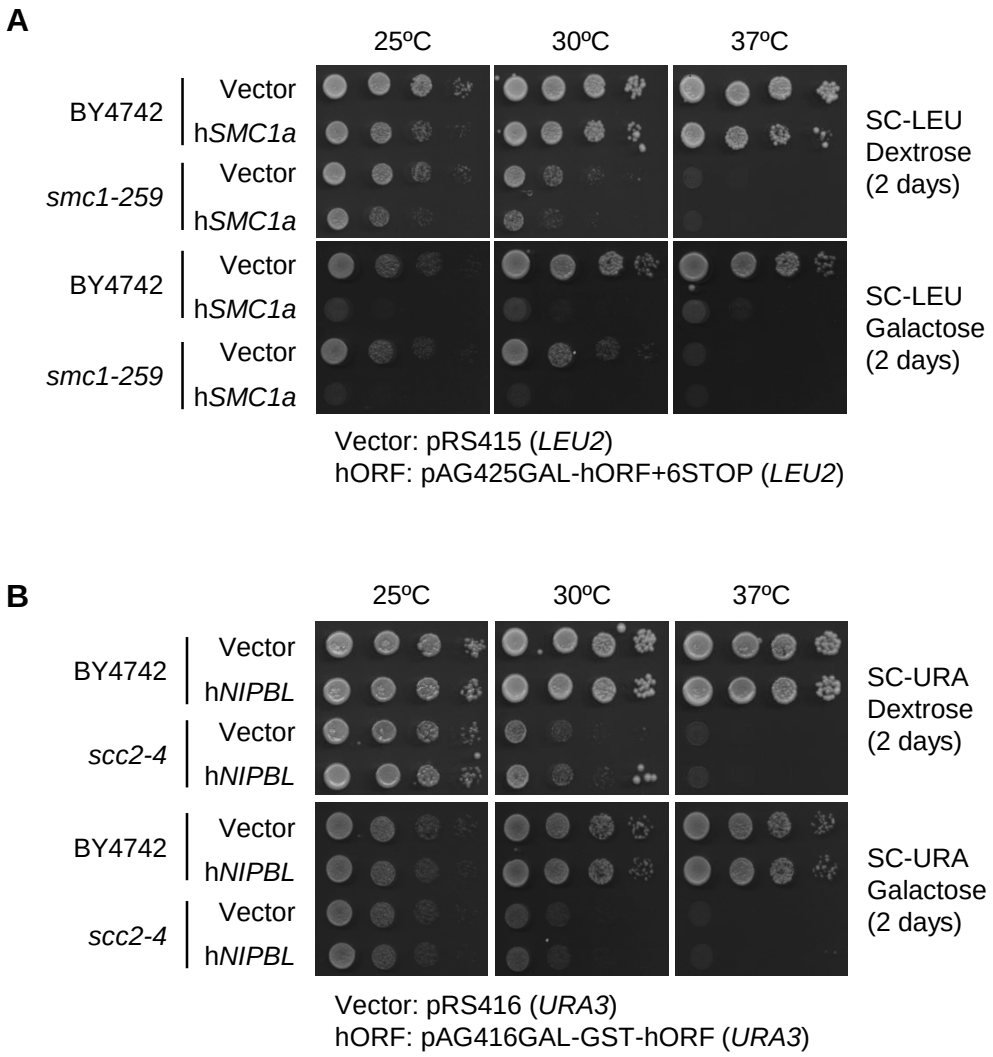

Figure 3.5. Testing complementation of single cohesin mutants by inducible expression of human cohesin genes.
Wild-type (BY4742) and yeast temperature-sensitive strains transformed with indicated plasmids were spotted in 10-fold serial dilutions to test rescue of temperature sensitivity. Strains were plated on galactose media to induce expression of human genes. **(A)** Human *SMC1A* overexpression causes fitness defects in yeast. **(B)** Human *NIPBL* overexpression does not rescue temperature sensitivity of yeast strain.

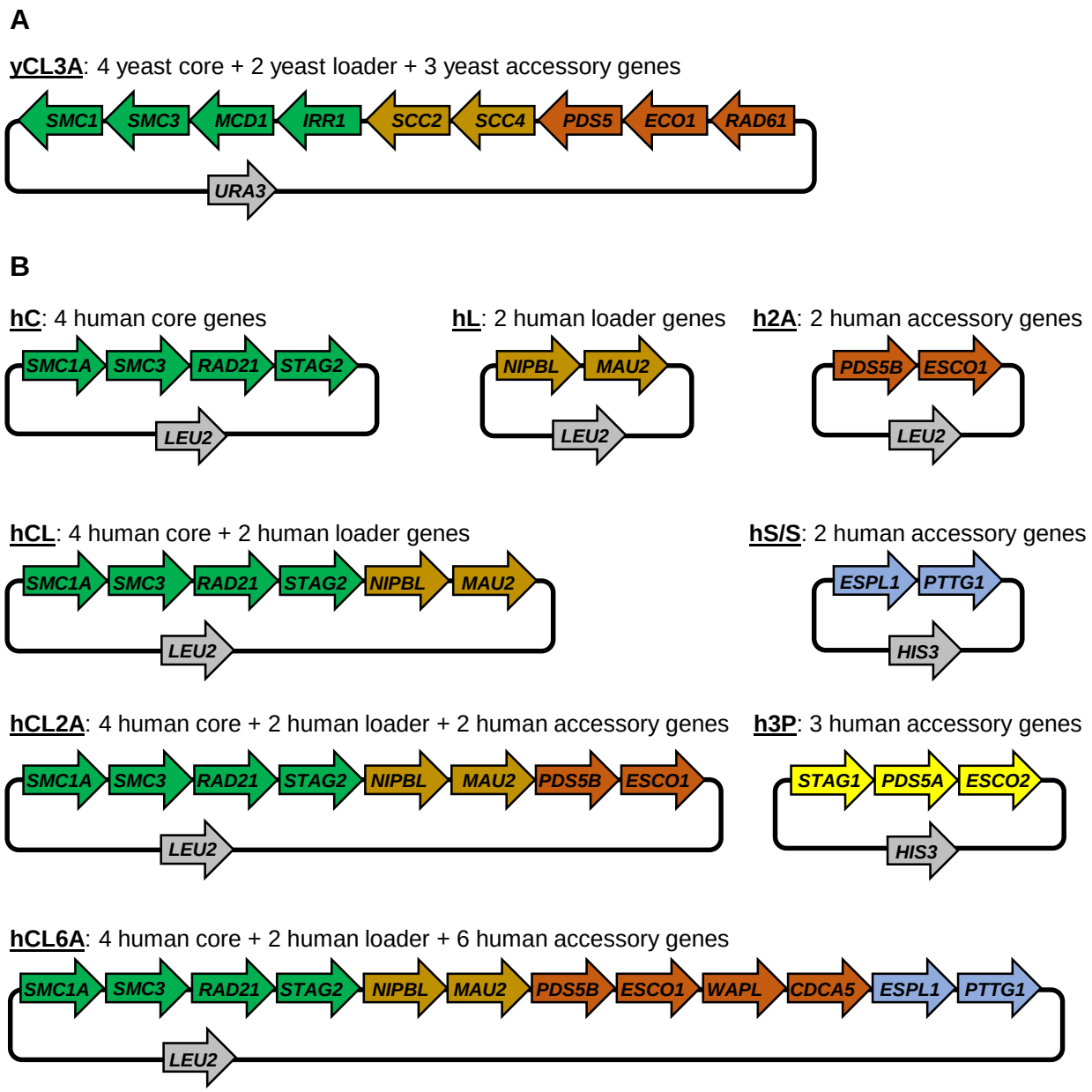

Figure 3.6. Design of yeast and human cohesin neochromosomes.
(A) yCL3A contains yeast cohesin genes and was cloned on the bottom strand. Yeast genes are flanked by endogenous promoters and heterologous terminators. **(B)** Human cohesin genes are flanked by the endogenous yeast promoter and terminator of the corresponding yeast ortholog (except for h*CDCA5* which has no known yeast homolog, and was designed with the yeast promoter of y*RPL13A* and terminator of y*RPL22B*. The neochromosome sizes are yCL3A: 40,321bp; hC: 22,139bp; hCL: 37,278bp; hCL2A: 45,451bp; hCL6A: 59,307bp.

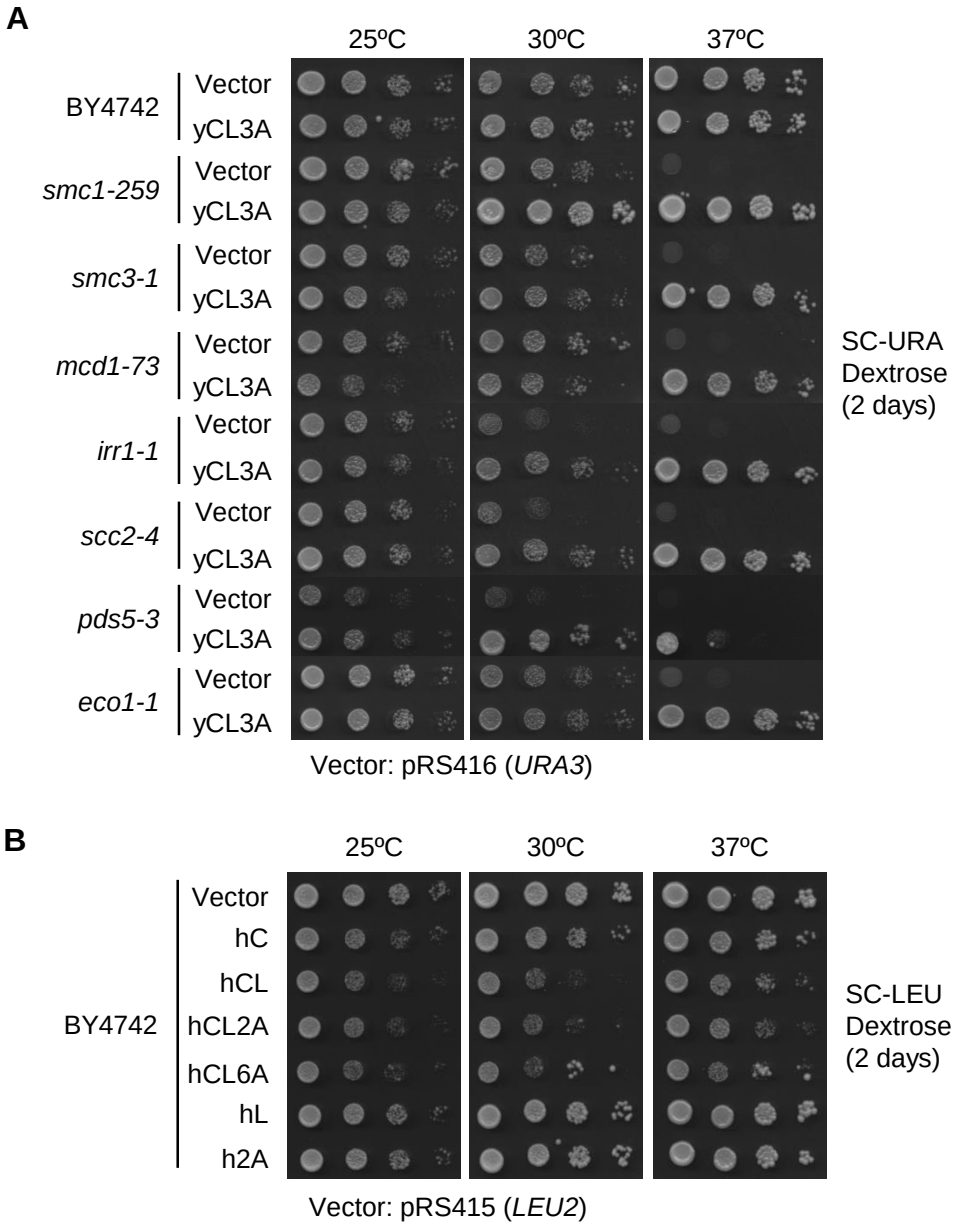

Figure 3.7. Expression of yeast and human cohesin neochromosomes in yeast.
(A) Wild-type (BY4742) and yeast cohesin temperature-sensitive strains transformed with indicated plasmids were spotted in 10-fold serial dilutions to test rescue of temperature sensitivity. Yeast cohesin neochromosome (yCL3A) rescues temperature sensitivity of cohesin temperature-sensitive strains. **(B)** Expression of human cohesin genes (hC, hCL, hCL2A, hCL6A) but not (hL, h2A) causes fitness defects in yeast. Wild-type (BY4742) strains with indicated plasmids were spotted in 10-fold serial dilutions.

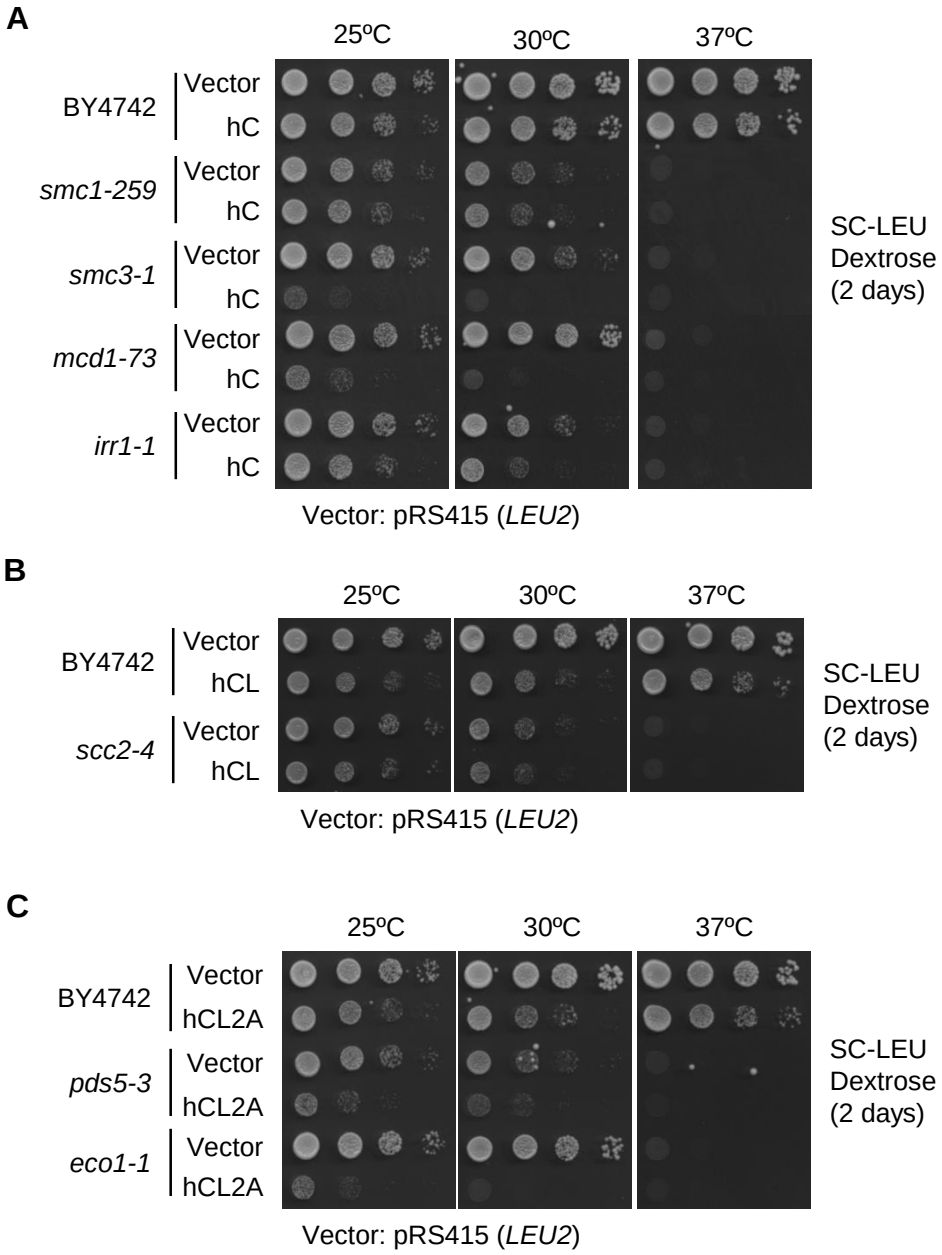

Figure 3.8. Testing complementation of single cohesin mutants by human neochromosomes hC, hCL, hCL2A.
Wild-type (BY4742) and yeast cohesin temperature-sensitive strains transformed with indicated plasmids were spotted in 10-fold serial dilutions to test rescue of temperature sensitivity. **(A)** hC does not rescue temperature sensitivity of yeast cohesin core temperature-sensitive mutants. hC causes fitness defects in WT yeast and this effect is amplified in some yeast cohesin mutants. **(B)** hCL does not rescue temperature sensitivity of a yeast cohesin loader temperature-sensitive mutant. hCL causes fitness defects in WT yeast. **(C)** hCL2A does not rescue temperature sensitivity of yeast cohesin accessory temperature-sensitive mutants. hCL2A causes fitness defects in WT yeast and this effect is amplified in some yeast cohesin mutants.

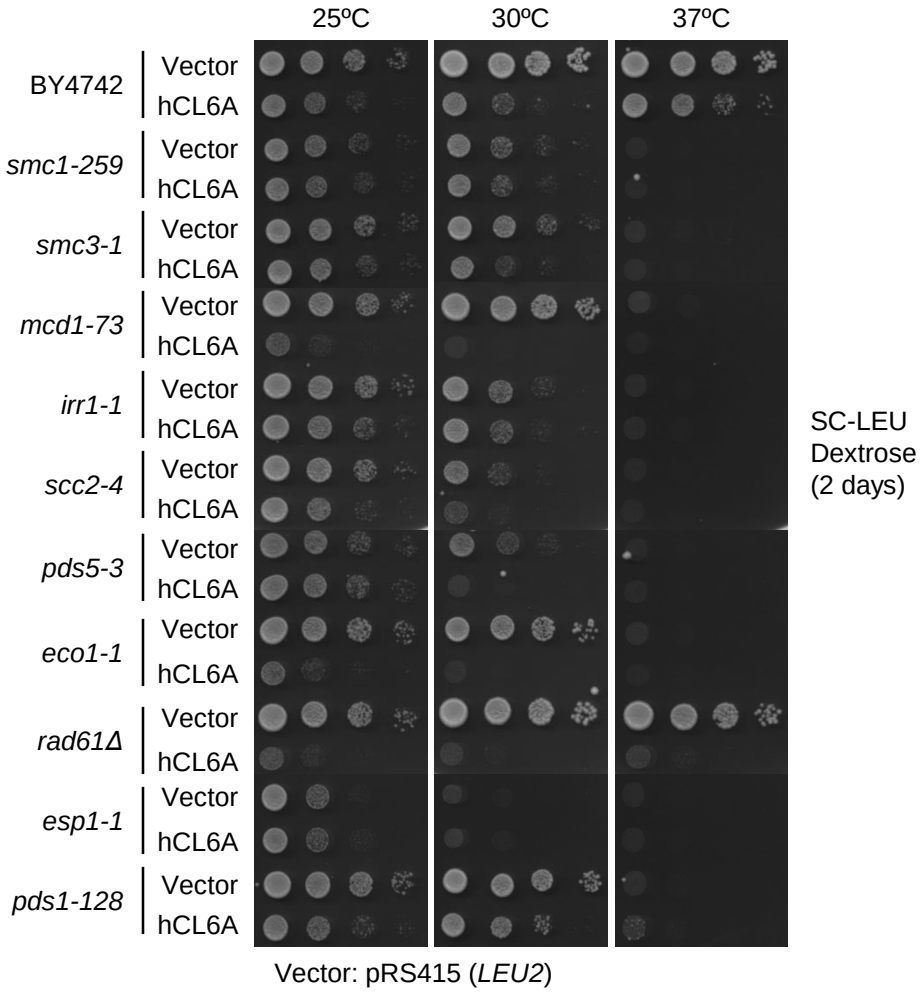

Figure 3.9. Testing complementation of single cohesin mutants by human neochromosomes hCL6A.
Wild-type (BY4742)**,** yeast *rad61Δ* deletion strain and cohesin temperature-sensitive strains transformed with indicated plasmids were spotted in 10-fold serial dilutions to test rescue of temperature sensitivity. hCL6A does not rescue temperature sensitivity of yeast cohesin temperature-sensitive mutants. hCL6A causes fitness defects in WT yeast and this effect is amplified in some yeast cohesin mutants.

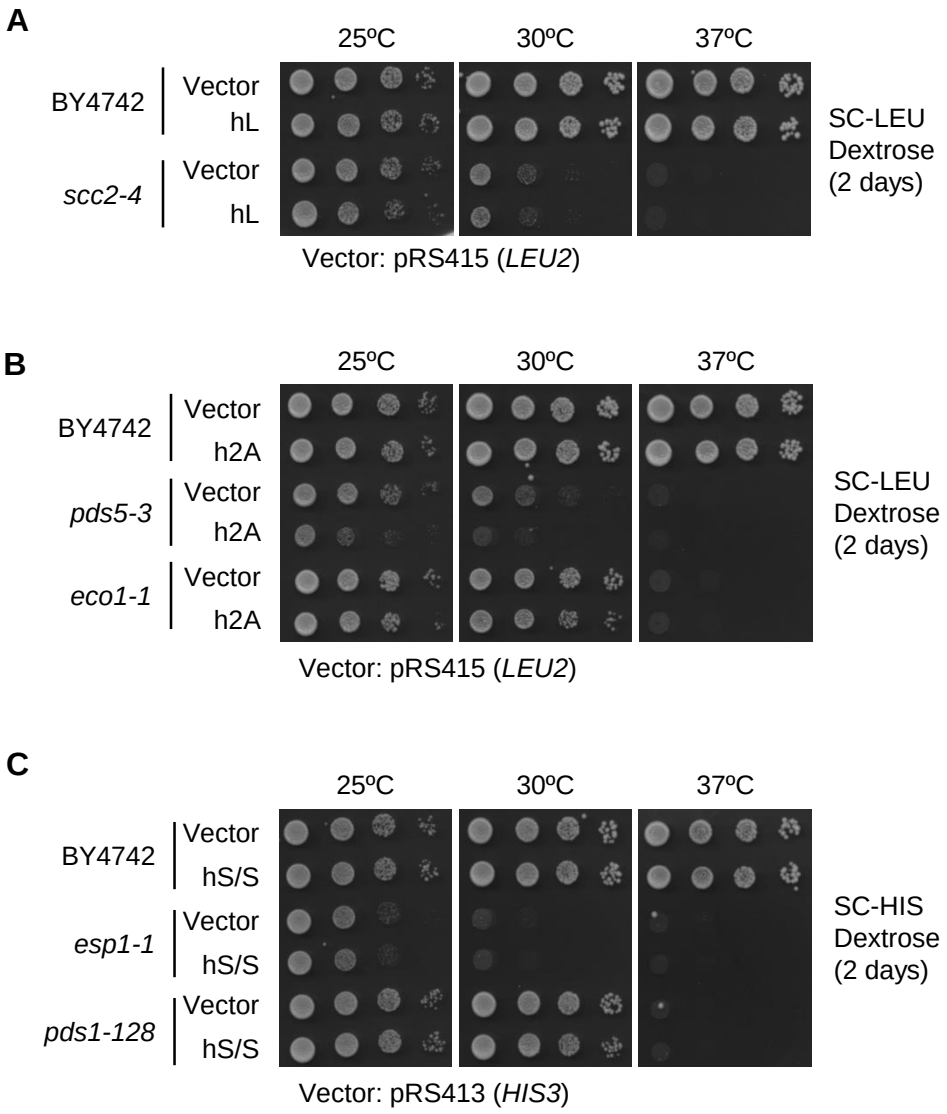

Figure 3.10. Testing complementation of single cohesin mutants by human neochromosomes hL, h2A, hS/S.
Wild-type (BY4742) and yeast cohesin temperature-sensitive strains transformed with indicated plasmids were spotted in 10-fold serial dilutions to test rescue of temperature sensitivity. **(A)** hL does not rescue temperature sensitivity of a yeast cohesin loader temperature-sensitive mutant. **(B)** h2A does not rescue temperature sensitivity of yeast cohesin accessory temperature-sensitive mutants. **(C)** hS/S does not rescue temperature sensitivity of yeast cohesin accessory temperature-sensitive mutants.

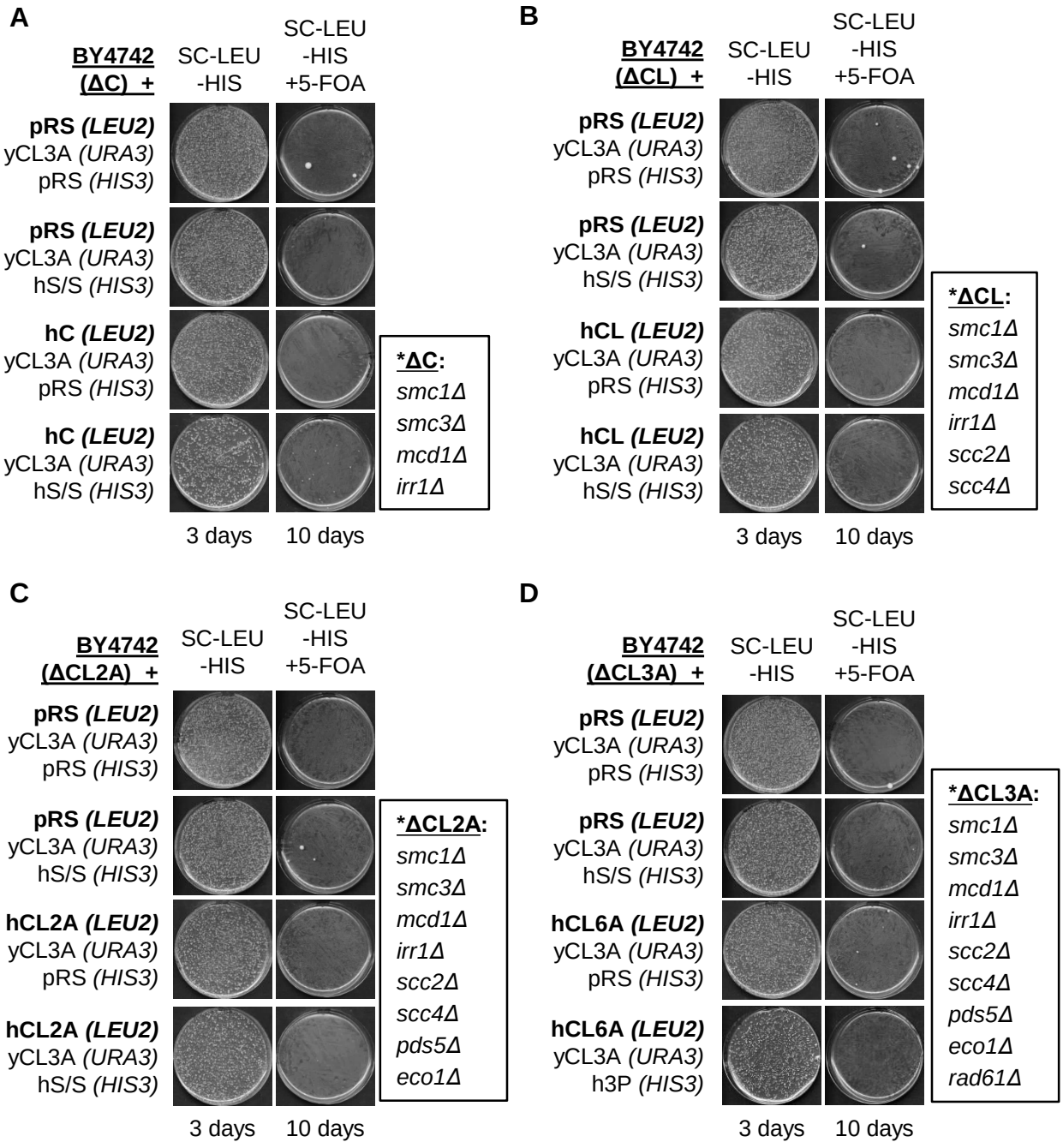

Figure 3.11. Testing complementation of complex cohesin deletion mutants by multiple combinations of human neochromosomes.
CRISPR/Cas9 was used to generate genomic deletions of yeast cohesin genes in the presence of yCL3A**.** Yeast knockout strains covered by *URA3*-marked vectors (yCL3A) were transformed with the indicated *LEU2*- and *HIS3*-marked vectors and maintained on −Ura −Leu −His media. Strains were plated on −Leu −His +5-FOA media to test complementation using 5-FOA plasmid shuffling. In the presented examples, yeast strains were plated 1000-fold higher on 5-FOA plates compared to −Leu −His plates. **(A)** hC does not rescue viability of a ΔC yeast strain +/- hS/S. **(B)** hCL does not rescue viability of a ΔCL yeast strain +/- hS/S. **(C)** hCL2A does not rescue viability of a ΔCL2A yeast strain +/- hS/S. **(D)** hCL6A does not rescue viability of a ΔCL3A yeast strain +/- h3P.

A

	YEAST STRAIN	hC	hCL	hCL2A	hCL6A	hL	h2A	hS/S
Core complex	*smc1-259*	NO			NO			
	smc3-1	TOXIC			NO			
	mcd1-73	TOXIC			TOXIC			
	irr1-1	NO			NO			
Loader complex	*scc2-4*		NO		NO	NO		
Accessory	*pds5-3*			NO	NO		NO	
	eco1-1			TOXIC	TOXIC		NO	
	rad61Δ				TOXIC			
	esp1-1				NO			NO
	pds1-128				NO			NO

B

YEAST STRAIN	hC	hCL	hCL2A	hCL6A	hC+ hS/S	hCL+ hS/S	hCL2A+ hS/S	hCL6A+ h3P
ΔC	NO				NO			
ΔCL		NO				NO		
ΔCL2A			NO				NO	
ΔCL3A				NO				NO

***ΔC**: *smc1Δ smc3Δ mcd1Δ irr1Δ*
***ΔCL**: *smc1Δ smc3Δ mcd1Δ irr1Δ scc2Δ scc4Δ*
***ΔCL2A**: *smc1Δ smc3Δ mcd1Δ irr1Δ scc2Δ scc4Δ pds5Δ eco1Δ*
***ΔCL3A**: *smc1Δ smc3Δ mcd1Δ irr1Δ scc2Δ scc4Δ pds5Δ eco1Δ rad61Δ*

Figure 3.12. Summary of complementation results for the yeast cohesin complex.
Red indicates no complementation was observed. **(A)** Complementation results of yeast cohesin temperature-sensitive strains with indicated human cohesin neochromosomes. **(B)** Complementation results of yeast cohesin deletion strains with indicated human cohesin neochromosomes.

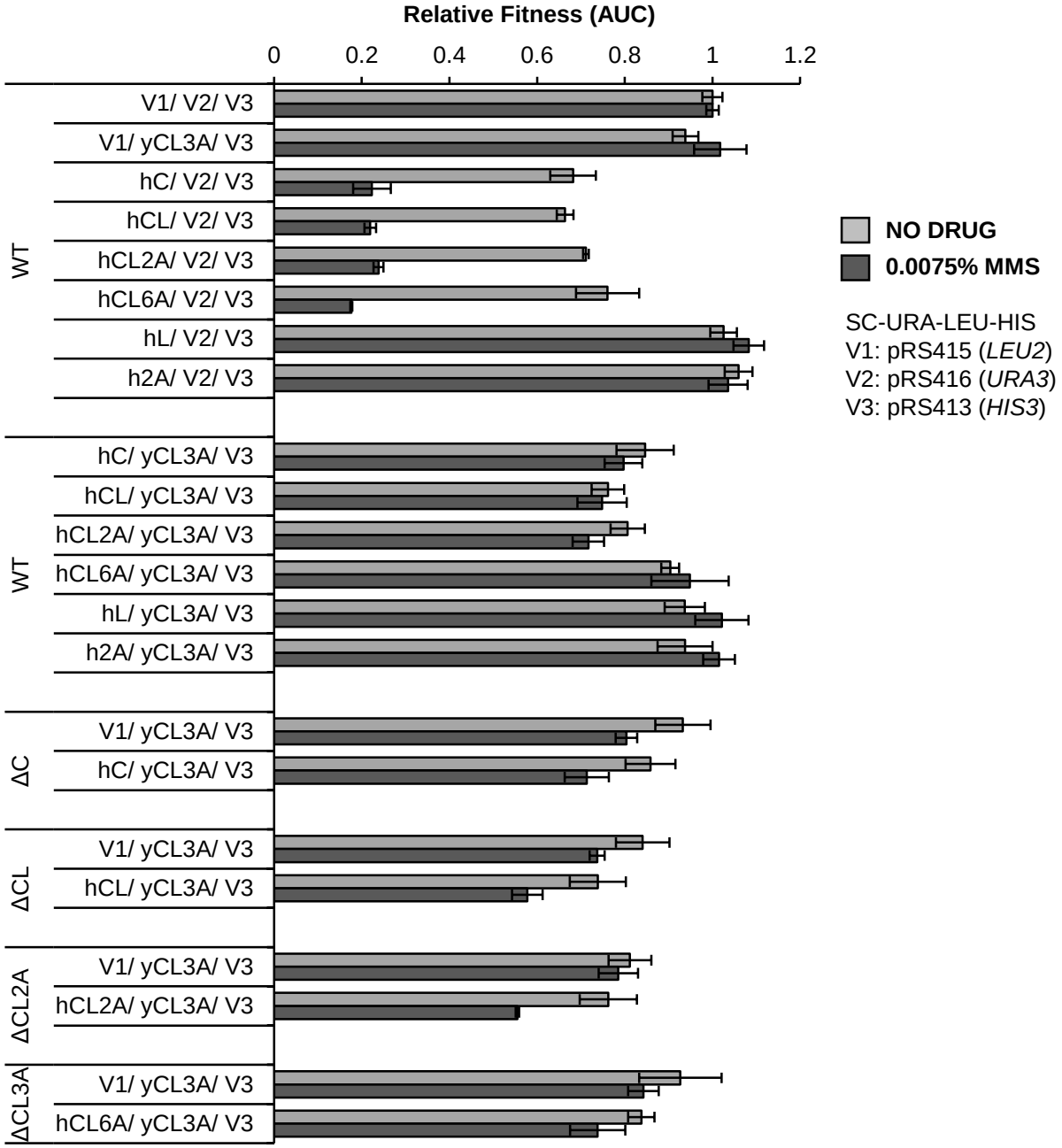

Figure 3.13. Fitness defects resulting from expression of human cohesin genes (without hS/S) are partially rescued by yCL3A.

Yeast neochromosome (yCL3A) rescues fitness defects of strains containing hC, hCL, hCL2A or hCL6A**.** Each strain was tested in three replicates per condition and area under the curve (AUC) value was calculated for each replicate independently. Strain fitness was defined as the AUC of each yeast strain relative to the AUC of the wild-type strain (BY4742) containing vector controls (V1, V2, V3) and grown in the same media condition (mean +/- SD).

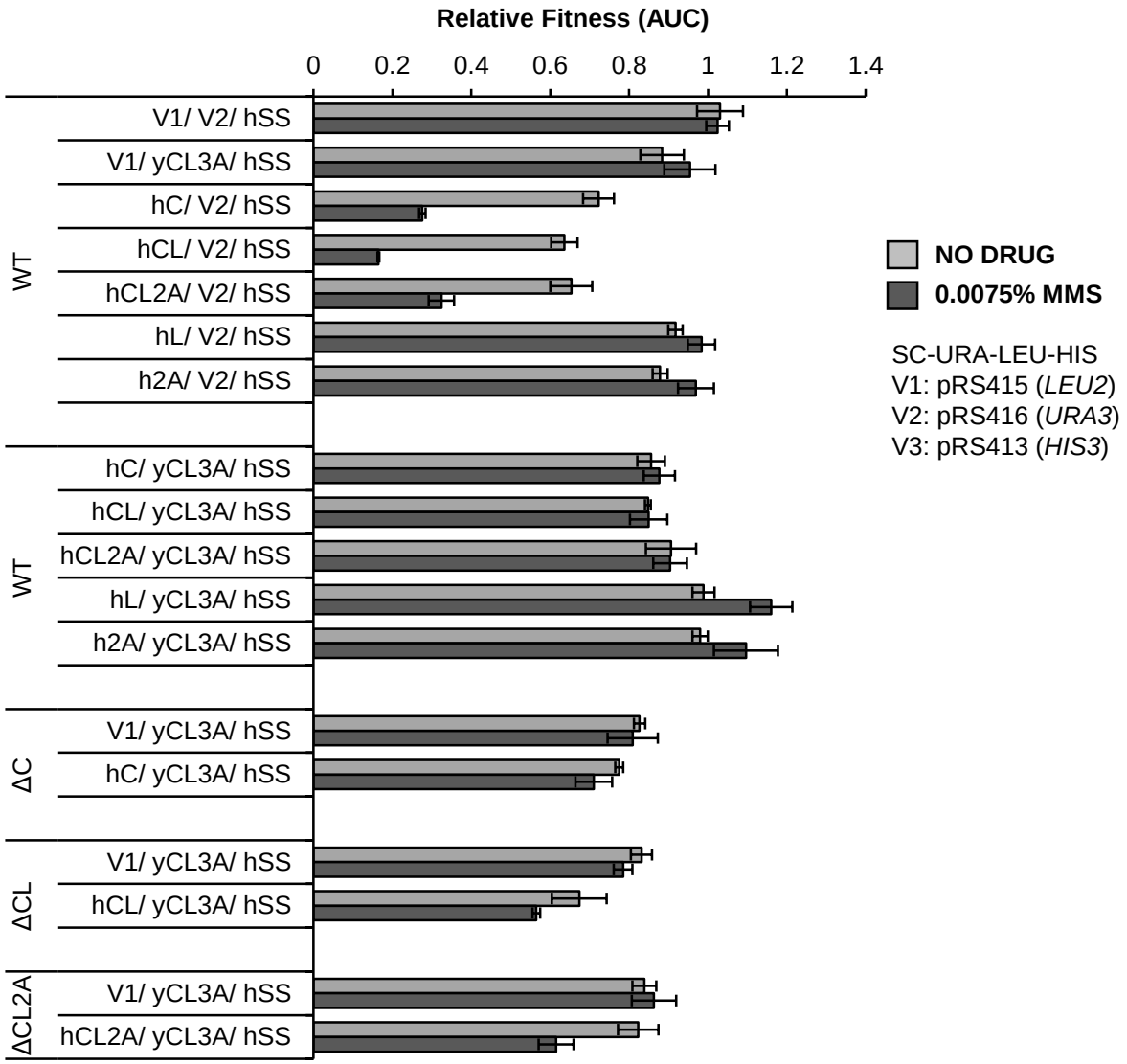

Figure 3.14. Fitness defects resulting from expression of human cohesin genes (with hS/S) are partially rescued by yCL3A.
Yeast neochromosome (yCL3A) rescues fitness defects of strains containing multiple combinations of hS/S with hC, hCL, hCL2A or hCL6A**.** Each strain was tested in three replicates per condition and area under the curve (AUC) value was calculated for each replicate independently. Strain fitness was defined as the AUC of each yeast strain relative to the AUC of the wild-type strain (BY4742) containing vector controls (V1, V2, V3) and grown in the same media condition (mean +/- SD).

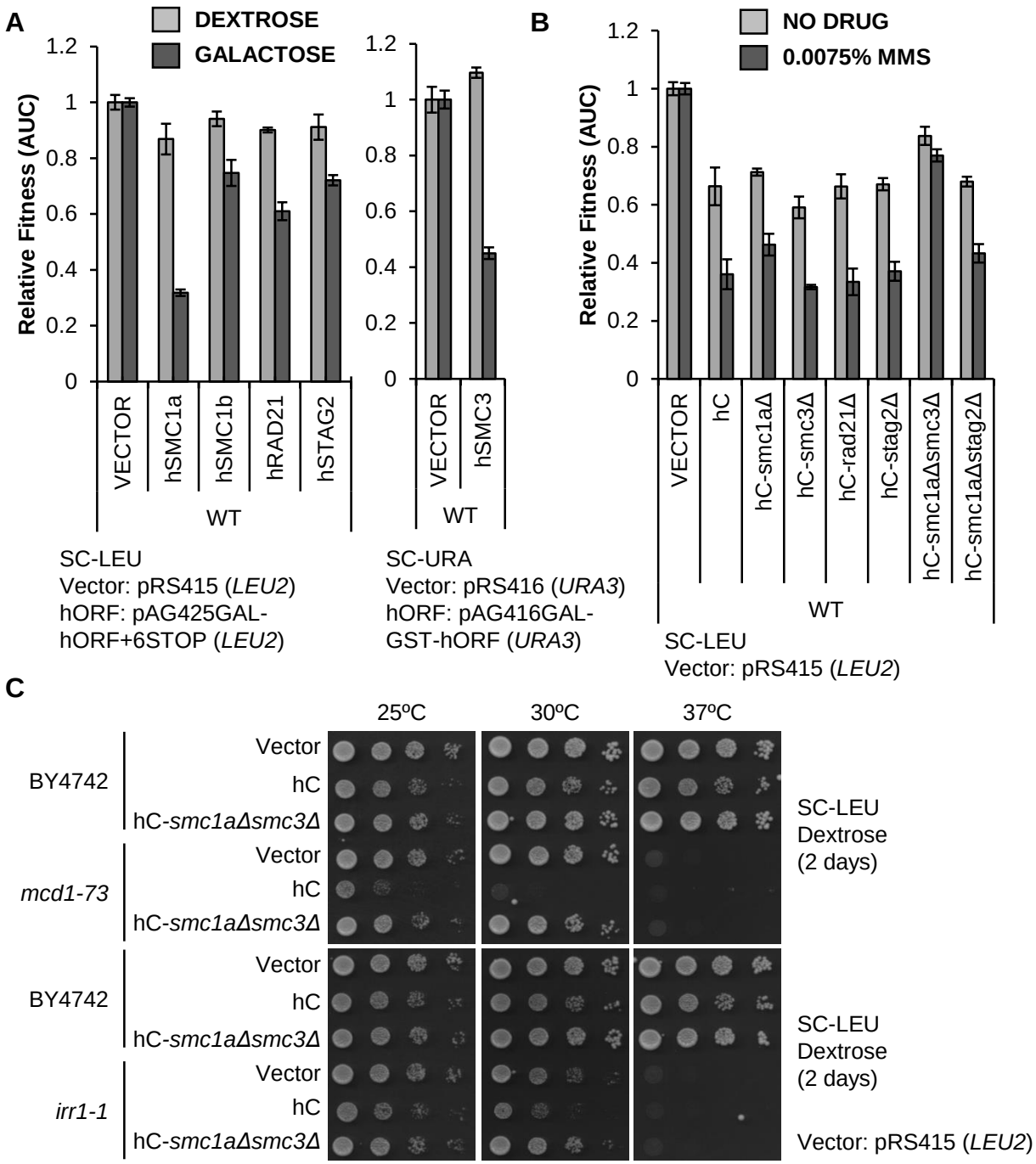

Figure 3.15. Expression of h*SMC1A* and h*SMC3* cause fitness defects in yeast.
(A) Overexpression of h*SMC1A* and h*SMC3* using galactose-inducible promoters cause the strongest fitness defects in yeast. h*SMC1B* is the meiosis-specific subunit. **(B)** Deleting h*SMC1A* and h*SMC3* from hC neochromosome rescues fitness defects and sensitivity to MMS in yeast. For liquid growth assays, each strain was tested in three replicates per condition and area under the curve (AUC) value was calculated for each replicate. Strain fitness was defined as the AUC of each yeast strain relative to the AUC of the wild-type strain (BY4742) containing the vector control and grown in the same media condition (mean +/- SD). **(C)** Deleting h*SMC1A* and h*SMC3* from hC neochromosome rescues fitness defects in yeast. Yeast strains transformed with indicated plasmids were spotted in 10-fold serial dilutions.

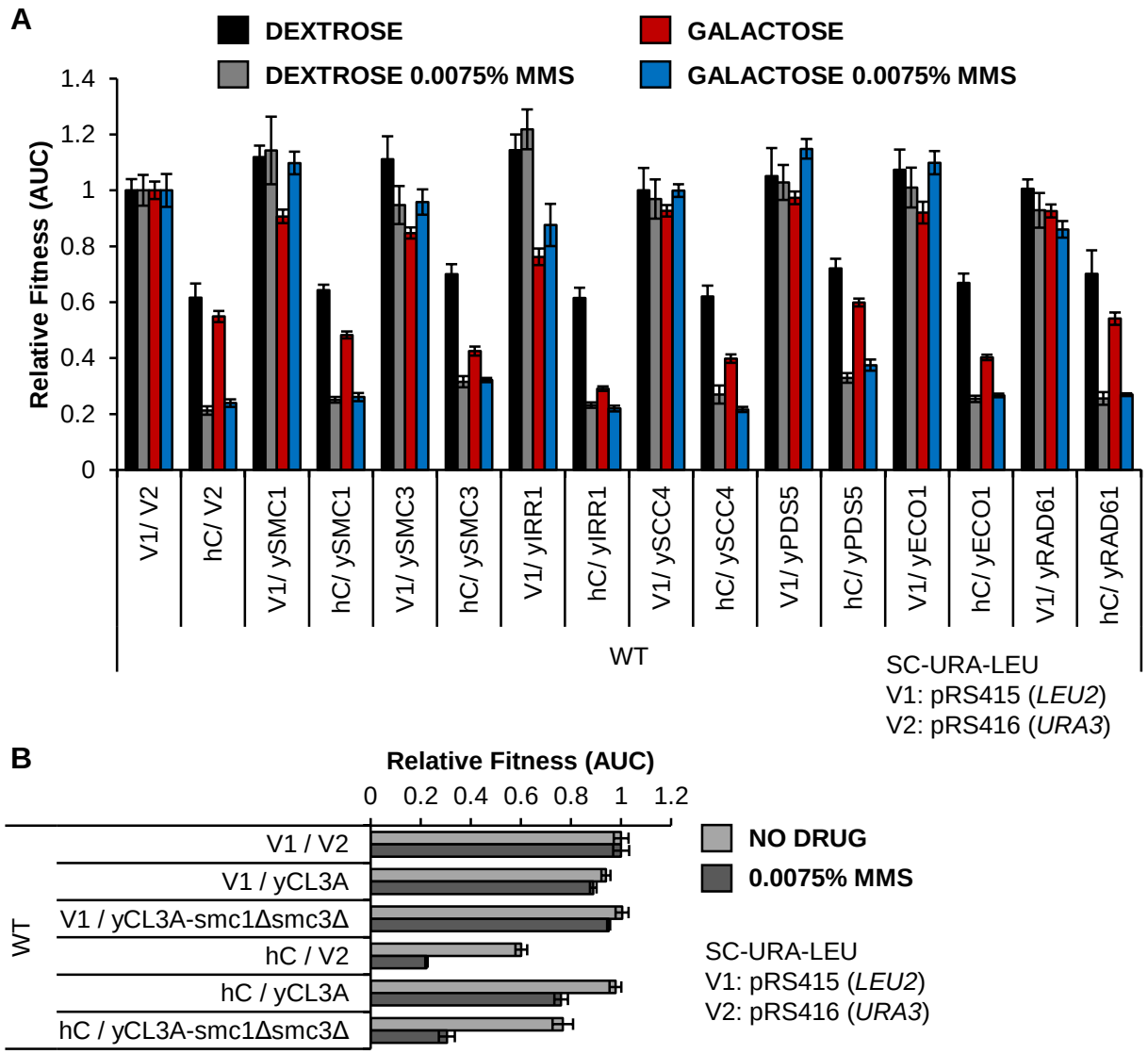

Figure 3.16. Yeast *SMC1* and *SMC3* are required to rescue fitness defects that result from expression of human cohesin genes in yeast.
For liquid growth assays, each strain was tested in three replicates per condition and area under the curve (AUC) value was calculated for each replicate. Strain fitness was defined as the AUC of each yeast strain relative to the AUC of the wild-type strain (BY4742) containing the vector controls and grown in the same media condition (mean +/- SD). **(A)** Overexpression of individual yeast cohesin genes does not rescue fitness defects resulting from the hC neochromosome in MMS. Yeast strains were grown in galactose media to induce expression. **(B)** Rescue of fitness defects of yeast containing hC by yCL3A is dependent on yeast *SMC1* and *SMC3*.

CHAPTER 4: APPLICATIONS OF HUMAN-YEAST CROSS-SPECIES COMPLEMENTATION

4.1 Introduction

4.1.1 Utilizing complementation to assess tumor-specific variants

Differentiating driver from passenger mutations in tumor genomes and understanding how driver mutations cause cancer cell phenotypes are major challenges. Driver mutations confer a selective growth advantage to the cell while passenger mutations have no effect on that growth advantage, and the number of somatic variants in human cancers can range from tens to hundreds per tumor (Vogelstein et al., 2013). The rate of discovery of somatic variants outpaces the rate at which they have been functionally tested (Pon and Marra, 2015), and as such, a platform to fill this gap and test variants is of great value.

An enabling characteristic of cancer is chromosome instability (CIN), which is an important predisposing factor in the progression and heterogeneity of tumors because it increases the likelihood of loss of tumor-suppressor genes, mutation/ amplification/ rearrangement of oncogenes, and accelerates the evolution of cancer cells to adapt to the tumor environment (Hanahan and Weinberg, 2011; Negrini et al., 2010). The budding yeast, *Saccharomyces cerevisiae*, has been used to define cellular pathways and catalog a comprehensive list of yeast genes required for the maintenance of chromosome stability (Stirling et al., 2011; Yuen et al., 2007). The yeast CIN gene list facilitates identification, by sequence homology, of candidate human CIN genes whose somatic variants may contribute to chromosome instability and tumorigenesis (Barber et al., 2008; Stirling et al., 2011). Budding yeast can be exploited to screen these human genetic variants using cross-species complementation for prioritizing and directing functional studies in mammalian models

(Dunham and Fowler, 2013). In this chapter, we demonstrate the feasibility of using yeast to screen cancer specific human gene variants by extending cross-species complementation to 45 tumor-specific mutations in CIN genes.

4.1.2 Utilizing complementation to generate SDL human-yeast genetic interaction networks for inactive hFen1

The yeast CIN gene list identifies candidate human CIN genes whose mutation or overexpression may contribute to tumorigenesis (Barber et al., 2008; Duffy et al., 2016; Stirling et al., 2011). Yeast assays have demonstrated that deletion or overexpression of y*RAD27* (ortholog of h*FEN1*) causes CIN and DNA damage in yeast (Duffy et al., 2016; Greene et al., 1999; Yuen et al., 2007), while studies using human cells confirmed that overexpression of h*FEN1* causes DNA damage (Becker et al., 2018; Jimeno et al., 2017). DNA flap endonuclease 1 (h*FEN1*) functions in DNA replication and repair and is required for Okazaki fragment maturation through removal of 5' flaps during lagging-strand synthesis (Balakrishnan and Bambara, 2013). Due to its key role in DNA replication, h*FEN1* has been shown to support rapid proliferation of cancer cells and is overexpressed in breast (Abdel-Fatah et al., 2014; He et al., 2016; Singh et al., 2008), lung (He et al., 2017; Nikolova et al., 2009), prostate (Lam et al., 2006), gastric (Wang et al., 2014), brain (Krause et al., 2005) and pancreatic (Iacobuzio-Donahue et al., 2003) cancer. Many studies have reported the screening and development of h*FEN1* inhibitors as potential anti-cancer therapeutics (Dorjsuren et al., 2011; Exell et al., 2016; He et al., 2016; McWhirter et al., 2013; Tumey et al., 2005; van Pel et al., 2013). Here, we carried out synthetic dosage lethal (SDL) screens using transcriptionally inducible forms of wild-type and catalytically-inactive human *FEN1*

as queries. We reasoned that the use of catalytically inactive forms of hFen1 would allow us to model hFen1 protein/small molecule inhibitor interactions in yeast to explore under which conditions an inhibited form of hFen1 exhibited a dominant SDL effect. The dominant synthetic lethal effect of inhibitor-mediated protein trapping on DNA has been shown for clinically-relevant inhibitors of PARP (Murai et al., 2012) and topoisomerase (Hsiang et al., 1989). The SDL screens described in this chapter, using overexpressed catalytically-inactive hFen1 as a query, identified synthetic lethal vulnerabilities that could potentially be targeted for the selective killing of tumor cells relative to normal cells due to the effects of protein trapping.

4.2 Methods

4.2.1 Generating variants and yeast strains for complementation of essential genes

Expression vectors and yeast strain construction: Human cDNAs h*LIG1*, h*SSRP1*, h*PPP1CA*, and h*PPP1CC* in Gateway-compatible entry clones were obtained from the hORFeome V8.1 collection (Yang et al., 2011) and shuttled into the yeast destination vectors pAG416GPD-ccdB-HA (*URA3*, CEN, constitutive GPD promoter, C-terminal HA tag) and pAG415GPD-ccdB-HA (*LEU2*, CEN, constitutive GPD promoter, C-terminal HA tag) (Alberti et al., 2007) using LR Clonase II (Invitrogen) to generate expression clones. Missense mutations were introduced in vector pAG415GPD-hORF-HA (*LEU2*) using the QuikChange Site-Directed Mutagenesis Kit (Agilent), and verified by Sanger sequencing (Table A.10). To generate the yeast haploid knockout strains, tetrads were dissected following transformation of the expression vector pAG416GPD-hORF-HA (*URA3*) to the corresponding heterozygous diploid deletion strain and then haploids were maintained on

SC−Ura media. To generate the strains used for liquid growth assays, expression clones containing wild-type and mutant human cDNA on pAG415GPD-hORF-HA (*LEU2*) were first transformed into both the generated haploid knockouts (covered by wild-type human cDNA marked by *URA3*) (*MAT*α *his3*Δ *leu2*Δ *ura3*Δ *yORF*Δ + hORF) and the isogenic wild-type strain (BY4742) (Brachmann et al., 1998) and maintained on SC−Ura−Leu or SC−Leu media, respectively. For the plasmid shuffle (Boeke et al., 1987), strains were then plated on SC−Leu +Ura +5-FOA (0.1%) media and individual colonies were picked and thereafter maintained on SC−Leu media. To confirm that the *URA3*-marked plasmid was lost, strains were streaked on SC−Ura media to observe lack of growth.

Growth curves: Unless otherwise indicated, all growth conditions were carried out in SC−Leu media at 30°C. Strains were inoculated overnight, diluted to a cell density of 0.1 OD_{600}, and then grown to mid-log phase. Strains were then diluted to OD_{600}=0.1 in 200µl SC−Leu media with no drug, 0.01% MMS, or 100mM HU in 96-well plates. OD_{600} readings were measured every 30 minutes over a period of 48h in a TECAN M200 plate reader. Prior to each reading, plates were shaken for 10 minutes. Each strain was tested in three to four replicates per plate per condition and area under the curve (AUC) value was calculated for each replicate independently. For growth curves in SC−Leu and SC−Leu +100 mM HU, AUC values were calculated from 0–24h, which is when most strains reached saturation. For growth curves in SC−Leu +0.01% MMS, AUC values were calculated from 0–48h. For each mutant, strain fitness was defined as the AUC of the mutant curves relative to the AUC of the wild-type allele grown on the same plate in the same media condition. Significant differences in growth in the “no drug” condition was determined against the wild-type allele in the same

condition, while significant differences in growth in the “drug” condition was determined against the same allele in the no drug condition using a Student’s t-test.

4.2.2 Generating variants and yeast strains for complementation of a nonessential gene

Expression vectors and yeast strain construction: Human *PPP2R1A* in a Gateway-compatible entry clone was obtained from hORFeome V8.1 (Yang et al., 2011); yeast *TPD3* was obtained from the Gateway-compatible FLEX array (Hu et al., 2007) and the cDNA was shuttled to a donor vector to generate the entry clone using BP Clonase II (Invitrogen). Missense mutations were introduced in the entry clones using the Quikchange site-directed mutagenesis kit (Agilent), and verified by Sanger sequencing. Wild-type and mutant y*TPD3* or h*PPP2R1A* entry clones were then shuttled into the yeast destination vector pAG416GPD-ccdB+6Stop (*URA3*, CEN, constitutive GPD promoter, 6-amino-acid C-terminal extension) (Alberti et al., 2007; Kachroo et al., 2015) using LR Clonase II (Invitrogen) to generate expression clones (Table A.10). Generated wild-type and mutant y*TPD3* or h*PPP2R1A* expression vectors and the vector control pRS416 (*URA3*) (Sikorski and Hieter, 1989) were transformed into wild-type *MAT*α BY4742 (Brachmann et al., 1998) and *tpd3*Δ from the *MAT*α yeast haploid knockout collection (Giaever et al., 2002) and maintained on SC−Ura media.

Growth and ALF assays: For spot assays, wild-type and mutant strains containing *URA3*-marked vectors were grown to saturation at 25°C then serially diluted in 10-fold increments and plated (5µl each spot) onto SC−Ura media at 25°C, 37°C and 30°C +/- chemicals. For ALF assays, colonies containing *URA3*-marked vectors were patched in 1-cm^2 squares on SC−Ura media and incubated at 30°C for 2 days. Patches were mated to a *MAT*α *his1* tester lawn by replica plating on YPD followed by incubation at 30°C for 24h. The mated lawn was

replica-plated to SC-6 (−Ura −Lys −Ade −His −Trp −Leu) media and incubated for 2 days at 30°C to select for His^+ products.

Whole cell extract and western blotting: Wild-type and the hR183W variant of h*PPP2R1A* in entry clones were shuttled into the yeast destination vector pAG416GPD-ccdB-HA (*URA3*, CEN, constitutive GPD promoter, C-terminal HA tag) as described previously in methods. Generated expression vectors and the vector control pRS416 were transformed into wild-type BY4742 and maintained on SC−Ura media. Yeast cells were grown in 50ml SC−Ura media at 30°C to mid-log phase and harvested before resuspension of cell pellets in equal volume of Tackett Extraction Buffer (20mM HEPES pH 7.4, 0.1% Tween20, 2mM $MgCl_2$, 200mM NaCl, protease inhibitors) (Hamza and Baetz, 2012). To lyse the cells, glass beads were added to the samples, and the mixture was vortexed in five-1 minute blasts with 1 minute incubation on ice between each vortex round. A 21-gauge needle (Becton Dickinson) was used to separate the crude whole cell extract from the beads into a new Eppendorf by poking a hole in the bottom of the tube and centrifuging at 1000rpm for 1 minute. Lysates were cleared via centrifugation at 3000rpm for 15 minutes at 4°C and normalized by protein concentration using the Bradford assay (Bio-Rad). Protein samples were subjected to SDS-PAGE and western blotting. Primary antibodies used included anti-HA (Abcam, catalog no. ab18181, 1:1000) and anti-PGK1 (Invitrogen catalog # 459250, 1:5000), while the secondary antibody used was goat anti-mouse horse-radish peroxidase (HRP) (1:10000).

4.2.3 Synthetic dosage lethality (SDL) screens

Expression vectors and yeast strains: Human *FEN1* in an entry clone was obtained from hORFeome V8.1 (Yang et al., 2011), and yeast *RAD27* from the Gateway-compatible FLEX array (Hu et al., 2007) was shuttled to a donor vector to generate the entry clone using BP

Clonase II (Invitrogen). Missense mutations (D179A [536A>C] for y*RAD27*; D181A [542A>C] and E158A [473A>C] for h*FEN1*) were introduced in the entry clone using the Quikchange site-directed mutagenesis kit (Agilent), and verified by Sanger sequencing. Wild-type and mutant y*RAD27* or h*FEN1* entry clones were then shuttled into the yeast destination vector pAG425GAL-ccdB+6Stop (*LEU2*, 2µ, inducible GAL promoter, 6-amino-acid C-terminal extension) (Alberti et al., 2007; Kachroo et al., 2015) as previously described in methods (Table A.10). Generated over-expression vectors and the vector control pRS425 (*LEU2*) (Christianson et al., 1992) were transformed into the SGA-starter strain (Y7092) (*MATα can1Δ::STE2pr-his5 lyp1Δ ura3Δ0 leu2Δ0 his3Δ1 met15Δ0*) and transformants were selected on SC−Leu media.

SDL screens and overexpression experiments: The SDL screens were performed as previously described (Duffy et al., 2016). Query strains (Y7092) containing *LEU2*-marked vectors were crossed to a mini-array comprising 332 *MAT*a yeast deletion strains and 50 wild-type strains using synthetic genetic array (SGA) technology (Tong et al., 2001). A series of replica-pinning steps using a Singer® RoToR robot generated an array of deletion mutants containing either a vector control or the overexpression plasmids which were induced by pinning on to media containing galactose. Initially, query strains were grown to saturation in triplicates in SC−Leu before plating on the same media to generate lawns of cells. Query strains were mated to the mini-array on YPD and diploids were selected on SC−Leu+G418 (200µg/ml) by two rounds of pinning. Diploids were pinned on sporulation media (+ 50µg/ml G418) and incubated for 7 days at 25°C. Haploids were selected on SD−HRLK + drugs (−His −Arg −Leu −Lys + 50µg/ml canavanine + 50µg/ml thyialysine + 200µg/ml G418 + 2% dextrose) for two rounds before pinning on the same haploid selection plates

containing either 2% dextrose or 2% galactose (two rounds of pinning on galactose). After the final plates were scanned, the area of each pinned spot was measured by Balony software (Young and Loewen, 2013), where the area of each deletion strain was normalized to the average area of all wild-type spots (n=50) on the same plate. Interactions with a cutoff of >20% change in growth differential compared to the vector control plate were chosen for validation (experimental-control values <-0.2). For confirmations and subsequent analysis using growth curves, sporulated diploids from the array (and sporulated diploids generated for h*FEN1*^{E158A} and h*FEN1*$^{D181A/E158A}$ with selected deletion strains) were streaked for single colonies on haploid-selection media to generate 3 independent haploid isolates. Each isolate was grown to mid-log phase in both dextrose and galactose SC−Leu media before diluting to OD_{600}=0.1 in the same media +/- 0.005% MMS for growth curve analysis as previously described in methods. To assess the effect of overexpression in the ALF assay, colonies containing *LEU2*-marked vectors were patched in 1-cm^2 squares on galactose SC−Leu media to induce transcription from the GAL-promoter for 2 rounds before mating to a *MATα his1* tester lawn on YPG (2% galactose) as described (Duffy et al., 2016). After 24h, the mated lawn was replica-plated to SC-6 (−Ura −Lys −Ade −His −Trp −Leu) media and incubated for 2 days to select for His^+ products. All SDL screens, growth curve validations, and dosage ALF assays were performed at 30°C unless otherwise indicated.

4.3 Results

4.3.1 Screening tumor-specific variants using complementation of essential genes

Human-yeast complementation enables direct testing of human gene variants for function. Genetic variants can be screened rapidly and are characterized in the context of the

human protein. For example, complementation of yeast *cys4*Δ by its human ortholog *CBS* gene enabled the testing of 84 variants from patients with homocystinuria for functionality and cofactor dependence (Mayfield et al., 2012). One resource from our human-yeast complementation screen is a list of human genes whose variants can be characterized in a yeast deletion strain. We focused on testing tumor-specific mutations found in human orthologs of yeast CIN genes. Our complementation set includes 28 essential yeast CIN genes rescued by 34 candidate human CIN genes and 20 nonessential yeast CIN genes rescued by 20 candidate human CIN genes. We observe that the replaceable yeast CIN genes function across diverse biological processes, including those pathways predicted to protect genome integrity (e.g., DNA replication/repair and chromatin-related processes) and more peripheral pathways (e.g., metabolism and cellular trafficking) (Figure 2.4).

We selected three essential yeast CIN genes corresponding to four complementation pairs (y*CDC9*:h*LIG1*, y*POB3*:h*SSRP1*, y*GLC7*:h*PPP1CA*, and y*GLC7*:h*PPP1CC*) and assessed the impact of single amino acid substitutions in the human protein. Briefly, y*CDC9* encodes DNA ligase, an essential enzyme that joins Okazaki fragments during DNA replication and also functions in DNA repair pathways (Lindahl and Barnes, 1992); y*POB3* is a subunit of the heterodimeric FACT complex (y*POB3*-y*SPT16*) that functions in nucleosome reorganization to facilitate transcription and replication processes (Formosa, 2008); y*GLC7* is the catalytic subunit of protein phosphatase which, depending on its bound regulatory subunit, regulates numerous cellular processes (Cannon, 2010). We selected one cancer type (colorectal cancer) and screened all reported missense mutations compiled in two databases: Catalogue of Somatic Mutations in Cancer (COSMIC) (Forbes et al., 2015) and cBIOPORTAL for Cancer Genomics (Cerami et al., 2012; Gao et al., 2013). In total, 35

single amino-acid substitutions were constructed corresponding to 16 in h*LIG1*, 12 in h*SSRP1*, 2 in h*PPP1CA*, and 5 in h*PPP1CC*. As a control, we expressed each human gene variant in a wild-type yeast strain and compared the growth of these yeast strains to the growth of the same yeast strain expressing the wild-type human allele. This step is required to identify any mutants whose ectopic expression may impact the growth phenotype of the yeast strain either by causing toxicity to the yeast cell or increasing the growth rate. Of the 35 mutants analyzed, the K228E mutation in h*SSRP1* is the only amino-acid substitution whose ectopic expression decreased fitness of wild-type yeast (Table A.11).

We used a plasmid shuffle strategy to introduce the human gene variants in the corresponding yeast gene deletion mutants. Haploid yeast gene knockout strains carrying the rescuing human cDNA on a *URA3*-marked plasmid were transformed with wild-type or mutated human cDNA on a *LEU2*-marked plasmid and plated on media containing 5-FOA (Figure 4.1A), which selects for cells that have lost the *URA3* plasmid. Growth on 5-FOA plates indicates that the mutant human cDNA is able to complement the essential gene. Lack of growth on 5-FOA indicates that the mutation in the human cDNA results in a nonfunctional protein. We observed that 4 of the 35 mutant alleles [2 in h*SSRP1* (K228E, S481P), 1 in h*PPP1CA* (Y272C), and 1 in h*PPP1CC* (L289R)] are nonfunctional. To determine the accuracy of our experimental readout, we surveyed the literature and found the conserved Y272 and L289 in PP1 phosphatases are essential for substrate binding (Egloff et al., 1995; Egloff et al., 1997; Zhang et al., 1996).

The remaining 31 mutant alleles were assessed for their ability to rescue growth of the null mutant (Figure 4.1B, Figure 4.2 and Table A.12). We observed that 19 of the 31 mutations cause a significant decrease in strain fitness relative to the wild-type allele, while

one mutant allele (h*PPP1CC*^{L201F}) grows considerably better than the corresponding wild-type allele. Notably, 16 of the 19 "slow growers" are substitutions in h*LIG1*, with the mutations dispersed throughout the protein. Given that mutants with defects in chromosome stability are often sensitive to DNA-damaging agents, we assayed our 31 mutants for growth in the presence of methyl methane sulfonate (MMS) and hydroxyurea (HU) (Figure 4.1C, Figure 4.2 and Table A.12). MMS is an alkylating agent (Beranek, 1990) while HU slows DNA replication by decreasing the rate of dNTP synthesis (Koc et al., 2004), and haploid viable mutant alleles of yeast *CDC9*, *POB3*, and *GLC7* have been shown to cause sensitivity to sublethal doses of MMS and/or HU (Bazzi et al., 2010; Prakash and Prakash, 1977; Schlesinger and Formosa, 2000). Twelve mutant alleles cause sensitivity to MMS, while two cause increased resistance to MMS. The majority of the mutants sensitive to HU are in h*LIG1* (12/14), which is expected given the major role of that protein in DNA replication.

4.3.2 Screening tumor-specific variants using complementation of a nonessential gene

We assessed the impact of recurrent mutations found in ovarian and endometrial carcinomas in protein phosphatase subunit h*PPP2R1A* (ortholog of nonessential yeast CIN gene y*TPD3*) (Seshacharyulu et al., 2013). Protein phosphatase 2A (PP2A) is a heterotrimeric serine/threonine phosphatase complex composed of a scaffolding (subunit A), regulatory (subunit B), and a catalytic (subunit C) (Figure 4.3A). Binding of at least 18 different regulatory (B) subunits defines substrate specificity, localization and enzymatic activity of the phosphatase complex. The scaffolding subunit (h*PPP2R1A*) is composed of 15 HEAT motifs, of which HEAT repeats 1-8 mediate interaction of the scaffold with regulatory (B) subunits, while HEAT repeats 11-15 mediate interaction with the catalytic subunit (C).

Missense mutations in h*PPP2R1A* occur in 5% to 40% in ovarian and endometrial carcinomas, are heterozygous and cluster in HEAT repeats 5 or 7 (Haesen et al., 2016).

The complementation screen of nonessential yeast CIN genes identified h*PPP2R1A* as able to partially rescue the growth defect, sensitivity to DNA-damaging agents and CIN defects of *tpd3*Δ (Table 2.2). To characterize recurrent mutations found in h*PPP2R1A*, we constructed 10 single amino acid substitutions in h*PPP2R1A*, and the corresponding 7 mutations in y*TPD3* (Figure 4.3A). As a control, we expressed each human and yeast gene variant in a wild-type yeast strain and compared the growth of these yeast strains to a vector control. Each variant was also screened in a wild-type background for increased CIN using the a-like faker (ALF) assay; which measures loss of the *MAT*α locus leading to de-differentiation to an a-mating phenotype and subsequent mating to a *MAT*α tester strain (Stirling et al., 2011; Yuen et al., 2007). None of the 17 mutants analyzed caused fitness (Figure 4.3B) or CIN defects (Figure 4.3C) when expressed ectopically in wild-type yeast.

The same variants were then introduced into *tpd3*Δ and assessed for their ability to rescue fitness and CIN defects of the null allele. Each yeast or human variant was compared to the deletion strain expressing the wild-type yeast or human allele, respectively. Indicative of CIN defects, a-like faker assays demonstrated that *tpd3*Δ increased ALF frequency compared to wild-type yeast, and expression of y*TPD3* or h*PPP2R1A* on a vector partially rescued CIN defects (Figure 4.4A). While the 7 yeast variants did not cause an increase in ALF compared to the wild-type yeast allele, one of the human variants displayed increased ALF compared to the wild-type human allele (hR183W) (Figure 4.4A and Figure 4.5). We assessed the impact of the variants on strain fitness in the absence of drug and demonstrated that hR183W was the only mutant that caused significant decrease in strain fitness relative to

the wild-type human allele (Figure 4.4B and Figure 4.5). Consistent with the ALF and fitness defects, hR183W was sensitive to MMS and HU and resembled *tpd3*Δ in these assays. Since hR183W was behaving as a loss-of-function mutant, we re-shuttled h*PPP2R1A*^{R183W} into a yeast expression vector that adds an HA-tag at the C-terminus (pAG416GPD-h*PPP2R1A*^{R183W}-HA) and checked for protein levels. Western blot analysis revealed that hR183W decreases protein levels of h*PPP2R1A* suggesting that this amino acid substitution impacts the stability of the protein (Figure 4.4C).

4.3.3 Comparing experimental to computational predictions

To assess whether computational predictions match empirical results, we used PredictSNP (a consensus classifier grouping six computational tools) (Bendl et al., 2014) to predict the effects of the mutations on protein function. Our results demonstrate that predicted effects do not always match observed results (Figure 4.2 and Figure 4.5). While some substitutions predicted to be neutral with high confidence displayed detrimental growth phenotypes (e.g., h*PPP1CC*^{E116D}), others predicted to be deleterious with high confidence exhibited no growth defects (e.g., h*SSRP1*^{R370C}). This was also observed for y*TPD3*:h*PPP2R1A* as all yeast and human variants were predicted to be deleterious with high confidence but only one of these variants (h*PPP2R1A*^{R183W}) was deleterious in the assays tested.

Although h*PPP2R1A*^{R183W} was found to be detrimental in the context of the human gene, the same substitution in the conserved site of the yeast protein (yTpd3^{R211W}) was tolerated. This was also the case for h*SSRP1*^{K228E}, as it was found to be nonfunctional in the context of the human gene, while the same substitution in the conserved site of the yeast protein (yPob3^{K271E}) is tolerated (VanDemark et al., 2006). These results corroborate

previous observations that amino acid substitutions in the context of the yeast gene do not necessarily have the same effect in the context of the human gene (Marini et al., 2010), emphasizing the importance of characterizing human variants in their native gene context. Overall, these results underscore the requirement for direct functional testing of variants in their native protein context.

4.3.4 Identifying synthetic dosage lethal targets of catalytically-inactive h*FEN1*

Our human-yeast complementation screens demonstrated that h*FEN1* can replace y*RAD27* (Table 2.2), thereby presenting a genetically amenable system with which to investigate the genetic interactions of h*FEN1* and allowing for the modelling of hFen1 inhibition since expression of catalytically inactive hFen1 should mimic inhibited hFen1 more effectively than a deletion allele. Expression of inactive hFen1 in the presence of endogenous yRad27 better models the effects of hFen1 inhibition *in vivo* as it allows for residual protein activity, which may be sufficient to perform its biological role, and mimics the presence of the inhibited enzyme. To identify mutations that have genetic interactions with catalytically inhibited h*FEN1* in the presence of functional yRad27, we performed SDL screens to find synthetic lethal vulnerabilities of inducibly overexpressed wild-type and catalytically-dead proteins (Figure 4.6A). We cloned the yeast and human ORFs into a multi-copy yeast plasmid under the transcriptional control of a galactose-inducible promoter (Alberti et al., 2007; Kachroo et al., 2015). Missense mutations that abolish h*FEN1* and y*RAD27* catalytic activity were constructed in the catalytic sites of the human and yeast ORFs. The resultant catalytically inactive mutant proteins yRad27^{D179A} and hFen1^{D181A} lack nuclease activity but retain binding to DNA flap substrates (Shen et al., 1996, 1997). Query strains containing the inducible expression plasmids were screened against a mini-array

comprising 332 yeast deletion mutants that function in various DNA transactions. Consistent with previous studies (Greene et al., 1999), induced overexpression of y*RAD27* or y*RAD27*^{D179A} causes profound growth defects in yeast (Figure 4.6B, C). However, induced overexpression of wild-type or catalytically-dead h*FEN1* in yeast did not impart severe growth defects and this was shown to be a result of the reduced binding affinity of human protein to yeast PCNA (a yRad27 binding partner) (Greene et al., 1999; Wu et al., 1996). The growth defects that resulted from overexpression of the yeast proteins were too severe to yield reliable data from an SDL screen in yeast. Therefore, we focused on confirming SDL target hits that utilized the human proteins as queries (Table A.13 and Table A.14). We did not find any mutants that had reduced fitness upon hFen1 overexpression, indicating that the 332 yeast deletion strains can tolerate elevated levels of the wild-type human protein.

We identified 22 putative SDL interactions that displayed >20% fitness defects, and subsequent growth curves validated 8 genetic interactions that resulted in SDL upon hFen1^{D181A} induction (Figure 4.7A). This included *rad27*Δ which was shown previously to have fitness defects in response to overexpression of the catalytically-dead human protein (endogenous yRad27 can minimize negative effects of elevated levels of inactive hFen1) (Greene et al., 1999). Notably, 7/8 hits function in the homologous recombination (HR) repair pathway including all members of the MRX complex (yMre11, yRad50, yXrs2) and yRad55-yRad57 complex. To identify any potential false-negative hits in our screen, we selected some mutants from the list of 332 yeast deletion strains for growth curve validations and determined that the null allele of another HR protein, *rad51*Δ, also had fitness defects upon hFen1^{D181A} induced expression (Table A.14). Given that HR repair is responsible for repairing DNA double-strand breaks in cells (Dudas and Chovanec, 2004), these results

suggested that hFen1^{D181A} overexpression contributed to DNA damage. Indeed, we found that yeast cells overexpressing hFen1^{D181A} showed increased levels of CIN in an ALF assay (Figure 4.7B), which would be consistent with hFen1^{D181A} resulting in DNA damage. In addition, yeast cells overexpressing hFen1^{D181A} were sensitized to the alkylating agent MMS (Figure 4.7C). These results align with data from other studies showing that overexpression of yRad27^{D179A} causes DNA damage in yeast (Becker et al., 2018), while overexpression of hFen1^{D181A} shows increased CIN as measured by other yeast-based CIN assays (Greene et al., 1999).

The nuclease-defective hFen1 retains its DNA flap binding ability and may remain bound due to its inability to process the flap. In turn, this bound protein-DNA complex could require HR proteins for efficient repair. To examine this, we introduced a second missense mutation (hFen1^{E158A}) that abolishes DNA binding (Shen et al., 1996, 1997) (Figure 4.8). We demonstrate that loss of DNA binding rescues fitness defects that result from induced expression of nuclease-defective hFen1 in HR mutants (Figure 4.9). These results are consistent with a 'trapped' hFen1-DNA complex model that causes DNA damage and indicate that elevated levels of inhibited hFen1 protein sensitizes cells that are defective in HR repair.

4.4 Discussion

4.4.1 Assessing the functional impact of tumor-specific variants in a humanized yeast system

We demonstrated an approach to determining the functional consequence of human gene variants in yeast. Because the functional effects of missense mutations are difficult to

predict, a quick yet systematic approach to screen and prioritize human gene variants for subsequent testing in mammalian models is of great value. As we have picked mutants of genes implicated in chromosome stability, mutant alleles that result in a nonfunctional protein, or reduction of function as displayed by decreased strain fitness, or increased sensitivity to DNA-damaging agents, are candidate mutations that might contribute to chromosome instability in tumor cells.

Yeast as a surrogate genetics system has been utilized extensively for assessing the pathogenicity of human disease variants. Ortholog- and paralog-based complementation assays have been shown to more likely identify disease-specific variants as deleterious in comparison to computational methods (Sun et al., 2016; Yang et al., 2017). Conversely, non-disease human variants found in the same disease genes were more likely to be identified as neutral when compared to computational predictions. In this study, we analyzed tumor-specific variants and determined that computational methods did not accurately predict the impact of missense mutations when compared to results obtained from yeast-based complementation assays. For instance, computational methods predicted 22 of 45 missense mutations to be deleterious with high-confidence, but our complementation assays demonstrated only five of these 22 variants to be loss-of-function. Moreover, amino-acid conservation alone or in combination with computational predictions did not accurately predict observable phenotypes. For instance, an amino-acid that is conserved between yeast and human proteins might be expected to be important for protein function. Indeed, most computational methods rely on sequence conservation as the main predictor that a missense mutation will be deleterious (Richards et al., 2015). Of the 22 human variants predicted to be deleterious, 20 correspond to sites conserved with the yeast protein, but only five of these

variants were loss-of-function mutants. In addition to sequence conservation, other criteria such as the identity of the amino-acid change and its location and context within the protein sequence are also utilized in computational prediction algorithms. In the set of h*SSRP1* variants assayed in this study, hR324C and hR370C are the same amino-acid substitution, but only hR324 is conserved with the yeast protein. However, computational methods predicted the substitution at the conserved site, hR324C, to be benign while the substitution at the non-conserved site, hR370C, to be deleterious. Nevertheless, complementation assays demonstrated that both variants had no impact on the ability of the human protein to rescue lethality of the yeast deletion mutant. Overall, these results support data showing computational methods tend to overpredict missense mutations as deleterious (Richards et al., 2015), and demonstrate the importance of functional assays in the annotation of missense changes.

The most reliable method for classifying driver genes as tumor-suppressors or oncogenes is the pattern of tumor-specific mutations (Vogelstein et al., 2013). Tumor-suppressor genes are mutated throughout their length and inactivate the protein product, while oncogenes are recurrently mutated at the same positions. Based on these parameters, the scaffold protein, h*PPP2R1A*, has been suggested to be an oncogene (Jones et al., 2010). However, the PP2A phosphatase complex acts as a tumor-suppressor (Janssens et al., 2005). Accordingly, and within the context of the PP2A complex activity, h*PPP2R1A* mutations found in recurrent hotpots have been shown to impact the binding of the scaffold to regulatory (B) subunits which in turn causes a loss of assembly and function of the PP2A complex (Haesen et al., 2016; Taylor et al., 2019). Notably, each mutation results in different interaction patterns with multiple regulatory (B) subunits, revealing the complexity of their

cellular regulation. The PP2A phosphatase complex regulates numerous cellular pathways including those involved in genome integrity (Seshacharyulu et al., 2013). Our ALF complementation assays demonstrated that almost all of the tumor-specific variants found in h*PPP2R1A* do not cause an increase in CIN, suggesting that the mutations do not impact regulation of genome integrity in the context of the yeast cell. While our complementation assays were restricted to rescue-of-lethality and CIN defects of the yeast ortholog deletion allele, other yeast-based assays can be utilized to measure the impact of mutations on PP2A complex assembly and activity. In turn, this may help pinpoint the cellular pathways impacted by mis-regulation of the PP2A complex.

Of the 10 h*PPP2R1A* variants assayed in this study, only hR183W resulted in a loss-of-function phenotype potentially due to its effect on protein stability. However, contrary to our results, expression of this variant in human cell lines did not impact protein levels (Haesen et al., 2016; Taylor et al., 2019), suggesting this result is restricted to expression in yeast. Furthermore, our results demonstrated that the yeast protein with the conserved mutation (yTpd3^{R211W}) behaved like the wild-type allele. One potential explanation is that the mutation causes a conformational change in the human protein leading to decreased protein levels. This has been shown for the hP179R variant, however, in this case the conformational changes in protein structure did not impact the stability of the protein (Taylor et al., 2019). Therefore, if hR183W is causing a conformational change that destabilizes the protein structure of hPpp2r1a, then this is specific only in the context of expression of the human protein in yeast.

Another unexplained finding was the decreased fitness observed for all h*LIG1* variants. Based solely on the growth assays, we cannot explain whether this result reflects the

experimental design or the reduced activity of these mutants. This phenomenon has been observed for other clinically-relevant mutations of argininosuccinate lyase, where yeast-based complementation assays determined that all 12 human variants of h*ASL* assessed for rescue of yeast growth defects resulted in either lethality or decreased fitness of the yeast strain (Trevisson et al., 2009). Alternatively, this may represent a limitation of yeast-based complementation assays. One study found complementation assays of h*DPAGT1* could not reliably predict pathogenicity of disease variants and this correlated with the tendency of the mutations to occur on sites not conserved between the human and yeast proteins (Sun et al., 2016). In our case, the majority of sites tested for h*LIG1* appear at non-conserved sites (14/16), and we observed that the only two conserved sites contained missense mutations that appeared to rescue better than the other non-conserved sites (i.e. fitness defects were not as strong: ~30% compared to ~40%-60%). However, these observations are only suggestive and do not reflect identity of the amino-acid change. Notably, one study found that the first 633 nucleotides of the human protein from the 5'end (encompassing 6/14 non-conserved sites tested in our study) is dispensable for complementation of the y*cdc9* temperature-sensitive strain (Barnes et al., 1990). However, while the study indicated that the yeast strain expressing truncated hLig1 produced only 25% as much ligase as the full-length hLig1, it was unclear whether this resulted in reduced complementation of growth defects. These results indicate that follow-up experiments to test human protein levels in yeast is required to explain the effect of all 16 variants. However, whether the results in yeast cells will reflect the same phenotypes in human cells remains unknown.

While the fitness defects associated with hLig1 mutations are difficult to explain, we did observe that the majority of the alleles caused sensitivity to hydroxyurea. This suggested

that the mutant alleles increased DNA replication stress in yeast as compared to the wild-type human allele, presumably due to reduced activity. Furthermore, some variants were found to cause sensitivity to MMS, suggesting that they affected DNA repair in yeast. Notably, two hLig1 variants grew significantly better in MMS than in the 'no drug' condition. The strongest rescue was the hK152E variant, which caused ~50% yeast fitness defects in the 'no drug' condition but grew in MMS at the same level as the wild-type human allele (i.e. ~50% rescue). In the context of cancer cells, tumor-specific variants that cause resistance to genotoxic agents would likely be genetic contexts not suitable for treatment with many common cancer chemotherapy drugs. Here, yeast-based assays were able to identify two candidate mutations that can be prioritized for testing resistance to genotoxic agents in human cell lines.

The experimental design utilized to assess variants had some limitations. We could not reliably test rescue of CIN defects for the essential yeast genes because the yeast deletion mutants rescued by the wild-type human alleles already had high levels of CIN (data not shown). In turn, this decreased the sensitivity of yeast CIN assays and made it more difficult to compare human variants to the wild-type human allele. This could be explained by several reasons. Although the homology between the yeast and human proteins is enough to elicit cross-species complementation of growth, the human allele represents a mutagenized version of the yeast protein that may only partially complement some phenotypes. This is not entirely different than yeast temperature-sensitive mutations where a single amino-acid change is sufficient for viability at the permissive temperatures but also causes CIN (Kofoed et al., 2015; Stirling et al., 2011). Another potential reason is that we used vector-based expression which results in more variability in expression and a constitutive promoter which prevents

endogenous transcriptional regulation of the human protein. These limitations can be addressed by using CRISPR/Cas9 technology, (which was not readily available at the onset of this study), to integrate the human ORF in the endogenous genomic loci.

4.4.2 Mimicking inhibition of hFen1 in a humanized yeast system

Chapter 3 discussed the impact of protein-protein interactions between the human protein and the cognate yeast interaction partners in relation to cross-species complementation. For some human-yeast pairs, altered interactions between the human protein and the interaction partners of the cognate yeast protein do not impact complementation. For example, hFen1 can replace the main function of yRad27 in processing flap substrates but has reduced binding affinity to yeast PCNA (Greene et al., 1999; Wu et al., 1996). Unlike hFen1, overexpression of yRad27 in yeast causes genetic instability and reduces viability in a PCNA-dependent manner (Becker et al., 2018; Greene et al., 1999). We took advantage of the differences in negative effects between the human and yeast protein to overexpress hFen1 and perform SDL screens in yeast.

In a proof-of-principle experiment, we inducibly overexpressed wild-type and catalytically-dead hFen1 and looked for mutants that resulted in synthetic dosage lethality. Given that inhibitors are being developed to target cancer cells with overexpressed hFen1, we wanted to model effects of the presence of chemically inhibited protein in yeast. In previous studies in mammalian cells, hFen1 inhibitors have been shown to (i) selectively impair proliferation of HR-defective cancer cell lines including h*MRE11A*-deficient colon cancer cell lines (van Pel et al., 2013; Ward et al., 2017), h*BRCA1*-deficient breast cancer cell lines (He et al., 2016), h*RAD54B*-deficient (Exell et al., 2016) and h*BRCA2*-deficient cervical cancer cell lines (Ward et al., 2017); (ii) increase endogenous DNA damage by causing the

accumulation of DNA double-strand breaks and chromosome breaks (Exell et al., 2016; He et al., 2017; He et al., 2016; van Pel et al., 2013; Ward et al., 2017); (iii) increase human cell line sensitivity to DNA damaging agents including temozolomide, 5FU (He et al., 2016), cisplatin (He et al., 2017; He et al., 2016; Ward et al., 2017) and MMS (Exell et al., 2016; Tumey et al., 2005); and (iv) induce cytotoxicity in a dose-dependent manner (higher levels of hFen1 or inhibitor is more toxic) (Exell et al., 2016; He et al., 2017; He et al., 2016; Ward et al., 2017). In the study presented here, we show that overexpressing catalytically-dead hFen1 in yeast (thus mimicking a mode-of-action inhibition) (a) reduces fitness of HR-defective mutants (identified from a screen of 332 yeast mutants); (b) causes chromosome instability as measured by different yeast assays that test ALF (this study), interchromosomal recombination, microsatellite instability and mutation rates (Greene et al., 1999); and (c) sensitizes yeast cells to the DNA damaging agent MMS (this study and (Greene et al., 1999)). These data are consistent with results observed using inhibitors in human cell lines and further demonstrates the utility of modelling this system in yeast.

Mimicking protein-inhibitor relationships using catalytically-dead mutants enables the study of the biological effects of protein inhibition using genetic approaches. Any observed phenotypes can be deduced to be a result of the inactive protein and not an effect of non-specific inhibition of secondary targets. We compared the results of our SDL screen to synthetic lethal (SL) screens of *rad27*Δ and found that SL screens of the deletion mutant identify a much larger and broader genetic interaction network of mutants that display negative interactions (Figure A.7). This demonstrates that genetic interaction network data generated from deletion or knockdown mutants may differ from cells expressing inhibited proteins. By introducing a DNA-binding mutant, we determined that the dominant-negative

effects exhibited by catalytically-dead hFen1 required the DNA binding activity which is consistent with the idea of forming trapped hFen1-DNA complexes that lead to DNA damage. This occurs even in the presence of wild-type yRad27 which suggests that inactive hFen1 competes with wild-type yRad27 for binding to flap substrates. This may explain how hFen1 inhibitors cause defects in a dose-dependent manner as higher levels of inhibited hFen1 will effectively compete with uninhibited hFen1 to form a trapped hFen1-DNA complex. This also indicates that inhibitors of hFen1 that disrupt binding to DNA may not be as effective in targeting cancer cells with defective HR repair. A similar mechanism was observed for *PARP* inhibitors which have been shown to cause trapped *PARP1*-DNA complexes that are more cytotoxic in HR-deficient cells than depleted *PARP1* (Murai et al., 2012). Overall, these results have implications for development of inhibitors that trap protein on DNA as an effective approach to targeting cancer cells that have synthetic lethal vulnerabilities in DNA repair pathways or in combination with other DNA damage inducing agents.

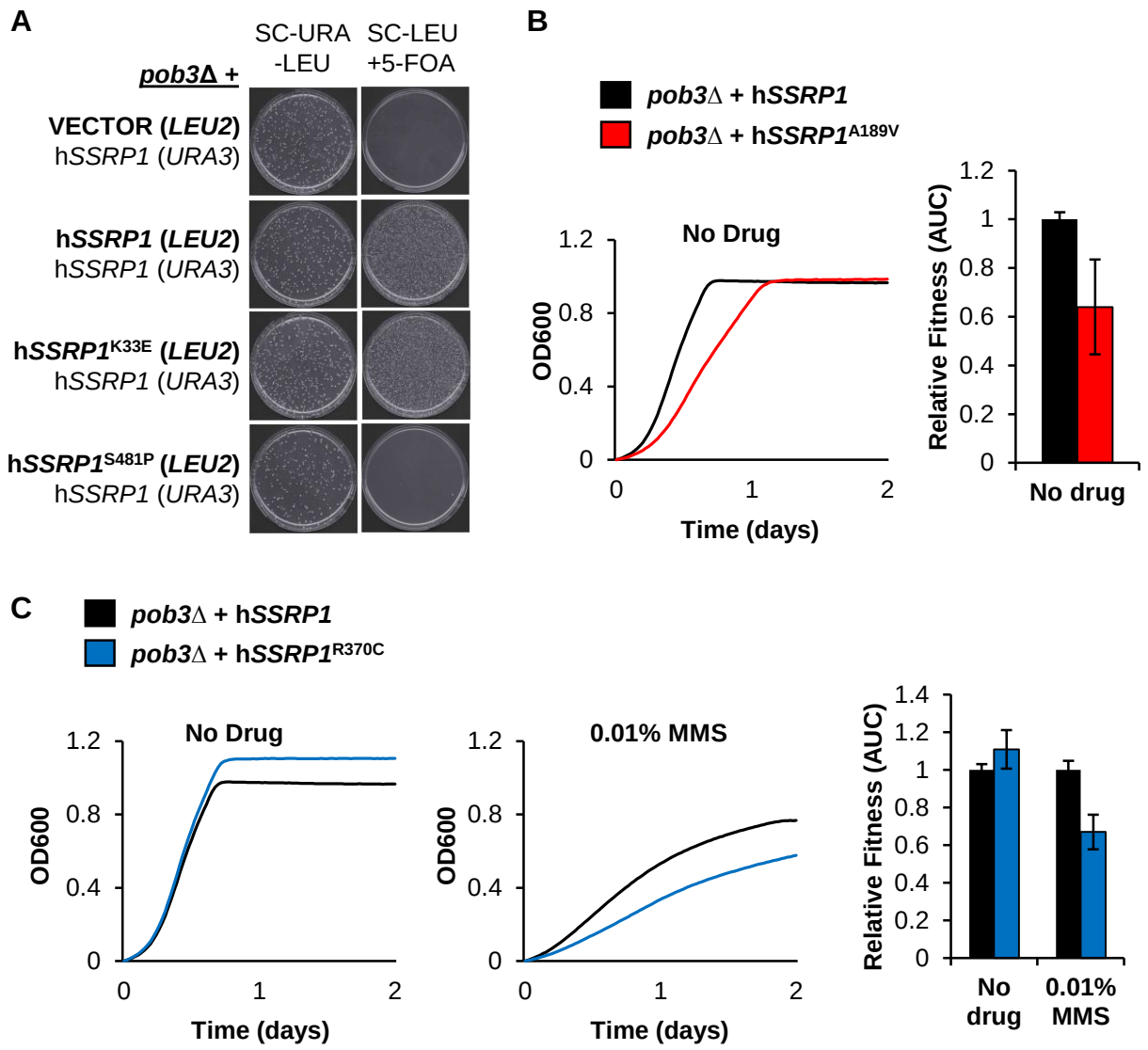

Figure 4.1. Utilizing complementation of essential yeast genes to characterize tumor-specific variants.
(A) Plasmid shuffle used to generate strains expressing human cDNAs with missense mutations. Yeast haploid knockout strains covered by wild-type human cDNAs on *URA3*-marked vectors were transformed with the following *LEU2*-marked vectors (empty, wild-type human cDNA, and human cDNA with missense mutation) and maintained on −Ura −Leu media. Strains were plated on −Leu +5-FOA media to generate haploid yeast knockouts covered by *LEU2*-marked vectors. Strains were confirmed to have lost the *URA3*-marked plasmid by streaking on −Ura media to observe no growth. In the presented example, hSsrp1-K33E is able to complement *pob3*Δ, but S481P results in a nonfunctional hSsrp1 protein. **(B, C)** Liquid growth curve assays were used to assess impact of tumor-specific variants on fitness of yeast strain (+/- chemical). In the presented examples, hA189V causes a decrease in strain fitness relative to the wild-type allele, while hR370C decreases fitness in MMS. Each represented curve is the average of three replicates per media condition. Fitness of each strain was quantified by calculating area under the curve (AUC) of each replicate independently. Strain fitness for each allele is expressed as a ratio relative to the yeast strain expressing the wild-type allele grown in the same plate in the same media condition (mean +/- SD).

DF: Decreased Fitness
IF: Increased Fitness
LOF: Loss-of-function
n/d: Not determined

	Nucleotide Mutation	Amino Acid Mutation	Conserved in Yeast	PredictSNP (Confidence)	Fitness (No Drug)	Fitness (MMS)	Fitness (HU)
h*LIG1*	179C>T	A60V	No	Neutral (83%)	DF		DF
	421A>G	S141G	No	Neutral (75%)	DF		DF
	454A>G	K152E	No	Neutral (83%)	DF	IF	
	455A>G	K152R	No	Neutral (83%)	DF		DF
	457G>A	E153K	No	Neutral (83%)	DF		DF
	488G>A	S163N	No	Neutral (83%)	DF		DF
	664C>T	R222C	No	Neutral (63%)	DF	DF	DF
	1045G>A	V349M	No	Neutral (60%)	DF	IF	DF
	1120G>A	A374T	No	Neutral (83%)	DF		DF
	1184C>A	P395Q	No	Neutral (83%)	DF	DF	DF
	1502T>C	M501T	No	Neutral (83%)	DF	DF	DF
	1835C>T	S612L	No	Neutral (74%)	DF	DF	
	1969T>G	L657V	Yes	Neutral (83%)	DF		DF
	2290G>A	A764T	Yes	Deleterious (87%)	DF	DF	
	2353G>A	E785K	No	Neutral (75%)	DF		
	2446G>A	V816M	No	Neutral (74%)	DF	DF	DF
h*SSRP1*	97A>G	K33E	Yes	Deleterious (87%)			
	566C>T	A189V	Yes	Deleterious (72%)	DF		
	626C>T	T209I	Yes	Deleterious (61%)		DF	
	682A>G	K228E	Yes	Deleterious (87%)	LOF	n/d	n/d
	970C>T	R324C	Yes	Neutral (60%)			
	1108C>T	R370C	No	Deleterious (65%)		DF	
	1306C>T	P436S	No	Neutral (83%)			
	1441T>C	S481P	No	Deleterious (61%)	LOF	n/d	n/d
	1493A>G	N498S	No	Neutral (74%)		DF	
	1723A>G	T575A	No	Neutral (83%)		DF	
	1724C>T	T575M	No	Neutral (60%)		DF	
	1950G>T	K650N	No	Neutral (83%)			
h*PPP1CA*	428G>A	R143H	Yes	Deleterious (87%)			
	815A>G	Y272C	Yes	Deleterious (87%)	LOF	n/d	n/d
h*PPP1CC*	348G>T	E116D	Yes	Neutral (75%)	DF	DF	DF
	559C>T	R187W	Yes	Deleterious (87%)	DF		DF
	601C>T	L201F	Yes	Deleterious (51%)	IF		
	610C>A	L204I	Yes	Neutral (63%)			
	866T>G	L289R	Yes	Deleterious (87%)	LOF	n/d	n/d

Figure 4.2. Summary of tumor-specific variants screened using complementation of essential genes in yeast.
Corresponding fitness values are summarized in Table A.12.

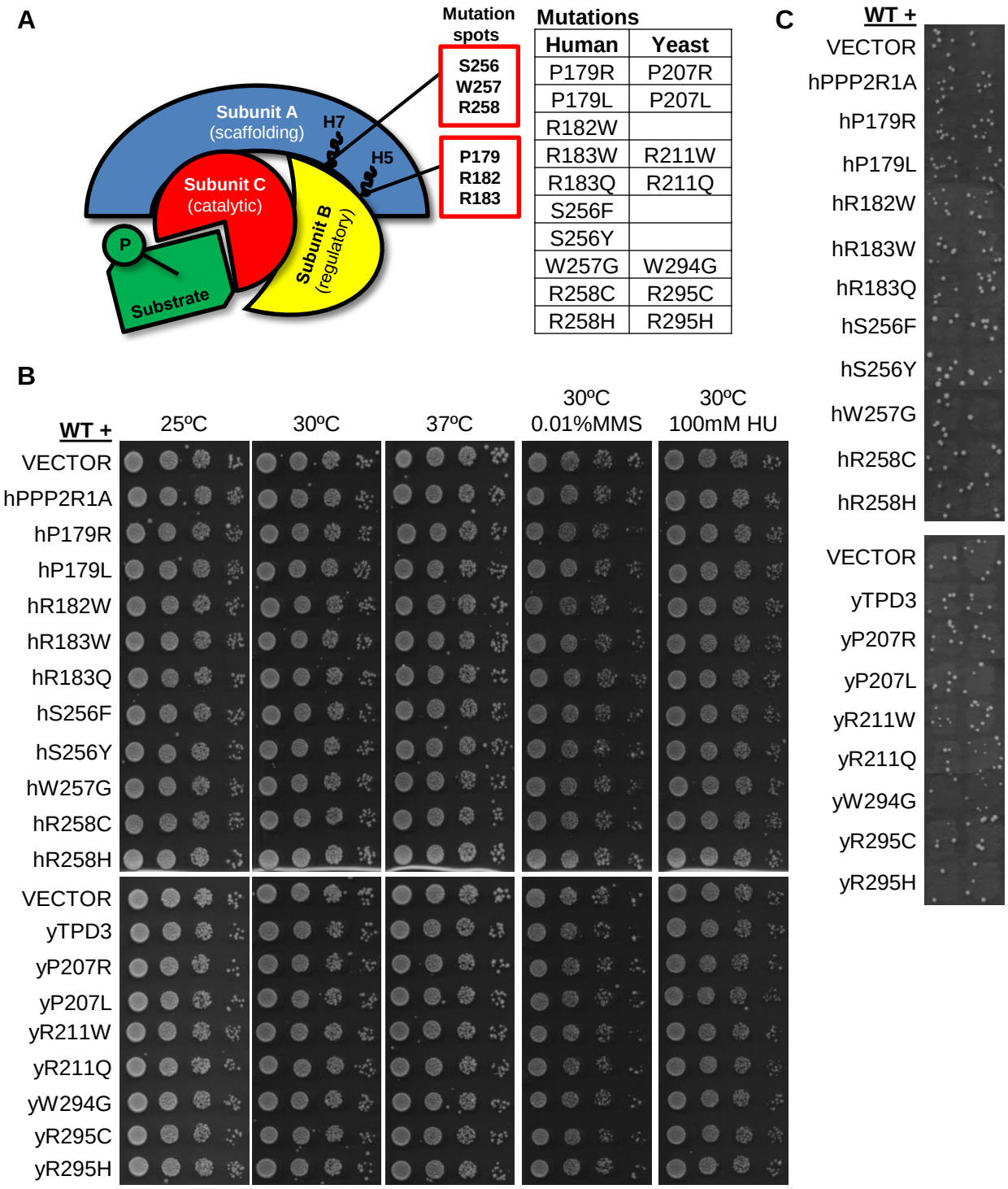

Figure 4.3. Utilizing complementation of a non-essential yeast gene to assay recurrent mutations found in protein phosphatase h*PPP2R1A.*

(A) Schematic of PP2A complex as adapted from PMID: 21432855. h*PPP2R1A* encodes subunit A. The human and corresponding yeast variants tested in this study are summarized in the table. **(B)** Constitutive expression of 10 h*PPP2R1A* or 7 y*TPD3* variants in WT (BY4742) yeast has no impact on strain fitness (+/- chemical). Yeast strains were spotted in 10-fold dilution on indicated media for 3 days. **(C)** A-like faker assays of WT strains ectopically expressing each variant demonstrates no CIN defects (2 independent isolates are shown per strain).

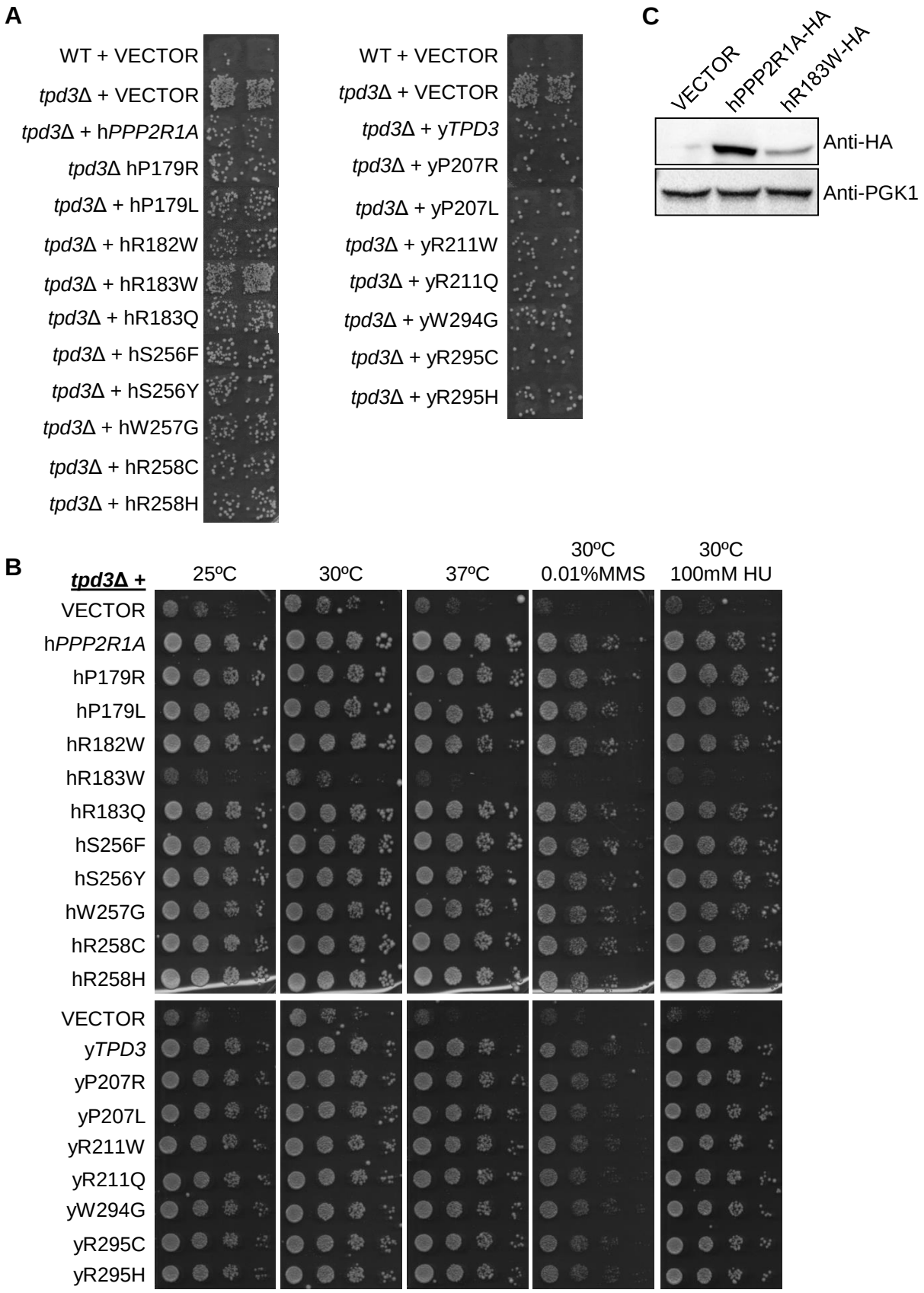
A
WT + VECTOR
tpd3Δ + VECTOR
tpd3Δ + hPPP2R1A
tpd3Δ hP179R
tpd3Δ + hP179L
tpd3Δ + hR182W
tpd3Δ + hR183W
tpd3Δ + hR183Q
tpd3Δ + hS256F
tpd3Δ + hS256Y
tpd3Δ + hW257G
tpd3Δ + hR258C
tpd3Δ + hR258H
WT + VECTOR
tpd3Δ + VECTOR
tpd3Δ + yTPD3
tpd3Δ + yP207R
tpd3Δ + yP207L
tpd3Δ + yR211W
tpd3Δ + yR211Q
tpd3Δ + yW294G
tpd3Δ + yR295C
tpd3Δ + yR295H
C
VECTOR
hPPP2R1A-HA
hR183W-HA
Anti-HA
Anti-PGK1
B
tpd3Δ +
25ºC
30ºC
37ºC
30ºC 0.01%MMS
30ºC 100mM HU
VECTOR
hPPP2R1A
hP179R
hP179L
hR182W
hR183W
hR183Q
hS256F
hS256Y
hW257G
hR258C
hR258H
VECTOR
yTPD3
yP207R
yP207L
yR211W
yR211Q
yW294G
yR295C
yR295H

Figure 4.4. Complementation assays of *tpd3*Δ identify h*PPP2R1A*^{R183W} as a loss-of-function allele.
(A) A-like faker assays demonstrate h*PPP2R1A* expression decreases the elevated frequency of ALF cells that result from deletion of y*TPD3* (2 independent isolates are shown per strain). One variant (hR183W) displays increased CIN compared to h*PPP2R1A*, while mutants in y*TPD3* did not show increased CIN. **(B)** Constitutive expression of 10 h*PPP2R1A* or 7 y*TPD3* variants in *tpd3*Δ yeast (+/- chemical) reveal hR183W as a loss-of-function allele. Yeast strains were spotted in 10-fold dilution on indicated media for 3 days. **(C)** hR183W variant decreases protein levels of h*PPP2R1A* in yeast.

DF: Decreased Fitness
IF: Increased Fitness
LOF: Loss-of-function
n/d: Not determined

	Nucleotide Mutation	Amino Acid Mutation	PredictSNP (Confidence)	A-like faker	Fitness (No Drug)	Fitness (MMS)	Fitness (HU)
h*PPP2R1A*	536C>T	hP179R	Deleterious(87%)				
	536C>T	hP179L	Deleterious(72%)				
	544C>T	hR182W	Deleterious(87%)				
	547C>T	hR183W	Deleterious(87%)	Increased	LOF	DF	DF
	548G>A	hR183Q	Deleterious(72%)				
	767C>T	hS256F	Deleterious(87%)				
	767C>A	hS256Y	Deleterious(87%)				
	769T>G	hW257G	Deleterious(87%)				
	772C>T	hR258C	Deleterious(87%)				
	773G>A	hR258H	Deleterious(87%)				
y*TPD3*	620C>G	yP207R	Deleterious(87%)				
	620C>T	yP207L	Deleterious(87%)				
	631A>T	yR211W	Deleterious(87%)				
	631A>C; 632G>A	yR211Q	Deleterious(87%)				
	880T>G	yW294G	Deleterious(87%)				
	883A>T; 885G>C	yR295C	Deleterious(87%)				
	883A>C; 884G>A; 885G>C	yR295H	Deleterious(87%)				

Figure 4.5. Summary of tumor-specific variants screened using complementation of y*TPD3* in yeast.
All amino acid changes were predicted to be deleterious by PredictSNP but only one of these variants (hR183W) was deleterious in the assays tested.

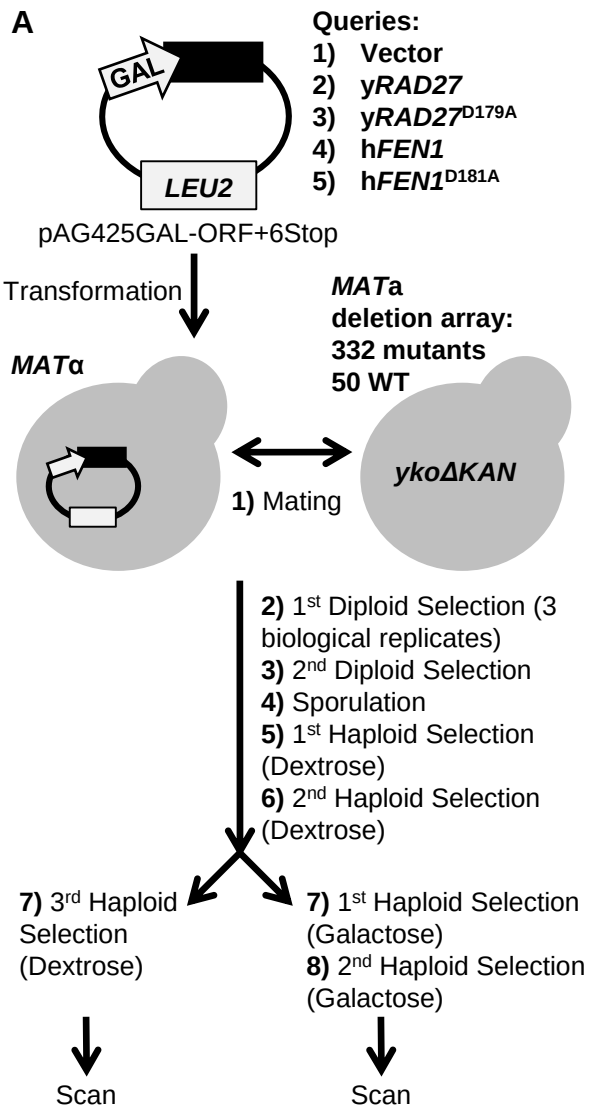
A
GAL
LEU2
pAG425GAL-ORF+6Stop
Queries:
1) Vector
2) yRAD27
3) yRAD27D179A
4) hFEN1
5) hFEN1D181A
Transformation
MATα
MATa
deletion array:
332 mutants
50 WT
ykoΔKAN
1) Mating
2) 1st Diploid Selection (3 biological replicates)
3) 2nd Diploid Selection
4) Sporulation
5) 1st Haploid Selection (Dextrose)
6) 2nd Haploid Selection (Dextrose)
7) 3rd Haploid Selection (Dextrose)
7) 1st Haploid Selection (Galactose)
8) 2nd Haploid Selection (Galactose)
Scan
Scan

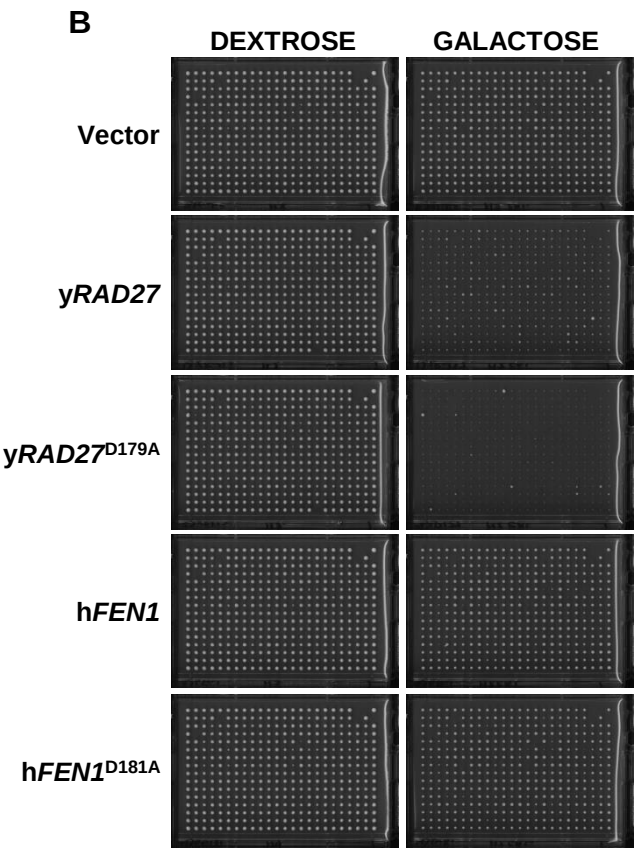
B
DEXTROSE
GALACTOSE
Vector
yRAD27
yRAD27D179A
hFEN1
hFEN1D181A

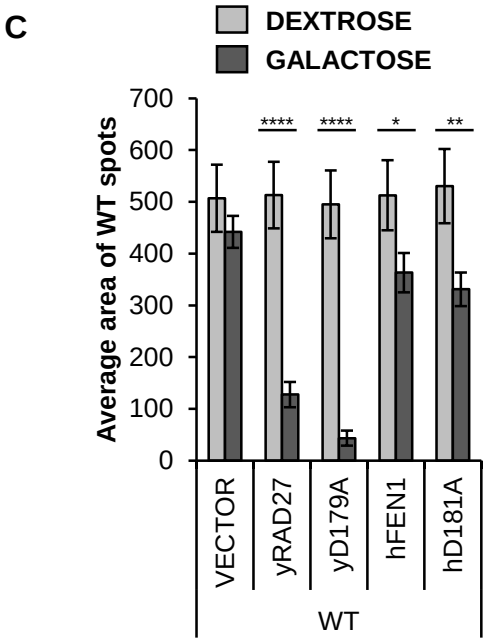
C
DEXTROSE
GALACTOSE
Average area of WT spots
700
600
500
400
300
200
100
0
****
****
*
**
VECTOR
yRAD27
yD179A
hFEN1
hD181A
WT

Figure 4.6. Workflow of the SDL screens.
(A) Inducible yeast expression vectors or a vector control were transformed to generate query strains for the SDL screens. Using synthetic genetic array technology, each query strain was mated to a pinned mini-array comprising 332 haploid yeast knockouts (*yko*Δ) and 50 wild-type strains to generate diploids. Following diploid selection (2 rounds) and sporulation, a series of replica-pinning steps generated a haploid array where each knockout mutant was combined with the overexpression vector. After 2 rounds of haploid selection, strains were pinned onto galactose media (2 rounds) to induce expression of the open reading frame (ORF). The final plates were scanned, and area of each pinned spot was determined to detect SDL interactions. **(B)** Overexpression of y*RAD27* or y*RAD27*^{D179A} causes growth defects in yeast. Haploid yeast cells (wild-type and knockout strains on the mini-array) containing y*RAD27* or y*RAD27*^{D179A} display severe fitness defects when pinned onto galactose media whereas fitness defects of haploid cells containing h*FEN1* or h*FEN1*^{D181A} are less pronounced. **(C)** Quantification of the fitness defects that result from overexpression of y*RAD27* or y*RAD27*^{D179A}. The average area of wild-type (WT) spots (n=50) on each haploid array (n=3) reveals that overexpression of the human proteins cause minimal growth defects compared to overexpression of the yeast proteins (mean +/- SD). Student's t-test. *p<0.05; **p<0.01; ****p<0.0001.

A

***Validated SDL interactions for* h*FEN1*^{D181A}**

Yeast systematic name	Yeast standard name
YMR224C	*MRE11*
YNL250W	*RAD50*
YDR369C	*XRS2*
YDR076W	*RAD55*
YDR004W	*RAD57*
YGL163C	*RAD54*
YML032C	*RAD52*
YER095W	*RAD51*
YKL113C	*RAD27*

B

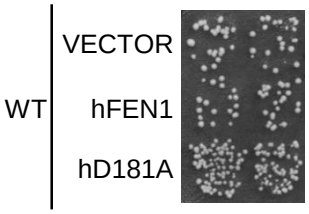

C

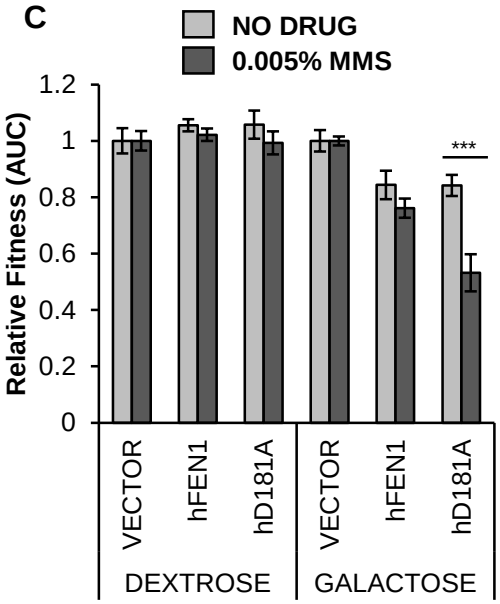

Figure 4.7. Overexpression of h*FEN1*^{D181A} decreases fitness of HR mutants and causes CIN.
(A) SDL interactions identified from the h*FEN1*^{D181A} screen were validated by growth curves. **(B)** Overexpression of h*FEN1*^{D181A} increases ALF frequency of yeast cells. Each strain (2 independent isolates are shown per strain) was grown on galactose media before assessing growth of diploid mating progeny on selective plates. **(C)** Wild-type haploids containing a vector control, h*FEN1*, or h*FEN1*^{D181A} plasmids were grown in dextrose or galactose media +/- 0.005% MMS. Each strain was tested in four replicates per condition and area under the curve (AUC) value was calculated for each replicate independently. Strain fitness was defined as the AUC of each yeast strain relative to the AUC of the vector control grown in the same media condition (mean +/- SD). Yeast cells overexpressing h*FEN1*^{D181A} display fitness defects in the presence of MMS. Corresponding growth curves are shown in Figure A.5. Student's t-test. ***p<0.001.

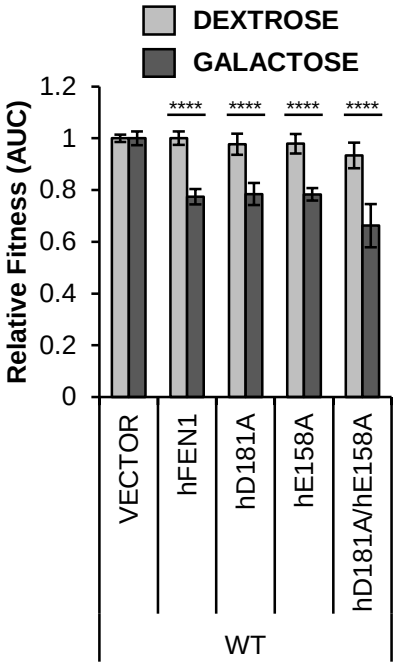

Figure 4.8. Overexpression of h*FEN1*^{E158A} or h*FEN1*$^{D181A/E158A}$ in wild-type yeast cells causes similar growth defects as h*FEN1* overexpression.
Each strain was tested in seven replicates per condition and area under the curve (AUC) value was calculated for each replicate independently. Strain fitness was defined as the AUC of each yeast strain relative to the AUC of the vector control grown in the same media condition (mean +/- SD). Corresponding growth curves are shown in Figure A.6. Student's t-test. ****p<0.0001.

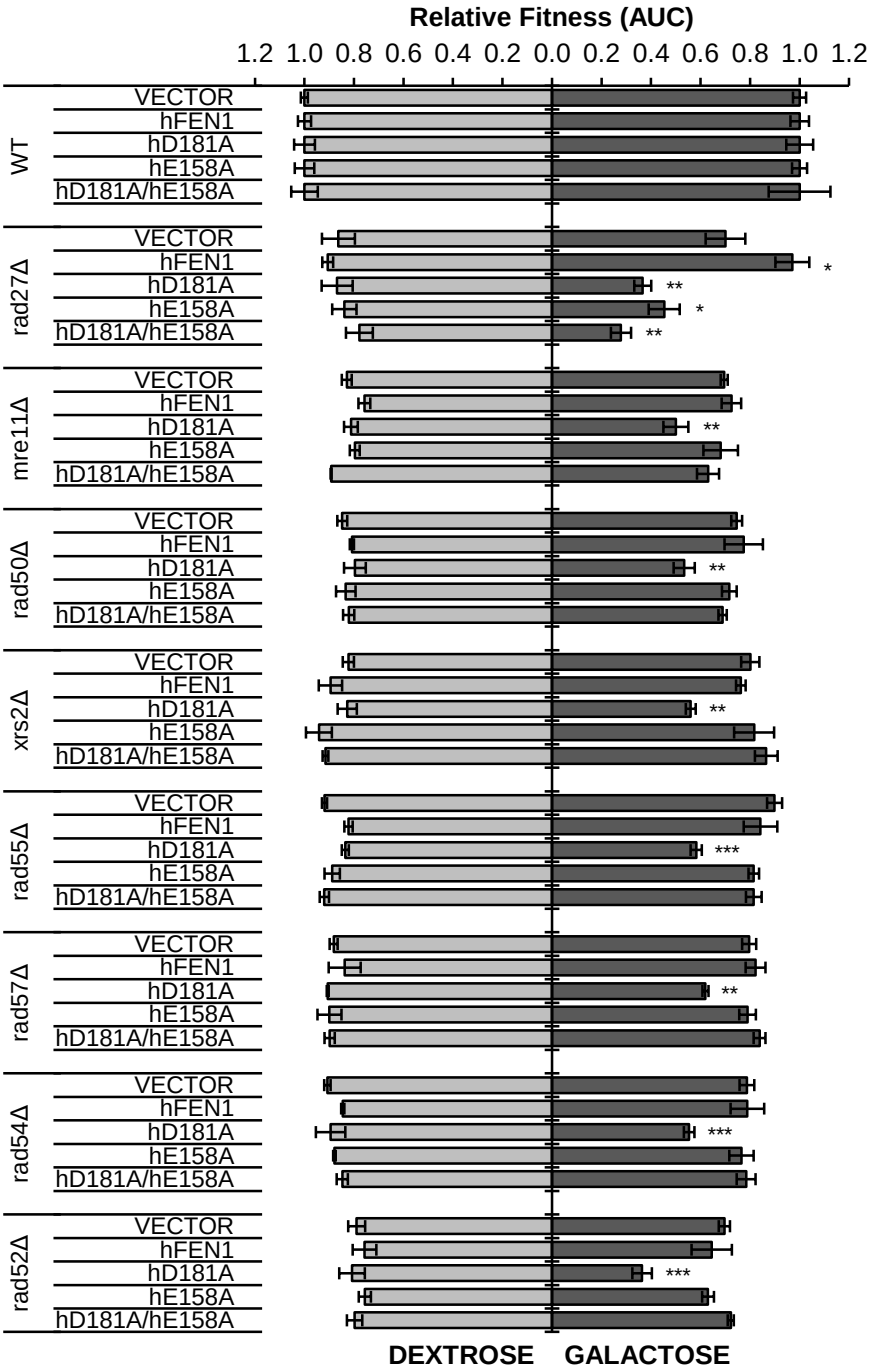

Figure 4.9. Introduction of a hFen1 DNA binding mutation rescues fitness defects of HR mutants overexpressing h*FEN1*^{D181A}.

Assessing the impact of a DNA binding mutant on SDL interaction hits identified from the h*FEN1*^{D181A} screen. Yeast knockout mutants containing a vector control or h*FEN1* (wild-type or mutant) plasmids were grown in galactose media to induce expression. h*FEN1* overexpression rescues fitness defects of *rad27Δ*, while overexpression of nuclease or DNA binding defective h*FEN1* decreases fitness of *rad27Δ*. For the HR mutants, only overexpression of h*FEN1*^{D181A} decreases fitness of the knockout strains. Strain fitness was defined as the AUC of each yeast knockout strain relative to the AUC of the wild-type strain containing the same plasmid and grown in the same media condition (mean +/- SD). Student's t-test. *p<0.05; **p<0.01; ***p<0.001. Corresponding growth curves are shown in Figure A.6.

CHAPTER 5: CONCLUSION AND FUTURE DIRECTIONS

5.1 A reference set of human-yeast complementation pairs

The development of high-throughput and large-scale technologies have expanded the screening capacity for human-yeast complementation pairs. As a result, several systematic screens (including our work presented in Chapter 2) have reported testing the essential yeast genes for replaceability (Hamza et al., 2015; Kachroo et al., 2015; Sun et al., 2016; Yang et al., 2017). Each study focused on a subset of the essential yeast genes, such as those implicated in CIN (our study), essential yeast genes that have human disease orthologs (Sun et al., 2016) or paralogs (Yang et al., 2017), and essential yeast genes that have one distinguishable ortholog (Kachroo et al., 2015). Notably, all studies generated overlapping lists of human-yeast complementation pairs and arrived at similar conclusions regarding features that predict replaceability of essential yeast genes. However, compared to the essential yeast genes, the nonessential genes are a much larger set and have a variety of different phenotypic readouts, making them more difficult to screen systematically for complementation. In this study, we have started this process by focusing on a subset of the nonessential yeast genes, specifically those required for chromosome maintenance. The accelerated pace of discovery for human-yeast complementation pairs has also led the Saccharomyces Genome Database (SGD) to curate complementation data in their Yeastmine database (Balakrishnan et al., 2012).

5.2 Limitations of cross-species complementation

One of the main limitations to cross-species human gene complementation using *S. cerevisiae* as the host is that not all human genes can complement a yeast loss-of-function

mutant. In these cases, human genes can be expressed ectopically in yeast and experiments are then designed based on an ability to induce a phenotypic readout. Moreover, representation of multicellular and developmental human pathways is absent in single-celled yeast. However, human genes that function in these pathways operate in the context of individual cells and may have a conserved function in yeast (Dunham and Fowler, 2013).

Assessing human gene variants in a yeast-based platform has some limitations. The functional impact of the mutations might be different outside the native context of the human cell. We observed an example of this in one of our assays; the h*PPP2R1A*^{R183W} allele was found to be nonfunctional in yeast cells, but published reports showed that this allele had an impact on protein interactions in human cell lines (Haesen et al., 2016; Taylor et al., 2019). Another limitation is that growth-based yeast complementation assays are less likely to detect gain-of-function mutations (Sun et al., 2016; Yang et al., 2017). In terms of tumor-specific variants, gain-of-function mutations in oncogenes are an important factor that drives tumorigenesis (Vogelstein et al., 2013). In these cases, other phenotypic readouts may be required to assess the impact of variants in a yeast-based platform. Taking these limitations into consideration, yeast-based assays remain an important screening platform for prioritizing experiments in mammalian models. Indeed, advances in sequencing technologies have led to the discovery of an overwhelming number of human genetic variants for which empirical assessment of their biological effects would be impractical without the support of yeast as a surrogate genetics system.

5.3 A utility for CRISPR/Cas9 in complementation assays

For our complementation screens, we designed and chose parameters that facilitated a systematic study of hundreds of human-yeast gene pairs. We chose vector-based expression to efficiently transform human cDNAs *en masse* as single clones or in a pooled format. We sought to minimize toxicity resulting from overexpression of human genes (Sekigawa et al., 2010) by using low-copy centromeric plasmids (~1-2 copies/cell) and a constitutive promoter. However, while this simplified the screening process, there were caveats to our method. In our study, we focused on assessing human complementation of yeast CIN mutants, which are defective in chromosome maintenance processes and may increase loss of centromeric plasmids. In some cases, our complementation screen tested processes involved in DNA transactions and the cell cycle, which tend to be endogenously regulated for periodic expression (Bahler, 2005). In this regard, the results from (Kachroo et al., 2015), whose study used constitutive and galactose-inducible regulation of expression to assess complementation of a more diverse set of essential yeast genes, found that DNA replication/repair and cell growth processes were the least likely to be replaceable by their human orthologs. Taken together, in some cases the use of plasmids introduces more variability in expression, and the use of a constitutive promoter could prevent endogenous transcriptional regulation of the human gene.

A systematic screening process for complementation that relies on a CRISPR/Cas9 mediated ORF replacement strategy on endogenous chromosomes will address these limitations and potentially identify a larger set of human-yeast complementation pairs for the CIN genes. Replacement of the chromosomal yeast ORF by a human ORF using a CRISPR/Cas9 replacement strategy also expands the potential for assessing human gene

variants in yeast. For instance, we assessed cancer-specific variants that were predominantly heteroallelic in the tumor environment, but our yeast-based complementation assays were restricted to haploid cells expressing the mutations in a homozygous context. In theory, experiments can be designed to introduce two plasmids into the yeast cell, where each plasmid expresses an allele to re-create the heteroallelic combination. However, given the copy number caveats mentioned including the fact that the variants are in candidate CIN genes, the variability in expression that results from using two plasmids is not ideal for these types of experiments. Instead, integration into the genome bypasses these limitations and allows testing different allelic combinations for functionality without the need for selective media. This includes assaying more complex combinations such as testing the impact of a variant in the context of mutations found in other genes.

5.4 Human-yeast genetic networks based on cross-species complementation

We demonstrated an application of humanized yeast where cross-species complementation experiments led to the strategy of inducibly overexpressing the human gene instead of the yeast gene to perform SDL screens in a model organism. Establishing cross-species genetic interaction networks typically involves identifying genetic interactions between two yeast genes before confirming the conservation of the genetic interaction in human cells (i.e. human-human) (Baryshnikova et al., 2013; Lehner, 2007). While humanized yeast has been utilized to screen yeast libraries and generate human-yeast genetic interaction networks, these screens have been mostly limited to identifying mutants that rescue growth defects resulting from the heterologous overexpression of human genes in yeast. Here, we used a human-yeast complementation pair to identify yeast mutants

sensitized to inducible expression of the human gene and demonstrated that results obtained from the yeast screen matched studies in human cell lines.

In this study, we restricted our SDL screens to testing a mini-array of 332 yeast deletion mutants that function in various DNA transactions. The next step is to expand to genome-wide yeast screens for the potential to generate a larger human-yeast genetic interaction network. Although our limited screens did not identify loss-of-function mutants sensitive to overexpression of wild-type h*FEN1*, a genome-wide screen may capture some yeast mutants that cannot tolerate elevated wild-type hFen1 protein levels. In turn, any second-site mutants that are identified may be candidate therapeutic targets for the selective killing of cancer cells that overexpress h*FEN1*. Moreover, genome-wide screens using catalytically inactive hFen1 as a query, may identify cancer targets other than HR-deficient genotypes where hFen1 inhibitors may be applied. Yeast can also be utilized to screen a query gene mutation against the whole-genome overexpression library (Hu et al., 2007). Here, a genetic network can be generated of overexpressed yeast genes that cause lethality in combination with catalytically inactive hFen1. In this case, these results may be applicable for hFen1 inhibitors to selectively target cancer cells that overexpress the conserved human gene.

Our studies showed the potential for generating genetic interaction networks that mimic the activity of chemically inhibited proteins. Genetic screens using loss- or reduction-of-function mutations would not accurately model synthetic lethal interactions that require the formation of cytotoxic protein-DNA complexes. Similar to the hFen1 screening strategy presented in this study, other DNA-binding enzymes that have catalytically inactive mutant forms that retain DNA binding are candidate queries for modelling the synthetic lethal effect

of protein trapping. For example, the catalytically inactive human *APE1* endonuclease binds substrate DNA with high affinity and induces DNA damage and sensitivity to DNA-damaging agents in mammalian cell lines (McNeill and Wilson, 2007). Overall, genetic screens utilizing gene mutations that mimic chemical inhibition in yeast or mammalian models will direct inhibitor screening approaches to identify which chemical inhibitors trap protein on the DNA.

5.5 Cross-species complementation as a platform for testing inhibitors

A humanized yeast system can also be utilized as an *in vivo* platform for inhibitor screening. This approach has been primarily used to screen for chemical inhibitors that rescue yeast growth defects caused by the heterologous expression of the human gene in yeast (Sekigawa et al., 2010; Tugendreich et al., 2001). In this study, we identified phenotypic readouts based on cross-species complementation in which inhibitors can be screened against the ability of human gene expression to rescue growth defects of the yeast null mutant. As a platform for inhibitor screening, human complementation of the yeast null mutant has several benefits over ectopic heterologous expression of human genes in yeast. Human proteins that complement yeast mutants are functional in a cellular system and in the context of other biological pathways, and inhibitors that prevent complementation may better reflect inhibition of the human protein activity in a cellular context. Screening in a null mutant background further eliminates the potential of non-specific inhibition of the cognate yeast protein. Moreover, growth defects caused by heterologous expression can be reversed by clonal selection of yeast that bypasses the fitness defects (either by a secondary unrelated mechanism or by turning off expression), and as such, large-scale screens for inhibitors that

rescue growth defects may have high background due to false-positives. This suppression of toxicity was apparent in our SDL screens that overexpressed wild-type and inactive y*RAD27*, and as such, was one of the contributing factors to the variability observed in growth rates in our screens. In contrast, inhibitors that prevent complementation are screened in a system where clonal selection of yeast favors rescue of growth by human gene expression. Complementation may also provide an alternative phenotypic readout for human proteins that do not induce severe toxicity in yeast. For example, we demonstrated that overexpression of h*FEN1* in wild-type yeast causes a minimal growth defect (~20%), which is not enough of a differential sensitivity for screening purposes. However, complementation of the y*RAD27* null allele by h*FEN1* in MMS media results in an ~80% rescue of growth defects as measured by liquid growth assays. In the case of essential yeast genes, inhibition of the complementing human protein may result in lethality.

Our study has further shown that hFen1 chemical inhibitors can be tested for induction of growth defects in HR-deficient yeast mutants. Preliminary experiments (data not shown) have revealed that hFen1 inhibitors are specific to the human protein and selectively induce growth defects in the HR-deficient *rad52*Δ strain. This system creates the potential to screen different parameters of hFen1 inhibition such as the trapping mechanism. For instance, in Chapter 4 we demonstrated that HR-deficient yeast mutant strains display no growth defects when wild-type or a DNA-binding mutant of h*FEN1* is ectopically expressed (in the presence of y*RAD27*). Based on these results, an experiment can be designed to screen for inhibitors that trap hFen1 on DNA as these inhibitors would elicit a growth defect in a HR-deficient yeast strain. In turn, these inhibitors could be more effective than those that block hFen1-DNA binding in targeting cancer cells with HR defects. This screening platform

would also identify inhibitors that cause growth defects in the presence of yRad27 activity. These represent inhibitors that can selectively target HR-defective mutants even when the inhibition is incomplete due to residual enzyme activity.

5.6 Concluding remarks

We have developed a reference set of human-yeast complementation pairs for CIN genes in order to use yeast as a surrogate genetics system to study cancer relevant processes. Our complementation screens identified 109 yeast-based assays where the functional status of 85 human genes can be assessed in a model organism. We further demonstrated applications of cross-species complementation to screen tumor-specific variants and model inhibitor-protein interactions for a cancer-relevant target. These results highlight the broad utility of humanized yeast to model and study human biology.

BIBLIOGRAPHY

Abdel-Fatah, T.M., Russell, R., Albarakati, N., Maloney, D.J., Dorjsuren, D., Rueda, O.M., Moseley, P., Mohan, V., Sun, H., Abbotts, R., *et al.* (2014). Genomic and protein expression analysis reveals flap endonuclease 1 (FEN1) as a key biomarker in breast and ovarian cancer. Molecular oncology *8*, 1326-1338.

Agmon, N., Temple, J., Tang, Z., Schraink, T., Baron, M., Chen, J., Mita, P., Martin, J.A., Tu, B.P., Yanai, I., *et al.* (2017). Human to yeast pathway transplantation: cross-species dissection of the adenine de novo pathway regulatory node. bioRxiv, 147579.

Alberti, S., Gitler, A.D., and Lindquist, S. (2007). A suite of Gateway cloning vectors for high-throughput genetic analysis in Saccharomyces cerevisiae. Yeast *24*, 913-919.

Alexandru, G., Uhlmann, F., Mechtler, K., Poupart, M.A., and Nasmyth, K. (2001). Phosphorylation of the cohesin subunit Scc1 by Polo/Cdc5 kinase regulates sister chromatid separation in yeast. Cell *105*, 459-472.

Andersen, M.P., Nelson, Z.W., Hetrick, E.D., and Gottschling, D.E. (2008). A genetic screen for increased loss of heterozygosity in Saccharomyces cerevisiae. Genetics *179*, 1179-1195.

Arnesen, T., Van Damme, P., Polevoda, B., Helsens, K., Evjenth, R., Colaert, N., Varhaug, J.E., Vandekerckhove, J., Lillehaug, J.R., Sherman, F., *et al.* (2009). Proteomics analyses reveal the evolutionary conservation and divergence of N-terminal acetyltransferases from yeast and humans. Proceedings of the National Academy of Sciences of the United States of America *106*, 8157-8162.

Arnoldo, A., Kittanakom, S., Heisler, L.E., Mak, A.B., Shukalyuk, A.I., Torti, D., Moffat, J., Giaever, G., and Nislow, C. (2014). A genome scale overexpression screen to reveal drug activity in human cells. Genome medicine *6*, 32.

Atorino, L., Silvestri, L., Koppen, M., Cassina, L., Ballabio, A., Marconi, R., Langer, T., and Casari, G. (2003). Loss of m-AAA protease in mitochondria causes complex I deficiency and increased sensitivity to oxidative stress in hereditary spastic paraplegia. The Journal of cell biology *163*, 777-787.

Bahler, J. (2005). Cell-cycle control of gene expression in budding and fission yeast. Annual review of genetics *39*, 69-94.

Balakrishnan, L., and Bambara, R.A. (2013). Flap endonuclease 1. Annual review of biochemistry *82*, 119-138.

Balakrishnan, R., Park, J., Karra, K., Hitz, B.C., Binkley, G., Hong, E.L., Sullivan, J., Micklem, G., and Cherry, J.M. (2012). YeastMine--an integrated data warehouse for Saccharomyces cerevisiae data as a multipurpose tool-kit. Database : the journal of biological databases and curation *2012*, bar062.

Barber, T.D., McManus, K., Yuen, K.W., Reis, M., Parmigiani, G., Shen, D., Barrett, I., Nouhi, Y., Spencer, F., Markowitz, S., *et al.* (2008). Chromatid cohesion defects may underlie chromosome instability in human colorectal cancers. Proceedings of the National Academy of Sciences of the United States of America *105*, 3443-3448.

Barnes, D.E., Johnston, L.H., Kodama, K., Tomkinson, A.E., Lasko, D.D., and Lindahl, T. (1990). Human DNA ligase I cDNA: cloning and functional expression in Saccharomyces cerevisiae. Proceedings of the National Academy of Sciences of the United States of America *87*, 6679-6683.

Baryshnikova, A., Costanzo, M., Myers, C.L., Andrews, B., and Boone, C. (2013). Genetic interaction networks: toward an understanding of heritability. Annual review of genomics and human genetics *14*, 111-133.

Bazzi, M., Mantiero, D., Trovesi, C., Lucchini, G., and Longhese, M.P. (2010). Dephosphorylation of gamma H2A by Glc7/protein phosphatase 1 promotes recovery from inhibition of DNA replication. Molecular and cellular biology *30*, 131-145.

Becker, J.R., Gallo, D., Leung, W., Croissant, T., Thu, Y.M., Nguyen, H.D., Starr, T.K., Brown, G.W., and Bielinsky, A.K. (2018). Flap endonuclease overexpression drives genome instability and DNA damage hypersensitivity in a PCNA-dependent manner. Nucleic acids research *46*, 5634-5650.

Ben-Aroya, S., Coombes, C., Kwok, T., O'Donnell, K.A., Boeke, J.D., and Hieter, P. (2008). Toward a comprehensive temperature-sensitive mutant repository of the essential genes of Saccharomyces cerevisiae. Molecular cell *30*, 248-258.

Bendl, J., Stourac, J., Salanda, O., Pavelka, A., Wieben, E.D., Zendulka, J., Brezovsky, J., and Damborsky, J. (2014). PredictSNP: robust and accurate consensus classifier for prediction of disease-related mutations. PLoS computational biology *10*, e1003440.

Beranek, D.T. (1990). Distribution of methyl and ethyl adducts following alkylation with monofunctional alkylating agents. Mutation research *231*, 11-30.

Blount, B.A., Driessen, M.R., and Ellis, T. (2016). GC Preps: Fast and Easy Extraction of Stable Yeast Genomic DNA. Scientific reports *6*, 26863.

Boeke, J.D., Trueheart, J., Natsoulis, G., and Fink, G.R. (1987). 5-Fluoroorotic acid as a selective agent in yeast molecular genetics. Methods in enzymology *154*, 164-175.

Botstein, D., and Fink, G.R. (2011). Yeast: an experimental organism for 21st Century biology. Genetics *189*, 695-704.

Brachmann, C.B., Davies, A., Cost, G.J., Caputo, E., Li, J., Hieter, P., and Boeke, J.D. (1998). Designer deletion strains derived from Saccharomyces cerevisiae S288C: a useful set of strains and plasmids for PCR-mediated gene disruption and other applications. Yeast *14*, 115-132.

Brooker, A.S., and Berkowitz, K.M. (2014). The roles of cohesins in mitosis, meiosis, and human health and disease. Methods in molecular biology *1170*, 229-266.

Burda, P., and Aebi, M. (1999). The dolichol pathway of N-linked glycosylation. Biochimica et biophysica acta *1426*, 239-257.

Cannon, J.F. (2010). Function of protein phosphatase-1, Glc7, in Saccharomyces cerevisiae. Advances in applied microbiology *73*, 27-59.

Cerami, E., Gao, J., Dogrusoz, U., Gross, B.E., Sumer, S.O., Aksoy, B.A., Jacobsen, A., Byrne, C.J., Heuer, M.L., Larsson, E., *et al.* (2012). The cBio cancer genomics portal: an open platform for exploring multidimensional cancer genomics data. Cancer discovery *2*, 401-404.

Ceulemans, H., and Bollen, M. (2004). Functional diversity of protein phosphatase-1, a cellular economizer and reset button. Physiological reviews *84*, 1-39.

Chen, C., and Kolodner, R.D. (1999). Gross chromosomal rearrangements in Saccharomyces cerevisiae replication and recombination defective mutants. Nature genetics *23*, 81-85.

Chen, J., Ghorai, M.K., Kenney, G., and Stubbe, J. (2008). Mechanistic studies on bleomycin-mediated DNA damage: multiple binding modes can result in double-stranded DNA cleavage. Nucleic acids research *36*, 3781-3790.

Christianson, T.W., Sikorski, R.S., Dante, M., Shero, J.H., and Hieter, P. (1992). Multifunctional yeast high-copy-number shuttle vectors. Gene *110*, 119-122.

Cooper, A.A., Gitler, A.D., Cashikar, A., Haynes, C.M., Hill, K.J., Bhullar, B., Liu, K., Xu, K., Strathearn, K.E., Liu, F., *et al.* (2006). Alpha-synuclein blocks ER-Golgi traffic and Rab1 rescues neuron loss in Parkinson's models. Science *313*, 324-328.

Davey, M.J., Andrighetti, H.J., Ma, X., and Brandl, C.J. (2011). A synthetic human kinase can control cell cycle progression in budding yeast. G3 *1*, 317-325.

Dehe, P.M., and Gaillard, P.H. (2017). Control of structure-specific endonucleases to maintain genome stability. Nature reviews Molecular cell biology *18*, 315-330.

Delgado, J.L., Hsieh, C.M., Chan, N.L., and Hiasa, H. (2018). Topoisomerases as anticancer targets. The Biochemical journal *475*, 373-398.

DiCarlo, J.E., Norville, J.E., Mali, P., Rios, X., Aach, J., and Church, G.M. (2013). Genome engineering in Saccharomyces cerevisiae using CRISPR-Cas systems. Nucleic acids research *41*, 4336-4343.

Dorjsuren, D., Kim, D., Maloney, D.J., Wilson, D.M., 3rd, and Simeonov, A. (2011). Complementary non-radioactive assays for investigation of human flap endonuclease 1 activity. Nucleic acids research *39*, e11.

Dudas, A., and Chovanec, M. (2004). DNA double-strand break repair by homologous recombination. Mutation research *566*, 131-167.

Duffy, S., Fam, H.K., Wang, Y.K., Styles, E.B., Kim, J.H., Ang, J.S., Singh, T., Larionov, V., Shah, S.P., Andrews, B., *et al.* (2016). Overexpression screens identify conserved dosage chromosome instability genes in yeast and human cancer. Proceedings of the National Academy of Sciences of the United States of America *113*, 9967-9976.

Dunham, M.J., and Fowler, D.M. (2013). Contemporary, yeast-based approaches to understanding human genetic variation. Current opinion in genetics & development *23*, 658-664.

Egloff, M.P., Cohen, P.T., Reinemer, P., and Barford, D. (1995). Crystal structure of the catalytic subunit of human protein phosphatase 1 and its complex with tungstate. Journal of molecular biology *254*, 942-959.

Egloff, M.P., Johnson, D.F., Moorhead, G., Cohen, P.T., Cohen, P., and Barford, D. (1997). Structural basis for the recognition of regulatory subunits by the catalytic subunit of protein phosphatase 1. The EMBO journal *16*, 1876-1887.

Elbatsh, A.M.O., Haarhuis, J.H.I., Petela, N., Chapard, C., Fish, A., Celie, P.H., Stadnik, M., Ristic, D., Wyman, C., Medema, R.H., *et al.* (2016). Cohesin Releases DNA through Asymmetric ATPase-Driven Ring Opening. Molecular cell *61*, 575-588.

Exell, J.C., Thompson, M.J., Finger, L.D., Shaw, S.J., Debreczeni, J., Ward, T.A., McWhirter, C., Sioberg, C.L., Martinez Molina, D., Abbott, W.M., *et al.* (2016). Cellularly active N-hydroxyurea FEN1 inhibitors block substrate entry to the active site. Nature chemical biology *12*, 815-821.

Forbes, S.A., Beare, D., Gunasekaran, P., Leung, K., Bindal, N., Boutselakis, H., Ding, M., Bamford, S., Cole, C., Ward, S., *et al.* (2015). COSMIC: exploring the world's knowledge of somatic mutations in human cancer. Nucleic acids research *43*, D805-811.

Formosa, T. (2008). FACT and the reorganized nucleosome. Molecular bioSystems *4*, 1085-1093.

Frank, C.G., Sanyal, S., Rush, J.S., Waechter, C.J., and Menon, A.K. (2008). Does Rft1 flip an N-glycan lipid precursor? Nature *454*, E3-4; discussion E4-5.

Frumkin, J.P., Patra, B.N., Sevold, A., Ganguly, K., Patel, C., Yoon, S., Schmid, M.B., and Ray, A. (2016). The interplay between chromosome stability and cell cycle control explored through gene-gene interaction and computational simulation. Nucleic acids research *44*, 8073-8085.

Gao, J., Aksoy, B.A., Dogrusoz, U., Dresdner, G., Gross, B., Sumer, S.O., Sun, Y., Jacobsen, A., Sinha, R., Larsson, E., *et al.* (2013). Integrative analysis of complex cancer genomics and clinical profiles using the cBioPortal. Science signaling *6*, pl1.

Gao, X.D., Tachikawa, H., Sato, T., Jigami, Y., and Dean, N. (2005). Alg14 recruits Alg13 to the cytoplasmic face of the endoplasmic reticulum to form a novel bipartite UDP-N-acetylglucosamine transferase required for the second step of N-linked glycosylation. The Journal of biological chemistry *280*, 36254-36262.

Giaever, G., Chu, A.M., Ni, L., Connelly, C., Riles, L., Veronneau, S., Dow, S., Lucau-Danila, A., Anderson, K., Andre, B., *et al.* (2002). Functional profiling of the Saccharomyces cerevisiae genome. Nature *418*, 387-391.

Giorgini, F., Guidetti, P., Nguyen, Q., Bennett, S.C., and Muchowski, P.J. (2005). A genomic screen in yeast implicates kynurenine 3-monooxygenase as a therapeutic target for Huntington disease. Nature genetics *37*, 526-531.

Gitler, A.D. (2008). Beer and bread to brains and beyond: can yeast cells teach us about neurodegenerative disease? Neuro-Signals *16*, 52-62.

Greene, A.L., Snipe, J.R., Gordenin, D.A., and Resnick, M.A. (1999). Functional analysis of human FEN1 in Saccharomyces cerevisiae and its role in genome stability. Human molecular genetics *8*, 2263-2273.

Guimier, A., Gordon, C.T., Godard, F., Ravenscroft, G., Oufadem, M., Vasnier, C., Rambaud, C., Nitschke, P., Bole-Feysot, C., Masson, C., *et al.* (2016). Biallelic PPA2 Mutations Cause Sudden Unexpected Cardiac Arrest in Infancy. American journal of human genetics *99*, 666-673.

Gupta, K., Bishop, J., Peck, A., Brown, J., Wilson, L., and Panda, D. (2004). Antimitotic antifungal compound benomyl inhibits brain microtubule polymerization and dynamics and cancer cell proliferation at mitosis, by binding to a novel site in tubulin. Biochemistry *43*, 6645-6655.

Haber, J.E. (1974). Bisexual mating behavior in a diploid of Saccharomyces cerevisiae: evidence for genetically controlled non-random chromosome loss during vegetative growth. Genetics *78*, 843-858.

Haesen, D., Abbasi Asbagh, L., Derua, R., Hubert, A., Schrauwen, S., Hoorne, Y., Amant, F., Waelkens, E., Sablina, A., and Janssens, V. (2016). Recurrent PPP2R1A Mutations in Uterine Cancer Act through a Dominant-Negative Mechanism to Promote Malignant Cell Growth. Cancer research *76*, 5719-5731.

Hamza, A., and Baetz, K. (2012). Iron-responsive transcription factor Aft1 interacts with kinetochore protein Iml3 and promotes pericentromeric cohesin. The Journal of biological chemistry *287*, 4139-4147.

Hamza, A., Tammpere, E., Kofoed, M., Keong, C., Chiang, J., Giaever, G., Nislow, C., and Hieter, P. (2015). Complementation of Yeast Genes with Human Genes as an Experimental Platform for Functional Testing of Human Genetic Variants. Genetics *201*, 1263-1274.

Hanahan, D., and Weinberg, R.A. (2011). Hallmarks of cancer: the next generation. Cell *144*, 646-674.

Hartley, J.L., Temple, G.F., and Brasch, M.A. (2000). DNA cloning using in vitro site-specific recombination. Genome research *10*, 1788-1795.

Hartwell, L.H., Szankasi, P., Roberts, C.J., Murray, A.W., and Friend, S.H. (1997). Integrating genetic approaches into the discovery of anticancer drugs. Science *278*, 1064-1068.

He, L., Luo, L., Zhu, H., Yang, H., Zhang, Y., Wu, H., Sun, H., Jiang, F., Kathera, C.S., Liu, L., *et al.* (2017). FEN1 promotes tumor progression and confers cisplatin resistance in non-small-cell lung cancer. Molecular oncology *11*, 1302-1303.

He, L., Zhang, Y., Sun, H., Jiang, F., Yang, H., Wu, H., Zhou, T., Hu, S., Kathera, C.S., Wang, X., *et al.* (2016). Targeting DNA Flap Endonuclease 1 to Impede Breast Cancer Progression. EBioMedicine *14*, 32-43.

Heidinger-Pauli, J.M., Mert, O., Davenport, C., Guacci, V., and Koshland, D. (2010a). Systematic reduction of cohesin differentially affects chromosome segregation, condensation, and DNA repair. Current biology : CB *20*, 957-963.

Heidinger-Pauli, J.M., Onn, I., and Koshland, D. (2010b). Genetic evidence that the acetylation of the Smc3p subunit of cohesin modulates its ATP-bound state to promote cohesion establishment in Saccharomyces cerevisiae. Genetics *185*, 1249-1256.

Heinicke, S., Livstone, M.S., Lu, C., Oughtred, R., Kang, F., Angiuoli, S.V., White, O., Botstein, D., and Dolinski, K. (2007). The Princeton Protein Orthology Database (P-POD): a comparative genomics analysis tool for biologists. PloS one *2*, e766.

Helenius, J., Ng, D.T., Marolda, C.L., Walter, P., Valvano, M.A., and Aebi, M. (2002). Translocation of lipid-linked oligosaccharides across the ER membrane requires Rft1 protein. Nature *415*, 447-450.

Hill, V.K., Kim, J.S., and Waldman, T. (2016). Cohesin mutations in human cancer. Biochimica et biophysica acta *1866*, 1-11.

Ho, C.H., Magtanong, L., Barker, S.L., Gresham, D., Nishimura, S., Natarajan, P., Koh, J.L.Y., Porter, J., Gray, C.A., Andersen, R.J., *et al.* (2009). A molecular barcoded yeast ORF library enables mode-of-action analysis of bioactive compounds. Nature biotechnology *27*, 369-377.

Hsiang, Y.H., Lihou, M.G., and Liu, L.F. (1989). Arrest of replication forks by drug-stabilized topoisomerase I-DNA cleavable complexes as a mechanism of cell killing by camptothecin. Cancer research *49*, 5077-5082.

Hu, B., Itoh, T., Mishra, A., Katoh, Y., Chan, K.L., Upcher, W., Godlee, C., Roig, M.B., Shirahige, K., and Nasmyth, K. (2011). ATP hydrolysis is required for relocating cohesin from sites occupied by its Scc2/4 loading complex. Current biology : CB *21*, 12-24.

Hu, Y., Rolfs, A., Bhullar, B., Murthy, T.V., Zhu, C., Berger, M.F., Camargo, A.A., Kelley, F., McCarron, S., Jepson, D., *et al.* (2007). Approaching a complete repository of sequence-verified protein-encoding clones for Saccharomyces cerevisiae. Genome research *17*, 536-543.

Iacobuzio-Donahue, C.A., Maitra, A., Olsen, M., Lowe, A.W., van Heek, N.T., Rosty, C., Walter, K., Sato, N., Parker, A., Ashfaq, R., *et al.* (2003). Exploration of global gene expression patterns in pancreatic adenocarcinoma using cDNA microarrays. The American journal of pathology *162*, 1151-1162.

Janssens, V., Goris, J., and Van Hoof, C. (2005). PP2A: the expected tumor suppressor. Current opinion in genetics & development *15*, 34-41.

Jimeno, S., Herrera-Moyano, E., Ortega, P., and Aguilera, A. (2017). Differential effect of the overexpression of Rad2/XPG family endonucleases on genome integrity in yeast and human cells. DNA repair *57*, 66-75.

Jo, M., Chung, A.Y., Yachie, N., Seo, M., Jeon, H., Nam, Y., Seo, Y., Kim, E., Zhong, Q., Vidal, M., *et al.* (2017). Yeast genetic interaction screen of human genes associated with amyotrophic lateral sclerosis: identification of MAP2K5 kinase as a potential drug target. Genome research *27*, 1487-1500.

Johnson, D.I. (1999). Cdc42: An essential Rho-type GTPase controlling eukaryotic cell polarity. Microbiology and molecular biology reviews : MMBR *63*, 54-105.

Jones, S., Wang, T.L., Shih Ie, M., Mao, T.L., Nakayama, K., Roden, R., Glas, R., Slamon, D., Diaz, L.A., Jr., Vogelstein, B., *et al.* (2010). Frequent mutations of chromatin remodeling gene ARID1A in ovarian clear cell carcinoma. Science *330*, 228-231.

Kachroo, A.H., Laurent, J.M., Akhmetov, A., Szilagyi-Jones, M., McWhite, C.D., Zhao, A., and Marcotte, E.M. (2017). Systematic bacterialization of yeast genes identifies a near-universally swappable pathway. eLife *6*.

Kachroo, A.H., Laurent, J.M., Yellman, C.M., Meyer, A.G., Wilke, C.O., and Marcotte, E.M. (2015). Evolution. Systematic humanization of yeast genes reveals conserved functions and genetic modularity. Science *348*, 921-925.

Katahira, J., Strasser, K., Podtelejnikov, A., Mann, M., Jung, J.U., and Hurt, E. (1999). The Mex67p-mediated nuclear mRNA export pathway is conserved from yeast to human. The EMBO journal *18*, 2593-2609.

Kataoka, T., Powers, S., Cameron, S., Fasano, O., Goldfarb, M., Broach, J., and Wigler, M. (1985). Functional homology of mammalian and yeast RAS genes. Cell *40*, 19-26.

Kato, S., Han, S.Y., Liu, W., Otsuka, K., Shibata, H., Kanamaru, R., and Ishioka, C. (2003). Understanding the function-structure and function-mutation relationships of p53 tumor suppressor protein by high-resolution missense mutation analysis. Proceedings of the National Academy of Sciences of the United States of America *100*, 8424-8429.

Kikuchi, K., Narita, T., Pham, V.T., Iijima, J., Hirota, K., Keka, I.S., Mohiuddin, Okawa, K., Hori, T., Fukagawa, T., *et al.* (2013). Structure-specific endonucleases xpf and mus81 play overlapping but essential roles in DNA repair by homologous recombination. Cancer research *73*, 4362-4371.

Kinsella, R.J., Kahari, A., Haider, S., Zamora, J., Proctor, G., Spudich, G., Almeida-King, J., Staines, D., Derwent, P., Kerhornou, A., *et al.* (2011). Ensembl BioMarts: a hub for data retrieval across taxonomic space. Database : the journal of biological databases and curation *2011*, bar030.

Koc, A., Wheeler, L.J., Mathews, C.K., and Merrill, G.F. (2004). Hydroxyurea arrests DNA replication by a mechanism that preserves basal dNTP pools. The Journal of biological chemistry *279*, 223-230.

Koerte, A., Chong, T., Li, X., Wahane, K., and Cai, M. (1995). Suppression of the yeast mutation rft1-1 by human p53. The Journal of biological chemistry *270*, 22556-22564.

Kofoed, M., Milbury, K.L., Chiang, J.H., Sinha, S., Ben-Aroya, S., Giaever, G., Nislow, C., Hieter, P., and Stirling, P.C. (2015). An Updated Collection of Sequence Barcoded Temperature-Sensitive Alleles of Yeast Essential Genes. G3 *5*, 1879-1887.

Koonin, E.V. (2005). Orthologs, paralogs, and evolutionary genomics. Annual review of genetics *39*, 309-338.

Krause, A., Combaret, V., Iacono, I., Lacroix, B., Compagnon, C., Bergeron, C., Valsesia-Wittmann, S., Leissner, P., Mougin, B., and Puisieux, A. (2005). Genome-wide analysis of gene expression in neuroblastomas detected by mass screening. Cancer letters *225*, 111-120.

Kroll, E.S., Hyland, K.M., Hieter, P., and Li, J.J. (1996). Establishing genetic interactions by a synthetic dosage lethality phenotype. Genetics *143*, 95-102.

Lam, J.S., Seligson, D.B., Yu, H., Li, A., Eeva, M., Pantuck, A.J., Zeng, G., Horvath, S., and Belldegrun, A.S. (2006). Flap endonuclease 1 is overexpressed in prostate cancer and is associated with a high Gleason score. BJU international *98*, 445-451.

Laurent, J.M., Young, J.H., Kachroo, A.H., and Marcotte, E.M. (2016). Efforts to make and apply humanized yeast. Briefings in functional genomics *15*, 155-163.

Lee, K.S., and Erikson, R.L. (1997). Plk is a functional homolog of Saccharomyces cerevisiae Cdc5, and elevated Plk activity induces multiple septation structures. Molecular and cellular biology *17*, 3408-3417.

Lee, M.E., DeLoache, W.C., Cervantes, B., and Dueber, J.E. (2015). A Highly Characterized Yeast Toolkit for Modular, Multipart Assembly. ACS synthetic biology *4*, 975-986.

Lee, M.G., and Nurse, P. (1987). Complementation used to clone a human homologue of the fission yeast cell cycle control gene cdc2. Nature *327*, 31-35.

Lehner, B. (2007). Modelling genotype-phenotype relationships and human disease with genetic interaction networks. The Journal of experimental biology *210*, 1559-1566.

Li, Z., Vizeacoumar, F.J., Bahr, S., Li, J., Warringer, J., Vizeacoumar, F.S., Min, R., Vandersluis, B., Bellay, J., Devit, M., *et al.* (2011). Systematic exploration of essential yeast gene function with temperature-sensitive mutants. Nature biotechnology *29*, 361-367.

Lindahl, T., and Barnes, D.E. (1992). Mammalian DNA ligases. Annual review of biochemistry *61*, 251-281.

Loeb, L.A. (2011). Human cancers express mutator phenotypes: origin, consequences and targeting. Nature reviews Cancer *11*, 450-457.

Losada, A. (2014). Cohesin in cancer: chromosome segregation and beyond. Nature reviews Cancer *14*, 389-393.

Maine, G.T., Sinha, P., and Tye, B.K. (1984). Mutants of S. cerevisiae defective in the maintenance of minichromosomes. Genetics *106*, 365-385.

Makrantoni, V., and Marston, A.L. (2018). Cohesin and chromosome segregation. Current biology : CB *28*, R688-R693.

Marini, N.J., Gin, J., Ziegle, J., Keho, K.H., Ginzinger, D., Gilbert, D.A., and Rine, J. (2008). The prevalence of folate-remedial MTHFR enzyme variants in humans. Proceedings of the National Academy of Sciences of the United States of America *105*, 8055-8060.

Marini, N.J., Thomas, P.D., and Rine, J. (2010). The use of orthologous sequences to predict the impact of amino acid substitutions on protein function. PLoS genetics *6*, e1000968.

Marston, A.L. (2014). Chromosome segregation in budding yeast: sister chromatid cohesion and related mechanisms. Genetics *196*, 31-63.

Mayfield, J.A., Davies, M.W., Dimster-Denk, D., Pleskac, N., McCarthy, S., Boydston, E.A., Fink, L., Lin, X.X., Narain, A.S., Meighan, M., *et al.* (2012). Surrogate genetics and metabolic profiling for characterization of human disease alleles. Genetics *190*, 1309-1323.

McCarrey, J.R., and Thomas, K. (1987). Human testis-specific PGK gene lacks introns and possesses characteristics of a processed gene. Nature *326*, 501-505.

McManus, K.J., Barrett, I.J., Nouhi, Y., and Hieter, P. (2009). Specific synthetic lethal killing of RAD54B-deficient human colorectal cancer cells by FEN1 silencing. Proceedings of the National Academy of Sciences of the United States of America *106*, 3276-3281.

McNeill, D.R., and Wilson, D.M., 3rd (2007). A dominant-negative form of the major human abasic endonuclease enhances cellular sensitivity to laboratory and clinical DNA-damaging agents. Molecular cancer research : MCR *5*, 61-70.

McWhirter, C., Tonge, M., Plant, H., Hardern, I., Nissink, W., and Durant, S.T. (2013). Development of a high-throughput fluorescence polarization DNA cleavage assay for the identification of FEN1 inhibitors. Journal of biomolecular screening *18*, 567-575.

Measday, V., Baetz, K., Guzzo, J., Yuen, K., Kwok, T., Sheikh, B., Ding, H., Ueta, R., Hoac, T., Cheng, B., *et al.* (2005). Systematic yeast synthetic lethal and synthetic dosage lethal screens identify genes required for chromosome segregation. Proceedings of the National Academy of Sciences of the United States of America *102*, 13956-13961.

Measday, V., and Stirling, P.C. (2016). Navigating yeast genome maintenance with functional genomics. Briefings in functional genomics *15*, 119-129.

Mighell, T.L., Evans-Dutson, S., and O'Roak, B.J. (2018). A Saturation Mutagenesis Approach to Understanding PTEN Lipid Phosphatase Activity and Genotype-Phenotype Relationships. American journal of human genetics *102*, 943-955.

Murai, J., Huang, S.Y., Das, B.B., Renaud, A., Zhang, Y., Doroshow, J.H., Ji, J., Takeda, S., and Pommier, Y. (2012). Trapping of PARP1 and PARP2 by Clinical PARP Inhibitors. Cancer research *72*, 5588-5599.

Nasmyth, K., and Haering, C.H. (2009). Cohesin: its roles and mechanisms. Annual review of genetics *43*, 525-558.

Negrini, S., Gorgoulis, V.G., and Halazonetis, T.D. (2010). Genomic instability--an evolving hallmark of cancer. Nature reviews Molecular cell biology *11*, 220-228.

Ng, D.T., Spear, E.D., and Walter, P. (2000). The unfolded protein response regulates multiple aspects of secretory and membrane protein biogenesis and endoplasmic reticulum quality control. The Journal of cell biology *150*, 77-88.

Nikolova, T., Christmann, M., and Kaina, B. (2009). FEN1 is overexpressed in testis, lung and brain tumors. Anticancer research *29*, 2453-2459.

O'Neil, N.J., Bailey, M.L., and Hieter, P. (2017). Synthetic lethality and cancer. Nature reviews Genetics *18*, 613-623.

Osborn, M.J., and Miller, J.R. (2007). Rescuing yeast mutants with human genes. Briefings in functional genomics & proteomics *6*, 104-111.

Osborne, A.R., Rapoport, T.A., and van den Berg, B. (2005). Protein translocation by the Sec61/SecY channel. Annual review of cell and developmental biology *21*, 529-550.

Ozanick, S., Krecic, A., Andersland, J., and Anderson, J.T. (2005). The bipartite structure of the tRNA m1A58 methyltransferase from S. cerevisiae is conserved in humans. Rna *11*, 1281-1290.

Pan, X., Yuan, D.S., Ooi, S.L., Wang, X., Sookhai-Mahadeo, S., Meluh, P., and Boeke, J.D. (2007). dSLAM analysis of genome-wide genetic interactions in Saccharomyces cerevisiae. Methods *41*, 206-221.

Pan, X., Yuan, D.S., Xiang, D., Wang, X., Sookhai-Mahadeo, S., Bader, J.S., Hieter, P., Spencer, F., and Boeke, J.D. (2004). A robust toolkit for functional profiling of the yeast genome. Molecular cell *16*, 487-496.

Paul, V.D., Muhlenhoff, U., Stumpfig, M., Seebacher, J., Kugler, K.G., Renicke, C., Taxis, C., Gavin, A.C., Pierik, A.J., and Lill, R. (2015). The deca-GX3 proteins Yae1-Lto1 function as adaptors recruiting the ABC protein Rli1 for iron-sulfur cluster insertion. eLife *4*, e08231.

Perkins, E., Sun, D., Nguyen, A., Tulac, S., Francesco, M., Tavana, H., Nguyen, H., Tugendreich, S., Barthmaier, P., Couto, J., *et al.* (2001). Novel inhibitors of poly(ADP-ribose) polymerase/PARP1 and PARP2 identified using a cell-based screen in yeast. Cancer research *61*, 4175-4183.

Peters, J.M., Tedeschi, A., and Schmitz, J. (2008). The cohesin complex and its roles in chromosome biology. Genes & development *22*, 3089-3114.

Peterson, T.A., Park, D., and Kann, M.G. (2013). A protein domain-centric approach for the comparative analysis of human and yeast phenotypically relevant mutations. BMC genomics *14 Suppl 3*, S5.

Pommier, Y., O'Connor, M.J., and de Bono, J. (2016). Laying a trap to kill cancer cells: PARP inhibitors and their mechanisms of action. Science translational medicine *8*, 362ps317.

Pon, J.R., and Marra, M.A. (2015). Driver and passenger mutations in cancer. Annual review of pathology *10*, 25-50.

Prakash, L., and Prakash, S. (1977). Isolation and characterization of MMS-sensitive mutants of Saccharomyces cerevisiae. Genetics *86*, 33-55.

Qian, Y., Kachroo, A.H., Yellman, C.M., Marcotte, E.M., and Johnson, K.A. (2014). Yeast cells expressing the human mitochondrial DNA polymerase reveal correlations between polymerase fidelity and human disease progression. The Journal of biological chemistry *289*, 5970-5985.

Richards, S., Aziz, N., Bale, S., Bick, D., Das, S., Gastier-Foster, J., Grody, W.W., Hegde, M., Lyon, E., Spector, E., *et al.* (2015). Standards and guidelines for the interpretation of sequence variants: a joint consensus recommendation of the American College of Medical Genetics and Genomics and the Association for Molecular Pathology. Genetics in medicine : official journal of the American College of Medical Genetics *17*, 405-424.

Rine, J. (2014). A future of the model organism model. Molecular biology of the cell *25*, 549-553.

Rothbauer, U., Hofmann, S., Muhlenbein, N., Paschen, S.A., Gerbitz, K.D., Neupert, W., Brunner, M., and Bauer, M.F. (2001). Role of the deafness dystonia peptide 1 (DDP1) in import of human Tim23 into the inner membrane of mitochondria. The Journal of biological chemistry *276*, 37327-37334.

Rush, J.S., Gao, N., Lehrman, M.A., Matveev, S., and Waechter, C.J. (2009). Suppression of Rft1 expression does not impair the transbilayer movement of Man5GlcNAc2-P-P-dolichol in sealed microsomes from yeast. The Journal of biological chemistry *284*, 19835-19842.

Ryan, O.W., Skerker, J.M., Maurer, M.J., Li, X., Tsai, J.C., Poddar, S., Lee, M.E., DeLoache, W., Dueber, J.E., Arkin, A.P., *et al.* (2014). Selection of chromosomal DNA libraries using a multiplex CRISPR system. eLife *3*.

Sanyal, S., Frank, C.G., and Menon, A.K. (2008). Distinct flippases translocate glycerophospholipids and oligosaccharide diphosphate dolichols across the endoplasmic reticulum. Biochemistry *47*, 7937-7946.

Schlesinger, M.B., and Formosa, T. (2000). POB3 is required for both transcription and replication in the yeast Saccharomyces cerevisiae. Genetics *155*, 1593-1606.

Schneider-Poetsch, T., Ju, J., Eyler, D.E., Dang, Y., Bhat, S., Merrick, W.C., Green, R., Shen, B., and Liu, J.O. (2010). Inhibition of eukaryotic translation elongation by cycloheximide and lactimidomycin. Nature chemical biology *6*, 209-217.

Sekigawa, M., Kunoh, T., Wada, S., Mukai, Y., Ohshima, K., Ohta, S., Goshima, N., Sasaki, R., and Mizukami, T. (2010). Comprehensive screening of human genes with inhibitory effects on yeast growth and validation of a yeast cell-based system for screening chemicals. Journal of biomolecular screening *15*, 368-378.

Seshacharyulu, P., Pandey, P., Datta, K., and Batra, S.K. (2013). Phosphatase: PP2A structural importance, regulation and its aberrant expression in cancer. Cancer letters *335*, 9-18.

Shaag, A., Walsh, T., Renbaum, P., Kirchhoff, T., Nafa, K., Shiovitz, S., Mandell, J.B., Welcsh, P., Lee, M.K., Ellis, N., *et al.* (2005). Functional and genomic approaches reveal an ancient CHEK2 allele associated with breast cancer in the Ashkenazi Jewish population. Human molecular genetics *14*, 555-563.

Shen, B., Nolan, J.P., Sklar, L.A., and Park, M.S. (1996). Essential amino acids for substrate binding and catalysis of human flap endonuclease 1. The Journal of biological chemistry *271*, 9173-9176.

Shen, B., Nolan, J.P., Sklar, L.A., and Park, M.S. (1997). Functional analysis of point mutations in human flap endonuclease-1 active site. Nucleic acids research *25*, 3332-3338.

Sikorski, R.S., and Hieter, P. (1989). A system of shuttle vectors and yeast host strains designed for efficient manipulation of DNA in Saccharomyces cerevisiae. Genetics *122*, 19-27.

Singh, P., Yang, M., Dai, H., Yu, D., Huang, Q., Tan, W., Kernstine, K.H., Lin, D., and Shen, B. (2008). Overexpression and hypomethylation of flap endonuclease 1 gene in breast and other cancers. Molecular cancer research : MCR *6*, 1710-1717.

Smith, S., Hwang, J.Y., Banerjee, S., Majeed, A., Gupta, A., and Myung, K. (2004). Mutator genes for suppression of gross chromosomal rearrangements identified by a genome-wide screening in Saccharomyces cerevisiae. Proceedings of the National Academy of Sciences of the United States of America *101*, 9039-9044.

Spencer, F., Gerring, S.L., Connelly, C., and Hieter, P. (1990). Mitotic chromosome transmission fidelity mutants in Saccharomyces cerevisiae. Genetics *124*, 237-249.

Stanley, D., Bandara, A., Fraser, S., Chambers, P.J., and Stanley, G.A. (2010). The ethanol stress response and ethanol tolerance of Saccharomyces cerevisiae. Journal of applied microbiology *109*, 13-24.

Stirling, P.C., Bloom, M.S., Solanki-Patil, T., Smith, S., Sipahimalani, P., Li, Z., Kofoed, M., Ben-Aroya, S., Myung, K., and Hieter, P. (2011). The complete spectrum of yeast chromosome instability genes identifies candidate CIN cancer genes and functional roles for ASTRA complex components. PLoS genetics *7*, e1002057.

Stoler, S., Keith, K.C., Curnick, K.E., and Fitzgerald-Hayes, M. (1995). A mutation in CSE4, an essential gene encoding a novel chromatin-associated protein in yeast, causes chromosome nondisjunction and cell cycle arrest at mitosis. Genes & development *9*, 573-586.

Stratton, M.R., Campbell, P.J., and Futreal, P.A. (2009). The cancer genome. Nature *458*, 719-724.

Sun, S., Yang, F., Tan, G., Costanzo, M., Oughtred, R., Hirschman, J., Theesfeld, C.L., Bansal, P., Sahni, N., Yi, S., *et al.* (2016). An extended set of yeast-based functional assays accurately identifies human disease mutations. Genome research *26*, 670-680.

Svensson, J.P., Fry, R.C., Wang, E., Somoza, L.A., and Samson, L.D. (2012). Identification of novel human damage response proteins targeted through yeast orthology. PloS one *7*, e37368.

Tamburini, B.A., Carson, J.J., Adkins, M.W., and Tyler, J.K. (2005). Functional conservation and specialization among eukaryotic anti-silencing function 1 histone chaperones. Eukaryotic cell *4*, 1583-1590.

Tanaka, K., and Hirota, T. (2016). Chromosomal instability: A common feature and a therapeutic target of cancer. Biochimica et biophysica acta *1866*, 64-75.

Tardiff, D.F., Khurana, V., Chung, C.Y., and Lindquist, S. (2014). From yeast to patient neurons and back again: powerful new discovery platform. Movement disorders : official journal of the Movement Disorder Society *29*, 1231-1240.

Tarnowski, L.J., Kowalec, P., Milewski, M., Jurek, M., Plochocka, D., Fronk, J., and Kurlandzka, A. (2012). Nuclear import and export signals of human cohesins SA1/STAG1 and SA2/STAG2 expressed in Saccharomyces cerevisiae. PloS one *7*, e38740.

Taylor, S.E., O'Connor, C.M., Wang, Z., Shen, G., Song, H., Leonard, D., Sangodkar, J., LaVasseur, C., Avril, S., Waggoner, S., *et al.* (2019). The highly recurrent PP2A Aalpha-subunit mutation P179R alters protein structure and impairs PP2A enzyme function to promote endometrial tumorigenesis. Cancer research.

Tong, A.H., Evangelista, M., Parsons, A.B., Xu, H., Bader, G.D., Page, N., Robinson, M., Raghibizadeh, S., Hogue, C.W., Bussey, H., *et al.* (2001). Systematic genetic analysis with ordered arrays of yeast deletion mutants. Science *294*, 2364-2368.

Treusch, S., Hamamichi, S., Goodman, J.L., Matlack, K.E., Chung, C.Y., Baru, V., Shulman, J.M., Parrado, A., Bevis, B.J., Valastyan, J.S., *et al.* (2011). Functional links between Abeta toxicity, endocytic trafficking, and Alzheimer's disease risk factors in yeast. Science *334*, 1241-1245.

Trevisson, E., Burlina, A., Doimo, M., Pertegato, V., Casarin, A., Cesaro, L., Navas, P., Basso, G., Sartori, G., and Salviati, L. (2009). Functional complementation in yeast allows molecular characterization of missense argininosuccinate lyase mutations. The Journal of biological chemistry *284*, 28926-28934.

Truong, D.M., and Boeke, J.D. (2017). Resetting the Yeast Epigenome with Human Nucleosomes. Cell *171*, 1508-1519 e1513.

Tugendreich, S., Perkins, E., Couto, J., Barthmaier, P., Sun, D., Tang, S., Tulac, S., Nguyen, A., Yeh, E., Mays, A., *et al.* (2001). A streamlined process to phenotypically profile heterologous cDNAs in parallel using yeast cell-based assays. Genome research *11*, 1899-1912.

Tumey, L.N., Bom, D., Huck, B., Gleason, E., Wang, J., Silver, D., Brunden, K., Boozer, S., Rundlett, S., Sherf, B., *et al.* (2005). The identification and optimization of a N-hydroxy urea series of flap endonuclease 1 inhibitors. Bioorganic & medicinal chemistry letters *15*, 277-281.

Tutaj, H., Pogoda, E., Tomala, K., and Korona, R. (2018). Gene overexpression screen for chromosome instability in yeast primarily identifies cell cycle progression genes. Current genetics.

van Pel, D.M., Barrett, I.J., Shimizu, Y., Sajesh, B.V., Guppy, B.J., Pfeifer, T., McManus, K.J., and Hieter, P. (2013). An evolutionarily conserved synthetic lethal interaction network identifies FEN1 as a broad-spectrum target for anticancer therapeutic development. PLoS genetics *9*, e1003254.

VanDemark, A.P., Blanksma, M., Ferris, E., Heroux, A., Hill, C.P., and Formosa, T. (2006). The structure of the yFACT Pob3-M domain, its interaction with the DNA replication factor RPA, and a potential role in nucleosome deposition. Molecular cell *22*, 363-374.

Vogelstein, B., Papadopoulos, N., Velculescu, V.E., Zhou, S., Diaz, L.A., Jr., and Kinzler, K.W. (2013). Cancer genome landscapes. Science *339*, 1546-1558.

Waizenegger, I., Gimenez-Abian, J.F., Wernic, D., and Peters, J.M. (2002). Regulation of human separase by securin binding and autocleavage. Current biology : CB *12*, 1368-1378.

Waizenegger, I.C., Hauf, S., Meinke, A., and Peters, J.M. (2000). Two distinct pathways remove mammalian cohesin from chromosome arms in prophase and from centromeres in anaphase. Cell *103*, 399-410.

Wang, K., Xie, C., and Chen, D. (2014). Flap endonuclease 1 is a promising candidate biomarker in gastric cancer and is involved in cell proliferation and apoptosis. International journal of molecular medicine *33*, 1268-1274.

Wang, Z., Cummins, J.M., Shen, D., Cahill, D.P., Jallepalli, P.V., Wang, T.L., Parsons, D.W., Traverso, G., Awad, M., Silliman, N., *et al.* (2004). Three classes of genes mutated in colorectal cancers with chromosomal instability. Cancer research *64*, 2998-3001.

Ward, T.A., McHugh, P.J., and Durant, S.T. (2017). Small molecule inhibitors uncover synthetic genetic interactions of human flap endonuclease 1 (FEN1) with DNA damage response genes. PloS one *12*, e0179278.

Whelan, W.L., Gocke, E., and Manney, T.R. (1979). The CAN1 locus of Saccharomyces cerevisiae: fine-structure analysis and forward mutation rates. Genetics *91*, 35-51.

Wieland, G., Orthaus, S., Ohndorf, S., Diekmann, S., and Hemmerich, P. (2004). Functional complementation of human centromere protein A (CENP-A) by Cse4p from Saccharomyces cerevisiae. Molecular and cellular biology *24*, 6620-6630.

Willingham, S., Outeiro, T.F., DeVit, M.J., Lindquist, S.L., and Muchowski, P.J. (2003). Yeast genes that enhance the toxicity of a mutant huntingtin fragment or alpha-synuclein. Science *302*, 1769-1772.

Wu, X., Li, J., Li, X., Hsieh, C.L., Burgers, P.M., and Lieber, M.R. (1996). Processing of branched DNA intermediates by a complex of human FEN-1 and PCNA. Nucleic acids research *24*, 2036-2043.

Yamagata, K., Kato, J., Shimamoto, A., Goto, M., Furuichi, Y., and Ikeda, H. (1998). Bloom's and Werner's syndrome genes suppress hyperrecombination in yeast sgs1 mutant: implication for genomic instability in human diseases. Proceedings of the National Academy of Sciences of the United States of America *95*, 8733-8738.

Yang, F., Sun, S., Tan, G., Costanzo, M., Hill, D.E., Vidal, M., Andrews, B.J., Boone, C., and Roth, F.P. (2017). Identifying pathogenicity of human variants via paralog-based yeast complementation. PLoS genetics *13*, e1006779.

Yang, X., Boehm, J.S., Yang, X., Salehi-Ashtiani, K., Hao, T., Shen, Y., Lubonja, R., Thomas, S.R., Alkan, O., Bhimdi, T., *et al.* (2011). A public genome-scale lentiviral expression library of human ORFs. Nature methods *8*, 659-661.

Young, B.P., and Loewen, C.J. (2013). Balony: a software package for analysis of data generated by synthetic genetic array experiments. BMC bioinformatics *14*, 354.

Yuen, K.W., Warren, C.D., Chen, O., Kwok, T., Hieter, P., and Spencer, F.A. (2007). Systematic genome instability screens in yeast and their potential relevance to cancer. Proceedings of the National Academy of Sciences of the United States of America *104*, 3925-3930.

Zhang, J., Shi, X., Li, Y., Kim, B.J., Jia, J., Huang, Z., Yang, T., Fu, X., Jung, S.Y., Wang, Y., *et al.* (2008). Acetylation of Smc3 by Eco1 is required for S phase sister chromatid cohesion in both human and yeast. Molecular cell *31*, 143-151.

Zhang, L., Zhang, Z., Long, F., and Lee, E.Y. (1996). Tyrosine-272 is involved in the inhibition of protein phosphatase-1 by multiple toxins. Biochemistry *35*, 1606-1611.

Zhang, N., Osborn, M., Gitsham, P., Yen, K., Miller, J.R., and Oliver, S.G. (2003). Using yeast to place human genes in functional categories. Gene *303*, 121-129.

Zhou, Z., and Reed, R. (1998). Human homologs of yeast prp16 and prp17 reveal conservation of the mechanism for catalytic step II of pre-mRNA splicing. The EMBO journal *17*, 2095-2106.

Zhu, J., Heinecke, D., Mulla, W.A., Bradford, W.D., Rubinstein, B., Box, A., Haug, J.S., and Li, R. (2015). Single-Cell Based Quantitative Assay of Chromosome Transmission Fidelity. G3 *5*, 1043-1056.

APPENDIX

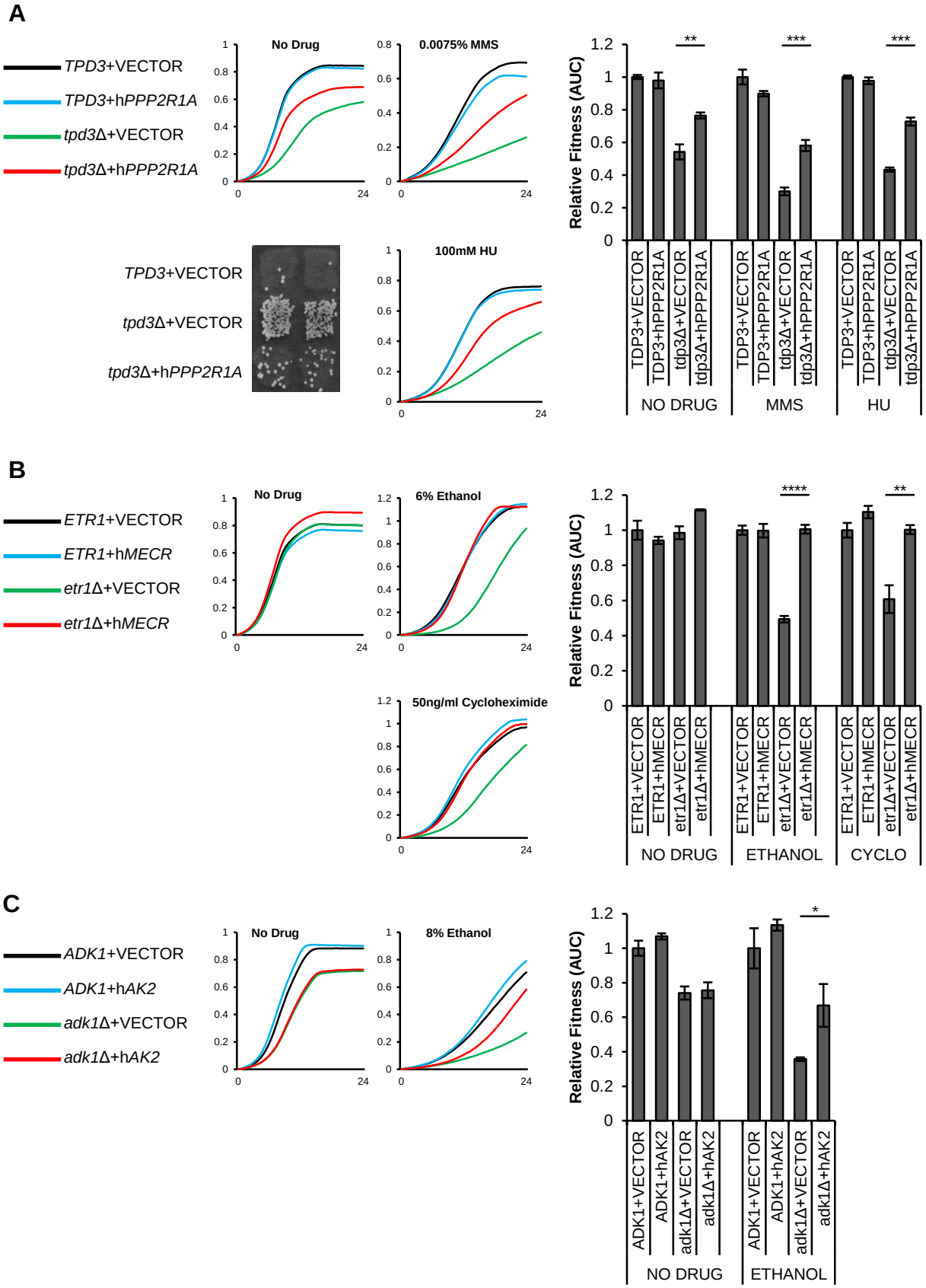
A
TPD3+VECTOR
TPD3+hPPP2R1A
tpd3Δ+VECTOR
tpd3Δ+hPPP2R1A
No Drug
0.0075% MMS
100mM HU
Relative Fitness (AUC)
NO DRUG
MMS
HU
B
ETR1+VECTOR
ETR1+hMECR
etr1Δ+VECTOR
etr1Δ+hMECR
No Drug
6% Ethanol
50ng/ml Cycloheximide
NO DRUG
ETHANOL
CYCLO
C
ADK1+VECTOR
ADK1+hAK2
adk1Δ+VECTOR
adk1Δ+hAK2
No Drug
8% Ethanol
NO DRUG
ETHANOL

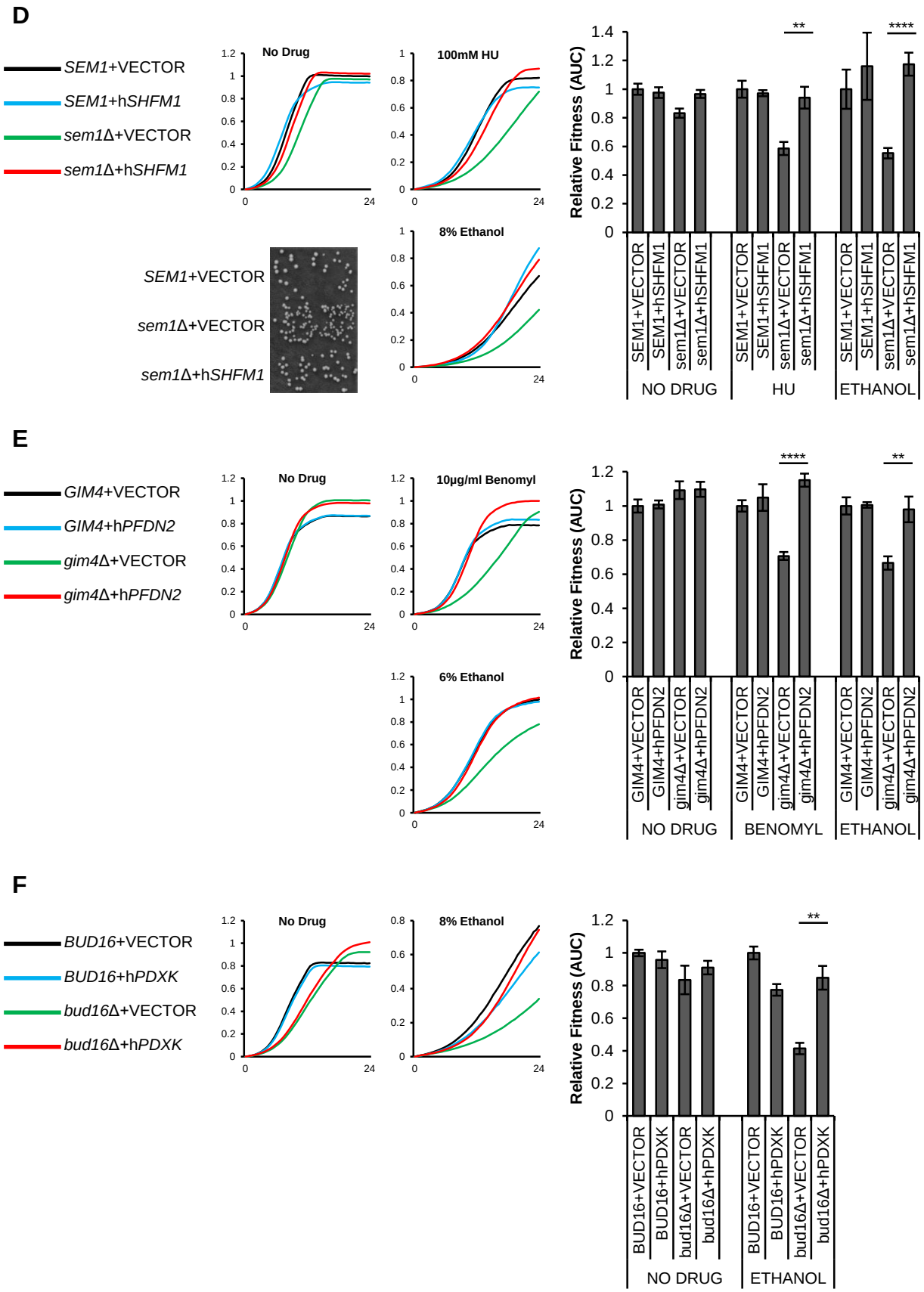
D
SEM1+VECTOR
SEM1+hSHFM1
sem1Δ+VECTOR
sem1Δ+hSHFM1
No Drug
100mM HU
8% Ethanol
Relative Fitness (AUC)
**
****
SEM1+VECTOR
SEM1+hSHFM1
sem1Δ+VECTOR
sem1Δ+hSHFM1
NO DRUG
HU
ETHANOL
E
GIM4+VECTOR
GIM4+hPFDN2
gim4Δ+VECTOR
gim4Δ+hPFDN2
No Drug
10µg/ml Benomyl
6% Ethanol
Relative Fitness (AUC)
****
**
GIM4+VECTOR
GIM4+hPFDN2
gim4Δ+VECTOR
gim4Δ+hPFDN2
NO DRUG
BENOMYL
ETHANOL
F
BUD16+VECTOR
BUD16+hPDXK
bud16Δ+VECTOR
bud16Δ+hPDXK
No Drug
8% Ethanol
Relative Fitness (AUC)
**
BUD16+VECTOR
BUD16+hPDXK
bud16Δ+VECTOR
bud16Δ+hPDXK
NO DRUG
ETHANOL

G

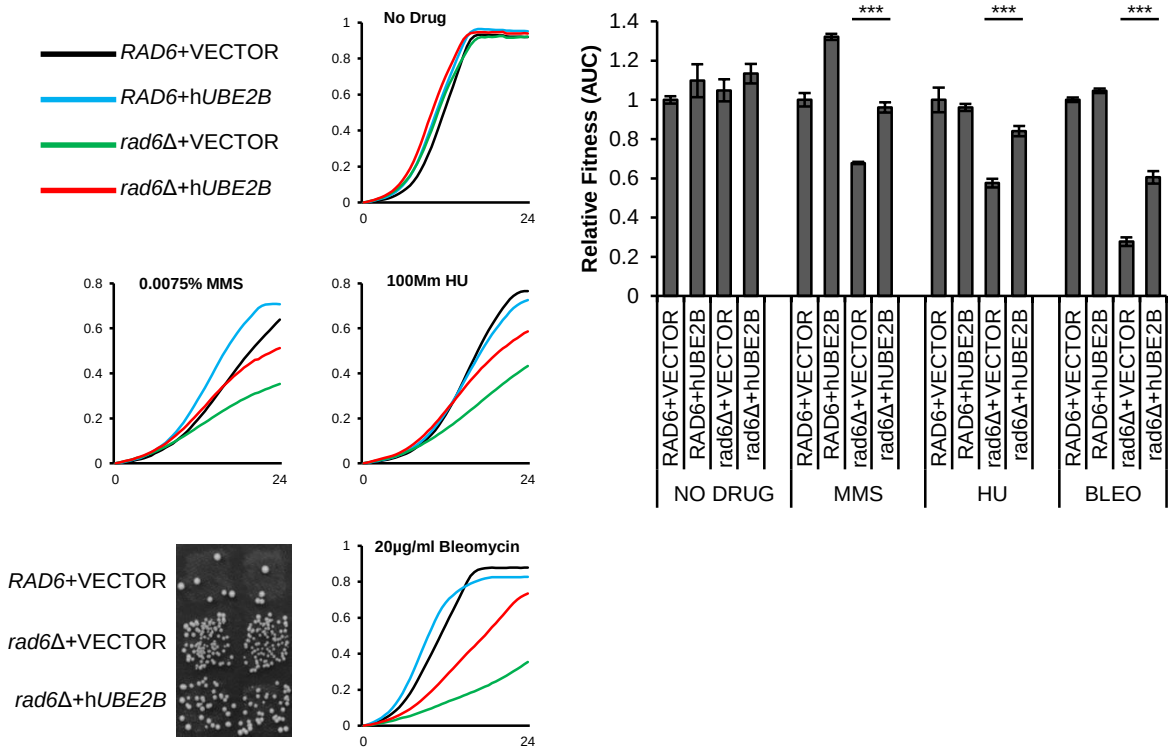
RAD6+VECTOR
RAD6+hUBE2B
rad6Δ+VECTOR
rad6Δ+hUBE2B
No Drug
0.0075% MMS
100Mm HU
20µg/ml Bleomycin
Relative Fitness (AUC)
***
***
***
RAD6+VECTOR
RAD6+hUBE2B
rad6Δ+VECTOR
rad6Δ+hUBE2B
NO DRUG
MMS
HU
BLEO

H

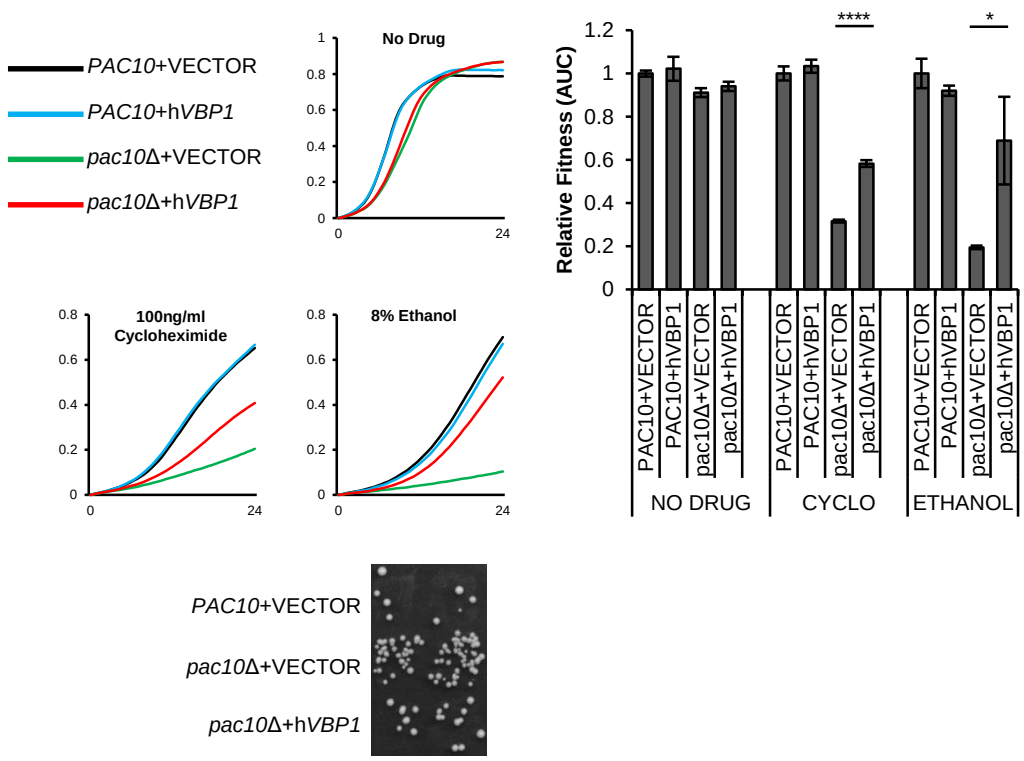
PAC10+VECTOR
PAC10+hVBP1
pac10Δ+VECTOR
pac10Δ+hVBP1
No Drug
100ng/ml Cycloheximide
8% Ethanol
Relative Fitness (AUC)
****
*
PAC10+VECTOR
PAC10+hVBP1
pac10Δ+VECTOR
pac10Δ+hVBP1
NO DRUG
CYCLO
ETHANOL

I

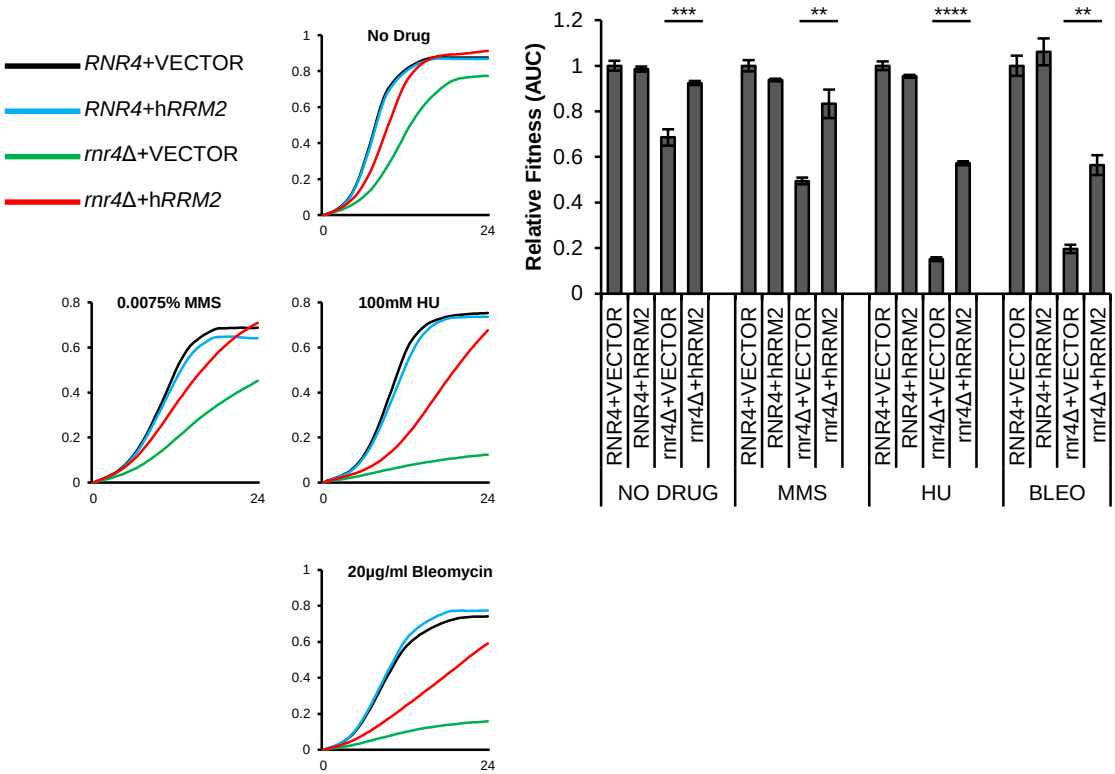
RNR4+VECTOR
RNR4+hRRM2
rnr4Δ+VECTOR
rnr4Δ+hRRM2
No Drug
0.0075% MMS
100mM HU
20µg/ml Bleomycin
Relative Fitness (AUC)
***
**
****
**
RNR4+VECTOR
RNR4+hRRM2
rnr4Δ+VECTOR
rnr4Δ+hRRM2
NO DRUG
MMS
HU
BLEO

J

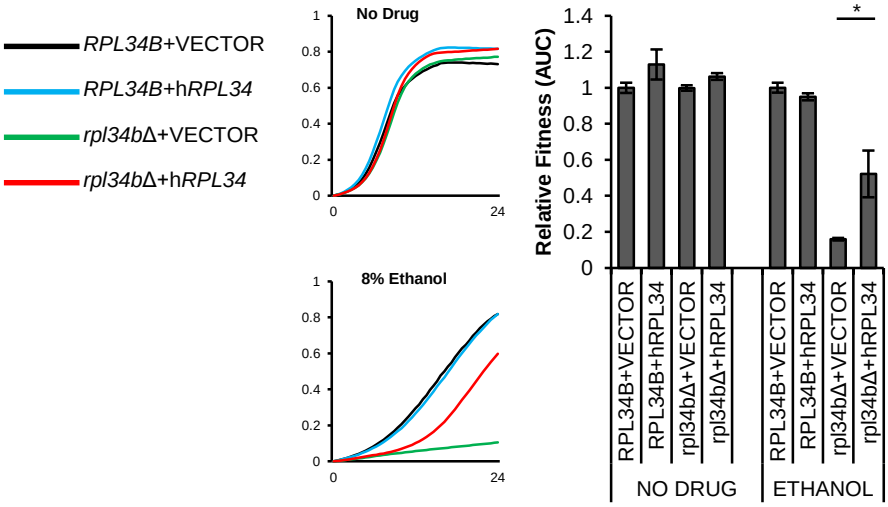
RPL34B+VECTOR
RPL34B+hRPL34
rpl34bΔ+VECTOR
rpl34bΔ+hRPL34
No Drug
8% Ethanol
Relative Fitness (AUC)
*
RPL34B+VECTOR
RPL34B+hRPL34
rpl34bΔ+VECTOR
rpl34bΔ+hRPL34
NO DRUG
ETHANOL

K

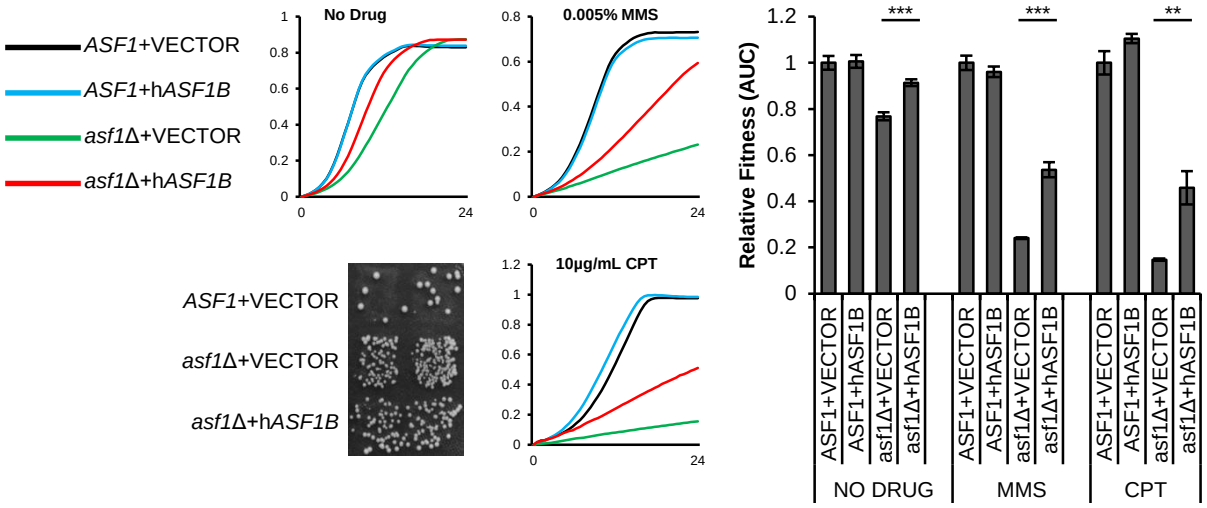
ASF1+VECTOR
ASF1+hASF1B
asf1Δ+VECTOR
asf1Δ+hASF1B
No Drug
0.005% MMS
10µg/mL CPT
ASF1+VECTOR
asf1Δ+VECTOR
asf1Δ+hASF1B
Relative Fitness (AUC)
***
***
**
ASF1+VECTOR
ASF1+hASF1B
asf1Δ+VECTOR
asf1Δ+hASF1B
NO DRUG
MMS
CPT

L

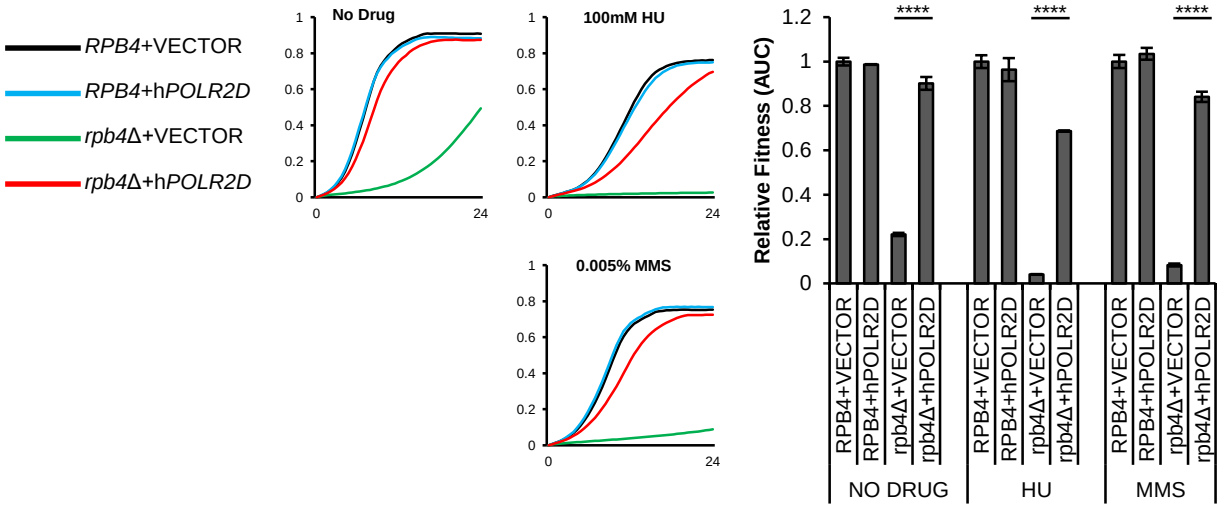
RPB4+VECTOR
RPB4+hPOLR2D
rpb4Δ+VECTOR
rpb4Δ+hPOLR2D
No Drug
100mM HU
0.005% MMS
Relative Fitness (AUC)
****
****
****
RPB4+VECTOR
RPB4+hPOLR2D
rpb4Δ+VECTOR
rpb4Δ+hPOLR2D
NO DRUG
HU
MMS

M

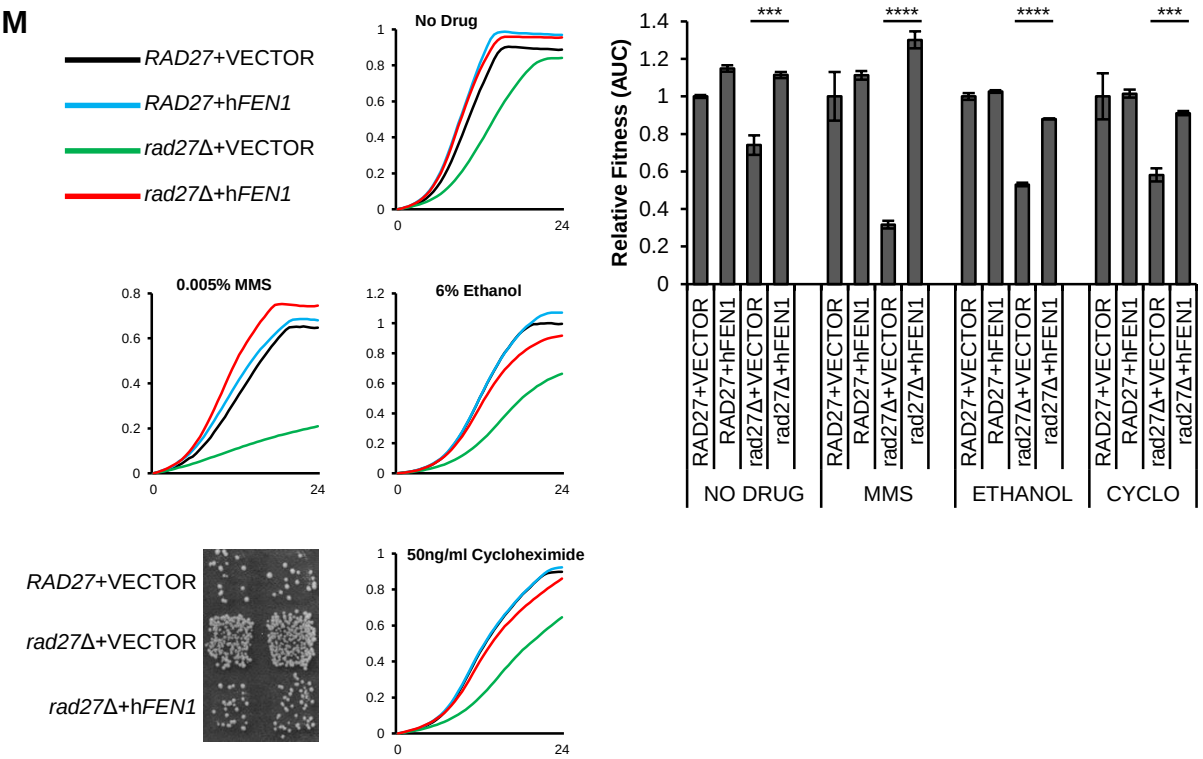
RAD27+VECTOR
RAD27+hFEN1
rad27Δ+VECTOR
rad27Δ+hFEN1
No Drug
0.005% MMS
6% Ethanol
50ng/ml Cycloheximide
Relative Fitness (AUC)
***
****
****
***
RAD27+VECTOR
RAD27+hFEN1
rad27Δ+VECTOR
rad27Δ+hFEN1
NO DRUG
MMS
ETHANOL
CYCLO

N

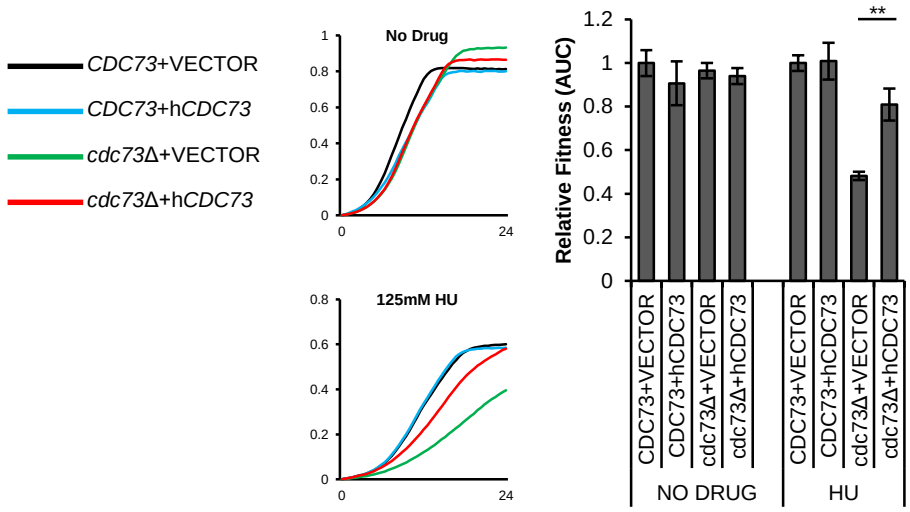
CDC73+VECTOR
CDC73+hCDC73
cdc73Δ+VECTOR
cdc73Δ+hCDC73
No Drug
125mM HU
Relative Fitness (AUC)
**
CDC73+VECTOR
CDC73+hCDC73
cdc73Δ+VECTOR
cdc73Δ+hCDC73
NO DRUG
HU

O

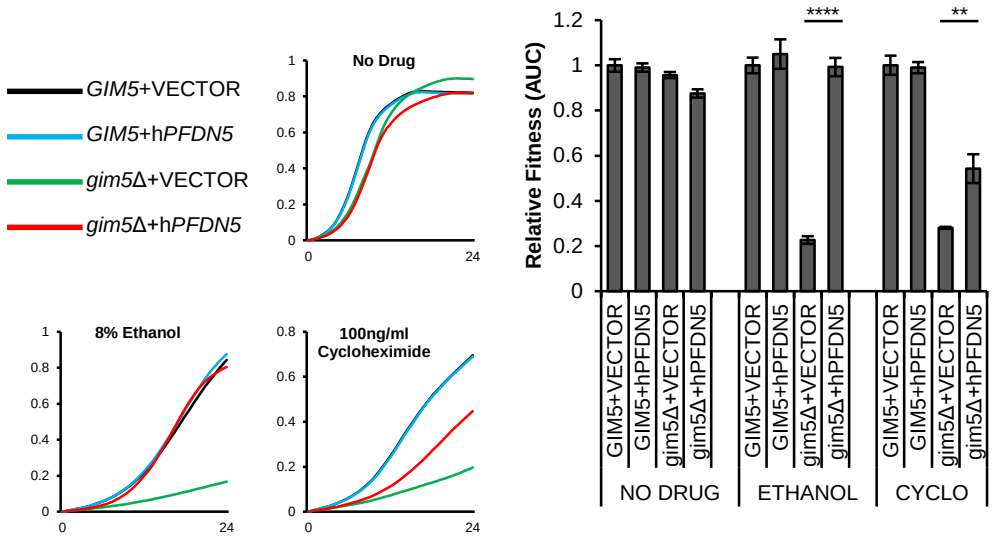
GIM5+VECTOR
GIM5+hPFDN5
gim5Δ+VECTOR
gim5Δ+hPFDN5
No Drug
8% Ethanol
100ng/ml Cycloheximide
Relative Fitness (AUC)
****
**
GIM5+VECTOR
GIM5+hPFDN5
gim5Δ+VECTOR
gim5Δ+hPFDN5
NO DRUG
ETHANOL
CYCLO

P

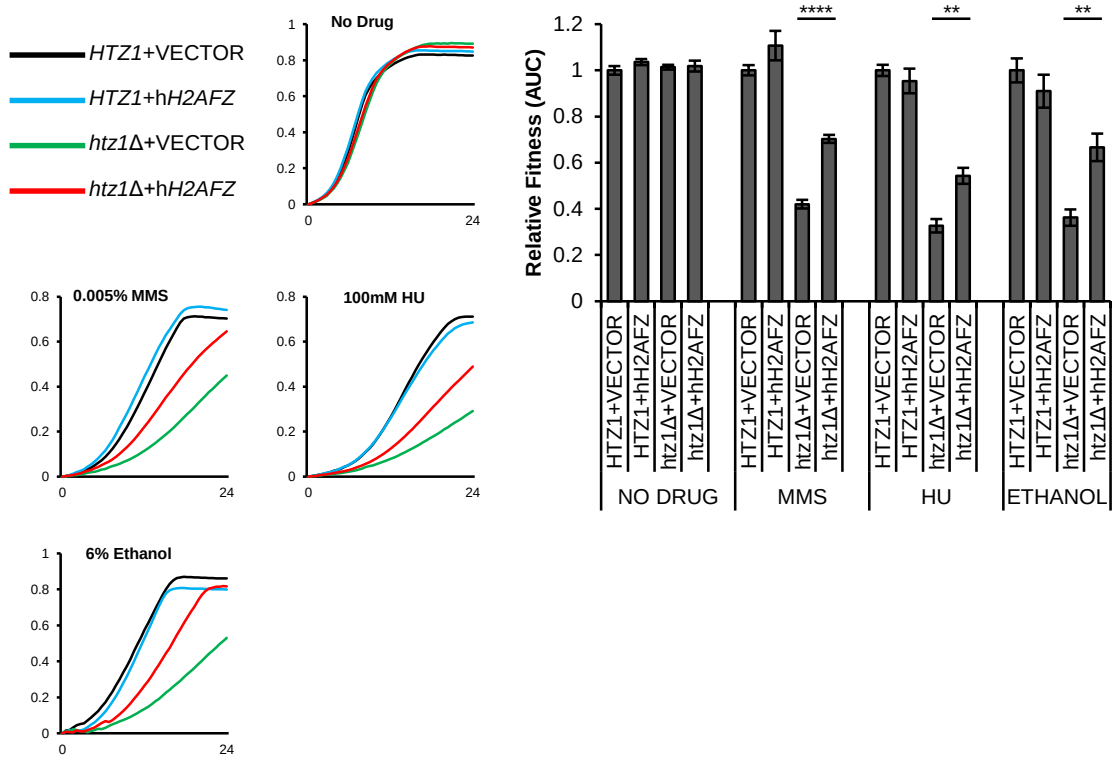
HTZ1+VECTOR
HTZ1+hH2AFZ
htz1Δ+VECTOR
htz1Δ+hH2AFZ
No Drug
0.005% MMS
100mM HU
6% Ethanol
Relative Fitness (AUC)
****
**
**
HTZ1+VECTOR
HTZ1+hH2AFZ
htz1Δ+VECTOR
htz1Δ+hH2AFZ
NO DRUG
MMS
HU
ETHANOL

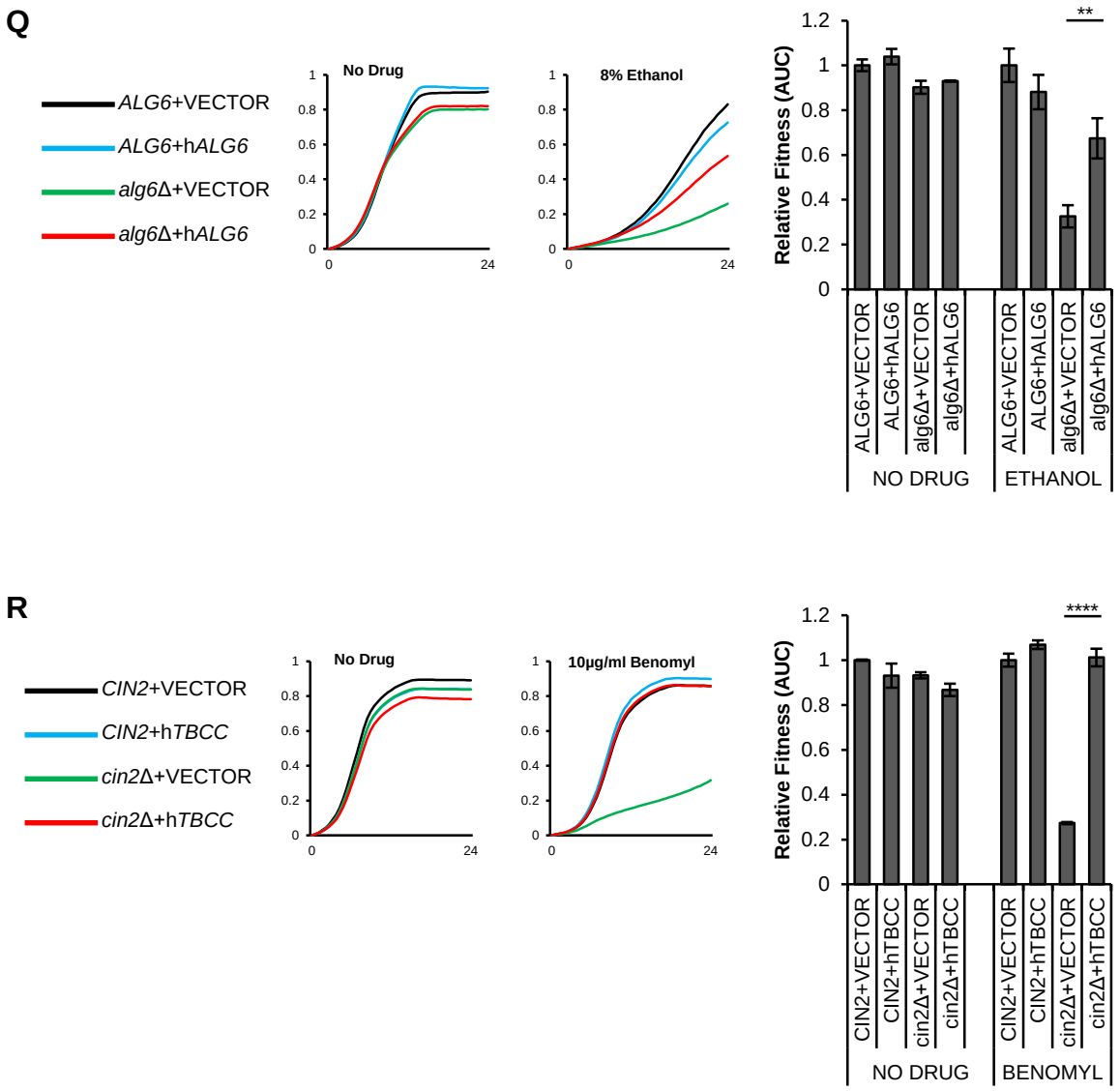

Figure A.1. Complementation assays identify human genes that rescue chemical sensitivity and/or CIN defects of nonessential yeast genes.
For each human-yeast pair, complementation that was observed in the screen using spot assays was validated with liquid growth assays (shown here). Yeast strains (wild-type or knockout mutants) containing a vector control or indicated human cDNA cloned in a yeast expression vector were grown in media +/- chemical at the indicated concentrations. Each represented curve is the average of 3 replicates per media condition. For each panel, x-axis represents time in hours, while y-axis represents OD600 readings. Fitness of each strain was quantified by calculating area under the curve (AUC) of each replicate independently. Strain fitness was defined as the AUC of each yeast strain relative to the AUC of the wild-type strain containing the vector control and grown in the same media condition (mean +/- SD). Student's t-test. *p<0.05; **p<0.01; ***p<0.001; ****p<0.0001. For ALF assays, 2 independent isolates are shown per strain. **(A)** h*PPP2R1A*/y*TPD3* **(B)** h*MECR*/y*ETR1* **(C)** h*AK2*/y*ADK1* **(D)** h*SHFM1*/y*SEM1* **(E)** h*PFDN2*/y*GIM4* **(F)** h*PDXK*/y*BUD16* **(G)** h*UBE2B*/y*RAD6* **(H)** h*VBP1*/y*PAC10* **(I)** h*RRM2*/y*RNR4* **(J)** h*RPL34*/y*RPL34B* **(K)** h*ASF1B*/y*ASF1* **(L)** h*POLR2D*/y*RPB4* **(M)** h*FEN1*/y*RAD27* **(N)** h*CDC73*/y*CDC73* **(O)** h*PFDN5*/y*GIM5* **(P)** h*H2AFZ*/y*HTZ1* **(Q)** h*ALG6*/y*ALG6* **(R)** h*TBCC*/y*CIN2*.

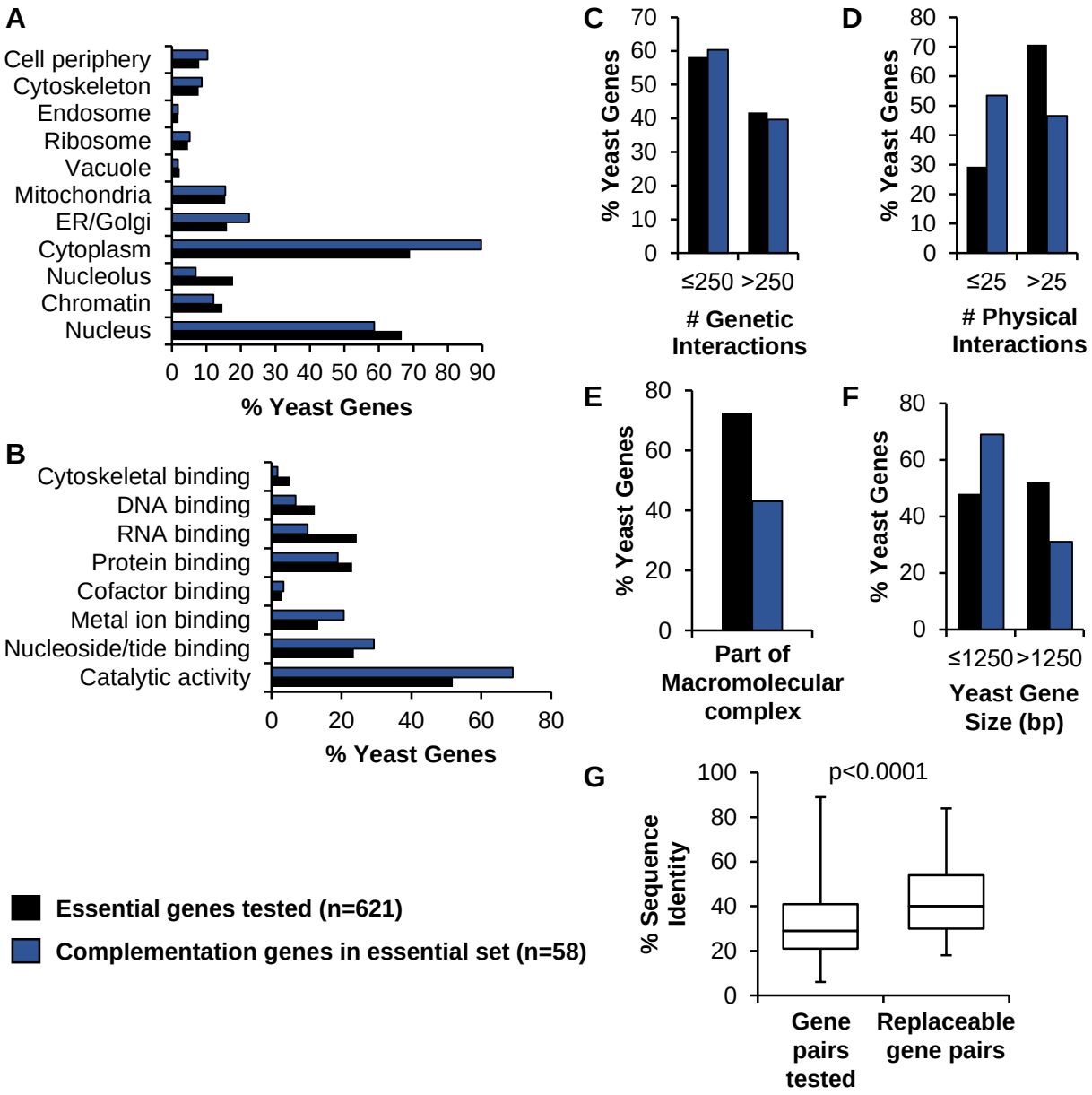

Figure A.2. Analyzing features of ESSENTIAL yeast genes that predict replaceability including (A) localization patterns, **(B)** molecular function, **(C)** no. of genetic interactions, **(D)** no. of physical interactions, **(E)** part of macromolecular complexes, **(F)** yeast gene size, and **(G)** human–yeast sequence identity. Localization data, Gene Ontology (GO) terms, no. of genetic/physical interactions, and gene size for each yeast gene were obtained from Yeastmine and each feature is represented as a proportion of the total number of genes input for each set (n = 621 for all essential yeast genes included in 2 screens and n = 58 for the complementation genes). Overall, the complementation set was enriched for yeast proteins that localize to the cytoplasm (P = 2.1E-03), have less physical interactions (P = 7.1E-04), are less likely to be part of macromolecular complexes (P = 1.0E-05), and have smaller gene size (P = 8.8E-03). For sequence identity, "essential gene pairs" refers to the 1076 human–yeast pairs included in this study corresponding to 621 yeast genes and "complementation gene pairs" refers to the 65 complementation pairs corresponding to 58 yeast genes. The box plot highlights the median and range of sequence identity for each set of gene pairs.

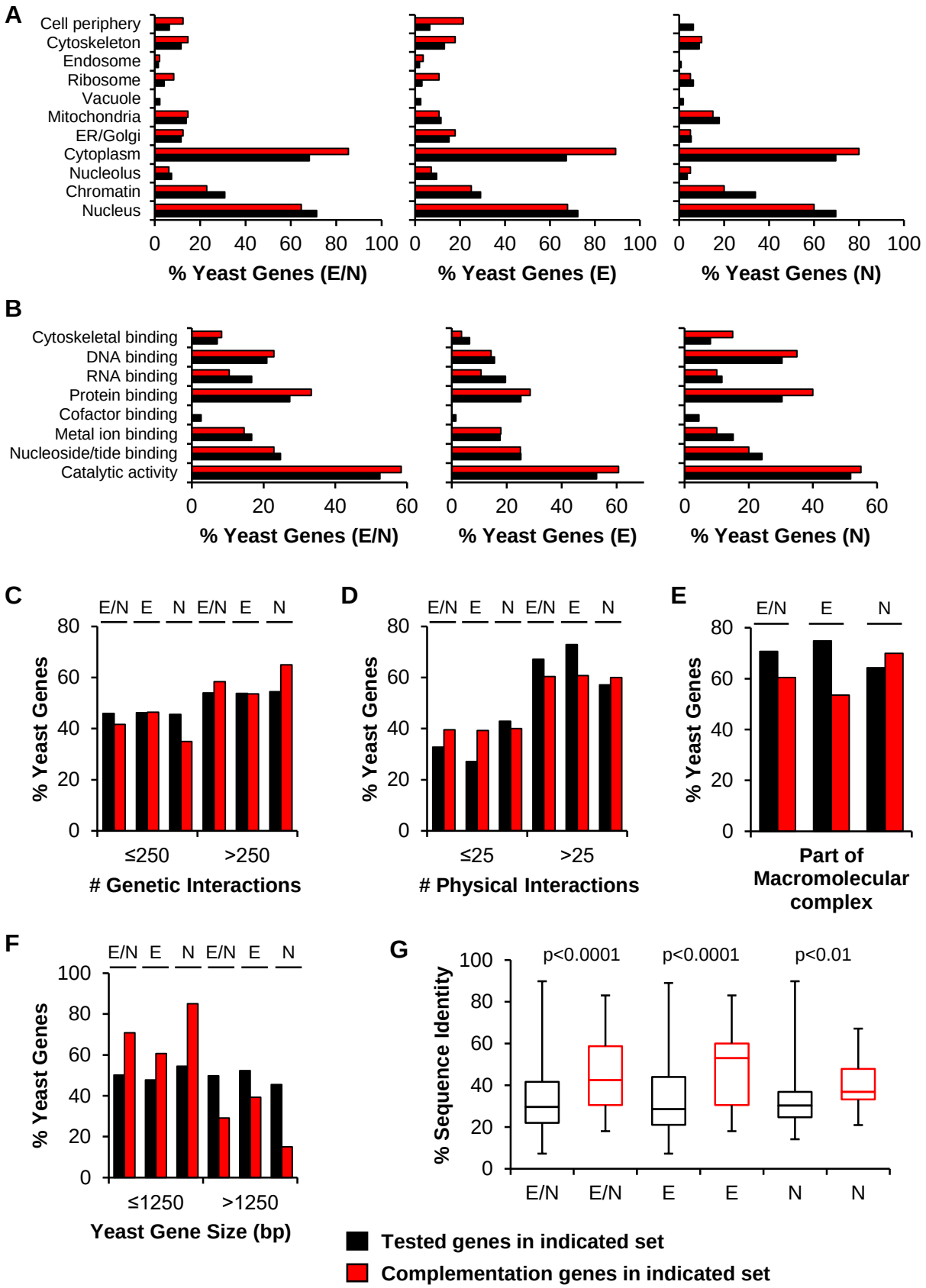
A
Cell periphery
Cytoskeleton
Endosome
Ribosome
Vacuole
Mitochondria
ER/Golgi
Cytoplasm
Nucleolus
Chromatin
Nucleus
0 20 40 60 80 100
% Yeast Genes (E/N)
% Yeast Genes (E)
% Yeast Genes (N)
B
Cytoskeletal binding
DNA binding
RNA binding
Protein binding
Cofactor binding
Metal ion binding
Nucleoside/tide binding
Catalytic activity
0 20 40 60
% Yeast Genes (E/N)
% Yeast Genes (E)
% Yeast Genes (N)
C
E/N E N E/N E N
% Yeast Genes
≤250 >250
Genetic Interactions
D
E/N E N E/N E N
% Yeast Genes
≤25 >25
Physical Interactions
E
E/N E N
% Yeast Genes
Part of Macromolecular complex
F
E/N E N E/N E N
% Yeast Genes
≤1250 >1250
Yeast Gene Size (bp)
G
% Sequence Identity
p<0.0001 p<0.0001 p<0.01
E/N E/N E E N N
Tested genes in indicated set
Complementation genes in indicated set

Figure A.3. Analyzing features of ESSENTIAL and NON-ESSENTIAL CIN yeast genes that predict replaceability including (A) localization patterns, **(B)** molecular function, **(C)** no. of genetic interactions, **(D)** no. of physical interactions, **(E)** part of macromolecular complexes, **(F)** yeast gene size, and **(G)** human–yeast sequence identity. Localization data, Gene Ontology (GO) terms, no. of genetic/physical interactions, and gene size for each yeast gene were obtained from Yeastmine and each feature is represented as a proportion of the total number of genes input for each set: n = 311 for essential and non-essential CIN yeast genes tested and n = 48 for essential and non-essential CIN complementation genes; n = 199 for essential CIN yeast genes tested and n = 28 for essential CIN complementation genes; n = 112 for non-essential CIN yeast genes tested and n = 20 for non-essential CIN complementation genes. For sequence identity, 'E/N' refers to the 443 human–yeast pairs tested and 54 pairs that complement; 'E' refers to the 322 human–yeast pairs tested and 34 pairs that complement; 'N' refers to the 121 human–yeast pairs tested and 20 pairs that complement;
The box plot highlights the median and range of sequence identity for each set of gene pairs.
Abbreviations: 'E/N': Essential and non-essential CIN genes; 'E': Essential CIN genes 'N': Non-essential CIN genes.

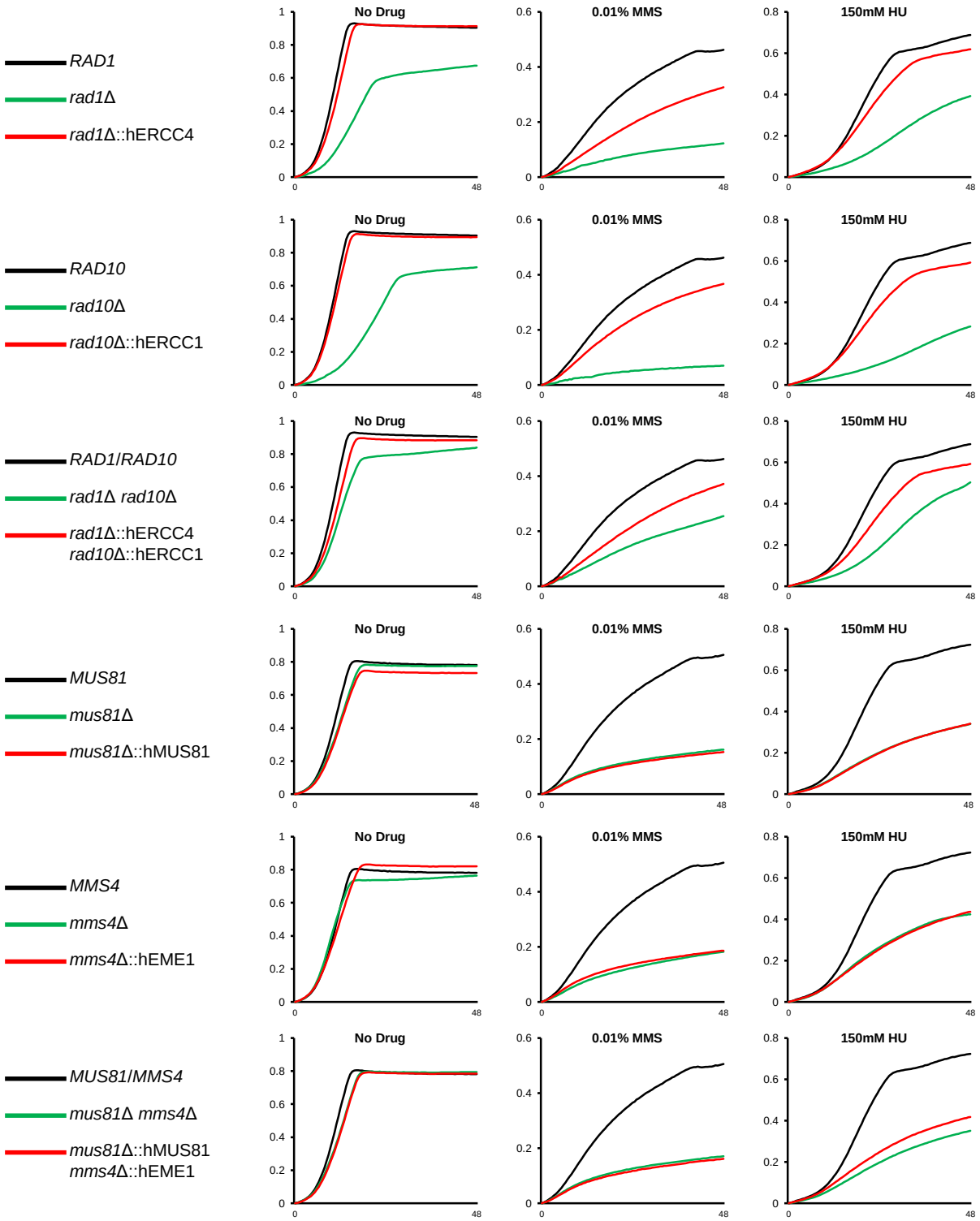

Figure A.4. Growth curve assays to assess complementation of two-subunit yeast complexes. Human cDNAs were integrated using CRISPR/Cas9 in the genomic location of the corresponding yeast gene. Yeast strains were grown in media +/- chemical at the indicated concentrations and each represented curve is the average of 3 replicates per media condition. For each panel, x-axis represents time in hours, while y-axis represents OD600 readings. Quantification of strain fitness is shown in Figure 3.2.

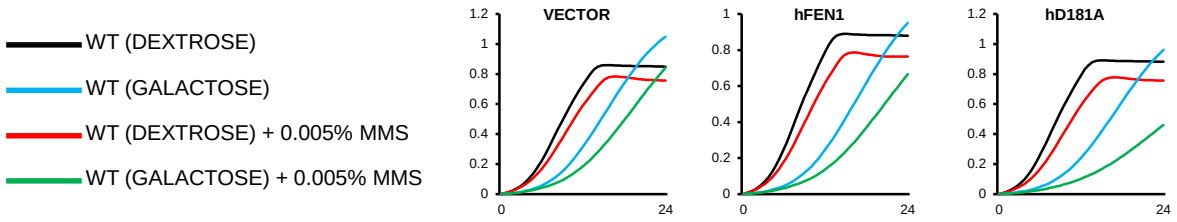

Figure A.5. Growth curve assays reveal h*FEN1*^{D181A} overexpression sensitizes yeast cells in MMS.

Wild-type yeast strains containing a vector control, h*FEN1*, or h*FEN1*^{D181A} cloned in a yeast expression vector were grown in dextrose or galactose media +/- 0.005% MMS. Each represented curve is the average of 4 replicates per media condition. For each panel, x-axis represents time in hours, while y-axis represents OD600 readings. Quantification of strain fitness is shown in Figure 4.7C.

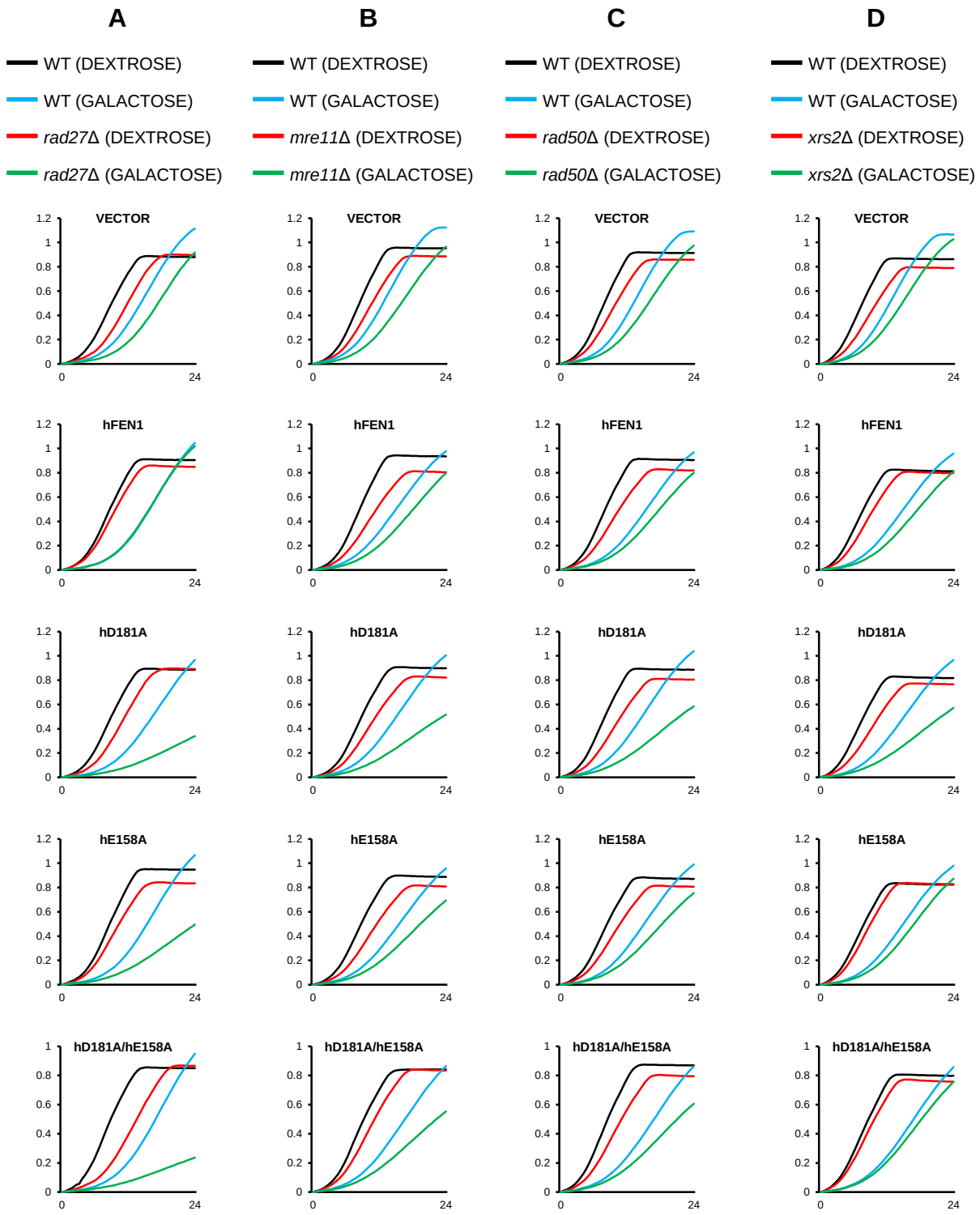
A
WT (DEXTROSE)
WT (GALACTOSE)
rad27Δ (DEXTROSE)
rad27Δ (GALACTOSE)
B
WT (DEXTROSE)
WT (GALACTOSE)
mre11Δ (DEXTROSE)
mre11Δ (GALACTOSE)
C
WT (DEXTROSE)
WT (GALACTOSE)
rad50Δ (DEXTROSE)
rad50Δ (GALACTOSE)
D
WT (DEXTROSE)
WT (GALACTOSE)
xrs2Δ (DEXTROSE)
xrs2Δ (GALACTOSE)
VECTOR
hFEN1
hD181A
hE158A
hD181A/hE158A
0
24

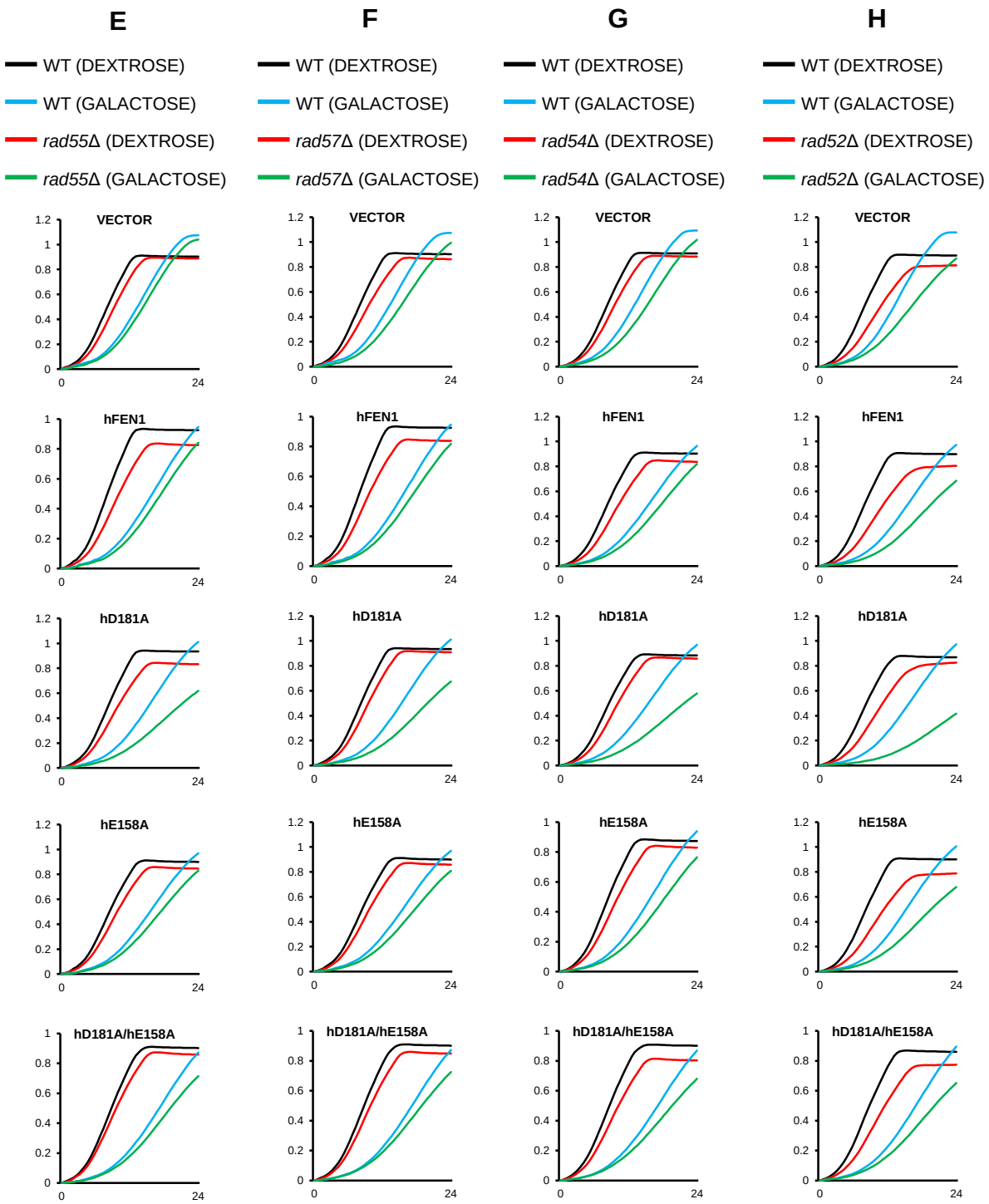

Figure A.6. Growth curve assays for validation of the h*FEN1*^{D181A} SDL screen and analysis using a DNA binding mutant.
Yeast strains (wild-type or knockout mutants) containing a vector control or indicated human cDNA cloned in a yeast expression vector were grown in dextrose or galactose media. Each represented curve is the average of 3 replicates per media condition. For each panel, x-axis represents time in hours, while y-axis represents OD600 readings. Quantification of strain fitness is shown in Figure 4.9. **(A)** *rad27*Δ **(B)** *mre11*Δ **(C)** *rad50*Δ **(D)** *xrs2*Δ **(E)** *rad55*Δ **(F)** *rad57*Δ **(G)** *rad54*Δ **(H)** *rad52*Δ.

Yeast systematic name	Yeast standard name
YAL040C	*CLN3*
YAR002W	*NUP60*
YBR098W	*MMS4*
YBR195C	*MSI1*
YBR223C	*TDP1*
YCL061C	*MRC1*
YCR066W	*RAD18*
YDL059C	*RAD59*
YDL074C	*BRE1*
YDR004W	*RAD57*
YDR075W	*PPH3*
YDR076W	*RAD55*
YDR217C	*RAD9*
YDR279W	*RNH202*
YDR369C	*XRS2*
YDR386W	*MUS81*
YDR440W	*DOT1*
YER095W	*RAD51*
YER164W	*CHD1*
YER169W	*RPH1*
YER173W	*RAD24*
YGL163C	*RAD54*
YGL175C	*SAE2*
YGR184C	*UBR1*
YGR270W	*YTA7*
YHR031C	*RRM3*
YHR154W	*RTT107*
YIL153W	*RRD1*
YJL092W	*SRS2*
YJR043C	*POL32*
YLL002W	*RTT109*
YLL019C	*KNS1*
YLR135W	*SLX4*
YLR154C	*RNH203*
YLR176C	*RFX1*
YLR234W	*TOP3*
YLR288C	*MEC3*
YLR320W	*MMS22*
YLR376C	*PSY3*
YML032C	*RAD52*
YML102W	*CAC2*
YMR048W	*CSM3*
YMR190C	*SGS1*
YMR216C	*SKY1*
YMR224C	*MRE11*
YNL072W	*RNH201*
YNL250W	*RAD50*
YNL307C	*MCK1*
YOL090W	*MSH2*
YOR025W	*HST3*
YOR033C	*EXO1*
YOR144C	*ELG1*
YOR368W	*RAD17*
YPL008W	*CHL1*
YPL024W	*RMI1*
YPL167C	*REV3*
YPL194W	*DDC1*
YPR018W	*RLF2*
YPR135W	*CTF4*
YPR164W	*MMS1*

Figure A.7. List of genes from the 332 mutants included in this study that display negative genetic interactions with *rad27Δ*.
Genetic interaction data was obtained from TheCellMap.org (PubMed PMID: 27708008). Genes that are SDL with catalytically-dead h*FEN1*^{D181A} are highlighted in red.

Table A.1. Essential yeast CIN genes and human homologs tested in the one-to-one complementation screen

Yeast Systematic Name	Yeast Standard Name	Human Entrez Gene ID	Human Standard Name	Complementation
YAL034W-A	*MTW1*	79003	*MIS12*	NO
YAL038W	*CDC19*	5313	*PKLR*	NO
YAL038W	*CDC19*	5315	*PKM*	NO
YAL041W	*CDC24*	7409	*VAV1*	NO
YAL041W	*CDC24*	8874	*ARHGEF7*	NO
YAL041W	*CDC24*	9459	*ARHGEF6*	NO
YAL041W	*CDC24*	23101	*MCF2L2*	NO
YAL041W	*CDC24*	23229	*ARHGEF9*	NO
YAL041W	*CDC24*	26030	*PLEKHG3*	NO
YAL041W	*CDC24*	55701	*ARHGEF40*	NO
YAL041W	*CDC24*	64857	*PLEKHG2*	NO
YAL041W	*CDC24*	84069	*PLEKHN1*	NO
YAL041W	*CDC24*	121512	*FGD4*	NO
YAL041W	*CDC24*	221178	*SPATA13*	NO
YAL041W	*CDC24*	221472	*FGD2*	NO
YAL041W	*CDC24*	440107	*PLEKHG7*	NO
YBL023C	*MCM2*	4171	*MCM2*	NO
YBL023C	*MCM2*	254394	*MCM9*	NO
YBL026W	*LSM2*	57819	*LSM2*	NO
YBL050W	*SEC17*	8775	*NAPA*	NO
YBL074C	*AAR2*	25980	*AAR2*	NO
YBL105C	*PKC1*	207	*AKT1*	NO
YBL105C	*PKC1*	208	*AKT2*	NO
YBL105C	*PKC1*	5578	*PRKCA*	NO
YBL105C	*PKC1*	5579	*PRKCB*	NO
YBL105C	*PKC1*	5581	*PRKCE*	NO
YBL105C	*PKC1*	5590	*PRKCZ*	NO
YBL105C	*PKC1*	10000	*AKT3*	NO
YBR055C	*PRP6*	24148	*PRPF6*	NO
YBR079C	*RPG1*	9667	*SAFB2*	NO
YBR088C	*POL30*	5111	*PCNA*	NO
YBR109C	*CMD1*	801	*CALM1*	YES
YBR109C	*CMD1*	805	*CALM2*	YES
YBR109C	*CMD1*	808	*CALM3*	YES
YBR109C	*CMD1*	810	*CALML3*	NO
YBR109C	*CMD1*	7125	*TNNC2*	NO
YBR109C	*CMD1*	7134	*TNNC1*	NO
YBR109C	*CMD1*	9478	*CABP1*	NO
YBR109C	*CMD1*	51806	*CALML5*	NO
YBR109C	*CMD1*	57010	*CABP4*	NO
YBR109C	*CMD1*	83698	*CALN1*	NO

Yeast Systematic Name	Yeast Standard Name	Human Entrez Gene ID	Human Standard Name	Complementation
YBR109C	*CMD1*	91860	*CALML4*	NO
YBR109C	*CMD1*	164633	*CABP7*	NO
YBR154C	*RPB5*	5434	*POLR2E*	NO
YBR160W	*CDC28*	983	*CDK1*	YES
YBR160W	*CDC28*	1017	*CDK2*	YES
YBR160W	*CDC28*	1019	*CDK4*	NO
YBR160W	*CDC28*	1021	*CDK6*	NO
YBR160W	*CDC28*	728642	*CDK11A*	NO
YBR167C	*POP7*	10248	*POP7*	NO
YBR198C	*TAF5*	27097	*TAF5L*	NO
YBR198C	*TAF5*	55023	*PHIP*	NO
YBR202W	*MCM7*	4176	*MCM7*	NO
YBR211C	*AME1*	79682	*MLF1IP*	NO
YCL052C	*PBN1*	54965	*PIGX*	NO
YCR012W	*PGK1*	5230	*PGK1*	YES
YCR012W	*PGK1*	5232	*PGK2*	YES
YCR035C	*RRP43*	11340	*EXOSC8*	NO
YCR057C	*PWP2*	5822	*PWP2*	NO
YDL003W	*MCD1*	5885	*RAD21*	NO
YDL003W	*MCD1*	9985	*REC8*	NO
YDL008W	*APC11*	51529	*ANAPC11*	NO
YDL017W	*CDC7*	8317	*CDC7*	NO
YDL028C	*MPS1*	7272	*TTK*	NO
YDL045C	*FAD1*	80308	*FLAD1*	YES
YDL064W	*UBC9*	7329	*UBE2I*	YES
YDL084W	*SUB2*	10212	*DDX39A*	NO
YDL097C	*RPN6*	9318	*COPS2*	NO
YDL098C	*SNU23*	153527	*ZMAT2*	NO
YDL105W	*NSE4*	54780	*NSMCE4A*	NO
YDL105W	*NSE4*	493861	*EID3*	NO
YDL126C	*CDC48*	7415	*VCP*	NO
YDL126C	*CDC48*	79029	*SPATA5L1*	NO
YDL139C	*SCM3*	55355	*HJURP*	NO
YDL140C	*RPO21*	5430	*POLR2A*	NO
YDL141W	*BPL1*	3141	*HLCS*	NO
YDL147W	*RPN5*	5718	*PSMD12*	YES
YDL164C	*CDC9*	3978	*LIG1*	YES
YDR002W	*YRB1*	202151	*RANBP3L*	NO
YDR013W	*PSF1*	9837	*GINS1*	NO
YDR045C	*RPC11*	51728	*POLR3K*	NO
YDR050C	*TPI1*	7167	*TPI1*	YES
YDR052C	*DBF4*	10926	*DBF4*	NO
YDR052C	*DBF4*	80174	*DBF4B*	NO
YDR091C	*RLI1*	6059	*ABCE1*	NO

Yeast Systematic Name	Yeast Standard Name	Human Entrez Gene ID	Human Standard Name	Complementation
YDR170C	*SEC7*	23362	*PSD3*	NO
YDR170C	*SEC7*	23550	*PSD4*	NO
YDR170C	*SEC7*	27128	*CYTH4*	NO
YDR170C	*SEC7*	84249	*PSD2*	NO
YDR172W	*SUP35*	10767	*HBS1L*	NO
YDR172W	*SUP35*	23708	*GSPT2*	NO
YDR182W	*CDC1*	65258	*MPPE1*	NO
YDR208W	*MSS4*	5305	*PIP4K2A*	NO
YDR208W	*MSS4*	8394	*PIP5K1A*	YES
YDR208W	*MSS4*	8395	*PIP5K1B*	YES
YDR208W	*MSS4*	8396	*PIP4K2B*	NO
YDR208W	*MSS4*	138429	*PIP5KL1*	NO
YDR288W	*NSE3*	56160	*NDNL2*	NO
YDR292C	*SRP101*	6734	*SRPR*	NO
YDR328C	*SKP1*	6500	*SKP1*	NO
YDR404C	*RPB7*	5436	*POLR2G*	YES
YDR460W	*TFB3*	4331	*MNAT1*	NO
YDR510W	*SMT3*	6612	*SUMO3*	NO
YDR510W	*SMT3*	6613	*SUMO2*	NO
YDR510W	*SMT3*	7341	*SUMO1*	YES
YDR510W	*SMT3*	387082	*SUMO4*	NO
YEL026W	*SNU13*	4809	*NHP2L1*	YES
YEL032W	*MCM3*	4172	*MCM3*	NO
YEL034W	*HYP2*	1984	*EIF5A*	NO
YER009W	*NTF2*	10204	*NUTF2*	NO
YER012W	*PRE1*	5690	*PSMB2*	NO
YER018C	*SPC25*	57405	*SPC25*	NO
YER018C	*SPC25*	147841	*SPC24*	NO
YER023W	*PRO3*	5831	*PYCR1*	NO
YER023W	*PRO3*	29920	*PYCR2*	NO
YER023W	*PRO3*	65263	*PYCRL*	NO
YER094C	*PUP3*	5691	*PSMB3*	YES
YER133W	*GLC7*	5499	*PPP1CA*	YES
YER133W	*GLC7*	5501	*PPP1CC*	YES
YER147C	*SCC4*	23383	*MAU2*	NO
YER165W	*PAB1*	5042	*PABPC3*	NO
YER165W	*PAB1*	5937	*RBMS1*	NO
YER165W	*PAB1*	22827	*PUF60*	NO
YER165W	*PAB1*	140886	*PABPC5*	NO
YFL008W	*SMC1*	27127	*SMC1B*	NO
YFL009W	*CDC4*	55294	*FBXW7*	NO
YFL017C	*GNA1*	64841	*GNPNAT1*	YES
YFL022C	*FRS2*	2193	*FARSA*	NO
YFL037W	*TUB2*	7280	*TUBB2A*	NO

Yeast Systematic Name	Yeast Standard Name	Human Entrez Gene ID	Human Standard Name	Complementation
YFL037W	*TUB2*	10381	*TUBB3*	NO
YFL037W	*TUB2*	10382	*TUBB4A*	NO
YFL037W	*TUB2*	10383	*TUBB4B*	NO
YFL037W	*TUB2*	51175	*TUBE1*	NO
YFL037W	*TUB2*	81027	*TUBB1*	NO
YFL037W	*TUB2*	84617	*TUBB6*	NO
YFL037W	*TUB2*	203068	*TUBB*	NO
YFL037W	*TUB2*	347733	*TUBB2B*	NO
YFL038C	*YPT1*	5861	*RAB1A*	NO
YFL038C	*YPT1*	9363	*RAB33A*	NO
YFL038C	*YPT1*	27314	*RAB30*	NO
YFL038C	*YPT1*	81876	*RAB1B*	NO
YFL038C	*YPT1*	83452	*RAB33B*	NO
YFL038C	*YPT1*	376267	*RAB15*	NO
YFL039C	*ACT1*	59	*ACTA2*	NO
YFL039C	*ACT1*	60	*ACTB*	NO
YFL039C	*ACT1*	70	*ACTC1*	NO
YFL039C	*ACT1*	71	*ACTG1*	NO
YFL039C	*ACT1*	84517	*ACTRT3*	NO
YFL039C	*ACT1*	139741	*ACTRT1*	NO
YFL039C	*ACT1*	140625	*ACTRT2*	NO
YFL039C	*ACT1*	345651	*ACTBL2*	NO
YFR027W	*ECO1*	114799	*ESCO1*	NO
YFR028C	*CDC14*	8556	*CDC14A*	NO
YFR028C	*CDC14*	54935	*DUSP23*	NO
YFR037C	*RSC8*	6601	*SMARCC2*	NO
YFR050C	*PRE4*	5692	*PSMB4*	NO
YFR052W	*RPN12*	5714	*PSMD8*	NO
YGL030W	*RPL30*	6156	*RPL30*	YES
YGL044C	*RNA15*	23283	*CSTF2T*	NO
YGL097W	*SRM1*	1102	*RCBTB2*	NO
YGL097W	*SRM1*	1104	*RCC1*	NO
YGL097W	*SRM1*	55213	*RCBTB1*	NO
YGL098W	*USE1*	55850	*USE1*	NO
YGL116W	*CDC20*	991	*CDC20*	NO
YGL116W	*CDC20*	166979	*CDC20B*	NO
YGL142C	*GPI10*	9488	*PIGB*	NO
YGR091W	*PRP31*	26121	*PRPF31*	NO
YGR172C	*YIP1*	285525	*YIPF7*	NO
YGR179C	*OKP1*	55166	*CENPQ*	NO
YGR218W	*CRM1*	7514	*XPO1*	NO
YGR253C	*PUP2*	5686	*PSMA5*	NO
YGR264C	*MES1*	9255	*AIMP1*	NO
YHL015W	*RPS20*	6224	*RPS20*	NO

Yeast Systematic Name	Yeast Standard Name	Human Entrez Gene ID	Human Standard Name	Complementation
YHR058C	*MED6*	10001	*MED6*	NO
YHR065C	*RRP3*	51202	*DDX47*	NO
YHR065C	*RRP3*	55794	*DDX28*	NO
YHR070W	*TRM5*	57570	*TRMT5*	NO
YHR085W	*IPI1*	54881	*TEX10*	NO
YHR088W	*RPF1*	80135	*RPF1*	NO
YHR107C	*CDC12*	1731	*SEPT1*	NO
YHR107C	*CDC12*	4735	*SEPT2*	NO
YHR107C	*CDC12*	23157	*SEPT6*	NO
YHR107C	*CDC12*	55752	*SEPT11*	NO
YHR107C	*CDC12*	151011	*SEPT10*	NO
YHR118C	*ORC6*	23594	*ORC6*	NO
YHR122W	*CIA2*	84191	*FAM96A*	NO
YHR164C	*DNA2*	1763	*DNA2*	NO
YHR166C	*CDC23*	8697	*CDC23*	NO
YIL004C	*BET1*	10282	*BET1*	NO
YIL021W	*RPB3*	5432	*POLR2C*	NO
YIL026C	*IRR1*	10734	*STAG3*	NO
YIL026C	*IRR1*	10735	*STAG2*	NO
YIL061C	*SNP1*	6625	*SNRNP70*	NO
YIL109C	*SEC24*	9871	*SEC24D*	NO
YIL143C	*SSL2*	2071	*ERCC3*	NO
YIL144W	*NDC80*	10403	*NDC80*	NO
YIL150C	*MCM10*	55388	*MCM10*	NO
YIR008C	*PRI1*	5557	*PRIM1*	NO
YIR010W	*DSN1*	79980	*DSN1*	NO
YIR015W	*RPR2*	79897	*RPP21*	NO
YJL001W	*PRE3*	5698	*PSMB9*	NO
YJL026W	*RNR2*	6241	*RRM2*	NO
YJL026W	*RNR2*	50484	*RRM2B*	NO
YJL031C	*BET4*	5875	*RABGGTA*	NO
YJL072C	*PSF2*	51659	*GINS2*	NO
YJL167W	*ERG20*	2224	*FDPS*	NO
YJR006W	*POL31*	5425	*POLD2*	YES
YKL013C	*ARC19*	10093	*ARPC4*	YES
YKL024C	*URA6*	51727	*CMPK1*	YES
YKL033W	*TTI1*	9675	*TTI1*	YES
YKL035W	*UGP1*	7360	*UGP2*	YES
YKL049C	*CSE4*	1058	*CENPA*	NO
YKL049C	*CSE4*	3021	*H3F3B*	NO
YKL089W	*MIF2*	1060	*CENPC*	NO
YKL104C	*GFA1*	9945	*GFPT2*	NO
YKL154W	*SRP102*	58477	*SRPRB*	NO
YKL173W	*SNU114*	9343	*EFTUD2*	NO

Yeast Systematic Name	Yeast Standard Name	Human Entrez Gene ID	Human Standard Name	Complementation
YKL192C	*ACP1*	4706	*NDUFAB1*	NO
YKL193C	*SDS22*	5510	*PPP1R7*	NO
YKL193C	*SDS22*	54839	*LRRC49*	NO
YKR025W	*RPC37*	55718	*POLR3E*	NO
YKR038C	*KAE1*	55644	*OSGEP*	NO
YKR062W	*TFA2*	2961	*GTF2E2*	NO
YKR071C	*DRE2*	57019	*CIAPIN1*	NO
YLL050C	*COF1*	1072	*CFL1*	NO
YLL050C	*COF1*	11034	*DSTN*	NO
YLR007W	*NSE1*	197370	*NSMCE1*	NO
YLR060W	*FRS1*	10056	*FARSB*	NO
YLR103C	*CDC45*	8318	*CDC45*	NO
YLR115W	*CFT2*	53981	*CPSF2*	NO
YLR116W	*MSL5*	9444	*QKI*	NO
YLR116W	*MSL5*	202559	*KHDRBS2*	NO
YLR163C	*MAS1*	9512	*PMPCB*	NO
YLR196W	*PWP1*	11137	*PWP1*	NO
YLR212C	*TUB4*	7283	*TUBG1*	NO
YLR212C	*TUB4*	27175	*TUBG2*	NO
YLR212C	*TUB4*	51174	*TUBD1*	NO
YLR229C	*CDC42*	57381	*RHOJ*	NO
YLR274W	*MCM5*	4174	*MCM5*	NO
YLR291C	*GCD7*	8892	*EIF2B2*	NO
YLR293C	*GSP1*	5901	*RAN*	NO
YLR298C	*YHC1*	6631	*SNRPC*	NO
YLR316C	*TAD3*	113179	*ADAT3*	NO
YLR378C	*SEC61*	29927	*SEC61A1*	NO
YLR378C	*SEC61*	55176	*SEC61A2*	NO
YLR409C	*UTP21*	134430	*WDR36*	NO
YLR424W	*SPP382*	24144	*TFIP11*	NO
YML010W	*SPT5*	6829	*SUPT5H*	NO
YML064C	*TEM1*	9364	*RAB28*	NO
YML069W	*POB3*	6749	*SSRP1*	YES
YML077W	*BET5*	58485	*TRAPPC1*	YES
YML085C	*TUB1*	7277	*TUBA4A*	NO
YML085C	*TUB1*	79861	*TUBAL3*	NO
YML085C	*TUB1*	84790	*TUBA1C*	NO
YML114C	*TAF8*	129685	*TAF8*	NO
YML130C	*ERO1*	30001	*ERO1L*	NO
YML130C	*ERO1*	56605	*ERO1LB*	NO
YMR033W	*ARP9*	10096	*ACTR3*	NO
YMR033W	*ARP9*	57180	*ACTR3B*	NO
YMR079W	*SEC14*	266629	*SEC14L3*	NO
YMR117C	*SPC24*	57405	*SPC25*	NO

Yeast Systematic Name	Yeast Standard Name	Human Entrez Gene ID	Human Standard Name	Complementation
YMR117C	*SPC24*	147841	*SPC24*	NO
YMR197C	*VTI1*	10490	*VTI1B*	NO
YMR203W	*TOM40*	84134	*TOMM40L*	NO
YMR218C	*TRS130*	7109	*TRAPPC10*	NO
YMR227C	*TAF7*	54457	*TAF7L*	NO
YMR308C	*PSE1*	3843	*IPO5*	YES
YMR308C	*PSE1*	26953	*RANBP6*	NO
YMR314W	*PRE5*	5682	*PSMA1*	YES
YNL002C	*RLP7*	6129	*RPL7*	NO
YNL002C	*RLP7*	285855	*RPL7L1*	NO
YNL118C	*DCP2*	167227	*DCP2*	NO
YNL126W	*SPC98*	10426	*TUBGCP3*	NO
YNL126W	*SPC98*	27229	*TUBGCP4*	NO
YNL131W	*TOM22*	56993	*TOMM22*	NO
YNL132W	*KRE33*	55226	*NAT10*	NO
YNL312W	*RFA2*	6118	*RPA2*	NO
YNL312W	*RFA2*	29935	*RPA4*	NO
YNL317W	*PFS2*	5542	*PRB1*	NO
YNL317W	*PFS2*	5554	*PRH1*	NO
YNL317W	*PFS2*	55339	*WDR33*	NO
YNR026C	*SEC12*	55250	*ELP2*	NO
YOL021C	*DIS3*	22894	*DIS3*	NO
YOL021C	*DIS3*	115752	*DIS3L*	NO
YOL069W	*NUF2*	83540	*NUF2*	NO
YOL123W	*HRP1*	3181	*HNRNPA2B1*	NO
YOL123W	*HRP1*	9987	*HNRNPDL*	NO
YOL123W	*HRP1*	124540	*MSI2*	NO
YOL144W	*NOP8*	81892	*SLIRP*	NO
YOL146W	*PSF3*	64785	*GINS3*	NO
YOR122C	*PFY1*	375189	*PFN4*	NO
YOR149C	*SMP3*	80235	*PIGZ*	YES
YOR168W	*GLN4*	5859	*QARS*	NO
YOR250C	*CLP1*	10978	*CLP1*	NO
YOR262W	*GPN2*	54707	*GPN2*	NO
YOR272W	*YTM1*	22884	*WDR37*	NO
YOR326W	*MYO2*	4646	*MYO6*	NO
YOR336W	*KRE5*	55757	*UGGT2*	NO
YPL082C	*MOT1*	50485	*SMARCAL1*	NO
YPL117C	*IDI1*	3422	*IDI1*	YES
YPL117C	*IDI1*	91734	*IDI2*	NO
YPL160W	*CDC60*	51520	*LARS*	NO
YPL190C	*NAB3*	3183	*HNRNPC*	NO
YPL190C	*NAB3*	22913	*RALY*	NO
YPL190C	*NAB3*	138046	*RALYL*	NO

Yeast Systematic Name	Yeast Standard Name	Human Entrez Gene ID	Human Standard Name	Complementation
YPL190C	*NAB3*	343069	*HNRNPCL1*	NO
YPL209C	*IPL1*	6795	*AURKC*	NO
YPL209C	*IPL1*	9212	*AURKB*	NO
YPL235W	*RVB2*	10856	*RUVBL2*	NO
YPR082C	*DIB1*	10907	*TXNL4A*	YES
YPR082C	*DIB1*	54957	*TXNL4B*	NO
YPR103W	*PRE2*	5696	*PSMB8*	NO
YPR133C	*SPN1*	3270	*HRC*	NO
YPR133C	*SPN1*	55677	*IWS1*	NO
YPR133C	*SPN1*	126637	*TCHHL1*	NO
YPR161C	*SGV1*	1025	*CDK9*	NO
YPR162C	*ORC4*	5000	*ORC4*	NO
YPR178W	*PRP4*	5048	*PAFAH1B1*	NO
YPR178W	*PRP4*	9128	*PRPF4*	NO
YPR178W	*PRP4*	10300	*KATNB1*	NO
YPR178W	*PRP4*	25886	*POC1A*	NO
YPR178W	*PRP4*	282809	*POC1B*	NO

Table A.2. Essential yeast genes and human homologs included in the pool-to-pool complementation screen

Yeast Systematic Name	Yeast Standard Name	Human Entrez Gene ID	Human Standard Name	Yeast Systematic Name	Yeast Standard Name	Human Entrez Gene ID	Human Standard Name
YAL003W	*EFB1*	1933	*EEF1B2*	YBL105C	*PKC1*	5590	*PRKCZ*
YAL003W	*EFB1*	1936	*EEF1D*	YBL105C	*PKC1*	10000	*AKT3*
YAL025C	*MAK16*	84549	*MAK16*	YBR002C	*RER2*	79947	*DHDDS*
YAL032C	*PRP45*	22938	*SNW1*	YBR004C	*GPI18*	55650	*PIGV*
YAL033W	*POP5*	51367	*POP5*	YBR011C	*IPP1*	27068	*PPA2*
YAL034W-A	*MTW1*	79003	*MIS12*	YBR029C	*CDS1*	1040	*CDS1*
YAL038W	*CDC19*	5313	*PKLR*	YBR029C	*CDS1*	8760	*CDS2*
YAL038W	*CDC19*	5315	*PKM*	YBR055C	*PRP6*	24148	*PRPF6*
YAL041W	*CDC24*	7409	*VAV1*	YBR079C	*RPG1*	9667	*SAFB2*
YAL041W	*CDC24*	8874	*ARHGEF7*	YBR088C	*POL30*	5111	*PCNA*
YAL041W	*CDC24*	9459	*ARHGEF6*	YBR102C	*EXO84*	149371	*EXOC8*
YAL041W	*CDC24*	23101	*MCF2L2*	YBR109C	*CMD1*	801	*CALM1*
YAL041W	*CDC24*	23229	*ARHGEF9*	YBR109C	*CMD1*	805	*CALM2*
YAL041W	*CDC24*	26030	*PLEKHG3*	YBR109C	*CMD1*	808	*CALM3*
YAL041W	*CDC24*	55701	*ARHGEF40*	YBR109C	*CMD1*	810	*CALML3*
YAL041W	*CDC24*	64857	*PLEKHG2*	YBR109C	*CMD1*	7125	*TNNC2*
YAL041W	*CDC24*	84069	*PLEKHN1*	YBR109C	*CMD1*	7134	*TNNC1*
YAL041W	*CDC24*	121512	*FGD4*	YBR109C	*CMD1*	9478	*CABP1*
YAL041W	*CDC24*	221178	*SPATA13*	YBR109C	*CMD1*	51806	*CALML5*
YAL041W	*CDC24*	221472	*FGD2*	YBR109C	*CMD1*	56344	*CABP5*
YAL041W	*CDC24*	440107	*PLEKHG7*	YBR109C	*CMD1*	57010	*CABP4*
YAR019C	*CDC15*	9064	*MAP3K6*	YBR109C	*CMD1*	83698	*CALN1*
YBL020W	*RFT1*	91869	*RFT1*	YBR109C	*CMD1*	84288	*EFCAB2*
YBL023C	*MCM2*	4171	*MCM2*	YBR109C	*CMD1*	91860	*CALML4*
YBL023C	*MCM2*	254394	*MCM9*	YBR109C	*CMD1*	164633	*CABP7*
YBL026W	*LSM2*	57819	*LSM2*	YBR110W	*ALG1*	200810	*ALG1L*
YBL030C	*PET9*	291	*SLC25A4*	YBR154C	*RPB5*	5434	*POLR2E*
YBL030C	*PET9*	292	*SLC25A5*	YBR155W	*CNS1*	7268	*TTC4*
YBL030C	*PET9*	293	*SLC25A6*	YBR160W	*CDC28*	983	*CDK1*
YBL030C	*PET9*	83447	*SLC25A31*	YBR160W	*CDC28*	1017	*CDK2*
YBL040C	*ERD2*	10945	*KDELR1*	YBR160W	*CDC28*	1019	*CDK4*
YBL040C	*ERD2*	11014	*KDELR2*	YBR160W	*CDC28*	1020	*CDK5*
YBL040C	*ERD2*	11015	*KDELR3*	YBR160W	*CDC28*	1021	*CDK6*
YBL041W	*PRE7*	5689	*PSMB1*	YBR160W	*CDC28*	728642	*CDK11A*
YBL050W	*SEC17*	8775	*NAPA*	YBR167C	*POP7*	10248	*POP7*
YBL074C	*AAR2*	25980	*AAR2*	YBR192W	*RIM2*	55186	*SLC25A36*
YBL084C	*CDC27*	996	*CDC27*	YBR198C	*TAF5*	27097	*TAF5L*
YBL105C	*PKC1*	207	*AKT1*	YBR198C	*TAF5*	55023	*PHIP*
YBL105C	*PKC1*	208	*AKT2*	YBR198C	*TAF5*	64326	*RFWD2*
YBL105C	*PKC1*	5578	*PRKCA*	YBR198C	*TAF5*	84292	*WDR83*
YBL105C	*PKC1*	5579	*PRKCB*	YBR202W	*MCM7*	4176	*MCM7*

Yeast Systematic Name	Yeast Standard Name	Human Entrez Gene ID	Human Standard Name	Yeast Systematic Name	Yeast Standard Name	Human Entrez Gene ID	Human Standard Name
YBL105C	*PKC1*	5581	*PRKCE*	YBR211C	*AME1*	79682	*CENPU*
YBR234C	*ARC40*	10095	*ARPC1B*	YDL064W	*UBC9*	7329	*UBE2I*
YBR234C	*ARC40*	10552	*ARPC1A*	YDL084W	*SUB2*	10212	*DDX39A*
YBR236C	*ABD1*	8731	*RNMT*	YDL087C	*LUC7*	51319	*RSRC1*
YBR247C	*ENP1*	705	*BYSL*	YDL087C	*LUC7*	51631	*LUC7L2*
YBR252W	*DUT1*	1854	*DUT*	YDL087C	*LUC7*	51747	*LUC7L3*
YBR257W	*POP4*	10775	*POP4*	YDL087C	*LUC7*	55119	*PRPF38B*
YBR265W	*TSC10*	2531	*KDSR*	YDL087C	*LUC7*	55692	*LUC7L*
YCL017C	*NFS1*	51540	*SCLY*	YDL087C	*LUC7*	84950	*PRPF38A*
YCL031C	*RRP7*	27341	*RRP7A*	YDL092W	*SRP14*	6727	*SRP14*
YCL043C	*PDI1*	5034	*P4HB*	YDL097C	*RPN6*	9318	*COPS2*
YCL043C	*PDI1*	10954	*PDIA5*	YDL098C	*SNU23*	153527	*ZMAT2*
YCL043C	*PDI1*	54431	*DNAJC10*	YDL105W	*NSE4*	54780	*NSMCE4A*
YCL043C	*PDI1*	63915	*BLOC1S5*	YDL105W	*NSE4*	493861	*EID3*
YCL043C	*PDI1*	81567	*TXNDC5*	YDL108W	*KIN28*	1022	*CDK7*
YCL043C	*PDI1*	121506	*ERP27*	YDL108W	*KIN28*	23552	*CDK20*
YCL052C	*PBN1*	54965	*PIGX*	YDL111C	*RRP42*	23016	*EXOSC7*
YCL054W	*SPB1*	117246	*FTSJ3*	YDL120W	*YFH1*	2395	*FXN*
YCL059C	*KRR1*	11103	*KRR1*	YDL126C	*CDC48*	7415	*VCP*
YCR012W	*PGK1*	5230	*PGK1*	YDL126C	*CDC48*	79029	*SPATA5L1*
YCR012W	*PGK1*	5232	*PGK2*	YDL139C	*SCM3*	55355	*HJURP*
YCR035C	*RRP43*	11340	*EXOSC8*	YDL140C	*RPO21*	5430	*POLR2A*
YCR052W	*RSC6*	6602	*SMARCD1*	YDL141W	*BPL1*	3141	*HLCS*
YCR057C	*PWP2*	5822	*PWP2*	YDL143W	*CCT4*	10575	*CCT4*
YCR072C	*RSA4*	14	*AAMP*	YDL147W	*RPN5*	5718	*PSMD12*
YDL003W	*MCD1*	5885	*RAD21*	YDL150W	*RPC53*	661	*POLR3D*
YDL003W	*MCD1*	9985	*REC8*	YDL153C	*SAS10*	57050	*UTP3*
YDL008W	*APC11*	51529	*ANAPC11*	YDL164C	*CDC9*	3978	*LIG1*
YDL014W	*NOP1*	2091	*FBL*	YDL166C	*FAP7*	50808	*AK3*
YDL017W	*CDC7*	8317	*CDC7*	YDL195W	*SEC31*	22872	*SEC31A*
YDL028C	*MPS1*	7272	*TTK*	YDL195W	*SEC31*	25956	*SEC31B*
YDL028C	*MPS1*	11011	*TLK2*	YDL205C	*HEM3*	3145	*HMBS*
YDL029W	*ARP2*	81569	*ACTL8*	YDL207W	*GLE1*	2733	*GLE1*
YDL031W	*DBP10*	79039	*DDX54*	YDL208W	*NHP2*	55651	*NHP2*
YDL045C	*FAD1*	80308	*FLAD1*	YDR002W	*YRB1*	202151	*RANBP3L*
YDL055C	*PSA1*	29925	*GMPPB*	YDR013W	*PSF1*	9837	*GINS1*
YDL055C	*PSA1*	29926	*GMPPA*	YDR021W	*FAL1*	9188	*DDX21*
YDL055C	*PSA1*	386724	*AMIGO3*	YDR021W	*FAL1*	9775	*EIF4A3*
YDL058W	*USO1*	2803	*GOLGA4*	YDR021W	*FAL1*	79009	*DDX50*
YDL058W	*USO1*	8615	*USO1*	YDR023W	*SES1*	6301	*SARS*
YDL058W	*USO1*	10900	*RUNDC3A*	YDR037W	*KRS1*	3735	*KARS*
YDL058W	*USO1*	23085	*ERC1*	YDR044W	*HEM13*	1371	*CPOX*
YDL058W	*USO1*	55680	*RUFY2*	YDR045C	*RPC11*	51728	*POLR3K*
YDL058W	*USO1*	80230	*RUFY1*	YDR047W	*HEM12*	635	*BHMT*

Yeast Systematic Name	Yeast Standard Name	Human Entrez Gene ID	Human Standard Name	Yeast Systematic Name	Yeast Standard Name	Human Entrez Gene ID	Human Standard Name
YDL060W	*TSR1*	55720	*TSR1*	YDR047W	*HEM12*	7389	*UROD*
YDR047W	*HEM12*	23743	*BHMT2*	YDR224C	*HTB1*	8970	*HIST1H2BJ*
YDR050C	*TPI1*	7167	*TPI1*	YDR224C	*HTB1*	85236	*HIST1H2BK*
YDR052C	*DBF4*	10926	*DBF4*	YDR224C	*HTB1*	128312	*HIST3H2BB*
YDR052C	*DBF4*	80174	*DBF4B*	YDR224C	*HTB1*	158983	*H2BFWT*
YDR054C	*CDC34*	54926	*UBE2R2*	YDR224C	*HTB1*	255626	*HIST1H2BA*
YDR062W	*LCB2*	9517	*SPTLC2*	YDR224C	*HTB1*	440689	*HIST2H2BF*
YDR062W	*LCB2*	55304	*SPTLC3*	YDR232W	*HEM1*	212	*ALAS2*
YDR064W	*RPS13*	6207	*RPS13*	YDR232W	*HEM1*	23464	*GCAT*
YDR081C	*PDC2*	23126	*POGZ*	YDR235W	*PRP42*	55015	*PRPF39*
YDR081C	*PDC2*	81789	*TIGD6*	YDR236C	*FMN1*	55312	*RFK*
YDR081C	*PDC2*	84948	*TIGD5*	YDR243C	*PRP28*	9416	*DDX23*
YDR081C	*PDC2*	91151	*TIGD7*	YDR243C	*PRP28*	55082	*ARGLU1*
YDR081C	*PDC2*	201798	*TIGD4*	YDR267C	*CIA1*	55884	*WSB2*
YDR081C	*PDC2*	220359	*TIGD3*	YDR280W	*RRP45*	11340	*EXOSC8*
YDR086C	*SSS1*	23480	*SEC61G*	YDR280W	*RRP45*	23016	*EXOSC7*
YDR087C	*RRP1*	8568	*RRP1*	YDR288W	*NSE3*	56160	*NDNL2*
YDR088C	*SLU7*	10569	*SLU7*	YDR292C	*SRP101*	6734	*SRPR*
YDR091C	*RLI1*	6059	*ABCE1*	YDR302W	*GPI11*	5281	*PIGF*
YDR113C	*PDS1*	9232	*PTTG1*	YDR308C	*SRB7*	9412	*MED21*
YDR145W	*TAF12*	6883	*TAF12*	YDR324C	*UTP4*	55294	*FBXW7*
YDR164C	*SEC1*	6812	*STXBP1*	YDR324C	*UTP4*	80227	*PAAF1*
YDR164C	*SEC1*	6814	*STXBP3*	YDR324C	*UTP4*	84916	*CIRH1A*
YDR164C	*SEC1*	152579	*SCFD2*	YDR324C	*UTP4*	151790	*WDR49*
YDR170C	*SEC7*	23362	*PSD3*	YDR324C	*UTP4*	157574	*FBXO16*
YDR170C	*SEC7*	23550	*PSD4*	YDR324C	*UTP4*	349136	*WDR86*
YDR170C	*SEC7*	27128	*CYTH4*	YDR325W	*YCG1*	64151	*NCAPG*
YDR170C	*SEC7*	84249	*PSD2*	YDR328C	*SKP1*	6500	*SKP1*
YDR172W	*SUP35*	10767	*HBS1L*	YDR331W	*GPI8*	5641	*LGMN*
YDR172W	*SUP35*	23708	*GSPT2*	YDR331W	*GPI8*	10026	*PIGK*
YDR177W	*UBC1*	3093	*UBE2K*	YDR339C	*FCF1*	51077	*FCF1*
YDR182W	*CDC1*	65258	*MPPE1*	YDR341C		5917	*RARS*
YDR190C	*RVB1*	8607	*RUVBL1*	YDR341C		57038	*RARS2*
YDR208W	*MSS4*	5305	*PIP4K2A*	YDR361C	*BCP1*	56647	*BCCIP*
YDR208W	*MSS4*	8394	*PIP5K1A*	YDR362C	*TFC6*	2976	*GTF3C2*
YDR208W	*MSS4*	8395	*PIP5K1B*	YDR373W	*FRQ1*	5957	*RCVRN*
YDR208W	*MSS4*	8396	*PIP4K2B*	YDR373W	*FRQ1*	23413	*NCS1*
YDR208W	*MSS4*	138429	*PIP5KL1*	YDR373W	*FRQ1*	30819	*KCNIP2*
YDR224C	*HTB1*	3017	*HIST1H2BD*	YDR373W	*FRQ1*	30820	*KCNIP1*
YDR224C	*HTB1*	8341	*HIST1H2BN*	YDR373W	*FRQ1*	51440	*HPCAL4*
YDR224C	*HTB1*	8342	*HIST1H2BM*	YDR373W	*FRQ1*	79645	*EFCAB1*
YDR224C	*HTB1*	8343	*HIST1H2BF*	YDR373W	*FRQ1*	80333	*KCNIP4*
YDR224C	*HTB1*	8345	*HIST1H2BH*	YDR373W	*FRQ1*	83988	*NCALD*
YDR224C	*HTB1*	8348	*HIST1H2BO*	YDR376W	*ARH1*	2232	*FDXR*

Yeast Systematic Name	Yeast Standard Name	Human Entrez Gene ID	Human Standard Name	Yeast Systematic Name	Yeast Standard Name	Human Entrez Gene ID	Human Standard Name
YDR224C	*HTB1*	8349	*HIST2H2BE*	YDR381W	*YRA1*	26097	*CHTOP*
YDR381W	*YRA1*	84271	*POLDIP3*	YER021W	*RPN3*	5709	*PSMD3*
YDR390C	*UBA2*	10054	*UBA2*	YER023W	*PRO3*	5831	*PYCR1*
YDR397C	*NCB2*	1810	*DR1*	YER023W	*PRO3*	29920	*PYCR2*
YDR404C	*RPB7*	5436	*POLR2G*	YER023W	*PRO3*	65263	*PYCRL*
YDR412W	*RRP17*	79159	*NOL12*	YER036C	*ARB1*	10061	*ABCF2*
YDR427W	*RPN9*	5719	*PSMD13*	YER043C	*SAH1*	191	*AHCY*
YDR437W	*GPI19*	51227	*PIGP*	YER043C	*SAH1*	10768	*AHCYL1*
YDR449C	*UTP6*	55813	*UTP6*	YER043C	*SAH1*	23382	*AHCYL2*
YDR454C	*GUK1*	1741	*DLG3*	YER082C	*UTP7*	9277	*WDR46*
YDR454C	*GUK1*	2987	*GUK1*	YER093C	*TSC11*	253260	*RICTOR*
YDR460W	*TFB3*	4331	*MNAT1*	YER094C	*PUP3*	5691	*PSMB3*
YDR468C	*TLG1*	10228	*STX6*	YER112W	*LSM4*	25804	*LSM4*
YDR472W	*TRS31*	126003	*TRAPPC5*	YER125W	*RSP5*	11059	*WWP1*
YDR473C	*PRP3*	9129	*PRPF3*	YER125W	*RSP5*	11060	*WWP2*
YDR478W	*SNM1*	9937	*DCLRE1A*	YER125W	*RSP5*	64750	*SMURF2*
YDR478W	*SNM1*	64421	*DCLRE1C*	YER126C	*NSA2*	10412	*NSA2*
YDR478W	*SNM1*	64858	*DCLRE1B*	YER127W	*LCP5*	25983	*NGDN*
YDR499W	*LCD1*	84126	*ATRIP*	YER133W	*GLC7*	5499	*PPP1CA*
YDR510W	*SMT3*	6612	*SUMO3*	YER133W	*GLC7*	5501	*PPP1CC*
YDR510W	*SMT3*	6613	*SUMO2*	YER136W	*GDI1*	2664	*GDI1*
YDR510W	*SMT3*	7341	*SUMO1*	YER136W	*GDI1*	2665	*GDI2*
YDR510W	*SMT3*	84901	*NFATC2IP*	YER146W	*LSM5*	23658	*LSM5*
YDR510W	*SMT3*	387082	*SUMO4*	YER147C	*SCC4*	23383	*MAU2*
YDR531W	*CAB1*	53354	*PANK1*	YER148W	*SPT15*	6908	*TBP*
YDR531W	*CAB1*	55229	*PANK4*	YER165W	*PAB1*	5042	*PABPC3*
YDR531W	*CAB1*	79646	*PANK3*	YER165W	*PAB1*	5937	*RBMS1*
YDR531W	*CAB1*	80025	*PANK2*	YER165W	*PAB1*	5939	*RBMS2*
YEL002C	*WBP1*	1650	*DDOST*	YER165W	*PAB1*	22827	*PUF60*
YEL026W	*SNU13*	4809	*NHP2L1*	YER165W	*PAB1*	140886	*PABPC5*
YEL032W	*MCM3*	4172	*MCM3*	YER168C	*CCA1*	51095	*TRNT1*
YEL034W	*HYP2*	1984	*EIF5A*	YFL002C	*SPB4*	57696	*DDX55*
YEL034W	*HYP2*	56648	*EIF5A2*	YFL005W	*SEC4*	5864	*RAB3A*
YEL058W	*PCM1*	5238	*PGM3*	YFL005W	*SEC4*	5874	*RAB27B*
YER003C	*PMI40*	4351	*MPI*	YFL005W	*SEC4*	10966	*RAB40B*
YER006W	*NUG1*	26354	*GNL3*	YFL005W	*SEC4*	25837	*RAB26*
YER006W	*NUG1*	54552	*GNL3L*	YFL005W	*SEC4*	51762	*RAB8B*
YER009W	*NTF2*	10204	*NUTF2*	YFL005W	*SEC4*	55647	*RAB20*
YER012W	*PRE1*	5690	*PSMB2*	YFL005W	*SEC4*	57799	*RAB40C*
YER013W	*PRP22*	1659	*DHX8*	YFL005W	*SEC4*	142684	*RAB40A*
YER013W	*PRP22*	8449	*DHX16*	YFL005W	*SEC4*	158158	*RASEF*
YER013W	*PRP22*	56919	*DHX33*	YFL005W	*SEC4*	282808	*RAB40AL*
YER013W	*PRP22*	79665	*DHX40*	YFL005W	*SEC4*	326624	*RAB37*
YER018C	*SPC25*	57405	*SPC25*	YFL005W	*SEC4*	376267	*RAB15*

Yeast Systematic Name	Yeast Standard Name	Human Entrez Gene ID	Human Standard Name	Yeast Systematic Name	Yeast Standard Name	Human Entrez Gene ID	Human Standard Name
YER018C	*SPC25*	147841	*SPC24*	YFL008W	*SMC1*	27127	*SMC1B*
YFL009W	*CDC4*	55294	*FBXW7*	YFR028C	*CDC14*	54935	*DUSP23*
YFL009W	*CDC4*	80227	*PAAF1*	YFR037C	*RSC8*	6601	*SMARCC2*
YFL009W	*CDC4*	151790	*WDR49*	YFR050C	*PRE4*	5692	*PSMB4*
YFL009W	*CDC4*	157574	*FBXO16*	YFR052W	*RPN12*	5714	*PSMD8*
YFL009W	*CDC4*	349136	*WDR86*	YGL001C	*ERG26*	50814	*NSDHL*
YFL017C	*GNA1*	64841	*GNPNAT1*	YGL018C	*JAC1*	150274	*HSCB*
YFL022C	*FRS2*	2193	*FARSA*	YGL022W	*STT3*	3703	*STT3A*
YFL024C	*EPL1*	26122	*EPC2*	YGL030W	*RPL30*	6156	*RPL30*
YFL024C	*EPL1*	80314	*EPC1*	YGL044C	*RNA15*	23283	*CSTF2T*
YFL029C	*CAK1*	1017	*CDK2*	YGL044C	*RNA15*	85437	*ZCRB1*
YFL037W	*TUB2*	7280	*TUBB2A*	YGL047W	*ALG13*	79868	*ALG13*
YFL037W	*TUB2*	10381	*TUBB3*	YGL048C	*RPT6*	5705	*PSMC5*
YFL037W	*TUB2*	10382	*TUBB4A*	YGL055W	*OLE1*	6319	*SCD*
YFL037W	*TUB2*	10383	*TUBB4B*	YGL055W	*OLE1*	79966	*SCD5*
YFL037W	*TUB2*	51175	*TUBE1*	YGL065C	*ALG2*	85365	*ALG2*
YFL037W	*TUB2*	81027	*TUBB1*	YGL068W	*MNP1*	6182	*MRPL12*
YFL037W	*TUB2*	84617	*TUBB6*	YGL073W	*HSF1*	3297	*HSF1*
YFL037W	*TUB2*	203068	*TUBB*	YGL073W	*HSF1*	3298	*HSF2*
YFL037W	*TUB2*	347733	*TUBB2B*	YGL073W	*HSF1*	86614	*HSFY1*
YFL038C	*YPT1*	5861	*RAB1A*	YGL091C	*NBP35*	4682	*NUBP1*
YFL038C	*YPT1*	5864	*RAB3A*	YGL091C	*NBP35*	80224	*NUBPL*
YFL038C	*YPT1*	9363	*RAB33A*	YGL097W	*SRM1*	1102	*RCBTB2*
YFL038C	*YPT1*	11020	*IFT27*	YGL097W	*SRM1*	1104	*RCC1*
YFL038C	*YPT1*	25837	*RAB26*	YGL097W	*SRM1*	6103	*RPGR*
YFL038C	*YPT1*	27314	*RAB30*	YGL097W	*SRM1*	55213	*RCBTB1*
YFL038C	*YPT1*	51762	*RAB8B*	YGL098W	*USE1*	55850	*USE1*
YFL038C	*YPT1*	81876	*RAB1B*	YGL099W	*LSG1*	2794	*GNL1*
YFL038C	*YPT1*	83452	*RAB33B*	YGL103W	*RPL28*	6157	*RPL27A*
YFL038C	*YPT1*	326624	*RAB37*	YGL111W	*NSA1*	54663	*WDR74*
YFL038C	*YPT1*	376267	*RAB15*	YGL112C	*TAF6*	10629	*TAF6L*
YFL039C	*ACT1*	59	*ACTA2*	YGL116W	*CDC20*	991	*CDC20*
YFL039C	*ACT1*	60	*ACTB*	YGL116W	*CDC20*	166979	*CDC20B*
YFL039C	*ACT1*	70	*ACTC1*	YGL120C	*PRP43*	55760	*DHX32*
YFL039C	*ACT1*	71	*ACTG1*	YGL120C	*PRP43*	165545	*DQX1*
YFL039C	*ACT1*	81569	*ACTL8*	YGL122C	*NAB2*	79882	*ZC3H14*
YFL039C	*ACT1*	84517	*ACTRT3*	YGL123W	*RPS2*	6187	*RPS2*
YFL039C	*ACT1*	139741	*ACTRT1*	YGL130W	*CEG1*	8732	*RNGTT*
YFL039C	*ACT1*	140625	*ACTRT2*	YGL142C	*GPI10*	9488	*PIGB*
YFL039C	*ACT1*	345651	*ACTBL2*	YGL150C	*INO80*	54617	*INO80*
YFR004W	*RPN11*	8667	*EIF3H*	YGL169W	*SUA5*	79693	*YRDC*
YFR005C	*SAD1*	10713	*USP39*	YGL171W	*ROK1*	11056	*DDX52*
YFR005C	*SAD1*	84196	*USP48*	YGL172W	*NUP49*	9818	*NUPL1*
YFR027W	*ECO1*	114799	*ESCO1*	YGL225W	*VRG4*	11046	*SLC35D2*

Yeast Systematic Name	Yeast Standard Name	Human Entrez Gene ID	Human Standard Name	Yeast Systematic Name	Yeast Standard Name	Human Entrez Gene ID	Human Standard Name
YFR028C	*CDC14*	8556	*CDC14A*	YGL225W	*VRG4*	23169	*SLC35D1*
YGL225W	*VRG4*	85019	*TMEM241*	YHR007C	*ERG11*	1595	*CYP51A1*
YGL233W	*SEC15*	54536	*EXOC6*	YHR007C	*ERG11*	56603	*CYP26B1*
YGR009C	*SEC9*	8773	*SNAP23*	YHR024C	*MAS2*	7385	*UQCRC2*
YGR009C	*SEC9*	9342	*SNAP29*	YHR024C	*MAS2*	23203	*PMPCA*
YGR024C	*THG1*	54974	*THG1L*	YHR058C	*MED6*	10001	*MED6*
YGR029W	*ERV1*	2671	*GFER*	YHR062C	*RPP1*	10556	*RPP30*
YGR047C	*TFC4*	9330	*GTF3C3*	YHR065C	*RRP3*	51202	*DDX47*
YGR060W	*ERG25*	9023	*CH25H*	YHR065C	*RRP3*	55794	*DDX28*
YGR060W	*ERG25*	10826	*FAXDC2*	YHR070W	*TRM5*	57570	*TRMT5*
YGR065C	*VHT1*	10050	*SLC17A4*	YHR072W	*ERG7*	4047	*LSS*
YGR065C	*VHT1*	10246	*SLC17A2*	YHR085W	*IPI1*	54881	*TEX10*
YGR065C	*VHT1*	10786	*SLC17A3*	YHR088W	*RPF1*	80135	*RPF1*
YGR065C	*VHT1*	246213	*SLC17A8*	YHR107C	*CDC12*	989	*SEPT7*
YGR075C	*PRP38*	55119	*PRPF38B*	YHR107C	*CDC12*	1731	*SEPT1*
YGR075C	*PRP38*	84950	*PRPF38A*	YHR107C	*CDC12*	4735	*SEPT2*
YGR083C	*GCD2*	8890	*EIF2B4*	YHR107C	*CDC12*	23157	*SEPT6*
YGR091W	*PRP31*	26121	*PRPF31*	YHR107C	*CDC12*	55752	*SEPT11*
YGR095C	*RRP46*	56915	*EXOSC5*	YHR107C	*CDC12*	55964	*SEPT3*
YGR103W	*NOP7*	23481	*PES1*	YHR107C	*CDC12*	124404	*SEPT12*
YGR113W	*DAM1*	10286	*BCAS2*	YHR107C	*CDC12*	151011	*SEPT10*
YGR119C	*NUP57*	9818	*NUPL1*	YHR118C	*ORC6*	23594	*ORC6*
YGR119C	*NUP57*	23636	*NUP62*	YHR122W	*CIA2*	84191	*FAM96A*
YGR119C	*NUP57*	53371	*NUP54*	YHR164C	*DNA2*	1763	*DNA2*
YGR119C	*NUP57*	54830	*NUP62CL*	YHR166C	*CDC23*	8697	*CDC23*
YGR120C	*COG2*	22796	*COG2*	YHR170W	*NMD3*	51068	*NMD3*
YGR145W	*ENP2*	79954	*NOL10*	YHR186C	*KOG1*	57521	*RPTOR*
YGR147C	*NAT2*	10	*NAT2*	YHR188C	*GPI16*	51604	*PIGT*
YGR156W	*PTI1*	1915	*EEF1A1*	YHR190W	*ERG9*	2222	*FDFT1*
YGR172C	*YIP1*	285525	*YIPF7*	YIL003W	*CFD1*	10101	*NUBP2*
YGR175C	*ERG1*	6713	*SQLE*	YIL004C	*BET1*	10282	*BET1*
YGR179C	*OKP1*	55166	*CENPQ*	YIL021W	*RPB3*	5432	*POLR2C*
YGR185C	*TYS1*	8565	*YARS*	YIL022W	*TIM44*	10469	*TIMM44*
YGR185C	*TYS1*	9255	*AIMP1*	YIL026C	*IRR1*	10734	*STAG3*
YGR195W	*SKI6*	54512	*EXOSC4*	YIL026C	*IRR1*	10735	*STAG2*
YGR216C	*GPI1*	9091	*PIGQ*	YIL031W	*ULP2*	26054	*SENP6*
YGR218W	*CRM1*	7514	*XPO1*	YIL061C	*SNP1*	6625	*SNRNP70*
YGR246C	*BRF1*	55290	*BRF2*	YIL062C	*ARC15*	10092	*ARPC5*
YGR253C	*PUP2*	5686	*PSMA5*	YIL068C	*SEC6*	11336	*EXOC3*
YGR264C	*MES1*	9255	*AIMP1*	YIL068C	*SEC6*	90332	*EXOC3L2*
YGR277C	*CAB4*	80347	*COASY*	YIL078W	*THS1*	54148	*MRPL39*
YGR278W	*CWC22*	5411	*PNN*	YIL083C	*CAB2*	79717	*PPCS*
YGR278W	*CWC22*	57703	*CWC22*	YIL091C	*UTP25*	27042	*DIEXF*
YGR280C	*PXR1*	54984	*PINX1*	YIL106W	*MOB1*	79817	*MOB3B*

Yeast Systematic Name	Yeast Standard Name	Human Entrez Gene ID	Human Standard Name	Yeast Systematic Name	Yeast Standard Name	Human Entrez Gene ID	Human Standard Name
YHL015W	*RPS20*	6224	*RPS20*	YIL106W	*MOB1*	81532	*MOB2*
YIL106W	*MOB1*	92597	*MOB1B*	YJL125C	*GCD14*	115708	*TRMT61A*
YIL106W	*MOB1*	148932	*MOB3C*	YJL143W	*TIM17*	10245	*TIMM17B*
YIL109C	*SEC24*	9871	*SEC24D*	YJL143W	*TIM17*	10440	*TIMM17A*
YIL126W	*STH1*	6595	*SMARCA2*	YJL167W	*ERG20*	2224	*FDPS*
YIL129C	*TAO3*	285527	*FRYL*	YJL203W	*PRP21*	6433	*SFSWAP*
YIL143C	*SSL2*	2071	*ERCC3*	YJL203W	*PRP21*	10291	*SF3A1*
YIL144W	*TID3*	10403	*NDC80*	YJR006W	*POL31*	5425	*POLD2*
YIL150C	*MCM10*	55388	*MCM10*	YJR013W	*GPI14*	93183	*PIGM*
YIR006C	*PAN1*	50618	*ITSN2*	YJR045C	*SSC1*	3313	*HSPA9*
YIR006C	*PAN1*	58513	*EPS15L1*	YJR057W	*CDC8*	1841	*DTYMK*
YIR006C	*PAN1*	85021	*REPS1*	YJR064W	*CCT5*	22948	*CCT5*
YIR008C	*PRI1*	5557	*PRIM1*	YJR065C	*ARP3*	10096	*ACTR3*
YIR010W	*DSN1*	79980	*DSN1*	YJR065C	*ARP3*	57180	*ACTR3B*
YIR012W	*SQT1*	14	*AAMP*	YJR072C	*NPA3*	11321	*GPN1*
YIR015W	*RPR2*	79897	*RPP21*	YJR076C	*CDC11*	989	*SEPT7*
YIR022W	*SEC11*	23478	*SEC11A*	YJR076C	*CDC11*	1731	*SEPT1*
YIR022W	*SEC11*	90701	*SEC11C*	YJR076C	*CDC11*	4735	*SEPT2*
YJL001W	*PRE3*	5698	*PSMB9*	YJR076C	*CDC11*	23157	*SEPT6*
YJL002C	*OST1*	6184	*RPN1*	YJR076C	*CDC11*	55752	*SEPT11*
YJL005W	*CYR1*	55631	*LRRC40*	YJR076C	*CDC11*	55964	*SEPT3*
YJL008C	*CCT8*	150160	*CCT8L2*	YJR076C	*CDC11*	124404	*SEPT12*
YJL010C	*NOP9*	161424	*NOP9*	YJR076C	*CDC11*	151011	*SEPT10*
YJL014W	*CCT3*	7203	*CCT3*	YJR112W	*NNF1*	64946	*CENPH*
YJL026W	*RNR2*	6241	*RRM2*	YKL012W	*PRP40*	25766	*PRPF40B*
YJL026W	*RNR2*	50484	*RRM2B*	YKL012W	*PRP40*	55660	*PRPF40A*
YJL031C	*BET4*	5875	*RABGGTA*	YKL013C	*ARC19*	10093	*ARPC4*
YJL035C	*TAD2*	134637	*ADAT2*	YKL018W	*SWD2*	80335	*WDR82*
YJL041W	*NSP1*	9883	*POM121*	YKL019W	*RAM2*	2339	*FNTA*
YJL041W	*NSP1*	23636	*NUP62*	YKL022C	*CDC16*	8881	*CDC16*
YJL041W	*NSP1*	54830	*NUP62CL*	YKL024C	*URA6*	51727	*CMPK1*
YJL041W	*NSP1*	1E+08	*POM121C*	YKL033W	*TTI1*	9675	*TTI1*
YJL050W	*MTR4*	23517	*SKIV2L2*	YKL035W	*UGP1*	7360	*UGP2*
YJL050W	*MTR4*	55601	*DDX60*	YKL049C	*CSE4*	1058	*CENPA*
YJL072C	*PSF2*	51659	*GINS2*	YKL049C	*CSE4*	3021	*H3F3B*
YJL081C	*ARP4*	86	*ACTL6A*	YKL049C	*CSE4*	8290	*HIST3H3*
YJL081C	*ARP4*	51412	*ACTL6B*	YKL049C	*CSE4*	8350	*HIST1H3A*
YJL085W	*EXO70*	23265	*EXOC7*	YKL049C	*CSE4*	8352	*HIST1H3C*
YJL090C	*DPB11*	11073	*TOPBP1*	YKL049C	*CSE4*	8353	*HIST1H3E*
YJL097W	*PHS1*	9200	*HACD1*	YKL049C	*CSE4*	8354	*HIST1H3I*
YJL097W	*PHS1*	201562	*HACD2*	YKL049C	*CSE4*	8357	*HIST1H3H*
YJL097W	*PHS1*	401494	*HACD4*	YKL049C	*CSE4*	8358	*HIST1H3B*
YJL104W	*PAM16*	51025	*PAM16*	YKL049C	*CSE4*	126961	*HIST2H3C*
YJL109C	*UTP10*	55127	*HEATR1*	YKL049C	*CSE4*	440093	*H3F3C*

Yeast Systematic Name	Yeast Standard Name	Human Entrez Gene ID	Human Standard Name	Yeast Systematic Name	Yeast Standard Name	Human Entrez Gene ID	Human Standard Name
YJL125C	*GCD14*	55006	*TRMT61B*	YKL058W	*TOA2*	2958	*GTF2A2*
YKL059C	*MPE1*	5930	*RBBP6*	YKR086W	*PRP16*	170506	*DHX36*
YKL078W	*DHR2*	22907	*DHX30*	YLL031C	*GPI13*	84720	*PIGO*
YKL078W	*DHR2*	55760	*DHX32*	YLL034C	*RIX7*	4931	*NVL*
YKL078W	*DHR2*	90957	*DHX57*	YLL035W	*GRC3*	79707	*NOL9*
YKL078W	*DHR2*	165545	*DQX1*	YLL036C	*PRP19*	27339	*PRPF19*
YKL078W	*DHR2*	170506	*DHX36*	YLL050C	*COF1*	1072	*CFL1*
YKL082C	*RRP14*	6838	*SURF6*	YLL050C	*COF1*	11034	*DSTN*
YKL089W	*MIF2*	1060	*CENPC*	YLR005W	*SSL1*	730394	*GTF2H2D*
YKL095W	*YJU2*	55702	*CCDC94*	YLR007W	*NSE1*	197370	*NSMCE1*
YKL095W	*YJU2*	81576	*CCDC130*	YLR008C	*PAM18*	29103	*DNAJC15*
YKL099C	*UTP11*	51118	*UTP11L*	YLR008C	*PAM18*	131118	*DNAJC19*
YKL104C	*GFA1*	9945	*GFPT2*	YLR022C	*SDO1*	51119	*SBDS*
YKL125W	*RRN3*	54700	*RRN3*	YLR026C	*SED5*	6811	*STX5*
YKL145W	*RPT1*	5701	*PSMC2*	YLR029C	*RPL15A*	6138	*RPL15*
YKL152C	*GPM1*	669	*BPGM*	YLR045C	*STU2*	9793	*CKAP5*
YKL152C	*GPM1*	5224	*PGAM2*	YLR051C	*FCF2*	30836	*DNTTIP2*
YKL154W	*SRP102*	58477	*SRPRB*	YLR060W	*FRS1*	10056	*FARSB*
YKL165C	*MCD4*	23556	*PIGN*	YLR066W	*SPC3*	60559	*SPCS3*
YKL172W	*EBP2*	10969	*EBNA1BP2*	YLR088W	*GAA1*	8733	*GPAA1*
YKL173W	*SNU114*	9343	*EFTUD2*	YLR100W	*ERG27*	51478	*HSD17B7*
YKL180W	*RPL17A*	6139	*RPL17*	YLR103C	*CDC45*	8318	*CDC45*
YKL182W	*FAS1*	27349	*MCAT*	YLR105C	*SEN2*	80746	*TSEN2*
YKL186C	*MTR2*	29107	*NXT1*	YLR106C	*MDN1*	55677	*IWS1*
YKL189W	*HYM1*	51719	*CAB39*	YLR106C	*MDN1*	126637	*TCHHL1*
YKL189W	*HYM1*	81617	*CAB39L*	YLR106C	*MDN1*	161394	*SAMD15*
YKL192C	*ACP1*	4706	*NDUFAB1*	YLR115W	*CFT2*	53981	*CPSF2*
YKL193C	*SDS22*	5510	*PPP1R7*	YLR116W	*MSL5*	9444	*QKI*
YKL193C	*SDS22*	54839	*LRRC49*	YLR116W	*MSL5*	202559	*KHDRBS2*
YKL193C	*SDS22*	83450	*LRRC48*	YLR129W	*DIP2*	10885	*WDR3*
YKL193C	*SDS22*	85444	*LRRCC1*	YLR132C	*USB1*	79650	*USB1*
YKL195W	*MIA40*	131474	*CHCHD4*	YLR153C	*ACS2*	6296	*ACSM3*
YKL196C	*YKT6*	10652	*YKT6*	YLR153C	*ACS2*	54988	*ACSM5*
YKL210W	*UBA1*	7318	*UBA7*	YLR153C	*ACS2*	55902	*ACSS2*
YKL210W	*UBA1*	55236	*UBA6*	YLR153C	*ACS2*	79611	*ACSS3*
YKR002W	*PAP1*	10914	*PAPOLA*	YLR153C	*ACS2*	80221	*ACSF2*
YKR002W	*PAP1*	64895	*PAPOLG*	YLR153C	*ACS2*	116285	*ACSM1*
YKR025W	*RPC37*	55718	*POLR3E*	YLR163C	*MAS1*	9512	*PMPCB*
YKR038C	*KAE1*	55644	*OSGEP*	YLR167W	*RPS31*	6233	*RPS27A*
YKR062W	*TFA2*	2961	*GTF2E2*	YLR175W	*CBF5*	1736	*DKC1*
YKR071C	*DRE2*	57019	*CIAPIN1*	YLR186W	*EMG1*	10436	*EMG1*
YKR079C	*TRZ1*	60528	*ELAC2*	YLR195C	*NMT1*	4836	*NMT1*
YKR086W	*PRP16*	9785	*DHX38*	YLR196W	*PWP1*	11137	*PWP1*
YKR086W	*PRP16*	22907	*DHX30*	YLR197W	*NOP56*	10528	*NOP56*

Yeast Systematic Name	Yeast Standard Name	Human Entrez Gene ID	Human Standard Name	Yeast Systematic Name	Yeast Standard Name	Human Entrez Gene ID	Human Standard Name
YKR086W	*PRP16*	90957	*DHX57*	YLR212C	*TUB4*	7283	*TUBG1*
YLR212C	*TUB4*	27175	*TUBG2*	YML064C	*TEM1*	51715	*RAB23*
YLR212C	*TUB4*	51174	*TUBD1*	YML069W	*POB3*	3146	*HMGB1*
YLR215C	*CDC123*	8872	*CDC123*	YML069W	*POB3*	3148	*HMGB2*
YLR222C	*UTP13*	54584	*GNB1L*	YML069W	*POB3*	3149	*HMGB3*
YLR229C	*CDC42*	23433	*RHOQ*	YML069W	*POB3*	6672	*SP100*
YLR229C	*CDC42*	29984	*RHOD*	YML069W	*POB3*	6749	*SSRP1*
YLR229C	*CDC42*	54509	*RHOF*	YML069W	*POB3*	10362	*HMG20B*
YLR229C	*CDC42*	57381	*RHOJ*	YML069W	*POB3*	10363	*HMG20A*
YLR243W	*GPN3*	51184	*GPN3*	YML077W	*BET5*	58485	*TRAPPC1*
YLR259C	*HSP60*	3329	*HSPD1*	YML085C	*TUB1*	7277	*TUBA4A*
YLR274W	*MCM5*	4174	*MCM5*	YML085C	*TUB1*	7846	*TUBA1A*
YLR275W	*SMD2*	6633	*SNRPD2*	YML085C	*TUB1*	10376	*TUBA1B*
YLR277C	*YSH1*	54973	*CPSF3L*	YML085C	*TUB1*	79861	*TUBAL3*
YLR291C	*GCD7*	8892	*EIF2B2*	YML085C	*TUB1*	84790	*TUBA1C*
YLR293C	*GSP1*	5901	*RAN*	YML085C	*TUB1*	112714	*TUBA3E*
YLR293C	*GSP1*	51715	*RAB23*	YML085C	*TUB1*	113457	*TUBA3D*
YLR298C	*YHC1*	6631	*SNRPC*	YML092C	*PRE8*	5683	*PSMA2*
YLR310C	*CDC25*	5923	*RASGRF1*	YML093W	*UTP14*	9724	*UTP14C*
YLR310C	*CDC25*	6655	*SOS2*	YML093W	*UTP14*	10813	*UTP14A*
YLR310C	*CDC25*	55103	*RALGPS2*	YML098W	*TAF13*	6884	*TAF13*
YLR314C	*CDC3*	989	*SEPT7*	YML114C	*TAF8*	129685	*TAF8*
YLR314C	*CDC3*	1731	*SEPT1*	YML125C	*PGA3*	51167	*CYB5R4*
YLR314C	*CDC3*	4735	*SEPT2*	YML125C	*PGA3*	51706	*CYB5R1*
YLR314C	*CDC3*	23157	*SEPT6*	YML126C	*ERG13*	3158	*HMGCS2*
YLR314C	*CDC3*	55752	*SEPT11*	YML130C	*ERO1*	30001	*ERO1L*
YLR314C	*CDC3*	55964	*SEPT3*	YML130C	*ERO1*	56605	*ERO1LB*
YLR314C	*CDC3*	124404	*SEPT12*	YMR001C	*CDC5*	5347	*PLK1*
YLR314C	*CDC3*	151011	*SEPT10*	YMR001C	*CDC5*	126520	*PLK5*
YLR316C	*TAD3*	113179	*ADAT3*	YMR033W	*ARP9*	10120	*ACTR1B*
YLR321C	*SFH1*	6598	*SMARCB1*	YMR033W	*ARP9*	10121	*ACTR1A*
YLR323C	*CWC24*	7737	*RNF113A*	YMR047C	*NUP116*	9818	*NUPL1*
YLR340W	*RPP0*	6175	*RPLP0*	YMR059W	*SEN15*	116461	*TSEN15*
YLR378C	*SEC61*	29927	*SEC61A1*	YMR076C	*PDS5*	23047	*PDS5B*
YLR378C	*SEC61*	55176	*SEC61A2*	YMR076C	*PDS5*	23244	*PDS5A*
YLR397C	*AFG2*	79029	*SPATA5L1*	YMR079W	*SEC14*	266629	*SEC14L3*
YLR409C	*UTP21*	134430	*WDR36*	YMR093W	*UTP15*	84135	*UTP15*
YLR424W	*SPP382*	24144	*TFIP11*	YMR112C	*MED11*	400569	*MED11*
YLR424W	*SPP382*	54923	*LIME1*	YMR117C	*SPC24*	57405	*SPC25*
YLR430W	*SEN1*	23064	*SETX*	YMR117C	*SPC24*	147841	*SPC24*
YML010W	*SPT5*	6829	*SUPT5H*	YMR128W	*ECM16*	57647	*DHX37*
YML025C	*YML6*	51073	*MRPL4*	YMR146C	*TIF34*	8668	*EIF3I*
YML046W	*PRP39*	55015	*PRPF39*	YMR146C	*TIF34*	11171	*STRAP*
YML049C	*RSE1*	23450	*SF3B3*	YMR149W	*SWP1*	6185	*RPN2*

Yeast Systematic Name	Yeast Standard Name	Human Entrez Gene ID	Human Standard Name	Yeast Systematic Name	Yeast Standard Name	Human Entrez Gene ID	Human Standard Name
YML064C	*TEM1*	9364	*RAB28*	YMR197C	*VTI1*	10490	*VTI1B*
YMR203W	*TOM40*	84134	*TOMM40L*	YNL178W	*RPS3*	6188	*RPS3*
YMR208W	*ERG12*	4598	*MVK*	YNL182C	*IPI3*	57418	*WDR18*
YMR211W	*DML1*	55154	*MSTO1*	YNL189W	*SRP1*	3836	*KPNA1*
YMR218C	*TRS130*	7109	*TRAPPC10*	YNL189W	*SRP1*	3838	*KPNA2*
YMR227C	*TAF7*	54457	*TAF7L*	YNL189W	*SRP1*	3840	*KPNA4*
YMR235C	*RNA1*	80790	*CMIP*	YNL189W	*SRP1*	3841	*KPNA5*
YMR240C	*CUS1*	10992	*SF3B2*	YNL189W	*SRP1*	23633	*KPNA6*
YMR260C	*TIF11*	9086	*EIF1AY*	YNL232W	*CSL4*	51013	*EXOSC1*
YMR268C	*PRP24*	9733	*SART3*	YNL240C	*NAR1*	64428	*NARFL*
YMR290C	*HAS1*	8886	*DDX18*	YNL244C	*SUI1*	10289	*EIF1B*
YMR298W	*LIP1*	11019	*LIAS*	YNL247W		833	*CARS*
YMR308C	*PSE1*	3843	*IPO5*	YNL260C	*LTO1*	220064	*ORAOV1*
YMR308C	*PSE1*	26953	*RANBP6*	YNL263C	*YIF1*	10897	*YIF1A*
YMR309C	*NIP1*	8663	*EIF3C*	YNL263C	*YIF1*	90522	*YIF1B*
YMR314W	*PRE5*	5682	*PSMA1*	YNL272C	*SEC2*	5866	*RAB3IL1*
YNL002C	*RLP7*	6129	*RPL7*	YNL287W	*SEC21*	22820	*COPG1*
YNL002C	*RLP7*	285855	*RPL7L1*	YNL290W	*RFC3*	5985	*RFC5*
YNL006W	*LST8*	64223	*MLST8*	YNL312W	*RFA2*	6118	*RPA2*
YNL007C	*SIS1*	3337	*DNAJB1*	YNL312W	*RFA2*	29935	*RPA4*
YNL007C	*SIS1*	10049	*DNAJB6*	YNL313C	*EMW1*	55622	*TTC27*
YNL007C	*SIS1*	11080	*DNAJB4*	YNL317W	*PFS2*	5542	*PRB1*
YNL007C	*SIS1*	25822	*DNAJB5*	YNL317W	*PFS2*	5554	*PRH1*
YNL007C	*SIS1*	80331	*DNAJC5*	YNL317W	*PFS2*	5555	*PRH2*
YNL007C	*SIS1*	85479	*DNAJC5B*	YNL317W	*PFS2*	55339	*WDR33*
YNL038W	*GPI15*	5283	*PIGH*	YNL317W	*PFS2*	84826	*SFT2D3*
YNL061W	*NOP2*	4839	*NOP2*	YNR011C	*PRP2*	8449	*DHX16*
YNL061W	*NOP2*	63899	*NSUN3*	YNR011C	*PRP2*	22907	*DHX30*
YNL062C	*GCD10*	51605	*TRMT6*	YNR011C	*PRP2*	90957	*DHX57*
YNL110C	*NOP15*	81892	*SLIRP*	YNR011C	*PRP2*	170506	*DHX36*
YNL110C	*NOP15*	84365	*NIFK*	YNR026C	*SEC12*	55250	*ELP2*
YNL112W	*DBP2*	10521	*DDX17*	YNR046W	*TRM112*	51504	*TRMT112*
YNL112W	*DBP2*	51428	*DDX41*	YNR053C	*NOG2*	26354	*GNL3*
YNL112W	*DBP2*	55510	*DDX43*	YNR053C	*NOG2*	29889	*GNL2*
YNL112W	*DBP2*	83479	*DDX59*	YNR053C	*NOG2*	54552	*GNL3L*
YNL112W	*DBP2*	168400	*DDX53*	YOL005C	*RPB11*	5439	*POLR2J*
YNL113W	*RPC19*	51082	*POLR1D*	YOL010W	*RCL1*	8634	*RTCA*
YNL118C	*DCP2*	167227	*DCP2*	YOL010W	*RCL1*	10171	*RCL1*
YNL126W	*SPC98*	10426	*TUBGCP3*	YOL021C	*DIS3*	22894	*DIS3*
YNL126W	*SPC98*	27229	*TUBGCP4*	YOL021C	*DIS3*	115752	*DIS3L*
YNL131W	*TOM22*	56993	*TOMM22*	YOL022C	*TSR4*	84306	*PDCD2L*
YNL132W	*KRE33*	55226	*NAT10*	YOL069W	*NUF2*	83540	*NUF2*
YNL151C	*RPC31*	84265	*POLR3GL*	YOL097C	*WRS1*	7453	*WARS*
YNL161W	*CBK1*	11329	*STK38*	YOL102C	*TPT1*	83707	*TRPT1*

Yeast Systematic Name	Yeast Standard Name	Human Entrez Gene ID	Human Standard Name	Yeast Systematic Name	Yeast Standard Name	Human Entrez Gene ID	Human Standard Name
YNL161W	*CBK1*	23012	*STK38L*	YOL120C	*RPL18A*	6141	*RPL18*
YOL123W	*HRP1*	3178	*HNRNPA1*	YOR210W	*RPB10*	5441	*POLR2L*
YOL123W	*HRP1*	3181	*HNRNPA2B1*	YOR224C	*RPB8*	5437	*POLR2H*
YOL123W	*HRP1*	9987	*HNRNPDL*	YOR232W	*MGE1*	80273	*GRPEL1*
YOL123W	*HRP1*	27316	*RBMX*	YOR232W	*MGE1*	134266	*GRPEL2*
YOL123W	*HRP1*	124540	*MSI2*	YOR236W	*DFR1*	1719	*DHFR*
YOL123W	*HRP1*	159163	*RBMY1F*	YOR236W	*DFR1*	200895	*DHFRL1*
YOL127W	*RPL25*	6147	*RPL23A*	YOR244W	*ESA1*	10524	*KAT5*
YOL133W	*HRT1*	9616	*RNF7*	YOR244W	*ESA1*	11143	*KAT7*
YOL133W	*HRT1*	9978	*RBX1*	YOR249C	*APC5*	51433	*ANAPC5*
YOL135C	*MED7*	9443	*MED7*	YOR250C	*CLP1*	10978	*CLP1*
YOL139C	*CDC33*	1977	*EIF4E*	YOR254C	*SEC63*	11231	*SEC63*
YOL139C	*CDC33*	9470	*EIF4E2*	YOR256C	*TRE2*	7036	*TFR2*
YOL139C	*CDC33*	317649	*EIF4E3*	YOR257W	*CDC31*	1068	*CETN1*
YOL144W	*NOP8*	23029	*RBM34*	YOR257W	*CDC31*	1070	*CETN3*
YOL146W	*PSF3*	64785	*GINS3*	YOR257W	*CDC31*	84288	*EFCAB2*
YOR004W	*UTP23*	84294	*UTP23*	YOR261C	*RPN8*	5713	*PSMD7*
YOR046C	*DBP5*	11269	*DDX19B*	YOR261C	*RPN8*	8665	*EIF3F*
YOR046C	*DBP5*	55308	*DDX19A*	YOR261C	*RPN8*	10980	*COPS6*
YOR048C	*RAT1*	22803	*XRN2*	YOR262W	*GPN2*	54707	*GPN2*
YOR056C	*NOB1*	28987	*NOB1*	YOR272W	*YTM1*	22884	*WDR37*
YOR057W	*SGT1*	7265	*TTC1*	YOR294W	*RRS1*	23212	*RRS1*
YOR063W	*RPL3*	6122	*RPL3*	YOR310C	*NOP58*	51602	*NOP58*
YOR075W	*UFE1*	53407	*STX18*	YOR319W	*HSH49*	10262	*SF3B4*
YOR103C	*OST2*	1603	*DAD1*	YOR319W	*HSH49*	11052	*CPSF6*
YOR110W	*TFC7*	57103	*C12orf5*	YOR319W	*HSH49*	79869	*CPSF7*
YOR117W	*RPT5*	5702	*PSMC3*	YOR319W	*HSH49*	93487	*MAPK1IP1L*
YOR117W	*RPT5*	83858	*ATAD3B*	YOR326W	*MYO2*	4646	*MYO6*
YOR117W	*RPT5*	219293	*ATAD3C*	YOR326W	*MYO2*	80179	*MYO19*
YOR122C	*PFY1*	375189	*PFN4*	YOR336W	*KRE5*	55757	*UGGT2*
YOR143C	*THI80*	27010	*TPK1*	YOR340C	*RPA43*	221830	*TWISTNB*
YOR145C	*PNO1*	56902	*PNO1*	YOR353C	*SOG2*	55222	*LRRC20*
YOR148C	*SPP2*	27238	*GPKOW*	YOR353C	*SOG2*	255252	*LRRC57*
YOR149C	*SMP3*	80235	*PIGZ*	YOR370C	*MRS6*	2664	*GDI1*
YOR157C	*PUP1*	5695	*PSMB7*	YOR370C	*MRS6*	2665	*GDI2*
YOR157C	*PUP1*	5699	*PSMB10*	YPL007C	*TFC8*	9329	*GTF3C4*
YOR159C	*SME1*	6635	*SNRPE*	YPL010W	*RET3*	22818	*COPZ1*
YOR168W	*GLN4*	5859	*QARS*	YPL020C	*ULP1*	29843	*SENP1*
YOR176W	*HEM15*	2235	*FECH*	YPL020C	*ULP1*	59343	*SENP2*
YOR181W	*LAS17*	8976	*WASL*	YPL020C	*ULP1*	205564	*SENP5*
YOR181W	*LAS17*	10810	*WASF3*	YPL028W	*ERG10*	38	*ACAT1*
YOR181W	*LAS17*	199720	*GGN*	YPL028W	*ERG10*	39	*ACAT2*
YOR194C	*TOA1*	2957	*GTF2A1*	YPL028W	*ERG10*	10449	*ACAA2*
YOR194C	*TOA1*	11036	*GTF2A1L*	YPL043W	*NOP4*	55131	*RBM28*

Yeast Systematic Name	Yeast Standard Name	Human Entrez Gene ID	Human Standard Name	Yeast Systematic Name	Yeast Standard Name	Human Entrez Gene ID	Human Standard Name
YOR206W	*NOC2*	26155	*NOC2L*	YPL063W	*TIM50*	92609	*TIMM50*
YPL082C	*MOT1*	50485	*SMARCAL1*	YPR034W	*ARP7*	10120	*ACTR1B*
YPL085W	*SEC16*	89866	*SEC16B*	YPR034W	*ARP7*	10121	*ACTR1A*
YPL093W	*NOG1*	23560	*GTPBP4*	YPR034W	*ARP7*	51412	*ACTL6B*
YPL117C	*IDI1*	3422	*IDI1*	YPR035W	*GLN1*	2752	*GLUL*
YPL117C	*IDI1*	91734	*IDI2*	YPR048W	*TAH18*	27158	*NDOR1*
YPL146C	*NOP53*	29997	*GLTSCR2*	YPR055W	*SEC8*	60412	*EXOC4*
YPL151C	*PRP46*	5356	*PLRG1*	YPR056W	*TFB4*	2967	*GTF2H3*
YPL151C	*PRP46*	6801	*STRN*	YPR082C	*DIB1*	10907	*TXNL4A*
YPL153C	*RAD53*	2872	*MKNK2*	YPR082C	*DIB1*	54957	*TXNL4B*
YPL153C	*RAD53*	5261	*PHKG2*	YPR085C	*ASA1*	54584	*GNB1L*
YPL160W	*CDC60*	51520	*LARS*	YPR086W	*SUA7*	2959	*GTF2B*
YPL169C	*MEX67*	10482	*NXF1*	YPR094W	*RDS3*	84844	*PHF5A*
YPL169C	*MEX67*	55998	*NXF5*	YPR103W	*PRE2*	5696	*PSMB8*
YPL169C	*MEX67*	56000	*NXF3*	YPR104C	*FHL1*	1112	*FOXN3*
YPL169C	*MEX67*	56001	*NXF2*	YPR104C	*FHL1*	2298	*FOXD4*
YPL175W	*SPT14*	5277	*PIGA*	YPR104C	*FHL1*	2299	*FOXI1*
YPL190C	*NAB3*	3183	*HNRNPC*	YPR104C	*FHL1*	2302	*FOXJ1*
YPL190C	*NAB3*	22913	*RALY*	YPR104C	*FHL1*	2305	*FOXM1*
YPL190C	*NAB3*	138046	*RALYL*	YPR104C	*FHL1*	2307	*FOXS1*
YPL190C	*NAB3*	196477	*CCER1*	YPR104C	*FHL1*	2309	*FOXO3*
YPL190C	*NAB3*	343069	*HNRNPCL1*	YPR104C	*FHL1*	3169	*FOXA1*
YPL204W	*HRR25*	1452	*CSNK1A1*	YPR104C	*FHL1*	3171	*FOXA3*
YPL204W	*HRR25*	1453	*CSNK1D*	YPR104C	*FHL1*	3344	*FOXN2*
YPL204W	*HRR25*	1454	*CSNK1E*	YPR104C	*FHL1*	27086	*FOXP1*
YPL204W	*HRR25*	1455	*CSNK1G2*	YPR104C	*FHL1*	50943	*FOXP3*
YPL204W	*HRR25*	1456	*CSNK1G3*	YPR104C	*FHL1*	93986	*FOXP2*
YPL204W	*HRR25*	53944	*CSNK1G1*	YPR104C	*FHL1*	116113	*FOXP4*
YPL204W	*HRR25*	122011	*CSNK1A1L*	YPR104C	*FHL1*	121643	*FOXN4*
YPL209C	*IPL1*	6795	*AURKC*	YPR104C	*FHL1*	139628	*FOXR2*
YPL209C	*IPL1*	9212	*AURKB*	YPR104C	*FHL1*	283150	*FOXR1*
YPL211W	*NIP7*	51388	*NIP7*	YPR104C	*FHL1*	653404	*FOXD4L6*
YPL217C	*BMS1*	9790	*BMS1*	YPR107C	*YTH1*	10898	*CPSF4*
YPL218W	*SAR1*	56681	*SAR1A*	YPR107C	*YTH1*	23144	*ZC3H3*
YPL231W	*FAS2*	2194	*FASN*	YPR107C	*YTH1*	642843	*CPSF4L*
YPL235W	*RVB2*	10856	*RUVBL2*	YPR110C	*RPC40*	9533	*POLR1C*
YPL242C	*IQG1*	128239	*IQGAP3*	YPR112C	*MRD1*	9904	*RBM19*
YPL243W	*SRP68*	6730	*SRP68*	YPR113W	*PIS1*	10423	*CDIPT*
YPL252C	*YAH1*	2230	*FDX1*	YPR133C	*SPN1*	3270	*HRC*
YPL252C	*YAH1*	112812	*FDX1L*	YPR133C	*SPN1*	55677	*IWS1*
YPL266W	*DIM1*	27292	*DIMT1*	YPR133C	*SPN1*	126637	*TCHHL1*
YPL266W	*DIM1*	51106	*TFB1M*	YPR161C	*SGV1*	1025	*CDK9*
YPR025C	*CCL1*	902	*CCNH*	YPR161C	*SGV1*	8621	*CDK13*
YPR033C	*HTS1*	23438	*HARS2*	YPR161C	*SGV1*	8814	*CDKL1*

Yeast Systematic Name	Yeast Standard Name	Human Entrez Gene ID	Human Standard Name		Yeast Systematic Name	Yeast Standard Name	Human Entrez Gene ID	Human Standard Name
YPR034W	*ARP7*	86	*ACTL6A*		YPR161C	*SGV1*	51265	*CDKL3*
YPR162C	*ORC4*	5000	*ORC4*					
YPR165W	*RHO1*	387	*RHOA*					
YPR165W	*RHO1*	389	*RHOC*					
YPR165W	*RHO1*	390	*RND3*					
YPR165W	*RHO1*	8153	*RND2*					
YPR165W	*RHO1*	27289	*RND1*					
YPR165W	*RHO1*	29984	*RHOD*					
YPR165W	*RHO1*	54509	*RHOF*					
YPR168W	*NUT2*	84246	*MED10*					
YPR169W	*JIP5*	54853	*WDR55*					
YPR175W	*DPB2*	5427	*POLE2*					
YPR176C	*BET2*	5876	*RABGGTB*					
YPR178W	*PRP4*	5048	*PAFAH1B1*					
YPR178W	*PRP4*	9128	*PRPF4*					
YPR178W	*PRP4*	9410	*SNRNP40*					
YPR178W	*PRP4*	10300	*KATNB1*					
YPR178W	*PRP4*	11091	*WDR5*					
YPR178W	*PRP4*	25886	*POC1A*					
YPR178W	*PRP4*	54554	*WDR5B*					
YPR178W	*PRP4*	282809	*POC1B*					
YPR182W	*SMX3*	6636	*SNRPF*					
YPR182W	*SMX3*	11157	*LSM6*					
YPR183W	*DPM1*	8813	*DPM1*					
YPR187W	*RPO26*	5435	*POLR2F*					

Table A.3. Comparing our compiled list of complementation pairs to literature sources

Yeast Systematic Name	Yeast Standard Name	Human Entrez Gene ID	Human Standard Name	Reported Complementation (Pubmed ID)[b]
YBR002C	*RER2*	79947	*DHDDS*	12591616 [CA], 14652022 [D]
YBR109C	*CMD1*	801	*CALM1*	12559573 [R], 7753022 [D], 1988945 [D]
		805	*CALM2*	12559573 [R]
YBR160W	*CDC28*	983	*CDK1*	1717994 [D,CA], 25541464 [D]
		1017	*CDK2*	1717994 [D,CA], 25541464 [D]
YBR252W	*DUT1*	1854	*DUT*	25999509 [D]
YCR012W	*PGK1*	5230	*PGK1*	21991399 [D]
YDL064W	*UBC9*	7329	*UBE2I*	25999509 [D,CA], 8668125 [CA]
YDL120W	*YFH1*	2395	*FXN*	11030757 [D], 15282205 [D]
YDL147W	*RPN5*	5718	*PSMD12*	25999509 [D,CA], 12559573 [R]
YDL164C	*CDC9*	3978	*LIG1*	25999509 [CA], 2204063 [CA]
YDL205C	*HEM3*	3145	*HMBS*	25999509 [D]
YDR050C	*TPI1*	7167	*TPI1*	25999509 [D,R], 24598263 [D]
YDR086C	*SSS1*	23480	*SEC61G*	25999509 [D]
YDR236C	*FMN1*	55312	*RFK*	25999509 [D]
YDR404C	*RPB7*	5436	*POLR2G*	25999509 [D], 7579693 [D]
YDR510W	*SMT3*	7341	*SUMO1*	25999509 [D,CA], 10364461 [D]
YEL026W	*SNU13*	4809	*NHP2L1*	25999509 [D]
YEL058W	*PCM1*	5238	*PGM3*	25999509 [D]
YER094C	*PUP3*	5691	*PSMB3*	25999509 [D]
YER112W	*LSM4*	25804	*LSM4*	25999509 [D]
YER133W	*GLC7*	5499	*PPP1CA*	12559573 [R], 17545157 [D]
		5501	*PPP1CC*	17545157 [D]
YFL017C	*GNA1*	64841	*GNPNAT1*	25999509 [D,CA]
YGL001C	*ERG26*	50814	*NSDHL*	25999509 [D,CA,R], 21129721 [D]
YGL030W	*RPL30*	6156	*RPL30*	25999509 [D]
YGL048C	*RPT6*	5705	*PSMC5*	25999509 [D,CA,R], 7870181 [CA,R]
YGR024C	*THG1*	54974	*THG1L*	25999509 [D]
YGR175C	*ERG1*	6713	*SQLE*	25999509 [D]
YGR185C	*TYS1*	8565	*YARS*	25999509 [D,CA], 9427763 [D]
YGR280C	*PXR1*	54984	*PINX1*	25999509 [D,R], 12107183 [D]
YIL083C	*CAB2*	79717	*PPCS*	25999509 [D]
YJL097W	*PHS1*	201562	*PTPLB*	18554506 [R]
YJR006W	*POL31*	5425	*POLD2*	25999509 [D]
YKL024C	*URA6*	51727	*CMPK1*	25999509 [CA]
YKL035W	*UGP1*	7360	*UGP2*	25999509 [D,R]
YKL145W	*RPT1*	5701	*PSMC2*	25999509 [D,CA]
YML069W	*POB3*	6749	*SSRP1*	25999509 [D,CA]
YML077W	*BET5*	58485	*TRAPPC1*	25999509 [D], 10582700 [D]
YMR208W	*ERG12*	4598	*MVK*	25999509 [D,R]
YMR308C	*PSE1*	3843	*IPO5*	10799599 [CA]
YMR314W	*PRE5*	5682	*PSMA1*	25999509 [D,R]

Yeast Systematic Name	Yeast Standard Name	Human Entrez Gene ID	Human Standard Name	Reported Complementation (Pubmed ID)[b]
YOL133W	*HRT1*	9978	*RBX1*	25999509 [D], 10213691 [D], 10385629 [D]
YOR143C	*THI80*	27010	*TPK1*	25999509 [D]
YOR149C	*SMP3*	80235	*PIGZ*	25999509 [D], 15208306 [D,CA]
YOR176W	*HEM15*	2235	*FECH*	25999509 [D]
YOR236W	*DFR1*	1719	*DHFR*	21991399 [D]
YPL117C	*IDI1*	3422	*IDI1*	25999509 [D]
YPR082C	*DIB1*	10907	*TXNL4A*	25999509 [D]
YPR113W	*PIS1*	10423	*CDIPT*	25999509 [D]
YBR026C	*ETR1* [a]	51102	*MECR*	12654921
YDR363W-A	*SEM1* [a]	7979	*SHFM1*	15117943, 20020775, 23620289
YGL058W	*RAD6* [a]	7320	*UBE2B*	19410543
YGR078C	*PAC10* [a]	7411	*VBP1*	9463374
YJL115W	*ASF1* [a]	55723	*ASF1B*	16151251
YKL113C	*RAD27* [a]	2237	*FEN1*	10545607, 16914748, 18443037, 9830061
YOR002W	*ALG6* [a]	29929	*ALG6*	10359825, 10914684, 10924277

[a] Nonessential yeast gene.

[b] Literature source reporting human complementation of essential yeast genes in the following yeast background: [D]=Deletion, [CA]=Conditional Allele, [R]=Repressible-promoter.

Table A.4. Nonessential yeast CIN genes and human homologs tested in complementation assays

Yeast systematic name	Yeast standard name	Human Entrez Gene ID	Human standard name	MMS[a]	BEN[a]	HU[a]	ETH[a]	BLEO[a]	CPT[a]	CYC[a]	ALF[a]	# OF ASSAYS
YAL016W	*TPD3*	5518	*PPP2R1A*	MMS (Y)		HU (Y)					ALF (Y)	3
YAL019W	*FUN30*	56916	*SMARCAD1*	MMS (N)		HU (N)						2
YAL021C	*CCR4*	57472	*CNOT6*		BEN (N)	HU (N)			CPT (N)	CYC (N)		4
YBL058W	*SHP1*	137886	*UBXN2B*		BEN (N)	HU (N)	ETH (N)			CYC (N)		4
YBR026C	*ETR1*	51102	*MECR*				ETH (Y)			CYC (Y)		2
YBR035C	*PDX3*	55163	*PNPO*			HU (N)	ETH (N)			CYC (N)		3
YBR073W	*RDH54*	25788	*RAD54B*	MMS (N)						CYC (N)	ALF (N)	3
YBR098W	*MMS4*	146956	*EME1*	MMS (N)		HU (N)						2
YBR282W	*MRPL27*	64975	*MRPL41*			HU (N)	ETH (N)					2
YCL016C	*DCC1*	79075	*DSCC1*	MMS (N)	BEN (N)	HU (N)			CPT (N)	CYC (N)	ALF (N)	6
YCL061C	*MRC1*	63967	*CLSPN*	MMS (N)		HU (N)		BLEO (N)		CYC (N)	ALF (N)	5
YCR065W	*HCM1*	2305	*FOXM1*		BEN (N)	HU (N)		BLEO (N)		CYC (N)		4
YCR094W	*CDC50*	55754	*TMEM30A*	MMS (N)				BLEO (N)		CYC (N)		3
YCR094W	*CDC50*	161291	*TMEM30B*	MMS (N)				BLEO (N)		CYC (N)		3
YDL074C	*BRE1*	9810	*RNF40*	MMS (N)		HU (N)		BLEO (N)		CYC (N)	ALF (N)	5
YDL101C	*DUN1*	8536	*CAMK1*	MMS (N)		HU (N)				CYC (N)	ALF (N)	4
YDL204W	*RTN2*	57142	*RTN4*				ETH (N)				ALF (N)	2
YDR004W	*RAD57*	5890	*RAD51B*	MMS (N)		HU (N)		BLEO (N)	CPT (N)			4
YDR014W	*RAD61*	23063	*WAPL*	MMS (N)						CYC (N)		2
YDR076W	*RAD55*	5892	*RAD51D*	MMS (N)		HU (N)		BLEO (N)	CPT (N)		ALF (N)	5
YDR176W	*NGG1*	10474	*TADA3*	MMS (N)			ETH (N)			CYC (N)		3
YDR200C	*VPS64*	283638	*CEP170B*							CYC (N)		1
YDR226W	*ADK1*	204	*AK2*				ETH (Y)					1
YDR289C	*RTT103*	55197	*RPRD1A*	MMS (N)		HU (N)						2
YDR289C	*RTT103*	58490	*RPRD1B*	MMS (N)		HU (N)				CYC (N)		3
YDR334W	*SWR1*	57634	*EP400*		BEN (N)	HU (N)		BLEO (N)		CYC (N)		4
YDR363W-A	*SEM1*	7979	*SHFM1*			HU (Y)	ETH (Y)				ALF (Y)	3
YDR386W	*MUS81*	80198	*MUS81*	MMS (N)		HU (N)						2
YEL003W	*GIM4*	5202	*PFDN2*		BEN (Y)		ETH (Y)					2
YEL029C	*BUD16*	8566	*PDXK*				ETH (Y)					1
YEL037C	*RAD23*	5887	*RAD23B*							CYC (N)		1
YEL050C	*RML2*	51069	*MRPL2*			HU (N)	ETH (N)					2
YEL061C	*CIN8*	11127	*KIF3A*		BEN (N)							1
YER016W	*BIM1*	22919	*MAPRE1*	MMS (N)	BEN (N)	HU (N)				CYC (N)	ALF (N)	5
YER095W	*RAD51*	5888	*RAD51*	MMS (N)		HU (N)		BLEO (N)	CPT (N)	CYC (N)	ALF (N)	6
YER161C	*SPT2*	144108	*SPTY2D1*								ALF (N)	1
YER162C	*RAD4*	7508	*XPC*	MMS (N)				BLEO (N)		CYC (N)		3
YER173W	*RAD24*	5884	*RAD17*	MMS (N)		HU (N)			CPT (N)		ALF (N)	4
YER177W	*BMH1*	7529	*YWHAB*			HU (N)	ETH (N)	BLEO (N)		CYC (N)		4
YFL016C	*MDJ1*	9093	*DNAJA3*				ETH (N)				ALF (N)	2
YGL003C	*CDH1*	51343	*FZR1*		BEN (N)		ETH (N)			CYC (N)		3
YGL003C	*CDH1*	991	*CDC20*		BEN (N)		ETH (N)			CYC (N)		3
YGL058W	*RAD6*	7320	*UBE2B*	MMS (Y)		HU (Y)		BLEO (Y)			ALF (Y)	4
YGL066W	*SGF73*	222255	*ATXN7L1*			HU (N)	ETH (N)			CYC (N)		3
YGL163C	*RAD54*	25788	*RAD54B*	MMS (N)		HU (N)		BLEO (N)	CPT (N)		ALF (N)	5
YGL173C	*XRN1*	22803	*XRN2*					BLEO (N)		CYC (N)		2
YGL240W	*DOC1*	10393	*ANAPC10*			HU (N)					ALF (N)	2
YGR027C	*RPS25A*	6230	*RPS25*				ETH (N)					1
YGR078C	*PAC10*	7411	*VBP1*				ETH (Y)			CYC (Y)	ALF (Y)	3
YGR171C	*MSM1*	92935	*MARS2*				ETH (N)				ALF (N)	2
YGR180C	*RNR4*	6241	*RRM2*	MMS (Y)		HU (Y)		BLEO (Y)				3
YGR188C	*BUB1*	701	*BUB1B*	MMS (N)	BEN (N)	HU (N)	ETH (N)			CYC (N)	ALF (N)	6
YHR031C	*RRM3*	80119	*PIF1*			HU (N)				CYC (N)	ALF (N)	3
YHR134W	*WSS1*	83932	*SPTN*			HU (N)					ALF (N)	2

Yeast systematic name	Yeast standard name	Human Entrez Gene ID	Human standard name	MMS[a]	BEN[a]	HU[a]	ETH[a]	BLEO[a]	CPT[a]	CYC[a]	ALF[a]	# OF ASSAYS
YHR191C	*CTF8*	54921	*CHTF8*	MMS (N)	BEN (N)	HU (N)			CPT (N)		ALF (N)	5
YHR206W	*SKN7*	3297	*HSF1*	MMS (N)		HU (N)		BLEO (N)				3
YIL018W	*RPL2B*	6132	*RPL8*							CYC (N)	ALF (N)	2
YIL052C	*RPL34B*	6164	*RPL34*				ETH (Y)					1
YIL084C	*SDS3*	64426	*SUDS3*							CYC (N)		1
YIL148W	*RPL40A*	7311	*UBA52*		BEN (N)							1
YIR002C	*MPH1*	57697	*FANCM*	MMS (N)								1
YIR004W	*DJP1*	84277	*DNAJC30*								ALF (N)	1
YJL030W	*MAD2*	4085	*MAD2L1*		BEN (N)							1
YJL102W	*MEF2*	84340	*GFM2*				ETH (N)					1
YJL115W	*ASF1*	25842	*ASF1A*	MMS (N)					CPT (N)		ALF (N)	3
YJL115W	*ASF1*	55723	*ASF1B*	MMS (Y)					CPT (Y)		ALF (Y)	3
YJL124C	*LSM1*	27257	*LSM1*	MMS (N)		HU (N)			CPT (N)	CYC (N)		4
YJL140W	*RPB4*	5433	*POLR2D*	MMS (Y)		HU (Y)						2
YJR005W	*APL1*	163	*AP2B1*							CYC (N)		1
YJR032W	*CPR7*	9360	*PPIG*							CYC (N)		1
YJR043C	*POL32*	10714	*POLD3*	MMS (N)		HU (N)	ETH (N)				ALF (N)	4
YJR063W	*RPA12*	30834	*ZNRD1*				ETH (N)			CYC (N)		2
YJR074W	*MOG1*	29098	*RANGRF*		BEN (N)	HU (N)	ETH (N)			CYC (N)		4
YKL006W	*RPL14A*	9045	*RPL14*				ETH (N)			CYC (N)		2
YKL113C	*RAD27*	2237	*FEN1*	MMS (Y)			ETH (Y)			CYC (Y)	ALF (Y)	4
YKR024C	*DBP7*	64794	*DDX31*	MMS (N)			ETH (N)			CYC (N)		3
YKR087C	*OMA1*	115209	*OMA1*								ALF (N)	1
YKR093W	*PTR2*	6564	*SLC15A1*							CYC (N)		1
YLL027W	*ISA1*	122961	*ISCA2*	MMS (N)			ETH (N)					2
YLR085C	*ARP6*	64431	*ACTR6*	MMS (N)	BEN (N)					CYC (N)		3
YLR154C	*RNH203*	84153	*RNASEH2C*								ALF (N)	1
YLR288C	*MEC3*	3364	*HUS1*	MMS (N)		HU (N)			CPT (N)		ALF (N)	4
YLR370C	*ARC18*	10094	*ARPC3*		BEN (N)					CYC (N)	ALF (N)	3
YLR418C	*CDC73*	79577	*CDC73*			HU (Y)						1
YLR429W	*CRN1*	84940	*CORO6*							CYC (N)		1
YLR429W	*CRN1*	11151	*CORO1A*							CYC (N)		1
YML028W	*TSA1*	10935	*PRDX3*	MMS (N)		HU (N)					ALF (N)	3
YML028W	*TSA1*	7001	*PRDX2*	MMS (N)		HU (N)					ALF (N)	3
YML062C	*MFT1*	80145	*THOC7*				ETH (N)			CYC (N)	ALF (N)	3
YML094W	*GIM5*	5204	*PFDN5*				ETH (Y)			CYC (Y)		2
YML095C	*RAD10*	2067	*ERCC1*	MMS (Y)		HU (Y)						2
YML102W	*CAC2*	8208	*CHAF1B*	MMS (N)								1
YML124C	*TUB3*	84790	*TUBA1C*		BEN (N)					CYC (N)		2
YML124C	*TUB3*	7846	*TUBA1A*		BEN (N)							1
YMR048W	*CSM3*	54962	*TIPIN*	MMS (N)		HU (N)		BLEO (N)	CPT (N)		ALF (N)	5
YMR138W	*CIN4*	402	*ARL2*		BEN (N)							1
YMR311C	*GLC8*	5504	*PPP1R2*				ETH (N)					1
YNL107W	*YAF9*	8089	*YEATS4*	MMS (N)	BEN (N)	HU (N)	ETH (N)					4
YNL136W	*EAF7*	55257	*MRGBP*	MMS (N)		HU (N)						2
YNL213C	*RRG9*	51335	*NGRN*								ALF (N)	1
YNR048W		55754	*TMEM30A*							CYC (N)		1
YNR048W		161291	*TMEM30B*							CYC (N)		1
YNR052C	*POP2*	29883	*CNOT7*	MMS (N)	BEN (N)	HU (N)	ETH (N)		CPT (N)	CYC (N)		6
YOL012C	*HTZ1*	3015	*H2AFZ*	MMS (Y)		HU (Y)	ETH (Y)					3
YOL115W	*PAP2*	11044	*PAPD7*	MMS (N)	BEN (N)	HU (N)	ETH (N)		CPT (N)	CYC (N)		6
YOR002W	*ALG6*	29929	*ALG6*				ETH (Y)					1
YOR014W	*RTS1*	5527	*PPP2R5C*	MMS (N)			ETH (N)	BLEO (N)		CYC (N)		4
YOR025W	*HST3*	23410	*SIRT3*	MMS (N)							ALF (N)	2
YOR026W	*BUB3*	9184	*BUB3*		BEN (N)			BLEO (N)			ALF (N)	3
YOR368W	*RAD17*	5810	*RAD1*	MMS (N)		HU (N)		BLEO (N)	CPT (N)		ALF (N)	5

Yeast systematic name	Yeast standard name	Human Entrez Gene ID	Human standard name	MMS[a]	BEN[a]	HU[a]	ETH[a]	BLEO[a]	CPT[a]	CYC[a]	ALF[a]	# OF ASSAYS
YPL008W	*CHL1*	1663	*DDX11*	MMS (N)		HU (N)					ALF (N)	3
YPL017C	*IRC15*	1738	*DLD*		BEN (N)							1
YPL022W	*RAD1*	2072	*ERCC4*	MMS (Y)		HU (Y)						2
YPL047W	*SGF11*	56970	*ATXN7L3*			HU (N)						1
YPL061W	*ALD6*	216	*ALDH1A1*				ETH (N)					1
YPL194W	*DDC1*	144715	*RAD9B*	MMS (N)		HU (N)			CPT (N)		ALF (N)	4
YPL213W	*LEA1*	6627	*SNRPA1*		BEN (N)					CYC (N)		2
YPL241C	*CIN2*	6903	*TBCC*		BEN (Y)							1
YPL268W	*PLC1*	84812	*PLCD4*		BEN (N)	HU (N)	ETH (N)			CYC (N)		4
YPL268W	*PLC1*	5336	*PLCG2*		BEN (N)	HU (N)	ETH (N)			CYC (N)		4
YPR067W	*ISA2*	122961	*ISCA2*				ETH (N)				ALF (N)	2

[a] For each assay, green and (Y) indicate that the human gene can complement the yeast deletion mutant in that assay, while red and (N) indicate that no complementation was observed. Assays include MMS: Methyl methanesulfonate; BEN: benomyl; HU: hydroxyurea; ETH: ethanol; BLEO: bleomycin; CPT: camptothecin; CYC: cycloheximide; ALF: a-like faker.

Table A.5. Select examples of essential yeast genes from the one-to-one screen that had multiple homologs tested for complementation

Yeast Systematic Name	Yeast Standard Name	Human Entrez Gene ID	Human Standard Name	Complementation	Sequence Identity[b]
YPR082C	*DIB1*	10907	*TXNL4A*	YES	64
YPR082C	*DIB1*	54957	*TXNL4B*	NO	34
YPL117C	*IDI1*	3422	*IDI1* [a]	YES	42
YPL117C	*IDI1*	91734	*IDI2*	NO	33
YDR510W	*SMT3*	7341	*SUMO1* [a]	YES	50
YDR510W	*SMT3*	6613	*SUMO2*	NO	44
YDR510W	*SMT3*	6612	*SUMO3*	NO	48
YDR510W	*SMT3*	387082	*SUMO4*	NO	39
YDR208W	*MSS4*	8394	*PIP5K1A* [a]	YES	23
YDR208W	*MSS4*	8395	*PIP5K1B*	YES	20
YDR208W	*MSS4*	138429	*PIP5KL1*	NO	15
YDR208W	*MSS4*	5305	*PIP4K2A*	NO	18
YDR208W	*MSS4*	8396	*PIP4K2B*	NO	19
YBR160W	*CDC28*	983	*CDK1*	YES	59
YBR160W	*CDC28*	1017	*CDK2* [a]	YES	62
YBR160W	*CDC28*	1019	*CDK4*	NO	14
YBR160W	*CDC28*	1021	*CDK6*	NO	46
YBR160W	*CDC28*	728642	*CDK11A*	NO	48
YBR109C	*CMD1*	801	*CALM1*	YES	61
YBR109C	*CMD1*	805	*CALM2*	YES	61
YBR109C	*CMD1*	808	*CALM3* [a]	YES	61
YBR109C	*CMD1*	164633	*CABP7*	NO	34
YBR109C	*CMD1*	51806	*CALML5*	NO	36
YBR109C	*CMD1*	57010	*CABP4*	NO	39
YBR109C	*CMD1*	7125	*TNNC2*	NO	43
YBR109C	*CMD1*	7134	*TNNC1*	NO	39
YBR109C	*CMD1*	810	*CALML3*	NO	58
YBR109C	*CMD1*	83698	*CALN1*	NO	36
YBR109C	*CMD1*	91860	*CALML4*	NO	39
YBR109C	*CMD1*	9478	*CABP1*	NO	33

[a] Identified by Yeastmine as the least diverged ortholog

[b] Sequence identity was determined using NWalign

Table A.6. Primers used for CRISPR-mediated insertion and deletion of 2-subunit yeast complexes

Guide sequences	
MMS4 guide sequence	CAACTATTTTGGGATCACAG
MUS81 guide sequence	AAAACGGTATTCGCTAACAG
RAD1 guide sequence	CTAATACCAGAAATGCGGGT
RAD10 guide sequence	GTCATCTGTAGCCTTTGAGT
Primers for amplifying humanizing donor DNA	
EME1 integration F	AAAGAACAATGTATGGATTATGGTATAGAATAATAGTAGTCACATATTGCAGCTAGTTAAATGGCTCTAAAGAAGTCATCAC
EME1 integration R	AGTGATTTTCAAAACGACTGCCTTAAGGTATGTTCTTATATACAAAGTTTCGTTCGATCATCAGTCAGCACTATCTAAAGAG
MUS81 integration F	ACATTGGCGTAAACAAAGTTTCAAAGGATTGATACGAACACACATTCCTAGCATGAAAGCATGGCGGCCCCGGTCCGCCTG
MUS81 integration R	AAAGAATATCATCACTTTTTTCTTTATAAAACCTTGCAGGGATGACTATATTTCAAATTGTCAGGTCAAGGGGCCGTAGCTGC
ERCC1 integration F	ACTTATGAGACAGCCACGCAACACAAAAAAGGGCATAAACAAAGTTGGTTATCCTAGAAGATGGACCCTGGGAAGGAC
ERCC1 -M13F integration R	AAAATGACAAAGGATGGTAATAAGCATGGAACAGATTTATTAAAAGAAAATAGGAATTGTGTAAAACGACGGCCAGT
ERCC4 integration F	GAGCATTTGCTAAATGTGTAAAAATAATATTGCACTATCCTGTTGAAAATATCTTTCCAGATGGAGTCAGGGCAGCCGGC
ERCC4 integration R	CTATAGTTAATCGCATTTTATACTGATGTTTTAACAGGGTTCGTTAAATTAAACAATATTTCACTTTTTCCCTTTTCCTTTTGATACGACTTC
Primers for donor DNAs to delete ORFs for creating double deletion strains	
MMS4 deletion F	GTATGGATTATGGTATAGAATAATAGTAGTCACATATTGCAGCTAGTTAATGATCGAACGAAACTTTGTATATAAGAACATACCTTAAGGCAGTCGTTTT
MMS4 deletion R (reverse complement of MMS4 deletion F)	AAAACGACTGCCTTAAGGTATGTTCTTATATACAAAGTTTCGTTCGATCATTAACTAGCTGCAATATGTGACTACTATTATTCTATACCATAATCCATAC
RAD10 deletion F	CAGCCACGCAACACAAAAAAGGGCATAAACAAAGTTGGTTATCCTAGAAGACAATTCCTATTTTCTTTTAATAAATCTGTTCCATGCTTATTACCATCCT
RAD10 deletion R (reverse complement of RAD10 deletion F)	AGGATGGTAATAAGCATGGAACAGATTTATTAAAAGAAAATAGGAATTGTCTTCTAGGATAACCAACTTTGTTTATGCCCTTTTTTGTGTTGCGTGGCTG

Table A.7. Primers for CRISPR-mediated editing of (hC)

Guide sequences	
h*SMC1A* guide sequence	GCTTACCAACTGGAGCACCG
h*SMC3* guide sequence	AGTTGTTCATAACGATACCG
h*RAD21* guide sequence	ATTGGTCTTCGTATTCCAAG
h*STAG2* guide sequence	CATGTGTCTGAACATTTCAG
Donor DNA	
h*SMC1A* deletion F	TAATTGTAGCTTATTTCCCGCCCTGTGATTGAGGCGGGATGGTGTCCCCAGACTAAGACTCTGGTCACGGTTCAGAAGTGGACGATGCATGTCGTCGGGC
h*SMC1A* deletion R	GCCCGACGACATGCATCGTCCACTTCTGAACCGTGACCAGAGTCTTAGTCTGGGGACACCATCCCGCCTCAATCACAGGGCGGGAAATAAGCTACAATTA
h*SMC3* deletion F	ACTCTGGTCACGGTTCAGAAGTGGACGATGCATGTCGTCGGGCTGATAGATGCACGGCGCTAGGTGTGATATCGTACACTTGGGAGAAGTCAGATACGAT
h*SMC3* deletion R	ATCGTATCTGACTTCTCCCAAGTGTACGATATCACACCTAGCGCCGTGCATCTATCAGCCCGACGACATGCATCGTCCACTTCTGAACCGTGACCAGAGT
h*RAD21* deletion F	CGCTAGGTGTGATATCGTACACTTGGGAGAAGTCAGATACGATTGCGGCTTAGCGGCGCCGGGAAATCCAGCATATTCTCGCGGCCCTGAGCAGTAGGTG
h*RAD21* deletion R	CACCTACTGCTCAGGGCCGCGAGAATATGCTGGATTTCCCGGCGCCGCTAAGCCGCAATCGTATCTGACTTCTCCCAAGTGTACGATATCACACCTAGCG
h*STAG2* deletion F	GCCGGGAAATCCAGCATATTCTCGCGGCCCTGAGCAGTAGGTGTCTCGGGGGAGGTACTGGCCTAGCGTCGTGGCCCGGGAGAGACAGTTTAGTAGTGAC
h*STAG2* deletion R	GTCACTACTAAACTGTCTCTCCCGGGCCACGACGCTAGGCCAGTACCTCCCCCGAGACACCTACTGCTCAGGGCCGCGAGAATATGCTGGATTTCCCGGC

Table A.8. Primers for CRISPR-mediated editing of (yCL3A)

Guide sequences	
Guide sequence targeting V17	GGTCCAGTGCCAAATATCGA
Guide sequence targeting V19	CTCTTCAGCAATGTTCGTGA
Donor DNA	
h*SMC1* -h*SMC3* deletion F	TCGCCCCGAGAACTGTAAACCTCAACATTTATAGATTATGCGGCCGCCATGTAATAGAATAGAGTCCGAGTCAGGACGAGAACTGTACATATGTATTTTC
h*SMC1* -h*SMC3* deletion R	GAAAATACATATGTACAGTTCTCGTCCTGACTCGGACTCTATTCTATTACATGGCGGCCGCATAATCTATAAATGTTGAGGTTTACAGTTCTCGGGGCGA

Table A.9. Primers used for creating the 9 gene cohesin deletion strain using CRISPR

Guide sequences (targeting the terminator, except for *SCC4* , which targeted the ORF)	
SMC1 guide sequence	TGACGGGTTATAGCAGAGGT
SMC3 guide sequence	AATTCCAATATAGGAGACAA
MCD1 guide sequence	GGTCCACCAAGAAATCCCCT
IRR1 guide sequence	CGAGTATAGTCTAATGCGAA
SCC2 guide sequence	ACCTGCGTGAAAAATCAGCA
SCC4 guide sequence	TGTTGCTAGAGTAGAACTCG
RAD61 guide sequence	AGCAGGGTGAAGATGAAGCC
PDS5 guide sequence	ACATATATACACACATACAT
ECO1 guide sequence	CTTTCGAAAAGACAGCGAGA
Primers for donor DNA to delete ORFs	
SMC1 deletion F	AAAATCACTTAAAGCAAGCATCCAGAGGCTATTGATAAAAAGCAGGCACA AGGAGACGCAAATAACTAATAATATCTATATAGGTCAACTAGCTAGTGC
SMC1 deletion R	GTCTTCCGTCTGCGGCATATAG
SMC3 deletion F	AGTTTCACCATTTTTTTACAAGACGACCTGCTGGAGTAACGGTAATAGTTC ACGTCTGCATTAAAAAATTTTCTTTTAAGATGATACTGTTACTAAAC
SMC3 deletion R	GAGAAGTCACAAACAAAAGCC
MCD1 deletion F	AAAGGACTGGTCAAAGAAAAGACAACTCAATTGCACAATTACTTTACAAG AAACACGACACAATAAGCTGATGCATATATAGATCAAAGAC
MCD1 deletion R	GATATCGTAAGACGTTCTAGGCGC
IRR1 deletion F	TAAACAAAAATAATAAAGAAAGGCGATTGACCTGAGAACAAGAGCTCGGA CGAAGGTAACCTGGATGATATTCGGCTATGTATTTTCC
IRR1 deletion R	GCGATTTCTTTTAGATAGTTTCCTTGG
SCC2 deletion F	TTTGTTGTGAGAGTATTGTTCTTATAACTATTCATTTTTTGAAAGAATTGGC GGCTAGCATTTGAGAAGCAACTATGAAATATTGAATTTCATTTAC
SCC2 deletion R	GAAAGCTCCTCGAATATCAACGC
SCC4 deletion F	GCTATCAGAGGGGAATCAGTATTGGTAGAAATTGAACGATTTCGAAAGAA GTACAAATTCACCAAAAAAAAAAAAAAGAAACACTTGATTTCCTTTATCTAT TTTTATACTTAATTATTTT
SCC4 deletion R	AAAATAATTAAGTATAAAAATAGATAAAGGAAATCAAGTGTTTCTTTTTTT TTTTTTGGTGAATTTGTACTTCTTTCGAAATCGTTCAATTTCTACCAATACT GATTCCCCTCTGATAGC
RAD61 deletion F	AGAGAAACTATCGCAAAACGAAACCATCTTCTTACCCTAAAGCATCCTGTT TCTGAAAAAGGCAACTATTGAAAAATTGTCCAG
RAD61 deletion R	CTTTCAGTTTTTTAAGCCCTTTCAACC
PDS5 deletion F	ATCCGGTCTCAATTTTTACAGGTATATTTGTAAAGAAGCAAGAAATAAAGT GCGAACAAAAAGGAAGGTGTTCACGTTCCTG
PDS5 deletion R	CGGGAACATTCAAATCATACCAAC
ECO1 deletion F	CATCAACATATATCTATGTTTACATATTAGGGTTCAACAGAATATAAATCG TTGCACAAAGACACTGGAAAAATGGCATAAAACTTTTC
ECO1 deletion R	GAAGTAATTCATTCAAGAGCTCAGC

Table A.10. Plasmids used in study

Plasmids used for screening tumor-specific variants in yeast	
(BPH#)	**Plasmid**
BPH1202	pAG416GPD-hLIG1-HA
BPH1203	pAG416GPD-hSSRP1-HA
BPH1204	pAG416GPD-hPPP1CA-HA
BPH1205	pAG416GPD-hPPP1CC-HA
BPH1206	pAG415GPD-hLIG1-HA
BPH1207	pAG415GPD-hSSRP1-HA
BPH1208	pAG415GPD-hPPP1CA-HA
BPH1209	pAG415GPD-hPPP1CC-HA
BPH1210	pAG415GPD-hLIG1(A60V)-HA
BPH1211	pAG415GPD-hLIG1(S141G)-HA
BPH1212	pAG415GPD-hLIG1(K152E)-HA
BPH1213	pAG415GPD-hLIG1(K152R)-HA
BPH1214	pAG415GPD-hLIG1(E153K)-HA
BPH1215	pAG415GPD-hLIG1(S163N)-HA
BPH1216	pAG415GPD-hLIG1(R222C)-HA
BPH1217	pAG415GPD-hLIG1(V349M)-HA
BPH1218	pAG415GPD-hLIG1(A374T)-HA
BPH1219	pAG415GPD-hLIG1(P395Q)-HA
BPH1220	pAG415GPD-hLIG1(M501T)-HA
BPH1221	pAG415GPD-hLIG1(S612L)-HA
BPH1222	pAG415GPD-hLIG1(L657V)-HA
BPH1223	pAG415GPD-hLIG1(A764T)-HA
BPH1224	pAG415GPD-hLIG1(E785K)-HA
BPH1225	pAG415GPD-hLIG1(V816M)-HA
BPH1226	pAG415GPD-hSSRP1(K33E)-HA
BPH1227	pAG415GPD-hSSRP1(A189V)-HA
BPH1228	pAG415GPD-hSSRP1(T209I)-HA
BPH1229	pAG415GPD-hSSRP1(K228E)-HA
BPH1230	pAG415GPD-hSSRP1(R324C)-HA
BPH1231	pAG415GPD-hSSRP1(R370C)-HA
BPH1232	pAG415GPD-hSSRP1(P436S)-HA
BPH1233	pAG415GPD-hSSRP1(S481P)-HA
BPH1234	pAG415GPD-hSSRP1(N498S)-HA
BPH1235	pAG415GPD-hSSRP1(T575A)-HA
BPH1236	pAG415GPD-hSSRP1(T575M)-HA
BPH1237	pAG415GPD-hSSRP1(K650N)-HA
BPH1238	pAG415GPD-hPPP1CA(R143H)-HA
BPH1239	pAG415GPD-hPPP1CA(Y272C)-HA
BPH1240	pAG415GPD-hPPP1CC(E116D)-HA
BPH1241	pAG415GPD-hPPP1CC(R187W)-HA
BPH1242	pAG415GPD-hPPP1CC(L201F)-HA
BPH1243	pAG415GPD-hPPP1CC(L204I)-HA
BPH1244	pAG415GPD-hPPP1CC(L289R)-HA

Plasmids used for screening tumor-specific variants in yeast	
TBA	pAG416GPD-hPPP2R1A+6Stop
TBA	pAG416GPD-hPPP2R1A(P179R)+6Stop
TBA	pAG416GPD-hPPP2R1A(P179L)+6Stop
TBA	pAG416GPD-hPPP2R1A(R182W)+6Stop
TBA	pAG416GPD-hPPP2R1A(R183W)+6Stop
TBA	pAG416GPD-hPPP2R1A(R183Q)+6Stop
TBA	pAG416GPD-hPPP2R1A(S256F)+6Stop
TBA	pAG416GPD-hPPP2R1A(S256Y)+6Stop
TBA	pAG416GPD-hPPP2R1A(W257G)+6Stop
TBA	pAG416GPD-hPPP2R1A(R258C)+6Stop
TBA	pAG416GPD-hPPP2R1A(R258H)+6Stop
TBA	pAG416GPD-yTPD3+6Stop
TBA	pAG416GPD-yTPD3(P207R)+6Stop
TBA	pAG416GPD-yTPD3(P20L)+6Stop
TBA	pAG416GPD-yTPD3(R211W)+6Stop
TBA	pAG416GPD-yTPD3(R211Q)+6Stop
TBA	pAG416GPD-yTPD3(W294G)+6Stop
TBA	pAG416GPD-yTPD3(R295C)+6Stop
TBA	pAG416GPD-yTPD3(R295H)+6Stop
Plasmids used for SDL screens	
(BPH#)	**Plasmid**
BPH1342	pAG425GAL-yRAD27+6Stop
BPH1343	pAG425GAL-yRAD27(D179A)+6Stop
BPH1344	pAG425GAL-hFEN1+6Stop
BPH1345	pAG425GAL-hFEN1(D181A)+6Stop
BPH1346	pAG425GAL-hFEN1(E158A)+6Stop
BPH1347	pAG425GAL-hFEN1(D181A/E158A)+6Stop

Table A.11. Tumor-specific variants tested in a yeast wild-type background

	Amino Acid Mutation	Relative Fitness (AUC) No Drug
h*LIG1*	A60V	0.95 ± 0.04
	S141G	1.02 ± 0.03
	K152E	1.07 ± 0.05
	K152R	1.05 ± 0.06
	E153K	1.01 ± 0.02
	S163N	1.05 ± 0.09
	R222C	1.00 ± 0.03
	V349M	0.99 ± 0.05
	A374T	1.08 ± 0.07
	P395Q	1.05 ± 0.05
	M501T	1.01 ± 0.08
	S612L	1.09 ± 0.04
	L657V	0.99 ± 0.05
	A764T	1.04 ± 0.05
	E785K	1.02 ± 0.05
	V816M	1.06 ± 0.03
h*SSRP1*	K33E	0.98 ± 0.06
	A189V	1.04 ± 0.04
	T209I	1.00 ± 0.09
	K228E	0.82 ± 0.03*
	R324C	0.89 ± 0.04
	R370C	1.01 ± 0.05
	P436S	0.99 ± 0.05
	S481P	0.92 ± 0.09
	N498S	0.99 ± 0.09
	T575A	0.98 ± 0.02
	T575M	0.97 ± 0.06
	K650N	1.05 ± 0.06
h*PPP1CA*	R143H	0.97 ± 0.01
	Y272C	0.94 ± 0.04
h*PPP1CC*	E116D	0.94 ± 0.02
	R187W	1.04 ± 0.03
	L201F	1.02 ± 0.01
	L204I	0.99 ± 0.04
	L289R	1.01 ± 0.07

Strain fitness for each allele is expressed as a ratio relative to the yeast strain expressing the corresponding wild-type allele grown in the same plate in the same media condition. Significance was calculated compared to the corresponding wild-type allele grown in the same plate to assess impact of missense mutation on strain fitness. Corresponding growth curves can be found in Supplementary Figure S1 of PMID: 26354769. Student's t-test *$p<0.01$.

Table A.12. Tumor-specific variants tested in a yeast deletion background

	Amino Acid Mutation	Zygosity	Relative Fitness (AUC) No Drug	Relative Fitness (AUC) 0.01% MMS	Relative Fitness (AUC) 100mM HU
h*LIG1*	A60V	Unknown	0.56 ± 0.06***	0.50 ± 0.05	0.38 ± 0.03*
	S141G	Heterozygous	0.45 ± 0.03***	0.50 ± 0.07	0.25 ± 0.05*
	K152E	Heterozygous	0.52 ± 0.06***	0.98 ± 0.06***	0.46 ± 0.03
	K152R	Heterozygous	0.50 ± 0.05***	0.50 ± 0.06	0.23 ± 0.01***
	E153K	Heterozygous	0.60 ± 0.12***	0.44 ± 0.06	0.30 ± 0.07**
	S163N	Unknown	0.60 ± 0.12***	0.49 ± 0.05	0.23 ± 0.06***
	R222C	Heterozygous	0.35 ± 0.01***	0.23 ± 0.01***	0.21 ± 0.02***
	V349M	Unknown	0.47 ± 0.03***	0.59 ± 0.04*	0.29 ± 0.05*
	A374T	Unknown	0.71 ± 0.03***	0.71 ± 0.06	0.51 ± 0.06**
	P395Q	Unknown	0.63 ± 0.05***	0.48 ± 0.04**	0.44 ± 0.04*
	M501T	Unknown	0.61 ± 0.06***	0.34 ± 0.01***	0.46 ± 0.03*
	S612L	Heterozygous	0.49 ± 0.04***	0.33 ± 0.02***	0.42 ± 0.04
	L657V	Heterozygous	0.71 ± 0.08***	0.70 ± 0.10	0.44 ± 0.04**
	A764T	Unknown	0.73 ± 0.09***	0.30 ± 0.02***	0.61 ± 0.04
	E785K	Unknown	0.59 ± 0.07***	0.52 ± 0.05	0.56 ± 0.09
	V816M	Unknown	0.70 ± 0.06***	0.36 ± 0.01***	0.47 ± 0.04*
h*SSRP1*	K33E	Heterozygous	1.02 ± 0.12	0.70 ± 0.08	0.95 ± 0.12
	A189V	Heterozygous	0.69 ± 0.11**	0.35 ± 0.03	0.79 ± 0.05
	T209I	Unknown	1.09 ± 0.14	0.68 ± 0.07*	1.00 ± 0.12
	K228E	Heterozygous	Nonfunctional	n/d	n/d
	R324C	Heterozygous	1.00 ± 0.06	0.80 ± 0.18	0.97 ± 0.10
	R370C	Heterozygous	1.05 ± 0.11	0.67 ± 0.06*	0.97 ± 0.17
	P436S	Heterozygous	0.94 ± 0.05	0.81 ± 0.10	1.01 ± 0.11
	S481P	Unknown	Nonfunctional	n/d	n/d
	N498S	Heterozygous	1.05 ± 0.06	0.70 ± 0.04*	1.08 ± 0.08
	T575A	Heterozygous	1.02 ± 0.06	0.76 ± 0.04*	1.22 ± 0.13
	T575M	Unknown	1.02 ± 0.05	0.78 ± 0.08*	1.07 ± 0.10
	K650N	Unknown	1.07 ± 0.16	0.82 ± 0.03	1.22 ± 0.03
h*PPP1CA*	R143H	Heterozygous	0.69 ± 0.08	0.72 ± 0.09	0.67 ± 0.03
	Y272C	Heterozygous	Nonfunctional	n/d	n/d
h*PPP1CC*	E116D	Unknown	0.57 ± 0.11**	0.24 ± 0.03*	0.33 ± 0.01*
	R187W	Unknown	0.05 ± 0.01***	0.05 ± 0.01	0.02 ± 0.01*
	L201F	Heterozygous	1.48 ± 0.18*	1.09 ± 0.24	1.10 ± 0.11
	L204I	Unknown	0.97 ± 0.10	0.89 ± 0.22	1.07 ± 0.14
	L289R	Heterozygous	Nonfunctional	n/d	n/d

Strain fitness for each allele is expressed as a ratio relative to the yeast strain expressing the wild-type allele grown in the same plate in the same media condition. For “no drug” condition, significance was calculated compared to the wild-type allele grown in the same plate to assess impact of missense mutation on strain fitness. For “drug” condition, significance was calculated compared to the same allele in the no drug condition grown in the same plate to assess impact of drug on strain fitness. Alleles were defined as nonfunctional based on inability to complement the corresponding deletion mutant yeast strain. Strain fitness values that were not determined are indicated (n/d). Corresponding growth curves can be found in Supplementary Figures S2, S3 and S4 of PMID: 26354769. Student’s t-test *$p < 0.01$, **$p < 0.001$, ***$p < 0.0001$.

Table A.13. Results of the SDL screen for hFEN1

Yeast systematic name	Yeast standard name	Vector Set 1	Vector Set 2	Vector Set 3	Vector Avg.	hFEN1 Set 1	hFEN1 Set 2	hFEN1 Set 3	hFEN1 Avg.	T-test	E-C[a]	GC Validations[b]
YNR023W	*SNF12*	0.2397	1.1313	1.1669	0.8460	0.2718	0.2880	0.3702	0.3100	0.1535541	-0.5360	No interaction
YDR079C-A	*TFB5*	1.0247	1.0233	1.0778	1.0419	0.6824	0.2179	0.7119	0.5374	0.0350470	-0.5045	No interaction
YIL128W	*MET18*	1.1763	0.9612	0.7669	0.9681	0.5153	0.4099	0.5211	0.4821	0.0170907	-0.4860	No interaction
YGR171C	*MSM1*	0.1907	0.3449	1.2083	0.5813	0.0000	0.0233	0.3531	0.1255	0.2470289	-0.4559	No interaction
YGL173C	*KEM1*	1.0026	1.0417	0.9306	0.9916	0.5861	0.6227	0.6635	0.6241	0.0007394	-0.3675	No interaction
YNL025C	*SSN8*	1.0393	1.0233	1.0695	1.0440	0.0736	1.1130	0.9482	0.7116	0.3613371	-0.3324	No interaction
YNL252C	*MRPL17*	0.6236	0.1656	0.2073	0.3321	0.0000	0.0623	0.0740	0.0454	0.1248093	-0.2867	No interaction
YHL025W	*SNF6*	0.5258	0.9704	0.7669	0.7543	0.4587	0.4774	0.4698	0.4686	0.0904760	-0.2857	No interaction
YJL006C	*CTK2*	0.4989	0.6025	1.2767	0.7927	0.4899	0.5267	0.5553	0.5239	0.3335568	-0.2688	No interaction
YKL139W	*CTK1*	0.5233	1.1107	0.9866	0.8735	0.5465	0.7394	0.5467	0.6109	0.2388931	-0.2626	No interaction
YPL042C	*SSN3*	1.0124	1.0325	0.9866	1.0105	0.0595	1.1649	1.0593	0.7612	0.5184387	-0.2493	No interaction
YOR026W	*BUB3*	0.9855	0.6967	1.0757	0.9193	0.7164	0.7316	0.5752	0.6744	0.1209292	-0.2449	No interaction
YGL115W	*SNF4*	0.9904	0.9175	0.8104	0.9061	0.6484	0.6875	0.6749	0.6703	0.0116423	-0.2358	No interaction
YNL330C	*RPD3*	0.5135	0.5703	0.8270	0.6369	0.4247	0.3892	0.4812	0.4317	0.1096198	-0.2052	No interaction
YJR074W	*MOG1*	0.9219	0.9382	0.9493	0.9365	0.7164	0.7057	0.7774	0.7332	0.0010136	-0.2033	No interaction
YOL072W	*THP1*	1.1298	1.0624	1.1607	1.1176	0.6626	0.9470	1.1419	0.9171	0.2312768	-0.2005	No interaction
YKL057C	*NUP120*	1.0638	1.0164	1.0322	1.0374	0.7504	0.8354	0.9255	0.8371	0.0187595	-0.2004	No interaction
YNL250W	*RAD50*	0.7825	0.7519	0.7254	0.7533	0.5295	0.5760	0.5809	0.5621	0.0011921	-0.1912	No interaction
YOL004W	*SIN3*	0.5307	0.5358	0.8581	0.6415	0.4304	0.3944	0.5496	0.4581	0.1951432	-0.1834	No interaction
YGR180C	*RNR4*	0.9195	1.1612	0.8394	0.9734	0.7475	0.8302	0.7973	0.7917	0.1423965	-0.1817	No interaction
YMR167W	*MLH1*	0.8926	1.0164	0.7669	0.8919	0.7079	0.8328	0.6265	0.7224	0.1447761	-0.1696	No interaction
YDR369C	*XRS2*	0.7850	0.7680	0.6425	0.7318	0.5663	0.6797	0.4471	0.5644	0.1069634	-0.1675	No interaction
YNL021W	*HDA1*	0.6187	0.7082	0.9990	0.7753	0.5465	0.6823	0.6008	0.6099	0.2446268	-0.1654	No interaction
YEL003W	*GIM4*	0.9464	0.9796	0.9348	0.9536	0.8325	0.7809	0.7546	0.7893	0.0034580	-0.1642	No interaction
YIL153W	*RRD1*	0.6603	0.6071	0.8083	0.6919	0.5465	0.5474	0.4983	0.5307	0.0610548	-0.1611	No interaction
YNL136W	*EAF7*	0.7679	0.8531	0.9493	0.8567	0.7107	0.7342	0.6492	0.6981	0.0526249	-0.1587	No interaction
YMR224C	*MRE11*	0.7679	0.7174	0.7710	0.7521	0.5918	0.5760	0.6435	0.6038	0.0052007	-0.1483	No interaction
YHR115C	*DMA1*	0.9880	0.9819	1.0177	0.9958	0.8297	0.8380	0.8799	0.8492	0.0015384	-0.1467	No interaction
YGL066W	*SGF73*	0.8486	0.9152	0.8560	0.8733	0.7022	0.6979	0.7945	0.7315	0.0201220	-0.1417	No interaction
YEL061C	*CIN8*	0.9611	0.9819	0.9845	0.9758	0.9033	0.7991	0.8030	0.8351	0.0157025	-0.1407	No interaction
YLR085C	*ARP6*	1.0760	1.1405	1.1234	1.1133	0.8919	1.0144	1.0194	0.9753	0.0397382	-0.1380	
YBR089C-A	*NHP6B*	0.8804	0.8876	1.0156	0.9279	0.7900	0.8458	0.7461	0.7940	0.0634331	-0.1339	
YCR065W	*HCM1*	0.9366	0.9566	0.9783	0.9572	0.8183	0.8198	0.8372	0.8251	0.0006062	-0.1320	
YKR092C	*SRP40*	0.9244	0.8462	0.9907	0.9204	0.7362	0.8536	0.7774	0.7891	0.0720641	-0.1314	
YGR285C	*ZUO1*	0.5184	0.4001	0.6259	0.5148	0.3115	0.4696	0.3759	0.3856	0.1805927	-0.1292	No interaction
YNL031C	*HHT2*	0.9073	0.9589	0.9886	0.9516	0.8721	0.8354	0.7631	0.8236	0.0325565	-0.1280	
YPR023C	*EAF3*	0.7850	0.8117	0.9700	0.8556	0.7702	0.6875	0.7261	0.7279	0.1105877	-0.1276	
YDR279W	*RNH202*	0.9073	0.8922	0.9472	0.9156	0.8183	0.8276	0.7318	0.7926	0.0237955	-0.1230	
YDL059C	*RAD59*	0.8901	0.8577	0.8705	0.8728	0.7532	0.7135	0.7888	0.7518	0.0069679	-0.1210	
YMR078C	*CTF18*	1.0173	1.0601	0.9824	1.0199	0.9288	0.9340	0.8400	0.9009	0.0347427	-0.1190	
YER142C	*MAG1*	0.9513	0.9405	0.9824	0.9581	0.8268	0.8769	0.8172	0.8403	0.0062407	-0.1177	
YPR164W	*MMS1*	0.8143	0.7565	0.7544	0.7751	0.6654	0.6564	0.6606	0.6608	0.0044732	-0.1143	
YLR233C	*EST1*	0.9782	0.9152	0.9078	0.9337	0.7957	0.7965	0.8685	0.8202	0.0260133	-0.1135	
YLL039C	*UBI4*	0.9709	0.9681	0.9824	0.9738	0.8665	0.8224	0.8941	0.8610	0.0061416	-0.1128	
YBR278W	*DPB3*	0.8999	0.9497	1.0197	0.9565	0.8636	0.8484	0.8201	0.8440	0.0385153	-0.1124	
YNL068C	*FKH2*	0.7752	0.8485	0.7793	0.8010	0.7730	0.6538	0.6435	0.6901	0.0814877	-0.1109	
YER162C	*RAD4*	1.0295	0.9382	1.0591	1.0089	0.7051	1.0196	0.9767	0.9005	0.3598450	-0.1085	
YNL273W	*TOF1*	1.0198	0.8531	0.8415	0.9048	0.7277	0.9158	0.7518	0.7984	0.2669740	-0.1064	
YML032C	*RAD52*	0.5649	0.6232	0.5783	0.5888	0.4417	0.5345	0.4784	0.4849	0.0320867	-0.1039	No interaction

Yeast systematic name	Yeast standard name	Vector Set 1	Vector Set 2	Vector Set 3	Vector Avg.	hFEN1 Set 1	hFEN1 Set 2	hFEN1 Set 3	hFEN1 Avg.	T-test	E-C[a]	GC Validations[b]
YDR359C	*EAF1*	1.0467	0.9934	1.0197	1.0199	0.8835	0.9496	0.9169	0.9166	0.0135482	-0.1033	
YER116C	*SLX8*	0.9122	0.9014	0.9223	0.9120	0.7815	0.8380	0.8087	0.8094	0.0041387	-0.1026	
YJR082C	*EAF6*	0.8730	0.8554	0.8187	0.8490	0.7843	0.7135	0.7489	0.7489	0.0182313	-0.1001	
YBR073W	*RDH54*	0.9244	0.9796	0.9741	0.9594	0.8183	0.9055	0.8571	0.8603	0.0321249	-0.0991	
YPL183W-A	*RTC6*	0.5845	0.6485	0.6819	0.6383	0.5663	0.4852	0.5667	0.5394	0.0660312	-0.0989	
YGL094C	*PAN2*	1.0589	0.9980	1.0570	1.0380	0.9004	0.9236	0.9938	0.9393	0.0457673	-0.0987	
YMR080C	*NAM7*	1.0418	0.9014	0.9140	0.9524	0.8297	0.8925	0.8400	0.8541	0.1144923	-0.0983	
YNL072W	*RNH201*	1.0247	1.0463	0.9969	1.0226	0.9599	0.9314	0.8913	0.9275	0.0178144	-0.0951	
YBR245C	*ISW1*	0.8950	0.8830	0.9306	0.9029	0.7815	0.7991	0.8486	0.8097	0.0194246	-0.0932	
YLR176C	*RFX1*	0.9122	0.8876	0.8954	0.8984	0.7815	0.8588	0.7802	0.8068	0.0273812	-0.0915	
YJL013C	*MAD3*	0.9709	1.0141	0.9161	0.9670	0.8495	0.7939	0.9881	0.8772	0.2349890	-0.0899	
YLL002W	*RTT109*	0.7654	0.8577	0.8456	0.8229	0.6937	0.7420	0.7745	0.7368	0.0818862	-0.0862	No interaction
YLR032W	*RAD5*	0.8632	0.7358	0.7586	0.7859	0.6909	0.6746	0.7347	0.7000	0.1174725	-0.0858	
YPL241C	*CIN2*	0.8608	0.9428	0.9783	0.9273	0.8070	0.8380	0.8884	0.8445	0.1206385	-0.0828	
YER173W	*RAD24*	0.8290	0.9014	0.8270	0.8525	0.7702	0.7835	0.7574	0.7704	0.0327324	-0.0821	
YGR270W	*YTA7*	1.1323	1.0900	0.8332	1.0185	0.9457	0.9158	0.9482	0.9366	0.4330378	-0.0819	
YGR184C	*UBR1*	0.9268	0.9842	0.9783	0.9631	0.8665	0.7731	1.0052	0.8816	0.3079715	-0.0815	
YER179W	*DMC1*	0.8437	0.8393	0.8104	0.8311	0.7107	0.7316	0.8087	0.7504	0.0627229	-0.0808	
YMR284W	*YKU70*	1.0124	1.0049	1.0736	1.0303	0.9373	0.8743	1.0394	0.9503	0.2042033	-0.0800	
YAL021C	*CCR4*	0.7190	0.6600	0.7607	0.7132	0.6456	0.6097	0.6492	0.6348	0.0695405	-0.0783	
YGR276C	*RNH70*	0.9660	0.9589	0.9783	0.9677	0.7787	0.8588	1.0365	0.8913	0.3739284	-0.0764	
YDR363W-A	*SEM1*	0.6236	0.5657	0.5783	0.5892	0.4899	0.5319	0.5211	0.5143	0.0257599	-0.0749	
YAR002W	*NUP60*	0.9562	1.0164	0.9700	0.9808	0.9118	0.8043	1.0052	0.9071	0.2919702	-0.0738	
YKL017C	*HCS1*	1.0491	0.9842	1.0342	1.0225	0.9911	0.8821	0.9739	0.9490	0.1333405	-0.0735	
YLR394W	*CST9*	0.7630	0.7450	0.8456	0.7845	0.7390	0.7057	0.6891	0.7113	0.0993806	-0.0733	
YNL116W	*DMA2*	0.9170	0.9198	1.0467	0.9612	0.9231	0.9548	0.7859	0.8879	0.3368260	-0.0733	
YDR176W	*NGG1*	0.2470	0.2368	0.2425	0.2421	0.0793	0.2101	0.2193	0.1696	0.1846186	-0.0725	
YGR271W	*SLH1*	0.9709	0.9911	0.9990	0.9870	0.8891	0.9833	0.8742	0.9155	0.1120011	-0.0714	
YML095C	*RAD10*	0.8828	0.8922	0.9410	0.9053	0.8240	0.9003	0.7802	0.8348	0.1483464	-0.0705	No interaction
YER176W	*ECM32*	0.8975	0.9175	0.9368	0.9173	0.8042	0.9989	0.7404	0.8478	0.4265245	-0.0695	
YDR523C	*SPS1*	1.0222	1.0831	1.0487	1.0513	0.9231	0.9833	1.0394	0.9819	0.1410089	-0.0694	
YLR240W	*VPS34*	0.8901	0.8508	0.8767	0.8726	0.8495	0.8484	0.7147	0.8042	0.2130273	-0.0684	No interaction
YDR440W	*DOT1*	0.8975	0.8853	0.9348	0.9058	0.8381	0.9599	0.7147	0.8376	0.3988833	-0.0682	
YJR035W	*RAD26*	0.9831	1.0440	0.9472	0.9914	0.9882	0.8769	0.9055	0.9236	0.1955912	-0.0679	
YIL009C-A	*EST3*	0.9635	0.9842	0.9576	0.9684	0.8608	0.9366	0.9084	0.9019	0.0476017	-0.0665	
YMR234W	*RNH1*	0.9024	0.9014	0.8974	0.9004	0.8013	0.7991	0.9027	0.8344	0.1256003	-0.0660	
YGR063C	*SPT4*	1.1274	1.0624	1.1109	1.1002	1.1383	0.9003	1.0650	1.0345	0.4192003	-0.0657	
YPR120C	*CLB5*	0.8999	0.9796	0.9348	0.9381	0.8013	0.8276	0.9909	0.8733	0.3661804	-0.0648	
YKL190W	*CNB1*	0.9611	0.8669	0.8933	0.9071	0.8183	0.8614	0.8486	0.8427	0.1050120	-0.0643	
YHR191C	*CTF8*	0.8828	0.8922	0.8788	0.8846	0.8410	0.7861	0.8343	0.8205	0.0224484	-0.0641	
YDR386W	*MUS81*	0.8632	0.8554	0.7814	0.8333	0.8693	0.7705	0.6692	0.7697	0.3719560	-0.0637	No interaction
YKL210W	*UBA1*	0.9733	1.0164	0.9617	0.9838	0.9542	0.9677	0.8400	0.9207	0.2228718	-0.0631	
YDR263C	*DIN7*	0.9635	0.9566	0.9886	0.9696	0.8693	0.9262	0.9255	0.9070	0.0419484	-0.0626	
YIR002C	*MPH1*	0.8119	0.7749	0.8518	0.8129	0.7532	0.8017	0.6976	0.7508	0.1721966	-0.0620	
YLR107W	*REX3*	0.9782	0.9980	1.0695	1.0152	0.8806	1.0144	0.9653	0.9535	0.2669219	-0.0618	
YFL003C	*MSH4*	1.0907	1.1084	1.0819	1.0936	0.9995	1.0741	1.0223	1.0320	0.0577783	-0.0617	
YPL022W	*RAD1*	0.8877	0.8761	0.8767	0.8802	0.7645	0.7628	0.9283	0.8185	0.3252233	-0.0616	No interaction
YBR186W	*PCH2*	0.9513	0.9221	0.9306	0.9347	0.8353	0.8328	0.9511	0.8731	0.1981069	-0.0616	
YLR318W	*EST2*	0.9537	0.9842	0.9430	0.9603	0.8410	0.9573	0.8998	0.8994	0.1637892	-0.0609	
YGL043W	*DST1*	0.6627	0.6760	0.6632	0.6673	0.5267	0.6901	0.6037	0.6068	0.2708976	-0.0605	
YHR200W	*RPN10*	0.6725	0.6692	0.6259	0.6559	0.5635	0.5734	0.6492	0.5954	0.1224063	-0.0605	

Yeast systematic name	Yeast standard name	Vector Set 1	Vector Set 2	Vector Set 3	Vector Avg.	hFEN1 Set 1	hFEN1 Set 2	hFEN1 Set 3	hFEN1 Avg.	T-test	E-C[a]	GC Validations[b]
YDR217C	*RAD9*	0.8706	0.8899	0.8933	0.8846	0.7843	0.8172	0.8713	0.8243	0.0839083	-0.0603	
YMR186W	*HSC82*	0.9660	0.8462	0.9140	0.9087	0.7759	0.9158	0.8543	0.8487	0.3228276	-0.0601	
YBR195C	*MSI1*	0.8510	0.9428	0.8705	0.8881	0.7447	0.8873	0.8571	0.8297	0.3208822	-0.0584	
YBR034C	*HMT1*	0.7997	0.8278	0.8643	0.8306	0.7249	0.8562	0.7375	0.7729	0.2760449	-0.0577	
YDL154W	*MSH5*	0.9415	0.9451	0.9824	0.9563	0.8551	0.9496	0.8941	0.8996	0.1350583	-0.0567	
YJL187C	*SWE1*	0.9170	0.8968	0.9223	0.9121	0.7985	0.8328	0.9368	0.8561	0.2562270	-0.0560	
YGL070C	*RPB9*	0.7948	0.7772	0.6881	0.7534	0.6937	0.7446	0.6578	0.6987	0.2584463	-0.0547	
YDL082W	*RPL13A*	0.8681	0.8922	0.8373	0.8659	0.7985	0.8717	0.7717	0.8140	0.1998787	-0.0519	
YER095W	*RAD51*	0.6040	0.6485	0.6674	0.6400	0.5918	0.6201	0.5553	0.5890	0.1275287	-0.0509	No interaction
YOL012C	*HTZ1*	0.9635	0.8623	0.8539	0.8932	0.8466	0.9003	0.7831	0.8433	0.3647178	-0.0499	
YOR156C	*NFI1*	0.9317	0.9313	0.8705	0.9112	0.8721	0.8562	0.8600	0.8627	0.0813894	-0.0484	
YKL203C	*TOR2*	0.9342	0.9359	0.9182	0.9294	0.8665	0.8302	0.9482	0.8816	0.2479910	-0.0478	
YMR201C	*RAD14*	1.0467	1.0141	0.9057	0.9888	0.9401	1.0015	0.8884	0.9433	0.4443825	-0.0455	
YOR144C	*ELG1*	0.8094	0.8324	0.7814	0.8077	0.7730	0.7109	0.8030	0.7623	0.2151242	-0.0454	
YHL022C	*SPO11*	0.8168	0.8485	0.7731	0.8128	0.7305	0.8380	0.7347	0.7677	0.3376066	-0.0451	
YPL024W	*RMI1*	0.7752	0.8071	0.8000	0.7941	0.7674	0.7965	0.6834	0.7491	0.2705215	-0.0450	
YDR225W	*HTA1*	0.7654	0.7864	0.7814	0.7777	0.8070	0.6746	0.7176	0.7330	0.3212170	-0.0447	
YJL065C	*DLS1*	0.8926	0.8324	0.8394	0.8548	0.7447	0.9859	0.7090	0.8132	0.6645557	-0.0416	
YOR073W	*SGO1*	0.9904	1.0325	1.0591	1.0273	0.9514	1.0378	0.9682	0.9858	0.2783700	-0.0415	
YKR028W	*SAP190*	0.8901	0.8922	0.8705	0.8843	0.8155	0.7913	0.9283	0.8450	0.4107604	-0.0393	
YOL054W	*PSH1*	0.9293	0.9658	0.8788	0.9246	0.9514	0.9055	0.8030	0.8866	0.4944771	-0.0380	
YNL107W	*YAF9*	1.1861	1.0670	1.1026	1.1185	1.0987	1.1052	1.0450	1.0830	0.4252009	-0.0356	
YBR272C	*HSM3*	0.8975	0.9152	0.9327	0.9151	0.8636	0.9470	0.8315	0.8807	0.3916634	-0.0344	
YGL100W	*SEH1*	0.9439	0.9152	0.8974	0.9189	0.8835	0.9548	0.8201	0.8861	0.4708664	-0.0328	
YIL112W	*HOS4*	1.0295	0.9129	0.9410	0.9611	0.9401	0.9885	0.8600	0.9295	0.5714747	-0.0316	
YML011C	*RAD33*	0.9611	0.9750	1.0508	0.9956	0.8835	1.0196	0.9938	0.9656	0.5823259	-0.0300	
YBL058W	*SHP1*	0.7654	0.7726	0.6259	0.7213	0.6739	0.7057	0.6948	0.6915	0.5724883	-0.0299	
YLR320W	*MMS22*	0.9464	0.8255	0.7461	0.8394	0.8070	0.7809	0.8457	0.8112	0.6695107	-0.0281	No interaction
YPL194W	*DDC1*	0.9880	0.9681	0.9866	0.9809	0.9033	1.0040	0.9511	0.9528	0.3995087	-0.0281	
YBR274W	*CHK1*	0.8828	0.8853	0.8581	0.8754	0.9599	0.7654	0.8172	0.8475	0.6600404	-0.0279	
YHR066W	*SSF1*	0.8730	0.8715	0.8518	0.8655	0.8127	0.8276	0.8742	0.8382	0.2389180	-0.0273	
YBR010W	*HHT1*	0.8950	0.8991	0.9576	0.9172	0.8495	0.9729	0.8486	0.8903	0.5897094	-0.0269	
YKR024C	*DBP7*	0.7116	0.8094	0.8063	0.7758	0.7334	0.7705	0.7432	0.7490	0.4752881	-0.0267	
YOL068C	*HST1*	0.9537	0.9336	0.9037	0.9303	0.8806	1.0222	0.8115	0.9048	0.7089322	-0.0255	
YJL030W	*MAD2*	0.7850	0.7473	0.7503	0.7609	0.7730	0.7109	0.7233	0.7357	0.3265084	-0.0251	
YJR047C	*ANB1*	0.9562	0.9359	0.9886	0.9602	0.8976	0.9236	0.9852	0.9355	0.4584491	-0.0247	
YCR008W	*SAT4*	0.7239	0.6692	0.7233	0.7055	0.6258	0.7394	0.6777	0.6810	0.5497386	-0.0245	
YLR399C	*BDF1*	1.0760	1.0095	1.0633	1.0496	1.0788	1.0430	0.9539	1.0252	0.5963528	-0.0243	
YLR035C	*MLH2*	1.0149	0.9313	0.9327	0.9596	0.9089	0.9859	0.9112	0.9353	0.5522875	-0.0243	
YHR086W	*NAM8*	0.9635	0.9543	0.9472	0.9550	0.8948	1.0066	0.8913	0.9309	0.5622070	-0.0241	
YOR191W	*ULS1*	0.8926	0.7910	0.8332	0.8389	0.8495	0.8121	0.7831	0.8149	0.5314104	-0.0241	
YMR106C	*YKU80*	1.0711	0.9612	0.8601	0.9641	0.9174	0.8951	1.0137	0.9421	0.7713713	-0.0221	
YIL139C	*REV7*	1.0222	0.9773	0.9886	0.9960	0.9429	0.9288	1.0536	0.9751	0.6419351	-0.0209	
YCL061C	*MRC1*	1.0173	0.9037	0.9368	0.9526	0.9174	0.9366	0.9482	0.9341	0.6236988	-0.0185	
YOR304W	*ISW2*	0.7239	0.8025	0.8063	0.7775	0.7192	0.8717	0.6863	0.7591	0.7843615	-0.0185	
YER070W	*RNR1*	0.9317	0.9474	1.0280	0.9690	0.9146	0.9444	0.9938	0.9509	0.6560824	-0.0181	
YPL096W	*PNG1*	0.9293	0.9520	0.9161	0.9325	0.9288	0.9366	0.8827	0.9160	0.4534164	-0.0164	
YER169W	*RPH1*	0.7434	0.8761	0.8394	0.8196	0.8212	0.8172	0.7745	0.8043	0.7352085	-0.0153	
YDL070W	*BDF2*	0.8950	0.9612	1.0280	0.9614	0.9316	1.0015	0.9055	0.9462	0.7664188	-0.0152	
YNL218W	*MGS1*	1.0002	0.9888	0.9907	0.9932	0.9259	0.9885	1.0223	0.9789	0.6406718	-0.0143	
YOL043C	*NTG2*	0.9660	0.9175	0.8995	0.9277	0.9316	0.9755	0.8343	0.9138	0.7792607	-0.0138	

Yeast systematic name	Yeast standard name	Vector Set 1	Vector Set 2	Vector Set 3	Vector Avg.	hFEN1 Set 1	hFEN1 Set 2	hFEN1 Set 3	hFEN1 Avg.	T-test	E-C[a]	GC Validations[b]
YGR188C	*BUB1*	1.1249	0.8922	0.8871	0.9681	0.9061	0.9444	1.0137	0.9547	0.8823231	-0.0133	
YJL047C	*RTT101*	1.1078	0.9428	0.9368	0.9958	0.9995	0.9314	1.0166	0.9825	0.8401010	-0.0133	
YLR306W	*UBC12*	0.9635	0.8807	0.8684	0.9042	0.8891	0.8873	0.8970	0.8911	0.6852795	-0.0131	
YJL115W	*ASF1*	0.9170	0.8117	0.7876	0.8388	0.8466	0.8276	0.8030	0.8258	0.7703111	-0.0130	
YPL256C	*CLN2*	0.8926	0.8393	0.8560	0.8626	0.8580	0.8172	0.8742	0.8498	0.6085107	-0.0128	
YFR040W	*SAP155*	0.9122	0.8278	0.7358	0.8253	0.7645	0.8743	0.8002	0.8130	0.8490345	-0.0122	
YER098W	*UBP9*	1.0173	0.8807	0.9120	0.9367	0.9514	0.9781	0.8486	0.9260	0.8615128	-0.0106	
YLR154C	*RNH203*	1.0198	1.0992	0.9824	1.0338	1.1779	1.0196	0.8799	1.0258	0.9356668	-0.0080	
YGL090W	*LIF1*	0.9024	0.8600	0.8746	0.8790	0.8580	0.9236	0.8343	0.8720	0.8229108	-0.0070	
YMR173W	*DDR48*	0.7899	0.7726	0.8933	0.8186	0.8042	0.9132	0.7176	0.8117	0.9236112	-0.0069	
YDR363W	*ESC2*	0.9122	0.8807	0.8746	0.8892	0.8495	0.8717	0.9283	0.8832	0.8299463	-0.0060	
YDL116W	*NUP84*	0.9709	0.9842	0.9555	0.9702	0.9656	1.0585	0.8685	0.9642	0.9194929	-0.0060	
YMR199W	*CLN1*	0.8339	0.8830	0.8498	0.8556	0.9627	0.7498	0.8372	0.8499	0.9332450	-0.0057	
YCL016C	*DCC1*	0.9024	0.9428	0.9140	0.9197	0.8721	0.9703	0.8998	0.9141	0.8669900	-0.0056	
YNL299W	*TRF5*	0.9439	0.9428	0.9430	0.9433	0.8806	1.0378	0.8970	0.9385	0.9279148	-0.0048	
YPL001W	*HAT1*	1.0564	0.9635	0.9430	0.9877	1.0590	0.9236	0.9710	0.9845	0.9558904	-0.0031	
YBR189W	*RPS9B*	0.8584	0.8669	1.0052	0.9102	0.8636	1.0585	0.8002	0.9074	0.9776059	-0.0027	
YBR098W	*MMS4*	0.8804	0.8991	0.8145	0.8647	0.9203	0.8302	0.8372	0.8626	0.9589704	-0.0021	No interaction
YOL087C	*DUF1*	0.9464	0.7565	0.7524	0.8184	0.8297	0.8847	0.7347	0.8163	0.9798017	-0.0021	
YGR258C	*RAD2*	0.9195	0.9083	0.9078	0.9119	0.9033	0.8743	0.9539	0.9105	0.9568031	-0.0014	
YIL018W	*RPL2B*	0.9660	0.9796	1.0094	0.9850	0.9514	1.0533	0.9482	0.9843	0.9869345	-0.0006	
YDR379W	*RGA2*	0.8901	0.9612	0.9472	0.9328	0.9231	0.9184	0.9568	0.9328	0.9977437	-0.0001	
YPL127C	*HHO1*	0.0000	0.0000	0.0000	0.0000	0.0000	0.0000	0.0000	0.0000		0.0000	
YDL042C	*SIR2*	0.0000	0.0000	0.0000	0.0000	0.0000	0.0000	0.0000	0.0000		0.0000	
YLR234W	*TOP3*	0.0000	0.0000	0.0000	0.0000	0.0000	0.0000	0.0000	0.0000		0.0000	
YLR418C	*CDC73*	0.0000	0.0000	0.0000	0.0000	0.0000	0.0000	0.0000	0.0000		0.0000	
YGL087C	*MMS2*	1.0100	1.0210	0.9824	1.0045	1.0392	0.9210	1.0536	1.0046	0.9975181	0.0001	
YMR190C	*SGS1*	0.9219	0.9221	0.8829	0.9090	0.9741	0.9392	0.8144	0.9092	0.9966426	0.0002	
YMR127C	*SAS2*	0.9366	0.9198	1.0156	0.9573	1.0392	0.9859	0.8486	0.9579	0.9935574	0.0005	
YER164W	*CHD1*	0.6798	0.8140	0.7835	0.7591	0.7390	0.8250	0.7176	0.7606	0.9792032	0.0014	
YPL240C	*HSP82*	0.8657	0.9060	0.9140	0.8952	0.9316	0.9703	0.7888	0.8969	0.9783304	0.0017	
YBL003C	*HTA2*	0.8510	0.8117	0.7752	0.8126	0.9146	0.7965	0.7318	0.8143	0.9783490	0.0017	
YOR386W	*PHR1*	0.9244	0.8784	0.9969	0.9332	0.8750	1.0222	0.9084	0.9352	0.9742364	0.0019	
YNL230C	*ELA1*	0.8632	0.8991	0.8477	0.8700	0.9571	0.8458	0.8144	0.8724	0.9607628	0.0024	
YKR056W	*TRM2*	1.0295	0.9520	0.9368	0.9728	0.9684	0.9989	0.9596	0.9756	0.9315372	0.0028	
YOR290C	*SNF2*	0.8192	0.8416	0.8083	0.8231	0.8778	0.9081	0.6948	0.8269	0.9574178	0.0038	
YLR247C	*IRC20*	0.9880	1.0256	1.0487	1.0208	1.0024	0.9989	1.0735	1.0249	0.8967628	0.0042	
YPL164C	*MLH3*	0.9317	1.0256	0.9430	0.9668	1.0024	1.0507	0.8600	0.9710	0.9506020	0.0042	
YDR334W	*SWR1*	1.1274	1.0946	1.0467	1.0895	1.1128	1.0611	1.1077	1.0939	0.8866509	0.0043	
YOR368W	*RAD17*	1.0124	0.9313	0.9576	0.9671	0.9401	1.0092	0.9682	0.9725	0.8709251	0.0054	
YNL246W	*VPS75*	0.8290	0.8255	0.8104	0.8216	0.8155	0.9288	0.7375	0.8273	0.9245164	0.0056	
YDL230W	*PTP1*	0.9562	0.8577	0.8518	0.8886	0.9259	0.9651	0.7916	0.8942	0.9323496	0.0056	
YLR357W	*RSC2*	1.0809	1.0578	1.0301	1.0563	1.0307	1.0248	1.1305	1.0620	0.8851538	0.0057	
YOR351C	*MEK1*	0.8975	0.9428	0.9306	0.9236	0.9854	0.9340	0.8770	0.9321	0.8150656	0.0085	
YMR137C	*PSO2*	0.7483	0.7450	0.7689	0.7541	0.7589	0.8172	0.7176	0.7646	0.7436532	0.0105	
YAL040C	*CLN3*	1.0467	0.9727	0.9555	0.9916	1.0647	0.9366	1.0109	1.0040	0.8022334	0.0124	
YOR025W	*HST3*	0.6970	0.6760	0.6777	0.6836	0.6201	0.7316	0.7375	0.6964	0.7572397	0.0128	
YBR026C	*ETR1*	0.5429	0.4346	0.4643	0.4806	0.4814	0.5656	0.4357	0.4942	0.7984393	0.0136	
YGR163W	*GTR2*	0.9562	0.9129	0.8539	0.9077	0.9259	0.9729	0.8657	0.9215	0.7633531	0.0138	
YBR158W	*AMN1*	0.8779	0.8784	0.8995	0.8853	0.8268	0.9029	0.9682	0.8993	0.7525456	0.0140	
YBL046W	*PSY4*	0.8730	0.8899	0.8560	0.8730	0.9571	0.8873	0.8172	0.8872	0.7491454	0.0142	

Yeast systematic name	Yeast standard name	Vector Set 1	Vector Set 2	Vector Set 3	Vector Avg.	hFEN1 Set 1	hFEN1 Set 2	hFEN1 Set 3	hFEN1 Avg.	T-test	E-C[a]	GC Validations[b]
YDL013W	*SLX5*	0.8412	0.8255	0.8083	0.8250	0.8013	0.8354	0.8884	0.8417	0.5705982	0.0167	
YNL138W	*SRV2*	0.9880	0.9336	0.8498	0.9238	0.9542	0.9599	0.9112	0.9418	0.6969151	0.0180	
YDR076W	*RAD55*	0.9219	0.8991	0.8353	0.8854	0.9174	0.8562	0.9425	0.9054	0.6136714	0.0199	No interaction
YPL181W	*CTI6*	0.8217	0.8439	0.8145	0.8267	0.8325	0.9522	0.7574	0.8474	0.7371125	0.0207	
YOR014W	*RTS1*	0.8315	0.9244	0.8767	0.8775	1.0137	0.7420	0.9397	0.8985	0.8183739	0.0209	
YPL008W	*CHL1*	0.8926	0.8715	0.8664	0.8768	0.9429	0.9340	0.8201	0.8990	0.6116973	0.0222	
YPR052C	*NHP6A*	0.8681	0.8623	0.7855	0.8387	0.9457	0.8172	0.8201	0.8610	0.6779345	0.0224	
YDL200C	*MGT1*	0.8730	0.9244	0.9285	0.9087	0.9429	0.9963	0.8543	0.9311	0.6441021	0.0225	
YDL216C	*RRI1*	0.8412	0.8577	0.8415	0.8468	0.9769	0.9158	0.7176	0.8701	0.7813457	0.0233	
YDL074C	*BRE1*	0.4206	0.4392	0.4104	0.4234	0.3568	0.4021	0.5837	0.4476	0.7469339	0.0242	
YBL088C	*TEL1*	1.0100	0.8508	0.8601	0.9070	0.9089	0.9288	0.9568	0.9315	0.6698466	0.0245	
YDR121W	*DPB4*	0.9831	0.9451	0.9700	0.9661	1.0562	0.8821	1.0337	0.9906	0.6820336	0.0246	
YGL240W	*DOC1*	0.7972	0.7634	0.8601	0.8069	0.7730	0.7913	0.9311	0.8318	0.6869852	0.0249	
YLR210W	*CLB4*	1.0516	1.0417	0.9451	1.0128	1.0194	0.9729	1.1248	1.0390	0.6654513	0.0262	
YIL066C	*RNR3*	0.8950	0.8853	0.9389	0.9064	0.8919	1.0066	0.8998	0.9328	0.5501540	0.0264	
YDR014W	*RAD61*	1.0002	1.0325	1.0570	1.0299	1.0137	1.0144	1.1419	1.0567	0.5893265	0.0268	
YDR030C	*RAD28*	0.8901	0.8370	0.8249	0.8507	0.9599	0.9184	0.7546	0.8776	0.7030507	0.0270	
YCR066W	*RAD18*	0.8657	0.8209	0.8083	0.8316	0.8891	0.8639	0.8229	0.8587	0.3570169	0.0270	
YER051W	*JHD1*	0.9757	1.0578	1.0633	1.0323	0.9627	1.0326	1.1846	1.0600	0.7174630	0.0277	
YHR031C	*RRM3*	0.9391	0.9911	0.9783	0.9695	1.1100	0.9081	0.9739	0.9973	0.6743159	0.0278	
YDR004W	*RAD57*	0.9366	0.8784	0.7917	0.8689	0.9231	0.8821	0.8856	0.8969	0.5597350	0.0280	No interaction
YML124C	*TUB3*	1.1371	0.9957	0.9658	1.0329	1.1100	1.0404	1.0394	1.0632	0.6271684	0.0303	
YCL029C	*BIK1*	1.0173	0.9566	0.9265	0.9668	1.0420	0.9937	0.9568	0.9975	0.4461760	0.0307	
YOR005C	*DNL4*	1.0222	0.9957	0.9513	0.9897	1.0392	0.9522	1.0707	1.0207	0.4928319	0.0309	
YMR216C	*SKY1*	0.8681	0.8462	0.8726	0.8623	0.8353	0.9522	0.8941	0.8939	0.4145518	0.0316	
YIL132C	*CSM2*	1.1323	1.0693	1.0342	1.0786	1.1355	1.0300	1.1675	1.1110	0.5558818	0.0324	
YGR108W	*CLB1*	1.0785	1.0854	0.9866	1.0501	1.1440	0.9807	1.1276	1.0841	0.6067387	0.0340	
YML021C	*UNG1*	0.8999	0.7151	0.7544	0.7898	0.8551	0.8276	0.7916	0.8248	0.5862239	0.0350	
YER177W	*BMH1*	0.6285	0.6301	0.4850	0.5812	0.6598	0.6227	0.5667	0.6164	0.5584402	0.0352	
YHR120W	*MSH1*	0.6187	0.6646	0.6467	0.6433	0.8438	0.6175	0.5752	0.6788	0.6956072	0.0355	
YER016W	*BIM1*	0.9488	0.9796	1.0259	0.9848	0.9373	1.1104	1.0137	1.0205	0.5511442	0.0357	
YDL047W	*SIT4*	0.0685	0.8623	0.0580	0.3296	0.0283	0.0259	1.0422	0.3655	0.9375954	0.0359	No interaction
YMR048W	*CSM3*	0.9855	0.9428	0.9410	0.9564	0.9769	1.1130	0.8913	0.9937	0.6031006	0.0373	
YCR014C	*POL4*	1.0711	0.9865	0.9804	1.0126	1.0902	1.0118	1.0479	1.0500	0.3704440	0.0373	
YBL067C	*UBP13*	0.8339	0.8163	0.7648	0.8050	0.9004	0.8406	0.7859	0.8423	0.3932305	0.0373	
YDR092W	*UBC13*	0.9635	0.8094	0.7192	0.8307	0.8665	0.8043	0.9340	0.8682	0.6655364	0.0375	
YLR135W	*SLX4*	0.9170	0.8232	0.8311	0.8571	0.9174	0.8302	0.9368	0.8948	0.4443310	0.0377	
YMR036C	*MIH1*	0.7654	0.7634	0.7669	0.7652	0.8608	0.7939	0.7546	0.8031	0.2893144	0.0379	
YAL015C	*NTG1*	1.0149	0.9474	0.9037	0.9553	0.9854	0.9184	1.0764	0.9934	0.5340295	0.0381	
YDR289C	*RTT103*	0.4622	0.5082	0.4705	0.4803	0.4899	0.5993	0.4727	0.5206	0.3923468	0.0403	
YLR288C	*MEC3*	1.0173	0.9911	1.0032	1.0038	1.0902	0.9625	1.0821	1.0449	0.3829632	0.0411	
YLL019C	*KNS1*	0.9831	0.9635	0.9990	0.9819	0.9514	1.0715	1.0479	1.0236	0.3352254	0.0417	
YBL002W	*HTB2*	0.8828	0.8554	0.8954	0.8779	0.9033	0.9755	0.8827	0.9205	0.2347189	0.0426	
YGL086W	*MAD1*	0.9439	0.9244	0.9037	0.9240	1.0307	0.8899	0.9824	0.9677	0.3665084	0.0437	
YJL101C	*GSH1*	0.0000	0.0000	0.0000	0.0000	0.1331	0.0000	0.0000	0.0444	0.3739010	0.0444	
YGL163C	*RAD54*	0.8070	0.8623	0.7586	0.8093	0.8183	0.8406	0.9027	0.8539	0.3187937	0.0446	No interaction
YLR265C	*NEJ1*	0.9464	0.9083	0.9057	0.9201	0.9514	0.9236	1.0194	0.9648	0.2272371	0.0447	
YOR033C	*EXO1*	1.0124	1.0256	0.9783	1.0054	1.0845	1.0040	1.0621	1.0502	0.1824740	0.0448	
YGL003C	*CDH1*	0.9562	0.8738	0.7627	0.8642	0.9373	0.9055	0.8884	0.9104	0.4697029	0.0461	
YKL113C	*RAD27*	0.8779	0.9152	0.8746	0.8893	0.9967	0.9184	0.8913	0.9355	0.2476585	0.0462	
YBR223C	*TDP1*	0.9097	0.9543	0.9120	0.9253	1.0194	1.0118	0.8856	0.9723	0.3628535	0.0469	

Yeast systematic name	Yeast standard name	Vector Set 1	Vector Set 2	Vector Set 3	Vector Avg.	hFEN1 Set 1	hFEN1 Set 2	hFEN1 Set 3	hFEN1 Avg.	T-test	E-C[a]	GC Validations[b]
YDR075W	*PPH3*	1.1127	1.0647	0.9886	1.0553	1.1581	1.0352	1.1162	1.1032	0.4016849	0.0478	
YGL175C	*SAE2*	0.9219	0.9428	0.8871	0.9173	1.0845	0.8977	0.9169	0.9664	0.4695526	0.0491	
YOR258W	*HNT3*	1.1249	1.0900	1.1337	1.1162	1.1779	1.0741	1.2472	1.1664	0.3892851	0.0502	
YEL056W	*HAT2*	1.1078	1.0279	1.0011	1.0456	1.0930	1.0300	1.1646	1.0959	0.3748364	0.0503	
YJR066W	*TOR1*	0.8632	0.8393	0.7710	0.8245	0.9486	0.8276	0.8514	0.8759	0.3284723	0.0513	
YDR097C	*MSH6*	0.9170	0.9359	0.8518	0.9016	0.9373	0.8769	1.0450	0.9531	0.4051988	0.0515	
YDR378C	*LSM6*	0.9684	1.0371	1.0467	1.0174	1.0987	1.0222	1.0906	1.0705	0.1993624	0.0531	
YFR014C	*CMK1*	1.0222	0.9658	0.9493	0.9791	1.0703	0.9496	1.0821	1.0340	0.3143597	0.0549	
YGL211W	*NCS6*	0.6089	0.6462	0.5202	0.5918	0.6456	0.7109	0.5866	0.6477	0.3410880	0.0559	
YFR034C	*PHO4*	0.9195	0.9037	0.8622	0.8951	0.9373	1.0482	0.8713	0.9523	0.3525368	0.0571	
YGR003W	*CUL3*	0.9855	0.8508	0.8933	0.9099	1.0052	0.9444	0.9539	0.9678	0.2583250	0.0580	
YGL229C	*SAP4*	0.8632	0.9267	0.8560	0.8820	0.9911	0.8925	0.9397	0.9411	0.1784090	0.0591	
YJR043C	*POL32*	0.8877	0.8692	0.8353	0.8641	1.0024	0.9392	0.8286	0.9234	0.3259045	0.0593	
YKL213C	*DOA1*	0.8828	0.8761	0.8394	0.8661	0.9288	0.8639	0.9852	0.9260	0.1860464	0.0599	
YPR141C	*KAR3*	1.0100	0.9704	0.9741	0.9848	1.0618	0.9807	1.0963	1.0463	0.1677135	0.0614	
YCR044C	*PER1*	1.0589	0.9911	0.9617	1.0039	1.1298	1.0663	1.0023	1.0661	0.2534298	0.0623	
YGL033W	*HOP2*	1.1469	1.1497	1.1462	1.1476	1.2742	1.1416	1.2159	1.2106	0.1765464	0.0629	
YDL155W	*CLB3*	0.9219	0.9589	0.9990	0.9599	0.9373	1.0741	1.0593	1.0235	0.2618869	0.0636	
YER045C	*ACA1*	1.0491	0.8761	0.8726	0.9326	1.0817	0.9573	0.9539	0.9976	0.4163869	0.0651	
YNL201C	*PSY2*	0.8461	0.7542	0.7586	0.7863	0.8410	0.7913	0.9255	0.8526	0.2500001	0.0663	
YBR228W	*SLX1*	1.0760	1.0578	0.9534	1.0291	1.1779	1.0741	1.0394	1.0971	0.2946473	0.0681	
YPR135W	*CTF4*	0.8779	0.8485	0.8311	0.8525	0.9741	0.9807	0.8115	0.9221	0.2889964	0.0696	
YOL006C	*TOP1*	0.9929	0.9635	0.9348	0.9637	1.0817	1.0793	0.9397	1.0335	0.2337144	0.0698	
YCR092C	*MSH3*	1.0687	1.0279	0.9513	1.0160	1.1751	0.9729	1.1105	1.0862	0.3652727	0.0702	
YPR018W	*RLF2*	0.7410	0.6967	0.6176	0.6851	0.7957	0.6875	0.7831	0.7554	0.2298768	0.0703	
YML060W	*OGG1*	1.0980	1.0394	0.9824	1.0399	1.1836	1.0144	1.1362	1.1114	0.3024769	0.0715	
YML028W	*TSA1*	1.0222	0.9888	0.8974	0.9695	1.0760	1.0144	1.0337	1.0414	0.1581657	0.0719	
YGL194C	*HOS2*	1.1029	1.0647	0.9762	1.0479	1.1326	1.0793	1.1504	1.1208	0.1668440	0.0729	
YNL030W	*HHF2*	0.8926	0.9474	0.9037	0.9145	1.1440	0.8795	0.9425	0.9887	0.4144624	0.0741	
YHR154W	*RTT107*	0.8608	0.8393	0.8104	0.8368	0.9401	0.8536	0.9397	0.9111	0.0827586	0.0743	
YMR156C	*TPP1*	0.9880	0.9037	0.9078	0.9332	1.0675	0.9366	1.0251	1.0097	0.1809474	0.0766	
YIR019C	*MUC1*	0.9586	0.8531	0.8228	0.8782	0.9627	0.9366	0.9653	0.9549	0.1430708	0.0767	
YGR129W	*SYF2*	0.9439	0.8968	0.9016	0.9141	1.0958	1.0482	0.8286	0.9909	0.4106507	0.0768	
YNL082W	*PMS1*	1.0149	0.9290	0.8456	0.9298	1.1156	0.9081	0.9966	1.0068	0.3768809	0.0769	
YJR063W	*RPA12*	0.8828	0.8048	0.7358	0.8078	0.9203	0.9703	0.7660	0.8855	0.3570763	0.0777	
YHR082C	*KSP1*	0.9562	0.9727	0.8871	0.9386	1.0477	0.9366	1.0678	1.0174	0.1799021	0.0787	
YLR376C	*PSY3*	0.9562	0.8439	0.8000	0.8667	1.0364	0.8380	0.9625	0.9456	0.3477687	0.0789	
YDR314C	*RAD34*	1.0149	0.9543	0.9223	0.9638	1.1213	0.9470	1.0707	1.0463	0.2310523	0.0825	
YOR308C	*SNU66*	1.0809	0.9635	0.9016	0.9820	1.0987	1.0611	1.0365	1.0654	0.2078316	0.0834	
YJR104C	*SOD1*	0.2592	1.0854	1.1006	0.8150	1.1156	0.4644	1.1162	0.8988	0.8240614	0.0837	
YPL046C	*ELC1*	0.8853	0.7519	0.6612	0.7661	0.8891	0.8588	0.8030	0.8503	0.2942432	0.0842	
YGL251C	*HFM1*	1.0344	0.9313	0.8684	0.9447	1.0335	0.9859	1.0678	1.0291	0.1926427	0.0844	
YLR270W	*DCS1*	1.0075	0.9244	0.8809	0.9376	1.0449	0.9314	1.0906	1.0223	0.2320084	0.0847	
YFR031C-A	*RPL2A*	1.0026	0.9474	0.9327	0.9609	1.0817	1.0015	1.0564	1.0465	0.0547570	0.0856	
YBL019W	*APN2*	1.0907	1.0762	0.9907	1.0525	1.1921	1.0533	1.1703	1.1386	0.1808957	0.0861	
YKL025C	*PAN3*	1.0418	0.9980	0.9244	0.9880	1.1298	1.1000	0.9938	1.0745	0.1821025	0.0865	
YOL090W	*MSH2*	1.2105	1.0072	0.8270	1.0149	1.1411	0.8977	1.2672	1.1020	0.6042057	0.0871	
YEL037C	*RAD23*	1.0198	0.9750	0.9120	0.9689	1.0732	1.0326	1.0650	1.0569	0.0589984	0.0880	
YML102W	*CAC2*	0.8363	0.7772	0.7772	0.7969	0.9174	0.8977	0.8400	0.8850	0.0444298	0.0881	
YBR289W	*SNF5*	0.4328	0.7404	0.4995	0.5576	1.1836	0.3684	0.3958	0.6493	0.7623172	0.0917	
YBR231C	*SWC5*	0.9782	1.1497	1.0301	1.0527	1.1864	1.1519	1.0992	1.1458	0.1761994	0.0932	

Yeast systematic name	Yeast standard name	Vector Set 1	Vector Set 2	Vector Set 3	Vector Avg.	hFEN1 Set 1	hFEN1 Set 2	hFEN1 Set 3	hFEN1 Avg.	T-test	E-C[a]	GC Validations[b]
YHL006C	*SHU1*	1.0882	1.0187	0.9804	1.0291	1.1553	1.0663	1.1476	1.1231	0.0915565	0.0940	
YBR009C	*HHF1*	0.8779	0.8922	0.9057	0.8920	1.0675	1.0300	0.8685	0.9887	0.1913656	0.0967	
YPL129W	*TAF14*	1.0198	1.0877	1.1026	1.0700	1.1723	1.2090	1.1305	1.1706	0.0421101	0.1006	
YGR109C	*CLB6*	0.8706	0.8370	0.7648	0.8241	0.9939	0.9262	0.8543	0.9248	0.1195720	0.1007	
YDR419W	*RAD30*	1.0833	1.0256	1.0135	1.0408	1.1949	1.0352	1.2017	1.1439	0.1528432	0.1031	
YML061C	*PIF1*	1.0222	1.0578	1.0301	1.0367	1.1270	1.2064	1.0906	1.1413	0.0432977	0.1046	
YAL019W	*FUN30*	1.0173	0.9060	0.8353	0.9195	1.0647	1.0170	0.9938	1.0252	0.1371859	0.1056	
YKL114C	*APN1*	1.0858	1.0095	1.0301	1.0418	1.1666	1.1338	1.1447	1.1484	0.0125880	0.1066	
YER041W	*YEN1*	1.0075	0.9382	0.9078	0.9512	1.1128	1.1182	0.9454	1.0588	0.1676595	0.1076	
YPR101W	*SNT309*	1.1274	0.8048	0.7710	0.9011	1.0024	0.8951	1.1305	1.0093	0.4594724	0.1082	
YJR090C	*GRR1*	0.6774	0.8094	0.6280	0.7049	0.9854	0.7835	0.6720	0.8136	0.3651127	0.1087	
YDR364C	*CDC40*	0.2739	0.3794	0.8000	0.4844	1.2799	0.1557	0.3446	0.5934	0.7901891	0.1089	No interaction
YOL115W	*PAP2*	0.9660	0.9221	0.8456	0.9112	1.0845	1.0793	0.8998	1.0212	0.1920418	0.1100	
YGL058W	*RAD6*	0.9880	0.9474	0.9057	0.9470	1.1100	1.0819	0.9796	1.0571	0.0757049	0.1101	
YOR346W	*REV1*	1.0638	0.9773	0.9037	0.9816	1.1355	1.0196	1.1561	1.1037	0.1236989	0.1222	
YPR119W	*CLB2*	1.0662	1.0578	1.0177	1.0472	1.2147	1.1831	1.1105	1.1695	0.0234785	0.1222	
YGR252W	*GCN5*	1.0075	0.9865	1.0280	1.0073	1.1071	1.1701	1.1134	1.1302	0.0062362	0.1229	
YDL101C	*DUN1*	0.9660	0.9221	0.8788	0.9223	1.1071	1.0637	0.9739	1.0482	0.0539942	0.1260	
YKL117W	*SBA1*	1.1200	1.0693	0.9949	1.0614	1.2459	1.0871	1.2358	1.1896	0.1111774	0.1282	
YGR056W	*RSC1*	1.0516	1.0647	1.0094	1.0419	1.2629	1.1000	1.1618	1.1749	0.0573046	0.1330	
YDR078C	*SHU2*	0.9660	0.9589	0.9016	0.9421	1.1496	1.0949	1.0080	1.0842	0.0366267	0.1420	
YJL092W	*SRS2*	1.0222	0.9267	0.9223	0.9571	1.1326	1.0923	1.0821	1.1023	0.0157652	0.1452	
YNL307C	*MCK1*	0.8388	0.8117	0.7316	0.7940	1.0873	1.0222	0.7432	0.9509	0.2281668	0.1569	
YOR080W	*DIA2*	0.9219	0.9014	0.8394	0.8876	0.9684	1.1649	1.0052	1.0462	0.0718531	0.1586	
YHR064C	*SSZ1*	0.4402	0.4944	0.3088	0.4145	0.3794	1.0663	0.2876	0.5778	0.5519528	0.1633	
YNR052C	*POP2*	0.6309	0.3771	0.4394	0.4825	0.4077	0.3866	1.1874	0.6606	0.5516008	0.1781	
YPL167C	*REV3*	1.0075	0.9198	0.8436	0.9236	1.1808	1.0663	1.0792	1.1088	0.0360300	0.1851	
YJL176C	*SWI3*	0.1052	0.1311	0.5990	0.2784	1.1609	0.1038	0.4613	0.5753	0.4433778	0.2969	

[a] Experimental-control or (hFen1 average)-(vector average). For each mutant, area of pinned spot was normalized to the average of WT spots on the same plate.

[b] Growth curve validations. Interactions with (experimental-control values <-0.2) and some selected mutants were chosen for validations by growth curves. "No interaction" indicates that mutant was tested by growth curves and no SDL interaction was observed.

Table A.14. Results of the SDL screen for hD181A

Yeast systematic name	Yeast standard name	Vector Set 1	Vector Set 2	Vector Set 3	Vector Avg.	D181A Set 1	D181A Set 2	D181A Set 3	D181A Avg.	T-test	E-C[a]	GC Validations[b]
YNR023W	*SNF12*	0.2397	1.1313	1.1669	0.8460	0.3199	0.2946	0.2948	0.3031	0.1481367	-0.5428	No interaction
YNL250W	*RAD50*	0.7825	0.7519	0.7254	0.7533	0.2285	0.2165	0.2347	0.2265	0.0000070	-0.5268	Negative
YMR224C	*MRE11*	0.7679	0.7174	0.7710	0.7521	0.2285	0.2014	0.2587	0.2296	0.0000263	-0.5226	Negative
YDR369C	*XRS2*	0.7850	0.7680	0.6425	0.7318	0.2803	0.1954	0.1775	0.2177	0.0007290	-0.5141	Negative
YIL128W	*MET18*	1.1763	0.9612	0.7669	0.9681	0.6246	0.2555	0.5355	0.4719	0.0377517	-0.4962	No interaction
YKL113C	*RAD27*	0.8779	0.9152	0.8746	0.8893	0.4509	0.3157	0.4483	0.4050	0.0004802	-0.4843	Negative
YDR364C	*CDC40*	0.2739	0.3794	0.8000	0.4844	0.0244	0.0000	0.0271	0.0172	0.0439592	-0.4673	No interaction
YGR171C	*MSM1*	0.1907	0.3449	1.2083	0.5813	0.3260	0.0391	0.0000	0.1217	0.2395051	-0.4596	No interaction
YML032C	*RAD52*	0.5649	0.6232	0.5783	0.5888	0.2224	0.1714	0.1685	0.1874	0.0000859	-0.4014	Negative
YKL139W	*CTK1*	0.5233	1.1107	0.9866	0.8735	0.5210	0.5622	0.4844	0.5225	0.1231603	-0.3510	No interaction
YDL047W	*SIT4*	0.0685	0.8623	0.0580	0.3296	0.0000	0.0000	0.0000	0.0000	0.2836124	-0.3296	No interaction
YNL252C	*MRPL17*	0.6236	0.1656	0.2073	0.3321	0.0305	0.0000	0.0000	0.0102	0.0929934	-0.3220	No interaction
YDR076W	*RAD55*	0.9219	0.8991	0.8353	0.8854	0.6459	0.5682	0.5235	0.5792	0.0022739	-0.3062	Negative
YDR004W	*RAD57*	0.9366	0.8784	0.7917	0.8689	0.6733	0.5983	0.4483	0.5733	0.0196001	-0.2956	Negative
YOR026W	*BUB3*	0.9855	0.6967	1.0757	0.9193	0.6124	0.6644	0.6107	0.6292	0.0661366	-0.2901	No interaction
YGR285C	*ZUO1*	0.5184	0.4001	0.6259	0.5148	0.2742	0.1984	0.2377	0.2368	0.0155747	-0.2781	No interaction
YJL006C	*CTK2*	0.4989	0.6025	1.2767	0.7927	0.5667	0.4991	0.5024	0.5227	0.3321023	-0.2700	No interaction
YLR320W	*MMS22*	0.9464	0.8255	0.7461	0.8394	0.6550	0.5682	0.5175	0.5802	0.0215188	-0.2591	No interaction
YGL163C	*RAD54*	0.8070	0.8623	0.7586	0.8093	0.7739	0.4630	0.4302	0.5557	0.0892216	-0.2536	Negative
YDR386W	*MUS81*	0.8632	0.8554	0.7814	0.8333	0.6002	0.5832	0.5927	0.5921	0.0008114	-0.2413	No interaction
YLR240W	*VPS34*	0.8901	0.8508	0.8767	0.8726	0.7007	0.5953	0.6288	0.6416	0.0022409	-0.2310	No interaction
YNL025C	*SSN8*	1.0393	1.0233	1.0695	1.0440	1.1760	1.0853	0.1986	0.8200	0.5125334	-0.2240	No interaction
YBR289W	*SNF5*	0.4328	0.7404	0.4995	0.5576	0.3321	0.3337	0.4122	0.3593	0.1106792	-0.1983	No interaction
YLL002W	*RTT109*	0.7654	0.8577	0.8456	0.8229	0.6276	0.5953	0.6830	0.6353	0.0083102	-0.1876	No interaction
YJL115W	*ASF1*	0.9170	0.8117	0.7876	0.8388	0.7160	0.6614	0.5987	0.6587	0.0260980	-0.1801	No interaction
YKL057C	*NUP120*	1.0638	1.0164	1.0322	1.0374	0.8683	0.8659	0.8725	0.8689	0.0002783	-0.1685	No interaction
YPR164W	*MMS1*	0.8143	0.7565	0.7544	0.7751	0.5576	0.6103	0.6769	0.6149	0.0157118	-0.1602	No interaction
YMR167W	*MLH1*	0.8926	1.0164	0.7669	0.8919	0.8165	0.6704	0.7130	0.7333	0.1322857	-0.1586	No interaction
YBR098W	*MMS4*	0.8804	0.8991	0.8145	0.8647	0.7647	0.6975	0.6649	0.7090	0.0162637	-0.1556	No interaction
YJR104C	*SOD1*	0.2592	1.0854	1.1006	0.8150	0.4204	0.3097	1.2516	0.6606	0.7235236	-0.1545	No interaction
YOR368W	*RAD17*	1.0124	0.9313	0.9576	0.9671	0.8622	0.8358	0.7431	0.8137	0.0239728	-0.1534	No interaction
YPL024W	*RMI1*	0.7752	0.8071	0.8000	0.7941	0.6368	0.6374	0.6619	0.6453	0.0003066	-0.1488	
YOL004W	*SIN3*	0.5307	0.5358	0.8581	0.6415	0.4875	0.4750	0.5175	0.4933	0.2456750	-0.1482	No interaction
YJL176C	*SWI3*	0.1052	0.1311	0.5990	0.2784	0.1158	0.1774	0.1053	0.1328	0.4197206	-0.1456	
YGL173C	*KEM1*	1.0026	1.0417	0.9306	0.9916	1.1090	0.6223	0.8093	0.8469	0.3758981	-0.1448	No interaction
YNL330C	*RPD3*	0.5135	0.5703	0.8270	0.6369	0.4814	0.4750	0.5205	0.4923	0.2119764	-0.1446	No interaction
YKR092C	*SRP40*	0.9244	0.8462	0.9907	0.9204	0.8074	0.7696	0.7522	0.7764	0.0324911	-0.1440	
YDR279W	*RNH202*	0.9073	0.8922	0.9472	0.9156	0.7678	0.7817	0.7672	0.7722	0.0011018	-0.1433	
YHR115C	*DMA1*	0.9880	0.9819	1.0177	0.9958	0.8013	0.8899	0.8725	0.8546	0.0084854	-0.1413	No interaction
YBR089C-A	*NHP6B*	0.8804	0.8876	1.0156	0.9279	0.7495	0.8087	0.8033	0.7872	0.0422947	-0.1407	
YDR363W-A	*SEM1*	0.6236	0.5657	0.5783	0.5892	0.4570	0.4540	0.4393	0.4501	0.0016487	-0.1391	
YER142C	*MAG1*	0.9513	0.9405	0.9824	0.9581	0.8196	0.8298	0.8093	0.8196	0.0005681	-0.1385	
YNL021W	*HDA1*	0.6187	0.7082	0.9990	0.7753	0.6794	0.6103	0.6228	0.6375	0.3032196	-0.1378	
YNL136W	*EAF7*	0.7679	0.8531	0.9493	0.8567	0.6855	0.7606	0.7160	0.7207	0.0746180	-0.1360	
YPR135W	*CTF4*	0.8779	0.8485	0.8311	0.8525	0.7861	0.6885	0.6890	0.7212	0.0202752	-0.1314	
YGR270W	*YTA7*	1.1323	1.0900	0.8332	1.0185	0.9384	0.8869	0.8394	0.8882	0.2534304	-0.1302	
YPL194W	*DDC1*	0.9880	0.9681	0.9866	0.9809	0.8836	0.8538	0.8153	0.8509	0.0033216	-0.1300	
YIL153W	*RRD1*	0.6603	0.6071	0.8083	0.6919	0.5606	0.5772	0.5566	0.5648	0.1037643	-0.1271	
YNL116W	*DMA2*	0.9170	0.9198	1.0467	0.9612	0.7922	0.8598	0.8575	0.8365	0.0607643	-0.1247	

Yeast systematic name	Yeast standard name	Vector Set 1	Vector Set 2	Vector Set 3	Vector Avg.	D181A Set 1	D181A Set 2	D181A Set 3	D181A Avg.	T-test	E-C[a]	GC Validations[b]
YDL074C	*BRE1*	0.4206	0.4392	0.4104	0.4234	0.2742	0.3277	0.2948	0.2989	0.0021602	-0.1245	
YNL031C	*HHT2*	0.9073	0.9589	0.9886	0.9516	0.7891	0.8508	0.8484	0.8295	0.0172934	-0.1221	
YBR034C	*HMT1*	0.7997	0.8278	0.8643	0.8306	0.6977	0.7095	0.7191	0.7088	0.0034729	-0.1218	
YER173W	*RAD24*	0.8290	0.9014	0.8270	0.8525	0.7708	0.7155	0.7130	0.7331	0.0181157	-0.1193	
YDR176W	*NGG1*	0.2470	0.2368	0.2425	0.2421	0.1401	0.1082	0.1324	0.1269	0.0003304	-0.1152	
YAL040C	*CLN3*	1.0467	0.9727	0.9555	0.9916	0.9506	0.8598	0.8244	0.8783	0.0728112	-0.1133	
YLR394W	*CST9*	0.7630	0.7450	0.8456	0.7845	0.6490	0.6915	0.6739	0.6715	0.0274841	-0.1131	
YGL066W	*SGF73*	0.8486	0.9152	0.8560	0.8733	0.6825	0.7606	0.8394	0.7608	0.0876477	-0.1124	
YEL003W	*GIM4*	0.9464	0.9796	0.9348	0.9536	0.8927	0.8478	0.7883	0.8429	0.0287408	-0.1107	No interaction
YGR184C	*UBR1*	0.9268	0.9842	0.9783	0.9631	0.8074	0.9019	0.8484	0.8526	0.0282655	-0.1105	
YNL068C	*FKH2*	0.7752	0.8485	0.7793	0.8010	0.7312	0.7095	0.6348	0.6919	0.0441665	-0.1092	
YMR173W	*DDR48*	0.7899	0.7726	0.8933	0.8186	0.6947	0.6975	0.7431	0.7118	0.0589581	-0.1068	
YJR082C	*EAF6*	0.8730	0.8554	0.8187	0.8490	0.7465	0.7276	0.7612	0.7451	0.0051543	-0.1040	
YER162C	*RAD4*	1.0295	0.9382	1.0591	1.0089	0.9445	0.9109	0.8725	0.9093	0.0762428	-0.0996	
YDR440W	*DOT1*	0.8975	0.8853	0.9348	0.9058	0.8287	0.7997	0.8003	0.8096	0.0055329	-0.0963	
YOR304W	*ISW2*	0.7239	0.8025	0.8063	0.7775	0.7221	0.6404	0.6860	0.6828	0.0571280	-0.0947	
YDR217C	*RAD9*	0.8706	0.8899	0.8933	0.8846	0.6947	0.8418	0.8484	0.7950	0.1517117	-0.0896	
YMR190C	*SGS1*	0.9219	0.9221	0.8829	0.9090	0.9201	0.7696	0.7702	0.8200	0.1604545	-0.0890	
YJL047C	*RTT101*	1.1078	0.9428	0.9368	0.9958	0.9750	0.9350	0.8123	0.9074	0.3004999	-0.0884	
YCR065W	*HCM1*	0.9366	0.9566	0.9783	0.9572	0.8622	0.9109	0.8364	0.8699	0.0249178	-0.0873	
YHR200W	*RPN10*	0.6725	0.6692	0.6259	0.6559	0.5789	0.5472	0.5807	0.5689	0.0093515	-0.0870	
YLL039C	*UBI4*	0.9709	0.9681	0.9824	0.9738	0.8013	0.9560	0.9086	0.8886	0.1377489	-0.0851	
YGR180C	*RNR4*	0.9195	1.1612	0.8394	0.9734	0.8196	1.0102	0.8364	0.8887	0.4999999	-0.0847	No interaction
YGL115W	*SNF4*	0.9904	0.9175	0.8104	0.9061	0.7251	1.0492	0.6950	0.8231	0.5426822	-0.0830	
YOL090W	*MSH2*	1.2105	1.0072	0.8270	1.0149	0.9658	0.8659	0.9658	0.9325	0.5155824	-0.0824	
YBR073W	*RDH54*	0.9244	0.9796	0.9741	0.9594	0.8744	0.9019	0.8575	0.8779	0.0202748	-0.0814	
YER095W	*RAD51*	0.6040	0.6485	0.6674	0.6400	0.6642	0.5382	0.4754	0.5592	0.2404617	-0.0807	Negative
YAR002W	*NUP60*	0.9562	1.0164	0.9700	0.9808	0.8836	0.8809	0.9417	0.9020	0.0429610	-0.0788	
YLR085C	*ARP6*	1.0760	1.1405	1.1234	1.1133	0.9475	1.1635	0.9989	1.0366	0.3221538	-0.0767	
YGL070C	*RPB9*	0.7948	0.7772	0.6881	0.7534	0.7830	0.6704	0.5777	0.6770	0.3240393	-0.0763	
YPL183W-A	*RTC6*	0.5845	0.6485	0.6819	0.6383	0.5301	0.5321	0.6258	0.5627	0.1505122	-0.0756	
YDR225W	*HTA1*	0.7654	0.7864	0.7814	0.7777	0.7465	0.6825	0.6860	0.7050	0.0285106	-0.0728	
YJL187C	*SWE1*	0.9170	0.8968	0.9223	0.9121	0.7891	0.8298	0.8996	0.8395	0.0939947	-0.0726	
YLR107W	*REX3*	0.9782	0.9980	1.0695	1.0152	0.9110	0.9651	0.9537	0.9433	0.0894793	-0.0720	
YNL273W	*TOF1*	1.0198	0.8531	0.8415	0.9048	0.9171	0.7276	0.8575	0.8340	0.4279197	-0.0708	
YER116C	*SLX8*	0.9122	0.9014	0.9223	0.9120	0.8226	0.8418	0.8605	0.8416	0.0048832	-0.0703	
YER176W	*ECM32*	0.8975	0.9175	0.9368	0.9173	0.8409	0.8749	0.8274	0.8477	0.0185107	-0.0696	
YPR023C	*EAF3*	0.7850	0.8117	0.9700	0.8556	0.7647	0.7666	0.8334	0.7883	0.3385466	-0.0673	
YNL072W	*RNH201*	1.0247	1.0463	0.9969	1.0226	0.9414	0.9621	0.9748	0.9594	0.0216025	-0.0632	
YDR379W	*RGA2*	0.8901	0.9612	0.9472	0.9328	0.8379	0.8538	0.9176	0.8698	0.1255248	-0.0631	
YBR278W	*DPB3*	0.8999	0.9497	1.0197	0.9565	0.8714	0.9260	0.8875	0.8950	0.1840132	-0.0615	
YBL058W	*SHP1*	0.7654	0.7726	0.6259	0.7213	0.7525	0.6524	0.5746	0.6599	0.4307843	-0.0615	
YDR121W	*DPB4*	0.9831	0.9451	0.9700	0.9661	1.0359	0.8809	0.7973	0.9047	0.4348787	-0.0614	
YHL025W	*SNF6*	0.5258	0.9704	0.7669	0.7543	0.5027	0.9591	0.6198	0.6938	0.7633817	-0.0605	
YML028W	*TSA1*	1.0222	0.9888	0.8974	0.9695	1.0633	0.8628	0.8033	0.9098	0.5307361	-0.0597	
YLR233C	*EST1*	0.9782	0.9152	0.9078	0.9337	0.8622	0.8809	0.8815	0.8749	0.0642720	-0.0589	
YKL203C	*TOR2*	0.9342	0.9359	0.9182	0.9294	0.8805	0.8598	0.8725	0.8709	0.0020906	-0.0585	
YMR201C	*RAD14*	1.0467	1.0141	0.9057	0.9888	0.9810	0.8959	0.9146	0.9305	0.3068717	-0.0583	
YGL094C	*PAN2*	1.0589	0.9980	1.0570	1.0380	0.9018	0.9981	1.0410	0.9803	0.2761061	-0.0577	
YGR271W	*SLH1*	0.9709	0.9911	0.9990	0.9870	0.8896	0.9530	0.9537	0.9321	0.0742741	-0.0548	
YDL154W	*MSH5*	0.9415	0.9451	0.9824	0.9563	0.9171	0.8989	0.8905	0.9022	0.0237483	-0.0542	

Yeast systematic name	Yeast standard name	Vector Set 1	Vector Set 2	Vector Set 3	Vector Avg.	D181A Set 1	D181A Set 2	D181A Set 3	D181A Avg.	T-test	E-C[a]	GC Validations[b]
YMR078C	*CTF18*	1.0173	1.0601	0.9824	1.0199	0.9201	1.0132	0.9658	0.9663	0.2006224	-0.0536	
YMR080C	*NAM7*	1.0418	0.9014	0.9140	0.9524	0.9414	0.8869	0.8695	0.8993	0.3461849	-0.0531	
YGR056W	*RSC1*	1.0516	1.0647	1.0094	1.0419	1.2492	1.0793	0.6378	0.9888	0.7860809	-0.0531	
YHL022C	*SPO11*	0.8168	0.8485	0.7731	0.8128	0.7586	0.8328	0.6890	0.7601	0.3245482	-0.0527	
YBR245C	*ISW1*	0.8950	0.8830	0.9306	0.9029	0.8165	0.8208	0.9146	0.8506	0.2103878	-0.0523	
YOR144C	*ELG1*	0.8094	0.8324	0.7814	0.8077	0.6977	0.7065	0.8635	0.7559	0.4056070	-0.0519	
YDR263C	*DIN7*	0.9635	0.9566	0.9886	0.9696	0.9140	0.8989	0.9477	0.9202	0.0470201	-0.0494	
YMR127C	*SAS2*	0.9366	0.9198	1.0156	0.9573	0.9932	0.9771	0.7552	0.9085	0.5848074	-0.0488	
YOL054W	*PSH1*	0.9293	0.9658	0.8788	0.9246	0.9049	0.8779	0.8544	0.8791	0.1928988	-0.0456	
YLR032W	*RAD5*	0.8632	0.7358	0.7586	0.7859	0.6916	0.6704	0.8605	0.7408	0.5643447	-0.0451	
YER098W	*UBP9*	1.0173	0.8807	0.9120	0.9367	1.0024	0.8298	0.8454	0.8925	0.5565846	-0.0441	
YDR363W	*ESC2*	0.9122	0.8807	0.8746	0.8892	0.8531	0.8689	0.8153	0.8458	0.0920727	-0.0434	
YGL043W	*DST1*	0.6627	0.6760	0.6632	0.6673	0.5972	0.6614	0.6138	0.6241	0.0937727	-0.0432	
YDR523C	*SPS1*	1.0222	1.0831	1.0487	1.0513	0.9597	1.0252	1.0410	1.0086	0.2337972	-0.0427	
YOL087C	*DUF1*	0.9464	0.7565	0.7524	0.8184	0.8775	0.6825	0.7702	0.7767	0.6503333	-0.0417	
YML095C	*RAD10*	0.8828	0.8922	0.9410	0.9053	0.8531	0.8478	0.8905	0.8638	0.1386913	-0.0415	No interaction
YEL056W	*HAT2*	1.1078	1.0279	1.0011	1.0456	1.2004	0.9410	0.8725	1.0046	0.7161813	-0.0409	
YLR399C	*BDF1*	1.0760	1.0095	1.0633	1.0496	1.0237	0.9891	1.0229	1.0119	0.1821742	-0.0377	
YKL017C	*HCS1*	1.0491	0.9842	1.0342	1.0225	1.0907	1.0252	0.8424	0.9861	0.6604816	-0.0364	
YOR351C	*MEK1*	0.8975	0.9428	0.9306	0.9236	0.9689	0.8659	0.8274	0.8874	0.4594491	-0.0363	
YPL129W	*TAF14*	1.0198	1.0877	1.1026	1.0700	1.0755	1.0162	1.0109	1.0342	0.3367056	-0.0358	
YLR176C	*RFX1*	0.9122	0.8876	0.8954	0.8984	0.8104	0.8809	0.8966	0.8626	0.2628615	-0.0358	
YLR288C	*MEC3*	1.0173	0.9911	1.0032	1.0038	0.9658	0.9981	0.9417	0.9685	0.1217563	-0.0353	
YMR234W	*RNH1*	0.9024	0.9014	0.8974	0.9004	0.8257	0.8418	0.9297	0.8657	0.3438222	-0.0347	
YOL068C	*HST1*	0.9537	0.9336	0.9037	0.9303	0.9323	0.8899	0.8665	0.8962	0.2305875	-0.0341	
YLR035C	*MLH2*	1.0149	0.9313	0.9327	0.9596	0.9963	0.8959	0.8845	0.9256	0.4914343	-0.0340	
YMR284W	*YKU70*	1.0124	1.0049	1.0736	1.0303	0.9018	0.9861	1.1011	0.9964	0.6116905	-0.0339	
YKR056W	*TRM2*	1.0295	0.9520	0.9368	0.9728	1.0146	0.8869	0.9176	0.9397	0.5285388	-0.0331	
YBR010W	*HHT1*	0.8950	0.8991	0.9576	0.9172	0.9201	0.8839	0.8484	0.8841	0.3163450	-0.0331	
YMR186W	*HSC82*	0.9660	0.8462	0.9140	0.9087	0.8592	0.9079	0.8605	0.8759	0.4380624	-0.0329	
YGL086W	*MAD1*	0.9439	0.9244	0.9037	0.9240	0.9232	0.9170	0.8334	0.8912	0.3519728	-0.0328	
YPL241C	*CIN2*	0.8608	0.9428	0.9783	0.9273	0.8470	0.8959	0.9447	0.8959	0.5216140	-0.0314	
YIL009C-A	*EST3*	0.9635	0.9842	0.9576	0.9684	0.9323	0.9380	0.9417	0.9373	0.0217911	-0.0311	
YER164W	*CHD1*	0.6798	0.8140	0.7835	0.7591	0.7647	0.7215	0.6980	0.7281	0.5291270	-0.0310	
YLR318W	*EST2*	0.9537	0.9842	0.9430	0.9603	0.9353	0.9230	0.9297	0.9293	0.0731350	-0.0310	
YER016W	*BIM1*	0.9488	0.9796	1.0259	0.9848	0.9323	0.9801	0.9507	0.9544	0.3131215	-0.0304	
YDR359C	*EAF1*	1.0467	0.9934	1.0197	1.0199	0.9536	0.9410	1.0741	0.9896	0.5379277	-0.0304	
YIL018W	*RPL2B*	0.9660	0.9796	1.0094	0.9850	0.9201	0.9951	0.9507	0.9553	0.3057706	-0.0296	
YCL061C	*MRC1*	1.0173	0.9037	0.9368	0.9526	0.9658	0.8839	0.9206	0.9234	0.5182860	-0.0292	
YOR386W	*PHR1*	0.9244	0.8784	0.9969	0.9332	0.8805	0.9410	0.8936	0.9050	0.5103975	-0.0282	
YDL070W	*BDF2*	0.8950	0.9612	1.0280	0.9614	0.9079	0.9591	0.9327	0.9332	0.5306068	-0.0282	
YML124C	*TUB3*	1.1371	0.9957	0.9658	1.0329	1.1547	0.9470	0.9146	1.0055	0.7801997	-0.0274	
YJR074W	*MOG1*	0.9219	0.9382	0.9493	0.9365	0.9475	0.9290	0.8575	0.9113	0.4288413	-0.0251	No interaction
YNL218W	*MGS1*	1.0002	0.9888	0.9907	0.9932	0.9750	0.9170	1.0139	0.9686	0.4345884	-0.0246	
YIL112W	*HOS4*	1.0295	0.9129	0.9410	0.9611	1.0298	0.9019	0.8785	0.9367	0.6991057	-0.0244	
YJR035W	*RAD26*	0.9831	1.0440	0.9472	0.9914	0.9902	0.9711	0.9447	0.9687	0.5058694	-0.0228	
YFL003C	*MSH4*	1.0907	1.1084	1.0819	1.0936	1.0024	1.1064	1.1042	1.0710	0.5541662	-0.0227	
YDL082W	*RPL13A*	0.8681	0.8922	0.8373	0.8659	0.8196	0.8508	0.8605	0.8436	0.3300858	-0.0223	
YDR075W	*PPH3*	1.1127	1.0647	0.9886	1.0553	1.1517	0.9981	0.9507	1.0335	0.7726152	-0.0218	
YML011C	*RAD33*	0.9611	0.9750	1.0508	0.9956	0.9110	1.0072	1.0049	0.9743	0.6405419	-0.0213	
YHR154W	*RTT107*	0.8608	0.8393	0.8104	0.8368	0.8592	0.8598	0.7281	0.8157	0.6709224	-0.0211	

Yeast systematic name	Yeast standard name	Vector Set 1	Vector Set 2	Vector Set 3	Vector Avg.	D181A Set 1	D181A Set 2	D181A Set 3	D181A Avg.	T-test	E-C[a]	GC Validations[b]
YKL213C	*DOA1*	0.8828	0.8761	0.8394	0.8661	0.9414	0.8598	0.7341	0.8451	0.7512699	-0.0210	
YDL155W	*CLB3*	0.9219	0.9589	0.9990	0.9599	0.8988	0.9230	0.9958	0.9392	0.6020749	-0.0207	
YIR002C	*MPH1*	0.8119	0.7749	0.8518	0.8129	0.8074	0.7727	0.8003	0.7934	0.4735816	-0.0194	
YPR120C	*CLB5*	0.8999	0.9796	0.9348	0.9381	0.8653	0.8989	0.9928	0.9190	0.6908216	-0.0191	
YNL138W	*SRV2*	0.9880	0.9336	0.8498	0.9238	0.8836	0.8869	0.9477	0.9061	0.7154270	-0.0177	
YGR276C	*RNH70*	0.9660	0.9589	0.9783	0.9677	0.8896	0.8689	1.0921	0.9502	0.8185514	-0.0175	
YPL008W	*CHL1*	0.8926	0.8715	0.8664	0.8768	0.8896	0.8508	0.8424	0.8610	0.3938722	-0.0159	
YKL210W	*UBA1*	0.9733	1.0164	0.9617	0.9838	0.9262	1.0252	0.9537	0.9684	0.6726374	-0.0154	
YOR191W	*ULS1*	0.8926	0.7910	0.8332	0.8389	0.8500	0.7967	0.8244	0.8237	0.6705037	-0.0152	
YCR008W	*SAT4*	0.7239	0.6692	0.7233	0.7055	0.6672	0.7185	0.6860	0.6906	0.5618099	-0.0149	
YGR129W	*SYF2*	0.9439	0.8968	0.9016	0.9141	1.0054	0.8208	0.8725	0.8996	0.8110519	-0.0146	
YNL299W	*TRF5*	0.9439	0.9428	0.9430	0.9433	0.9018	0.9170	0.9688	0.9292	0.5257512	-0.0141	
YKL117W	*SBA1*	1.1200	1.0693	0.9949	1.0614	1.1699	1.0102	0.9658	1.0486	0.8677318	-0.0128	
YOL043C	*NTG2*	0.9660	0.9175	0.8995	0.9277	0.9506	0.8959	0.9026	0.9164	0.6893255	-0.0113	
YDL216C	*RRI1*	0.8412	0.8577	0.8415	0.8468	0.8318	0.8508	0.8274	0.8366	0.3232838	-0.0102	
YDL059C	*RAD59*	0.8901	0.8577	0.8705	0.8728	0.8531	0.8659	0.8695	0.8628	0.4024539	-0.0100	
YGR108W	*CLB1*	1.0785	1.0854	0.9866	1.0501	1.1060	1.0673	0.9477	1.0403	0.8724188	-0.0098	
YCR014C	*POL4*	1.0711	0.9865	0.9804	1.0126	1.1090	0.9621	0.9417	1.0043	0.8960186	-0.0084	
YBR272C	*HSM3*	0.8975	0.9152	0.9327	0.9151	0.9536	0.8779	0.8905	0.9074	0.7760942	-0.0078	
YPL181W	*CTI6*	0.8217	0.8439	0.8145	0.8267	0.8165	0.8238	0.8183	0.8195	0.4753234	-0.0072	
YKL190W	*CNB1*	0.9611	0.8669	0.8933	0.9071	0.8653	0.9500	0.8845	0.8999	0.8600074	-0.0071	
YBR231C	*SWC5*	0.9782	1.1497	1.0301	1.0527	1.0816	1.0703	0.9868	1.0462	0.9182508	-0.0064	
YDR079C-A	*TFB5*	1.0247	1.0233	1.0778	1.0419	1.0816	0.9591	1.0681	1.0362	0.9009861	-0.0057	No interaction
YGR003W	*CUL3*	0.9855	0.8508	0.8933	0.9099	1.0389	0.8779	0.8003	0.9057	0.9612331	-0.0042	
YPL164C	*MLH3*	0.9317	1.0256	0.9430	0.9668	1.0207	0.9290	0.9387	0.9628	0.9277612	-0.0040	
YHR086W	*NAM8*	0.9635	0.9543	0.9472	0.9550	0.9323	0.9981	0.9236	0.9514	0.8868516	-0.0036	
YJL013C	*MAD3*	0.9709	1.0141	0.9161	0.9670	0.9536	0.9290	1.0079	0.9635	0.9284413	-0.0035	
YBL088C	*TEL1*	1.0100	0.8508	0.8601	0.9070	0.9963	0.8749	0.8394	0.9035	0.9630414	-0.0035	
YOR033C	*EXO1*	1.0124	1.0256	0.9783	1.0054	1.1121	0.9530	0.9417	1.0023	0.9582794	-0.0032	
YGR188C	*BUB1*	1.1249	0.8922	0.8871	0.9681	1.1090	0.9530	0.8364	0.9661	0.9870767	-0.0019	
YKL025C	*PAN3*	1.0418	0.9980	0.9244	0.9880	1.1547	0.8779	0.9267	0.9864	0.9866941	-0.0016	
YBR228W	*SLX1*	1.0760	1.0578	0.9534	1.0291	1.1395	0.9891	0.9567	1.0284	0.9932276	-0.0006	
YPL127C	*HHO1*	0.0000	0.0000	0.0000	0.0000	0.0000	0.0000	0.0000	0.0000		0.0000	
YDL042C	*SIR2*	0.0000	0.0000	0.0000	0.0000	0.0000	0.0000	0.0000	0.0000		0.0000	
YLR234W	*TOP3*	0.0000	0.0000	0.0000	0.0000	0.0000	0.0000	0.0000	0.0000		0.0000	
YLR418C	*CDC73*	0.0000	0.0000	0.0000	0.0000	0.0000	0.0000	0.0000	0.0000		0.0000	
YIL066C	*RNR3*	0.8950	0.8853	0.9389	0.9064	0.8805	0.8869	0.9537	0.9070	0.9834896	0.0006	
YDR289C	*RTT103*	0.4622	0.5082	0.4705	0.4803	0.4601	0.5231	0.4603	0.4812	0.9740419	0.0009	
YJL065C	*DLS1*	0.8926	0.8324	0.8394	0.8548	0.9750	0.7967	0.7973	0.8563	0.9818642	0.0015	
YBL002W	*HTB2*	0.8828	0.8554	0.8954	0.8779	0.8531	0.8779	0.9086	0.8799	0.9252734	0.0020	
YCL029C	*BIK1*	1.0173	0.9566	0.9265	0.9668	1.0755	0.9140	0.9176	0.9690	0.9718268	0.0022	
YDR092W	*UBC13*	0.9635	0.8094	0.7192	0.8307	0.8531	0.8659	0.7822	0.8337	0.9702304	0.0030	
YJR047C	*ANB1*	0.9562	0.9359	0.9886	0.9602	0.9232	0.9981	0.9718	0.9644	0.8851995	0.0041	
YBR223C	*TDP1*	0.9097	0.9543	0.9120	0.9253	0.9750	0.9260	0.8875	0.9295	0.8930936	0.0042	
YLR247C	*IRC20*	0.9880	1.0256	1.0487	1.0208	0.9871	1.0041	1.0861	1.0258	0.8934687	0.0050	
YBR009C	*HHF1*	0.8779	0.8922	0.9057	0.8920	0.9597	0.8659	0.8665	0.8974	0.8750162	0.0054	
YHR120W	*MSH1*	0.6187	0.6646	0.6467	0.6433	0.6185	0.6674	0.6679	0.6513	0.7252410	0.0080	
YGL100W	*SEH1*	0.9439	0.9152	0.8974	0.9189	0.9262	0.9440	0.9116	0.9273	0.6364150	0.0084	
YGR063C	*SPT4*	1.1274	1.0624	1.1109	1.1002	1.3010	1.0372	0.9898	1.1093	0.9308466	0.0091	
YER179W	*DMC1*	0.8437	0.8393	0.8104	0.8311	0.7647	0.8508	0.9056	0.8404	0.8376414	0.0092	
YAL021C	*CCR4*	0.7190	0.6600	0.7607	0.7132	0.6794	0.6975	0.7913	0.7227	0.8436801	0.0095	

Yeast systematic name	Yeast standard name	Vector Set 1	Vector Set 2	Vector Set 3	Vector Avg.	D181A Set 1	D181A Set 2	D181A Set 3	D181A Avg.	T-test	E-C[a]	GC Validations[b]
YOR290C	*SNF2*	0.8192	0.8416	0.8083	0.8231	0.8927	0.7546	0.8514	0.8329	0.8262509	0.0099	
YER177W	*BMH1*	0.6285	0.6301	0.4850	0.5812	0.6429	0.6283	0.5054	0.5922	0.8732202	0.0110	
YPL096W	*PNG1*	0.9293	0.9520	0.9161	0.9325	0.9323	0.9350	0.9658	0.9444	0.4719999	0.0119	
YPL240C	*HSP82*	0.8657	0.9060	0.9140	0.8952	0.8744	0.9290	0.9206	0.9080	0.6024784	0.0128	
YOL072W	*THP1*	1.1298	1.0624	1.1607	1.1176	1.1608	1.1575	1.0771	1.1318	0.7402979	0.0142	No interaction
YBR186W	*PCH2*	0.9513	0.9221	0.9306	0.9347	0.8836	0.9560	1.0079	0.9492	0.7157543	0.0145	
YMR048W	*CSM3*	0.9855	0.9428	0.9410	0.9564	1.0816	0.9019	0.9297	0.9711	0.8123369	0.0146	
YJL092W	*SRS2*	1.0222	0.9267	0.9223	0.9571	1.0999	0.8779	0.9387	0.9721	0.8481652	0.0151	
YOL012C	*HTZ1*	0.9635	0.8623	0.8539	0.8932	0.8561	0.9109	0.9628	0.9099	0.7391318	0.0167	
YOR073W	*SGO1*	0.9904	1.0325	1.0591	1.0273	1.0603	1.0342	1.0380	1.0441	0.4794555	0.0168	
YMR137C	*PSO2*	0.7483	0.7450	0.7689	0.7541	0.7160	0.8057	0.7973	0.7730	0.5575348	0.0189	
YDL230W	*PTP1*	0.9562	0.8577	0.8518	0.8886	1.0511	0.8659	0.8063	0.9078	0.8246591	0.0192	
YBR026C	*ETR1*	0.5429	0.4346	0.4643	0.4806	0.5149	0.5171	0.4693	0.5004	0.6092092	0.0199	
YER070W	*RNR1*	0.9317	0.9474	1.0280	0.9690	0.9262	1.0162	1.0289	0.9904	0.6521162	0.0214	
YDR314C	*RAD34*	1.0149	0.9543	0.9223	0.9638	1.0846	0.9681	0.9056	0.9861	0.7252493	0.0223	
YLR154C	*RNH203*	1.0198	1.0992	0.9824	1.0338	1.0572	1.0853	1.0259	1.0562	0.5918234	0.0224	
YOR308C	*SNU66*	1.0809	0.9635	0.9016	0.9820	1.1639	0.9320	0.9176	1.0045	0.8254131	0.0225	
YOR080W	*DIA2*	0.9219	0.9014	0.8394	0.8876	0.9384	0.9170	0.8755	0.9103	0.5035086	0.0227	
YGL090W	*LIF1*	0.9024	0.8600	0.8746	0.8790	0.8988	0.8869	0.9206	0.9021	0.2193561	0.0231	
YDR334W	*SWR1*	1.1274	1.0946	1.0467	1.0895	1.1699	1.0943	1.0741	1.1128	0.5678817	0.0233	
YHR064C	*SSZ1*	0.4402	0.4944	0.3088	0.4145	0.7160	0.2375	0.3610	0.4382	0.8848193	0.0237	
YML102W	*CAC2*	0.8363	0.7772	0.7772	0.7969	0.8683	0.8598	0.7431	0.8238	0.5827358	0.0268	
YOL006C	*TOP1*	0.9929	0.9635	0.9348	0.9637	1.0389	0.9681	0.9658	0.9909	0.4053093	0.0272	
YAL015C	*NTG1*	1.0149	0.9474	0.9037	0.9553	0.9871	0.9621	0.9989	0.9827	0.4672372	0.0274	
YLL019C	*KNS1*	0.9831	0.9635	0.9990	0.9819	0.9932	0.9981	1.0380	1.0098	0.1857392	0.0279	
YBR189W	*RPS9B*	0.8584	0.8669	1.0052	0.9102	0.9232	0.9350	0.9567	0.9383	0.5936535	0.0281	
YGL003C	*CDH1*	0.9562	0.8738	0.7627	0.8642	1.0085	0.9019	0.7672	0.8925	0.7677600	0.0283	
YPL001W	*HAT1*	1.0564	0.9635	0.9430	0.9877	1.1121	1.0222	0.9206	1.0183	0.6637777	0.0306	
YGL175C	*SAE2*	0.9219	0.9428	0.8871	0.9173	0.9810	0.9560	0.9116	0.9496	0.2821427	0.0323	
YJL030W	*MAD2*	0.7850	0.7473	0.7503	0.7609	0.8165	0.8448	0.7191	0.7935	0.4605345	0.0326	
YKR024C	*DBP7*	0.7116	0.8094	0.8063	0.7758	0.8500	0.8388	0.7371	0.8086	0.5322469	0.0329	
YGR163W	*GTR2*	0.9562	0.9129	0.8539	0.9077	1.0146	0.8899	0.9206	0.9417	0.5157067	0.0340	
YBR274W	*CHK1*	0.8828	0.8853	0.8581	0.8754	0.8927	0.9079	0.9297	0.9101	0.0657929	0.0347	
YEL037C	*RAD23*	1.0198	0.9750	0.9120	0.9689	1.0938	0.9591	0.9658	1.0062	0.5265935	0.0373	
YLR357W	*RSC2*	1.0809	1.0578	1.0301	1.0563	1.1974	1.0072	1.0771	1.0939	0.5483934	0.0376	
YHR191C	*CTF8*	0.8828	0.8922	0.8788	0.8846	0.9201	0.9230	0.9236	0.9222	0.0007942	0.0376	
YLR210W	*CLB4*	1.0516	1.0417	0.9451	1.0128	1.0633	1.1034	0.9898	1.0522	0.4537189	0.0394	
YMR199W	*CLN1*	0.8339	0.8830	0.8498	0.8556	0.8896	0.9170	0.8785	0.8950	0.0988687	0.0395	
YEL061C	*CIN8*	0.9611	0.9819	0.9845	0.9758	1.0207	1.0462	0.9808	1.0159	0.1212677	0.0401	
YBR195C	*MSI1*	0.8510	0.9428	0.8705	0.8881	0.9262	0.9230	0.9357	0.9283	0.2269504	0.0402	
YGL087C	*MMS2*	1.0100	1.0210	0.9824	1.0045	1.0542	1.1124	0.9688	1.0451	0.4005017	0.0406	
YCR044C	*PER1*	1.0589	0.9911	0.9617	1.0039	1.1699	0.9591	1.0049	1.0446	0.5928896	0.0407	
YIL139C	*REV7*	1.0222	0.9773	0.9886	0.9960	0.9780	1.0372	1.0951	1.0368	0.3257253	0.0407	
YNL107W	*YAF9*	1.1861	1.0670	1.1026	1.1185	1.2827	1.1064	1.0891	1.1594	0.5970009	0.0408	
YML061C	*PIF1*	1.0222	1.0578	1.0301	1.0367	1.1303	1.0673	1.0350	1.0775	0.2451692	0.0408	
YPR018W	*RLF2*	0.7410	0.6967	0.6176	0.6851	0.7982	0.7396	0.6408	0.7262	0.5204126	0.0411	
YPR141C	*KAR3*	1.0100	0.9704	0.9741	0.9848	1.0603	1.0282	0.9898	1.0261	0.1600222	0.0413	
YML021C	*UNG1*	0.8999	0.7151	0.7544	0.7898	1.0146	0.7787	0.7010	0.8314	0.7240968	0.0416	
YMR216C	*SKY1*	0.8681	0.8462	0.8726	0.8623	0.8714	0.9350	0.9056	0.9040	0.1069624	0.0417	
YNL307C	*MCK1*	0.8388	0.8117	0.7316	0.7940	0.8683	0.8478	0.7943	0.8368	0.3347234	0.0428	
YGL229C	*SAP4*	0.8632	0.9267	0.8560	0.8820	0.9110	0.9140	0.9507	0.9252	0.1695475	0.0432	

Yeast systematic name	Yeast standard name	Vector Set 1	Vector Set 2	Vector Set 3	Vector Avg.	D181A Set 1	D181A Set 2	D181A Set 3	D181A Avg.	T-test	E-C[a]	GC Validations[b]
YCL016C	*DCC1*	0.9024	0.9428	0.9140	0.9197	0.9140	0.9981	0.9778	0.9633	0.1950482	0.0436	
YER051W	*JHD1*	0.9757	1.0578	1.0633	1.0323	0.9932	1.0763	1.1583	1.0760	0.4745509	0.0437	
YGL211W	*NCS6*	0.6089	0.6462	0.5202	0.5918	0.7129	0.6283	0.5656	0.6356	0.4824567	0.0439	
YGL194C	*HOS2*	1.1029	1.0647	0.9762	1.0479	1.2492	1.0883	0.9417	1.0931	0.6639719	0.0451	
YNL246W	*VPS75*	0.8290	0.8255	0.8104	0.8216	0.8561	0.7937	0.9507	0.8669	0.3813462	0.0452	
YKL114C	*APN1*	1.0858	1.0095	1.0301	1.0418	1.1517	1.0703	1.0410	1.0876	0.3175878	0.0459	
YOR156C	*NFI1*	0.9317	0.9313	0.8705	0.9112	0.9232	0.9591	1.0049	0.9624	0.1760661	0.0512	
YDR030C	*RAD28*	0.8901	0.8370	0.8249	0.8507	0.9719	0.8839	0.8514	0.9024	0.2775822	0.0517	
YLR306W	*UBC12*	0.9635	0.8807	0.8684	0.9042	1.0664	0.9230	0.8785	0.9559	0.4646327	0.0517	
YKR028W	*SAP190*	0.8901	0.8922	0.8705	0.8843	0.9079	0.9200	0.9808	0.9362	0.0924423	0.0519	
YFR040W	*SAP155*	0.9122	0.8278	0.7358	0.8253	0.9658	0.9109	0.7552	0.8773	0.5558226	0.0521	
YBL019W	*APN2*	1.0907	1.0762	0.9907	1.0525	1.1669	1.1184	1.0320	1.1057	0.3496003	0.0532	
YER045C	*ACA1*	1.0491	0.8761	0.8726	0.9326	1.0877	0.9771	0.8936	0.9861	0.5447629	0.0535	
YPL256C	*CLN2*	0.8926	0.8393	0.8560	0.8626	0.8866	0.9230	0.9417	0.9171	0.0732984	0.0545	
YGR258C	*RAD2*	0.9195	0.9083	0.9078	0.9119	0.9628	0.9621	0.9748	0.9665	0.0006267	0.0547	
YFR014C	*CMK1*	1.0222	0.9658	0.9493	0.9791	1.0938	1.0583	0.9507	1.0343	0.3174743	0.0552	
YBL046W	*PSY4*	0.8730	0.8899	0.8560	0.8730	0.9658	0.8689	0.9537	0.9295	0.1526130	0.0565	
YBR158W	*AMN1*	0.8779	0.8784	0.8995	0.8853	0.9384	0.9380	0.9507	0.9424	0.0022918	0.0571	
YHR066W	*SSF1*	0.8730	0.8715	0.8518	0.8655	0.9018	0.9140	0.9567	0.9242	0.0309991	0.0587	
YGL033W	*HOP2*	1.1469	1.1497	1.1462	1.1476	1.2309	1.2086	1.1824	1.2073	0.0132129	0.0597	
YOR258W	*HNT3*	1.1249	1.0900	1.1337	1.1162	1.2339	1.1695	1.1252	1.1762	0.1548183	0.0600	
YNL082W	*PMS1*	1.0149	0.9290	0.8456	0.9298	1.0877	0.9771	0.9056	0.9901	0.4498413	0.0603	
YLR135W	*SLX4*	0.9170	0.8232	0.8311	0.8571	0.9293	0.9290	0.8966	0.9183	0.1281851	0.0611	
YOR025W	*HST3*	0.6970	0.6760	0.6777	0.6836	0.6855	0.7125	0.8364	0.7448	0.2620270	0.0612	
YDL200C	*MGT1*	0.8730	0.9244	0.9285	0.9087	1.0511	0.9230	0.9387	0.9709	0.2309949	0.0623	
YLR270W	*DCS1*	1.0075	0.9244	0.8809	0.9376	1.0389	1.0072	0.9537	0.9999	0.2356294	0.0623	
YPL022W	*RAD1*	0.8877	0.8761	0.8767	0.8802	0.8500	0.9260	1.0530	0.9430	0.3492689	0.0628	No interaction
YJR043C	*POL32*	0.8877	0.8692	0.8353	0.8641	1.0785	0.8358	0.8665	0.9269	0.4645589	0.0629	
YPL042C	*SSN3*	1.0124	1.0325	0.9866	1.0105	0.9993	1.0883	1.1403	1.0760	0.2044818	0.0655	No interaction
YBL003C	*HTA2*	0.8510	0.8117	0.7752	0.8126	0.9475	0.8328	0.8575	0.8793	0.1810271	0.0666	
YDL013W	*SLX5*	0.8412	0.8255	0.8083	0.8250	0.9049	0.8478	0.9267	0.8931	0.0549197	0.0681	
YPR119W	*CLB2*	1.0662	1.0578	1.0177	1.0472	1.2553	1.0132	1.0861	1.1182	0.3875148	0.0710	
YGR109C	*CLB6*	0.8706	0.8370	0.7648	0.8241	0.9963	0.8448	0.8514	0.8975	0.2777035	0.0734	
YHL006C	*SHU1*	1.0882	1.0187	0.9804	1.0291	1.2065	1.0583	1.0440	1.1029	0.2913891	0.0738	
YOR014W	*RTS1*	0.8315	0.9244	0.8767	0.8775	0.9018	0.9861	0.9688	0.9522	0.1146452	0.0747	
YGL240W	*DOC1*	0.7972	0.7634	0.8601	0.8069	0.8653	0.8869	0.8936	0.8819	0.0644230	0.0750	
YJR090C	*GRR1*	0.6774	0.8094	0.6280	0.7049	0.7617	0.8147	0.7642	0.7802	0.2560614	0.0753	
YMR156C	*TPP1*	0.9880	0.9037	0.9078	0.9332	1.0968	1.0192	0.9116	1.0092	0.2758052	0.0760	
YAL019W	*FUN30*	1.0173	0.9060	0.8353	0.9195	1.2156	0.8869	0.8845	0.9957	0.5665051	0.0762	
YIR019C	*MUC1*	0.9586	0.8531	0.8228	0.8782	1.0846	0.8959	0.8845	0.9550	0.3738953	0.0768	
YHR082C	*KSP1*	0.9562	0.9727	0.8871	0.9386	1.0359	1.0372	0.9748	1.0160	0.0812102	0.0773	
YFR031C-A	*RPL2A*	1.0026	0.9474	0.9327	0.9609	1.1273	1.0793	0.9086	1.0384	0.3284914	0.0775	
YDR014W	*RAD61*	1.0002	1.0325	1.0570	1.0299	1.0907	1.1184	1.1132	1.1074	0.0138406	0.0775	
YGL251C	*HFM1*	1.0344	0.9313	0.8684	0.9447	1.1242	0.9951	0.9477	1.0224	0.3390605	0.0776	
YBL067C	*UBP13*	0.8339	0.8163	0.7648	0.8050	0.8531	0.9019	0.8966	0.8839	0.0380868	0.0789	
YML060W	*OGG1*	1.0980	1.0394	0.9824	1.0399	1.1242	1.1244	1.1102	1.1196	0.0773130	0.0797	
YLR376C	*PSY3*	0.9562	0.8439	0.8000	0.8667	0.9567	0.9380	0.9447	0.9465	0.1636493	0.0798	
YCR066W	*RAD18*	0.8657	0.8209	0.8083	0.8316	0.9201	0.8989	0.9176	0.9122	0.0124410	0.0806	
YIL132C	*CSM2*	1.1323	1.0693	1.0342	1.0786	1.2248	1.1124	1.1493	1.1622	0.1289128	0.0836	
YNL230C	*ELA1*	0.8632	0.8991	0.8477	0.8700	0.9475	0.9801	0.9357	0.9544	0.0139206	0.0844	
YJR066W	*TOR1*	0.8632	0.8393	0.7710	0.8245	0.9262	0.9470	0.8575	0.9102	0.0910390	0.0857	

Yeast systematic name	Yeast standard name	Vector Set 1	Vector Set 2	Vector Set 3	Vector Avg.	D181A Set 1	D181A Set 2	D181A Set 3	D181A Avg.	T-test	E-C[a]	GC Validations[b]
YDR078C	*SHU2*	0.9660	0.9589	0.9016	0.9421	1.1303	0.9290	1.0289	1.0294	0.2294498	0.0873	
YFR034C	*PHO4*	0.9195	0.9037	0.8622	0.8951	1.1791	0.8749	0.8966	0.9835	0.4244935	0.0884	
YDR378C	*LSM6*	0.9684	1.0371	1.0467	1.0174	1.0968	1.1334	1.0921	1.1075	0.0319837	0.0901	
YCR092C	*MSH3*	1.0687	1.0279	0.9513	1.0160	1.1121	1.0733	1.1373	1.1075	0.0791852	0.0916	
YMR036C	*MIH1*	0.7654	0.7634	0.7669	0.7652	0.8500	0.9049	0.8183	0.8578	0.0216741	0.0925	
YLR265C	*NEJ1*	0.9464	0.9083	0.9057	0.9201	1.0237	1.0523	0.9748	1.0169	0.0208535	0.0968	
YJR063W	*RPA12*	0.8828	0.8048	0.7358	0.8078	1.0389	0.8388	0.8364	0.9047	0.2894622	0.0969	
YDL116W	*NUP84*	0.9709	0.9842	0.9555	0.9702	1.0603	1.0342	1.1072	1.0672	0.0132845	0.0970	
YPR052C	*NHP6A*	0.8681	0.8623	0.7855	0.8387	0.9567	0.9260	0.9357	0.9394	0.0230781	0.1008	
YER041W	*YEN1*	1.0075	0.9382	0.9078	0.9512	1.2035	0.9560	0.9989	1.0528	0.2822665	0.1016	
YNR052C	*POP2*	0.6309	0.3771	0.4394	0.4825	1.1090	0.3247	0.3279	0.5872	0.7196500	0.1047	
YNL030W	*HHF2*	0.8926	0.9474	0.9037	0.9145	0.9993	1.0222	1.0470	1.0228	0.0074957	0.1083	
YHR031C	*RRM3*	0.9391	0.9911	0.9783	0.9695	1.0633	1.0763	1.0951	1.0782	0.0039159	0.1088	
YOR005C	*DNL4*	1.0222	0.9957	0.9513	0.9897	1.0907	1.1124	1.1042	1.1024	0.0064563	0.1127	
YOL115W	*PAP2*	0.9660	0.9221	0.8456	0.9112	1.1882	0.9290	0.9628	1.0267	0.2627727	0.1154	
YPL046C	*ELC1*	0.8853	0.7519	0.6612	0.7661	0.9963	0.8177	0.8394	0.8845	0.2408474	0.1184	
YDR097C	*MSH6*	0.9170	0.9359	0.8518	0.9016	1.0420	1.0222	1.0079	1.0240	0.0109723	0.1224	
YDR419W	*RAD30*	1.0833	1.0256	1.0135	1.0408	1.2035	1.2116	1.0831	1.1661	0.0554502	0.1252	
YER169W	*RPH1*	0.7434	0.8761	0.8394	0.8196	0.9414	0.9831	0.9116	0.9454	0.0480524	0.1257	
YNL201C	*PSY2*	0.8461	0.7542	0.7586	0.7863	0.9079	0.9651	0.8725	0.9152	0.0329627	0.1288	
YGL058W	*RAD6*	0.9880	0.9474	0.9057	0.9470	1.2126	0.9651	1.0530	1.0769	0.1637082	0.1299	
YDL101C	*DUN1*	0.9660	0.9221	0.8788	0.9223	1.1974	0.9621	1.0109	1.0568	0.1514436	0.1345	
YJL101C	*GSH1*	0.0000	0.0000	0.0000	0.0000	0.0000	0.4209	0.0000	0.1403	0.3739010	0.1403	
YPR101W	*SNT309*	1.1274	0.8048	0.7710	0.9011	1.0481	1.0342	1.0590	1.0471	0.2686652	0.1460	
YGR252W	*GCN5*	1.0075	0.9865	1.0280	1.0073	1.1791	1.1214	1.1734	1.1579	0.0023508	0.1506	
YOR346W	*REV1*	1.0638	0.9773	0.9037	0.9816	1.2217	1.1154	1.0981	1.1451	0.0534133	0.1635	
YPL167C	*REV3*	1.0075	0.9198	0.8436	0.9236	1.2035	0.9981	1.0620	1.0879	0.0997648	0.1643	
YMR106C	*YKU80*	1.0711	0.9612	0.8601	0.9641	1.0328	1.1695	1.3118	1.1714	0.1094024	0.2072	

[a] Experimental-control or (hD181A average)-(vector average). For each mutant, area of pinned spot was normalized to the average of WT spots on the same plate.

[b] Growth curve validations. Interactions with (experimental-control values <-0.2) and some selected mutants were chosen for validations by growth curves. "No interaction" indicates that mutant was tested by growth curves and no SDL interaction was observed. "Negative" and highlighted in yellow indicate that growth curves validated the SDL interaction of that deletion mutant.